A METHODOLOGY TO ENABLE RAPID EVALUATION OF AVIATION ENVIRONMENTAL IMPACTS AND AIRCRAFT TECHNOLOGIES

A Dissertation
Presented to
The Academic Faculty

By

Keith Frederick Becker

In Partial Fulfillment
Of the Requirements for the Degree
Doctor of Philosophy in the
School of Aerospace Engineering

Georgia Institute of Technology

August 2011

A METHODOLOGY TO ENABLE RAPID EVALUATION OF AVIATION ENVIRONMENTAL IMPACTS AND AIRCRAFT TECHNOLOGIES

Approved by:

Dr. Dimitri Mavris, Advisor
School of Aerospace Engineering
Georgia Institute of Technology

Dr. Michelle Kirby
School of Aerospace Engineering
Georgia Institute of Technology

Dr. Daniel Schrage
School of Aerospace Engineering
Georgia Institute of Technology

Dr. Mohan Gupta
Office of Environment & Energy
Federal Aviation Administration

Dr. Vitali Volovoi
School of Aerospace Engineering
Georgia Institute of Technology

Date Approved: May 12, 2011

ACKNOWLEDGEMENTS

First and foremost I give praise to the Lord Jesus Christ. Living, breathing, and finishing this thesis are only possible by the grace of God.

Next I would like to thank my advisor Dr. Dimitri Mavris. As his student, he has provided me with innumerable opportunities, including sharing his vast wisdom of different perspectives within engineering and how the world operates. I also recognize the rest of my committee: Dr. Michelle Kirby, Dr. Mohan Gupta, Dr. Daniel Schrage, and Dr. Vitali Volovoi. Each member of my committee provided valuable input during the proposal and defense stages of this work. In particular I thank Dr. Kirby for her leadership of the EDS team, helping me to find a thesis topic, and her willingness to meet the challenges along the way. I also recognize Dr. Gupta for his support of this thesis.

Over the years I have worked with many research engineers and students that have contributed to my learning and graduate school experience. Dr. Taewoo Nam, though not on my committee, helped me to develop many of the concepts that contributed to my thesis. Dr. Jimmy Tai, Dr. Jeff Schutte, Mr. Russell Denney, Mr. Graham Burdette, Mr. Chris Perullo, Mr. Paul Brett, Mr. William Engler, Mr. Eric Hendricks, Mr. Damon Rousis, Mr. Scott Wilson, and countless others worked diligently with me on various projects and also graciously reviewed my work throughout the dissertation process.

Finally, I recognize my family. My mom and dad have always supported me throughout my time in school and always desire to see me do my best. Together with my amazing fiancée Christy, I have been blessed with an incredible love that has continually provided me with encouragement as our relationship has grown deeper. Last, but most

certainly not least, I also thank all of my good friends here in Atlanta for their fellowship and prayer through the completion of this work.

TABLE OF CONTENTS

LIST OF TABLES

LIST OF FIGURES

NOMENCLATURE

ACC	Active Clearance Control
AEDT	Aviation Environmental Design Tool
AEE	Office of Environment and Energy
AIM	Aviation Integrated Modelling
ANCAT	Abatement of Nuisances Caused by Air Transport
ANOPP	Aircraft Noise Prediction Program
APMT	Aviation Environmental Portfolio Management Tool
ASDL	Aerospace Systems Design Lab
BADA	Base of Aircraft Data
CAEP	Committee on Aviation Environmental Protection
CDF	Cumulative Distribution Function
CLEEN	Continuous Lower Energy, Emissions, and Noise
CMC	Ceramic Matrix Composite
CO	Carbon Monoxide
CO_2	Carbon Dioxide
DAC	Dual Annular Combustor
DOE	Design of Experiments
EDMS	Emissions and Dispersion Modeling System
EDS	Environmental Design Space
EINOX	Emissions Index for NO_x
EPA	Environmental Protection Agency

EPNL	Effective Perceived Noise Level
ETMS	Enhanced Traffic Management System
FAA	Federal Aviation Administration
FESG	Forecasting and Economics Support Group
FLOPS	Flight Optimization System
FOM	Fleet and Operations Module
GDP	Gross Domestic Product
HLFC	Hybrid Laminar Flow Control
IATA	International Air Transport Association
ICAO	International Civil Aviation Organization
ICCAIA	International Coordinating Council of Aerospace Industries Associations
INM	Integrated Noise Module
IOAG	International Official Airline Guide
ISA	International Standard Atmosphere
JPDO	Joint Planning and Development Office
LDI	Lean Direct Injection
LTO	Landing-takeoff cycle
M&S	Modeling and Simulation
MAGENTA	Model for Assessing Global Exposure from Noise of Transport Airplanes
MCF	Monte Carlo Filtering
MCS	Monte Carlo Simulation
MODTF	Modelling and Database Task Force
NAS	National Airspace System

NASA	National Aeronautics and Space Administration
NextGen	Next Generation Air Transportation System
NO_x	Nitrous Oxides
NPSS	Numerical Propulsion System Simulation
OD	Origin-Destination
PDF	Probability Density Function
PIANO	Project Interactive Analysis and Optimization
RPK	Revenue Passenger Kilometer
SAC	Single Annular Combustor
SAE	Society of Automotive Engineers
SAGE	System for Assessing Aviation's Global Emissions
SARP	Standards and Recommended Practices
SFW	Subsonic Fixed Wing
SG	Steering Group
SLS	Sea Level Static
SO_x	Sulfurous Oxides
TAPS	Twin Annular Premixing Swirler
TBC	Thermal Barrier Coating
TOGW	Takeoff Gross Weight
UN	United Nations
U.S.	United States of America
WATE	Weight Analysis of Turbine Engines
WG	Working Group

SUMMARY

Commercial aviation has become an integral part of modern society and enables unprecedented global connectivity by increasing rapid business, cultural, and personal connectivity. In the decades following World War II, passenger travel through commercial aviation quickly grew at a rate of roughly 8% per year globally. The FAA's most recent Terminal Area Forecast predicts growth to continue at a rate of 2.5% domestically, and the market outlooks produced by Airbus and Boeing generally predict growth to continue at a rate of 5% per year globally over the next several decades, which translates into a need for up to 30,000 new aircraft produced by 2025.

With such large numbers of new aircraft potentially entering service, any negative consequences of commercial aviation must undergo examination and mitigation by governing bodies so that growth may still be achieved. Options to simultaneously grow while reducing environmental impact include evolution of the commercial fleet through changes in operations, aircraft mix, and technology adoption. Methods to rapidly evaluate fleet environmental metrics are needed to enable decision makers to quickly compare the impact of different scenarios and weigh the impact of multiple policy options.

As the fleet evolves, interdependencies may emerge in the form of tradeoffs between improvements in different environmental metrics as new technologies are brought into service. In order to include the impacts of these interdependencies on fleet evolution, physics-based modeling is required at the appropriate level of fidelity. Evaluation of environmental metrics in a physics-based manner can be done at the individual aircraft level, but will then not capture aggregate fleet metrics. Contrastingly, evaluation of

environmental metrics at the fleet level is already being done for aircraft in the commercial fleet, but current tools and approaches require enhancement because they currently capture technology implementation through post-processing, which does not capture physical interdependencies that may arise at the aircraft-level.

The goal of the work that has been conducted here was the development of a methodology to develop surrogate fleet approaches that leverage the capability of physics-based aircraft models and the development of connectivity to fleet-level analysis tools to enable rapid evaluation of fuel burn and emissions metrics. Instead of requiring development of an individual physics-based model for each vehicle in the fleet, the surrogate fleet approaches seek to reduce the number of such models needed while still accurately capturing performance of the fleet. By reducing the number of models, both development time and execution time to generate fleet-level results may also be reduced.

The initial steps leading to surrogate fleet formulation were a characterization of the commercial fleet into groups based on capability followed by the selection of a reference vehicle model and a reference set of operations for each group. Next, three potential surrogate fleet approaches were formulated. These approaches include the parametric correction factor approach, in which the results of a reference vehicle model are corrected to match the aggregate results of each group; the average replacement approach, in which a new vehicle model is developed to generate aggregate results of each group, and the best-in-class replacement approach, in which results for a reference vehicle are simply substituted for the entire group. Once candidate surrogate fleet approaches were developed, they were each applied to and evaluated over the set of reference operations. Then each approach was evaluated for their ability to model variations in operations.

Finally, the ability of each surrogate fleet approach to capture implementation of different technology suites along with corresponding interdependencies between fuel burn and emissions was evaluated using the concept of a virtual fleet to simulate the technology response of multiple aircraft families.

The results of experimentation led to a down selection to the best approach to use to rapidly characterize the performance of the commercial fleet for accurately in the context of acceptability of current fleet evaluation methods. The parametric correction factor and average replacement approaches were shown to be successful in capturing reference fleet results as well as fleet performance with variations in operations. The best-in-class replacement approach was shown to be unacceptable as a model for the larger fleet in each of the scenarios tested. Finally, the average replacement approach was the only one that was successful in capturing the impact of technologies on a larger fleet.

These results are meaningful because they show that it is possible to calculate the fuel burn and emissions of a larger fleet with a reduced number of physics-based models within acceptable bounds of accuracy. At the same time, the physics-based modeling also provides the ability to evaluate the impact of technologies on fleet-level fuel burn and emissions metrics. The value of such a capability is that multiple future fleet scenarios involving changes in both aircraft operations and technology levels may now be rapidly evaluated to inform and equip policy makers of the implications of impacts of changes on fleet-level metrics.

CHAPTER I

INTRODUCTION

"I believe the present status and future potential of aviation is a testimonial to the value of aeronautical research and development. The most distant lands are now merely hours away...and the aviation industry, which ranks seventh among the Nation's leading industries, is considered by economists as a key factor in our sustained national economic growth."

-Senator Margaret Chase Smith, 1967[1]

The importance of commercial aviation to modern society is beyond doubt. In the four decades since Senator Smith's statement, commercial aviation has grown worldwide, and today aviation enplanes almost 2 billion passengers per year, provides 28 million jobs, and transports 40% of world trade by value.[2] It is an enabler for global travel on a scale never before seen in human history, leading to increased business, cultural, and personal connectivity.

Commercial aviation blossomed significantly in the second half of the twentieth century. Between 1960 and 2005, passenger travel on commercial flights worldwide, represented by the product of revenue passengers and kilometers traveled (RPK), increased by an average rate of 7.9% per year.[3] This was significantly higher than the average Gross Domestic Product (GDP) growth rate over the same timeframe,[4,5] as illustrated in Figure 1. Despite slowdowns after the terrorist attacks of September 11, 2001 and the worldwide economic downturn in 2009, the growth of commercial aviation

is expected to recover and resume growth at a rapid pace over the next few decades. Both Airbus and Boeing predict that global passenger traffic will maintain an average growth rate of around 5% per year (based on revenue passenger kilometer (RPK)) over the next 20 years, resulting in a need for between 25,000 and 30,000 new aircraft deliveries by 2027.[6,7] The Terminal Area Forecast produced by the Federal Aviation Administration predicts recovery to an average annual growth domestically of 2.4% and 2.9% for traffic at large and medium hub airports between 2011 and 2031.[8] These numbers also suggest corresponding growth in airport and airspace capacity.

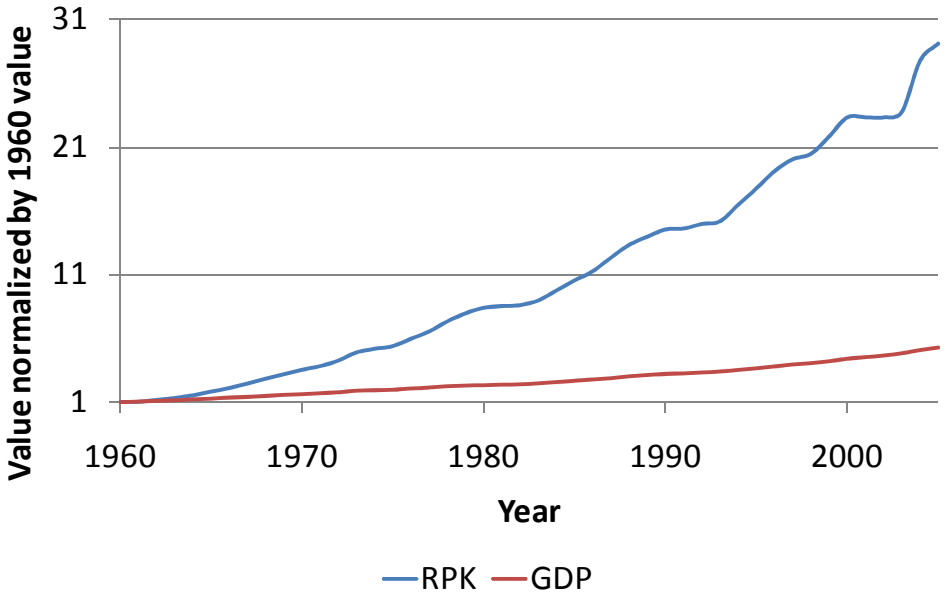

Figure 1. Growth in RPK and GDP, 1960-2005.

Like other large multinational industries, commercial aviation can potentially impact the global environment negatively if these impacts are not mitigated. One common avenue of exposure of the general public to potential negative impacts occurs in the form of aircraft noise during the landing and takeoff cycle (LTO). In addition to noise, the emission of pollutants, which include nitrous oxides (NO_x), sulfurous oxides (SO_x), carbon monoxide (CO), and carbon dioxide (CO_2), occurs during both in the terminal

area below 3000ft altitude, where local air quality in the vicinity of airports may be effected, and en route operations, which may have a deeper impact on the atmosphere and global climate change because of the high altitudes at which they are generated.[9] Despite the great strides that have been made to improve environmental performance of individual aircraft at the vehicle level, growth in demand and operations has resulted in ever increasing values for aggregate fuel burn and emissions of commercial aviation.[10] Although commercial aviation only represents a small portion of anthropogenic impacts on the environment, e.g. contributing about 2% of all CO_2 emissions, its growth in relation to other contributing industries, combined with the pursuit of alternative fuels and the aforementioned fact that much of its emissions occur at high altitudes, makes this a problem of significant interest for the international community.[11]

Regulating Aviation

Because of the desire to mitigate potential negative impacts of aviation, various regulatory bodies have been formed both domestically and internationally to evaluate policy and implement environmental goals for aviation. The International Civil Aviation Organization (ICAO) is a United Nations (UN) body founded in 1945 that governs standards for aviation worldwide. ICAO's environmental efforts are coordinated by the Committee on Aviation Environmental Protection (CAEP). Founded in 1983, CAEP replaced two previously existing organizations within ICAO: the Committee on Aircraft Noise and the Committee on Aircraft Engine Emissions[12]. CAEP consists of 22 member nations and 12 observers representing other nations and organizational bodies that have an interest in its work, such as the International Coordinating Council of Aerospace Industries Associations (ICCAIA), the International Air Transport Association (IATA),

and the World Meteorological Organization.[13] CAEP meets on a roughly triennial basis, as illustrated in Table 1. It is interesting to note that each individual meeting between 1986 and 2007 tended to focus on implementing either new NO_x or noise standards. The major contributing factor to this independence in the past has been a lack of capability to simultaneously capture interdependencies between noise and emissions when evaluating the impact of such policy scenarios, which requires enhancement of current tools.[14]

Table 1. Schedule of past CAEP meetings, 1986-2007.

Meeting	Year	NOx Standard	Noise Standard
CAEP/1	1986	Initial NOx Standard Set (Chapter 2)	Initial Noise Standard Set (Chapter 2)
CAEP/2	1991	New NOx Standard 20% below CAEP/1	No Reductions
CAEP/3	1995	New NOx Standard 16% below CAEP/2	No Reductions
CAEP/4	1998	No Reductions	New Noise Standard (Chapter 3) Specified Regulations by Aircraft Weight
CAEP/5	2001	No Reductions	New noise standard (Chapter 4) Cumulutive 10EPNLdB below Chapter 3
CAEP/6	2004	New NOx Standard 12% below CAEP/3	No Reductions
CAEP/7	2007	No Reductions	No Reductions

At the CAEP/6 meeting in 2004, members reached three key conclusions:[15]

- Recognition that implementing steps to achieve effective mitigation of environmental impacts will require consideration of potential interdependencies between environmental metrics.
- Selection of three environmental goals to focus on: limitation of local air quality emissions, greenhouse gas emissions, and noise exposure.
- Development of analytical tools and supporting databases that can capture interdependencies between these goals and be used to optimize the environmental benefit of mitigation measures would greatly facilitate progress toward these goals.

The regulations and certification standards that are developed by ICAO and CAEP are called Standards and Recommended Practices (SARPs), and these are passed on to the ICAO member nations, who are each individually responsible for their implementation. Within the United States, the Environmental Protection Agency (EPA) is responsible for enacting SARPs related to emissions by establishing emissions standards, and the Federal Aviation Administration (FAA) is responsible for enacting SARPs related to aircraft noise, and enforcing standards for both noise and emissions.[16] NO_x and other emissions regulations are often first imposed on aircraft or engines that are being newly certified. An example of how engine NO_x levels are calculated for certification is given in ICAO Annex 16 to the Convention on International Civil Aviation[17].

Because of the limitations that new environmental limits may have on the growth of the National Aerospace System (NAS), the Congress and President George Bush enacted the VISION 100 – Century of Aviation Reauthorization Act in 2003. Under the terms of this act, another entity known as the Joint Planning and Development Office (JPDO) was established to coordinate the efforts of the Department of Transportation, Department of Commerce, Department of Homeland Security, Department of Defense, National Aeronautics and Space Administration (NASA), FAA, and the White House Office of Science and Technology Policy in the development of the Next Generation Air Transportation System (NextGen).[18] The broad goal of JPDO and NextGen is to enable the NAS to meet the levels of demand and environmental stringencies forecast for the year 2025. Options to meet increasingly stringent regulations while accommodating the projected growth in commercial aviation include application of new technologies and changes in operational procedures. Like CAEP, the tasks undertaken by JPDO include

traffic/demand forecasting, technology identification and evaluation, and environmental modeling.

Modeling Aviation

Each of the entities mentioned here conduct different analyses of the commercial fleet with different goals and different fidelity requirements, which is illustrated in Figure 2.

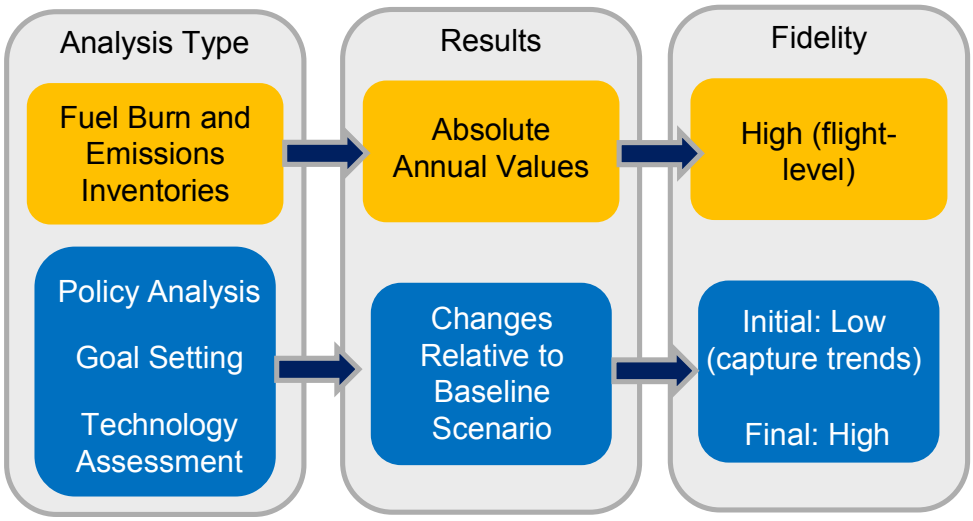

Figure 2. Overview of analyses.

One example of a high fidelity commercial fleet analysis is a fuel burn and emissions inventory study. Over the past few decades, a number of attempts have been made to quantify the entire global emissions inventory of commercial aviation, including efforts by NASA/Boeing in 1976, 1984, 1992, and the European Abatement of Nuisances Caused by Air Transport (ANCAT) working group for the European Commission for 1992, which represented the first estimates of "good quality" global emissions.[19,20] By law, the FAA conducts detailed fuel burn and emissions inventories on an annual basis, which requires absolute values and high fidelity results. Since 2000, the FAA has generated emissions inventories at the airport, regional, and global levels, a process that includes approximately 30 million flights per year (through 2005), individual segments within each flight, over

20,000 individual aircraft (roughly 200 unique aircraft types), and for which outputs may be tracked over each square degree of the Earth's surface for each hour of the year.[21] Needless to say, this requires the ability to track billions of pieces of data.[22] Each flight over the course of a year must be tracked, meaning that its fuel burn and emissions are recorded to produce a global sum of emissions and fuel burn.[23] A typical process for emissions inventory analysis using SAGE is given by Fleming[24] and in the SAGE Technical Manual.[25] While this is a task that must be completed as described to generate inventory data required by law, the large amounts of data that must be computed make this ill-suited for rapid decision making capabilities.

For other studies, such as examining the impact of different policies or goals, and the potential impact of new technologies, the desired result is the determination of how these changes may improve or degrade a given baseline scenario. Examples of these studies include scenario analysis by JPDO[26,27] and conducting cost-benefit analyses by CAEP.[28] In these cases, a tradeoff to initially use lower fidelity modeling with faster run times (on the order of minutes) that make simplifying assumptions to quickly evaluate a large number of future scenarios may be acceptable. Lower fidelity modeling could then be followed by selection of the most interesting scenarios to reanalyze with the higher fidelity modeling, which is more time consuming, but also more accurate.

An example of a simplified analysis may be found in the simplification of inventory modeling conducted by the FAA. Instead of modeling the roughly 20,000 unique aircraft ("tail numbers") in the commercial fleet, they may be grouped into unique engine/airframe combinations, of which there are just over 400, as illustrated in Figure 3.

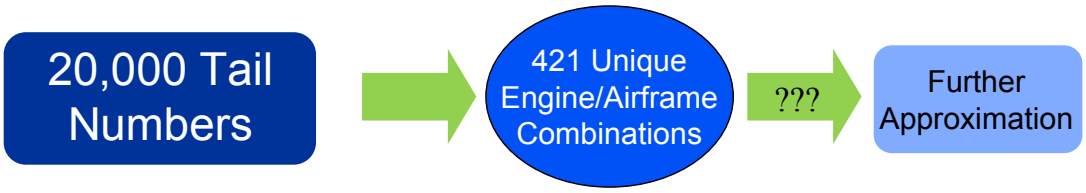

Figure 3. Simplifying the commercial fleet.

Assessment of this approach has found it to be within 5% of the actual fleet's fuel burn and emissions results.[29] However, developing hundreds of physics-based models with the fidelity to actually model the impact of technology infusion for each engine and airframe combination in the fleet would be impractical due to time and computing constraints. These current approaches to fleet analysis are still not well suited to rapid scenario evaluation and decision making. Thus, new techniques to represent the entire fleet using only a limited number of existing aircraft models spanning the seat classes of the fleet must be examined. One outstanding issue that will be addressed by this work is whether even further approximation may be conducted to generate fleet-level results faster and within a reasonable accuracy.

In order for an approximate technique to be useful for evaluating future fleet scenarios, it must be able to capture the influential factors that contribute to fleet evolution. The major contributing factors may be grouped into changes to the fleet mix, changes to operations, and application of new technologies,[30] as illustrated in Figure 4. Fleet mix changes include anything that changes the composition of the fleet, such as retirement of old aircraft, replacement by new aircraft, and growth with new aircraft. Operational changes include variations in the frequencies of flights at different distances, changes to routing structure, which includes airline scheduling, and procedural changes, such as continuous descent approach or reduced vertical separation. The latter two groups, routing and procedures, are highly specialized fields[31,32,33] and will not be addressed by this current

work, but do present challenges for future work. Finally, technology infusion may impact the fleet in the form of retrofits on currently in-production vehicles or in the form of newly design platforms.

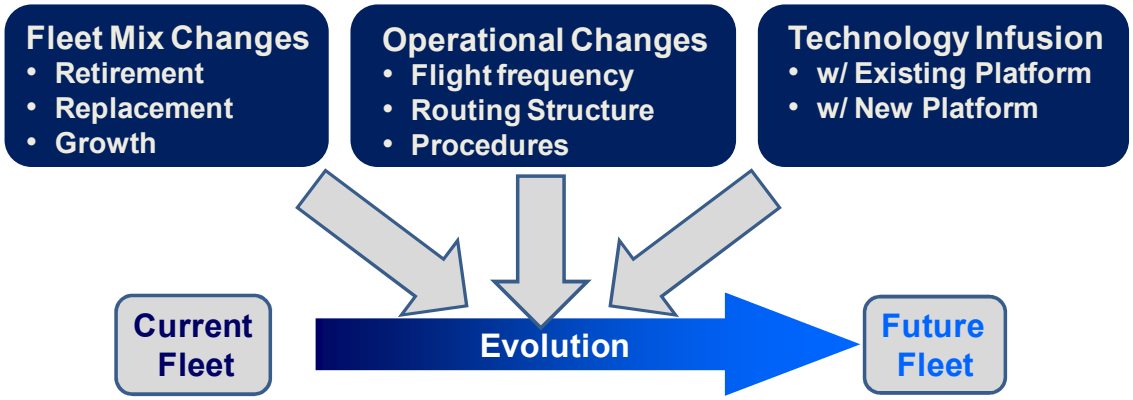

Figure 4. Factors that influence fleet evolution.

The challenge that arises in modeling new technologies is that physical interdependencies may emerge between environmental metrics. The following examples illustrate this point: high temperatures and pressures generated by advanced compressors within the engine can lead to more efficient fuel burn, but will often result in higher NO_x production.[9] Contrastingly, the opposite may occur if an advanced combustor is installed in an engine to reduce NO_x production, resulting in a fuel burn penalty. The impact of a technology that may be used in meeting stringencies should therefore be evaluated in a modeling environment with the fidelity to capture these types of interdependencies; otherwise the unforeseen negative impacts of technologies would be overlooked when evaluating potential future policy scenarios. However, the existing analytical tools and approaches used by CAEP, which will be described in more detail later in this document, require enhancement to model the impact of technologies at the vehicle level and roll them up to analyze their costs and benefits relative to proposed mitigation actions at the fleet level.[34] As a result, the process of relating changes in aircraft technologies to the

fleet level is derived through the input of ICCAIA members, who determine levels of impacts based on expert input rather than transparent modeling.[20,35]

In examining the elements discussed in this chapter thus far, a number of needs emerge. Broadly speaking, a need exists for a rapid screening capability to determine the impact of aircraft-level technologies at the fleet level to better inform aviation policy decisions. This type of decision making includes the scenario analyses that are conducted by JPDO and cost-benefit analyses that are conducted by CAEP, which would benefit from having the capability to rapidly evaluate large numbers of potential future scenarios. Developing such a capability presents a number of corresponding needs in itself:

- Categorization of the fleet of aircraft in an efficient manner that facilitates reduction of computational complexity
- Capturing the impact of changes in operational variations that represent potential future scenarios
- Translating the impact of technologies at the aircraft level to the corresponding effects at the fleet level using appropriate modeling and simulation (M&S)

Meeting these needs ties back into enhancing current techniques by enabling regulatory bodies and organizations to conduct tradeoffs between large numbers of different policy scenarios involving environmental goals and evolving the fleet to meet them.

1.2 Research Objectives

The objectives of the work conducted here arise out of the needs outlined in the previous section. The main objective is to address these needs by developing a methodology that captures the physical interdependencies that emerge at the aircraft level

when evaluating different future fleet scenarios, does so quickly, and does so within acceptable bounds of accuracy when compared to current global fleet analysis methods. It must consider the many different engine and airframe combinations acting in concert at the aggregate fleet level.

To capture aircraft performance and interdependencies that may emerge at the aircraft-level, an aircraft-level M&S tool must be selected. Such a tool must be of the appropriate fidelity level to capture the physics involved in this problem. At the same time, a similarly appropriate fleet-level M&S tool must be selected that can be used to roll up these aircraft-level results to fleet-level performance.

At the same time, the fleet itself must be examined to identify how to analyze it in the most efficient way. Different groups, such as CAEP or JPDO, have an interest in capturing fleet performance. As will be discussed in Chapter 2, they can employ different definitions to categorize the entire commercial fleet to simplify analysis. An investigation must be undertaken to define a consistent approach to generalize the fleet that will enable effective use of the appropriate M&S tools for the creation of a methodology in this work. Just as different entities characterize the fleet differently, they also employ different forecasts of the fleet. Thus, this method must be flexible enough to incorporate future variations in fleet mix and composition. The impact of retirement, replacement, growth on operations that represent potential fleet scenarios may then be captured.

Finally, the methodology must capture the interdependencies that emerge as aircraft respond to technology adoption to meet new stringencies. Vehicles within the fleet that are likely to receive a technology upgrades must be identified. However, creating a detailed, physics-based M&S representation of every aircraft in the fleet that will respond

to technology application is not a practical approach because of its resource intensive nature. Thus, in the absence of models for each aircraft, the method must be able to capture technology impacts rapidly and in a physics-based manner.

If these objectives are met, a methodology would exist to rapidly inform decision makers of the effect of a wide range of policy scenarios involving commercial fleet operations and technologies. It will provide a standard approach for physically quantifying aircraft-level impacts that are propagated to fleet analysis for different operations and technology sets. This will result in the ability to quantify policy scenario trade-offs in a more transparent fashion than current expert driven approaches.

1.3 Research Questions

The introduction and motivation presented above allows observations to be made on current methods fleet analysis and gaps in their capabilities. The first observation to be addressed is that developing individual physics-based vehicle models for every aircraft in the commercial fleet is an extremely cost prohibitive process, requiring months to construct, validate, and parameterize a model for any given engine/airframe combination. This leads to the first research question:

> **Research Question 1**: How can aggregate fuel burn and NO_x metrics be rapidly captured for a fleet of aircraft with a set of reference operations in a physics-based manner?

This research question focuses on addressing fuel burn and emissions. Although the ability to capture noise will be important for the development of a complete fleet evaluation approach, acoustics is such a complex area that a surrogate approach for noise would alone be a worthy doctoral thesis topic. The current work will focus on fuel burn

and emissions and form the building blocks to incrementally add a noise analysis capability later. The importance of using physics-based modeling for capturing a set of reference operations may not seem obvious, but it will allow the approaches developed to potentially be used to capture technology implementation at the aircraft level.

The second observation to be addressed is that the commercial fleet is constantly undergoing changes in makeup because of retirement of out-of-production aircraft, replacement or growth with in-production aircraft, and changes to frequency of flights over different flight distances. Any approach meant to capture fleet performance must also be able to capture these changes. The surrogate fleet approaches, which may each be able to generate a representation of the reference fleet for baseline operations, must next be compared according to their ability to capture these variations in operations. This leads into the second research question:

Research Question 2: How can the acceptability of surrogate fleet approaches be evaluated over wide variations of operations representing future fleet scenarios?

Because the future is uncertain, any surrogate fleet approach must have the flexibility to incorporate results from different forecasts, representing potential scenarios. In order to test this flexibility, results for surrogate fleet approaches must be rapidly evaluated over a wide range of operations.

The third observation is that current technology assessment is either conducted on a single aircraft or relies on post-processing approaches that lack transparency. An approach is needed that can transparently capture the impact of technologies on a fleet of aircraft. The next research question arises out of the need to address this point.

Research Question 3: How can the acceptability of surrogate fleet approaches be evaluated for implementation of technologies at the aircraft-level?

As previously stated, a limited number of calibrated physics-based vehicle models exist or may be created within a reasonable amount of time. However, capturing the impact of technologies on each individual aircraft of the entire fleet would require a larger number of physics-based models. Here again, acceptability is defined relative to current fleet evaluation methods and is further discussed in Chapters 3 and 4.

CHAPTER II

LITERATURE REVIEW

In order to develop a rapid analysis capability for aviation environmental impacts, a number of elements must be reviewed. First, the methods used by various entities to characterize the current fleet and forecast the behavior of the fleet in the future, which include flight frequency and aircraft mix, will be described. Characterizing the current fleet is an important first step toward modeling fleet behavior. In terms of the forecasting elements, the goal of this work is not to develop new forecasting techniques; however, the impact of future forecasts is important because they provide bounds of operations within which any rapid analysis capability would be expected to be accurate. Next, previous efforts to model and assess the fleet will be reviewed along with their accuracy, execution time, and ability to capture a number of essential elements of fleet evolution as shown previously in Figure 4: changes in fleet mix, operations, and technology levels. Chapter 1 touched on some of these methods in the context of framing the motivation for this problem; this chapter will focus more on how they incorporate tools, fleet characterization, and technology modeling. Finally, the different analytical and design tools that are available for use in aircraft and fleet M&S are surveyed for applicability in this work based on needs that have been identified.

2.1 Fleet Categorization and Forecasting

Categorizing the fleet includes a careful examination of the fleet's makeup and determination of what aircraft types may be grouped together for analysis based on capability, operations, geometry, etc. As stated in Chapter 1, the categorization of the

fleet plays a critical role in modeling the fleet because it defines the scope of the fleet that is to be studied and may provide avenues to segment the fleet for effective M&S. Forecasting then studies changes to the fleet's makeup and operational distributions over time, which provides insight to the bounds within which M&S should be accurate.

2.1.1 Categorizing Aviation

Commercial aviation is comprised of many different elements: aircraft, operators, passengers, air traffic control, regulators, airports, engine/airframe manufacturers, and fuel suppliers. All together these components make up the NAS. As such, it is an oft cited example of a complex system of systems, the characterization of which is an extremely challenging task.[36] It is further complicated when there is a need or desire to investigate the impact of future growth and application of technologies within the NAS.

Because CAEP, FAA, JPDO, aircraft manufacturers, and other entities are interested in capturing the performance of the fleet, both in the present day and in the form of predictions of future performance, they conduct studies to forecast how fleet composition changes over time due to retirement, replacement, and growth. Each entity takes a slightly different perspective when compiling forecasts. All of the forecasts generally include broad assumptions for economic growth, passenger demand prediction, retirement curves, and capacity assumptions, all of which are used to predict growth for various seat classes. An example of differences in how the different entities categorize aircraft into seat classes is illustrated in Figure 5, using data from their respective forecasts.[7,37,38] The seat classes used between entities are inconsistent, underscoring the need to be able to indentify an approach to categorize the fleet into groups for effective modeling in a way that is consistent and repeatable.

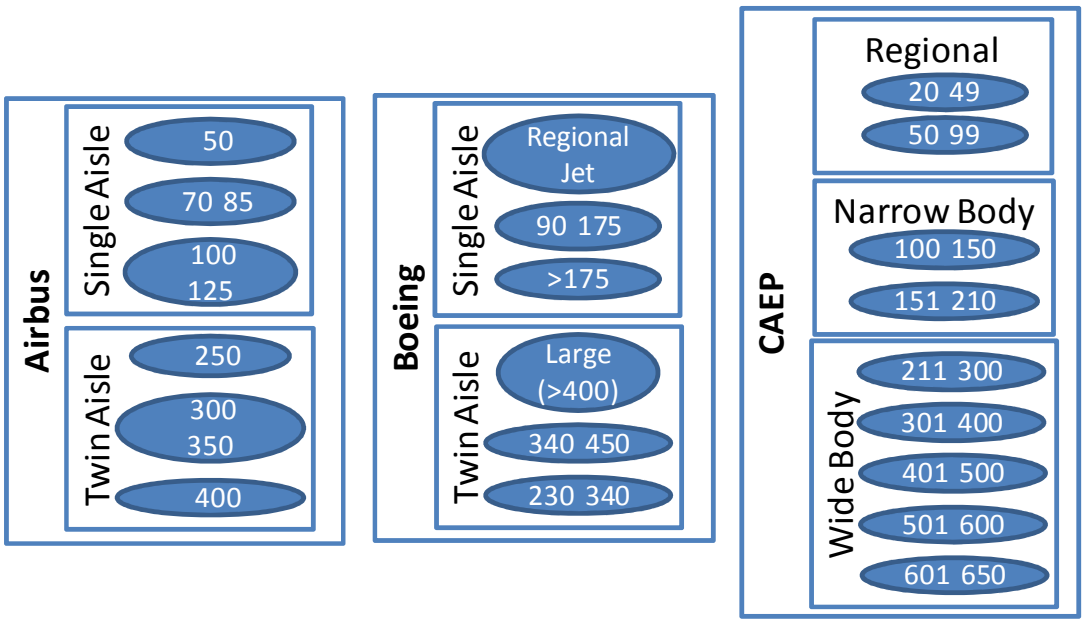

Figure 5. Characterization of seat classes by various forecasting entities.

These traditional methods of categorizing the entire fleet of passenger aircraft worldwide center around a single metric, i.e. the number of passengers that may be carried. However, use of a single metric may not create strong enough distinctions with which to definitively assign vehicles into groups. Because number of passengers may change based on internal seating configuration, the potential exists for an aircraft to shift groups (as listed in Figure 5) without having significantly changed performance. A few examples of aircraft that may fall between groups as a result are:

- The Embraer ERJ-190 may range from 94 to 114 passengers[39]
- The Airbus A321 may range from 185-220 passengers[40]
- The Boeing 767-300ER may range from 218-350 passengers[41]

Avoiding such lack of distinction between groups may potentially be avoided by grouping based on multiple metrics, which will be described in Chapter 3.

Once the fleet has been characterized into groups, manufacturers and regulators forecast growth within each group. Aviation forecasts created by the FAA, assisted by the

MITRE Corporation, focus on aircraft types sold to domestic carriers and flown on domestic flights within the U.S., and may therefore not encompass all aircraft types worldwide. The most recent FAA forecast[8] makes predictions through 2030. Retirement is modeled by retiring passenger aircraft after 25 years, with half of all retiring passenger aircraft being converted to freighters, which are assumed to never retire. In order to determine the distribution of aircraft types among new replacement and growth aircraft, MITRE examines actual fleet counts, adds firm order data, subtracts retirements, adds back in cargo conversions, then projects the gap relative to the FAA forecast. The gap for each MITRE category is then split 50/50 between new orders for Airbus/Boeing aircraft or Bombardier/Embraer aircraft.

Each year, Airbus and Boeing present forecasts of traffic demand and fleet mix by aircraft size for all regions of the world[6,7]. Predictions for demand are created based on current economic trends, for which numbers are given, but with little other justification. Forecast documents do not specify how aircraft are retired or how new aircraft are distributed by manufacturer, and final results do not include specific vehicle models.

An example of a recent CAEP forecast[38] was one that was prepared for the CAEP/6 meetings, and CAEP/7 extrapolated growth based on the CAEP/6 forecast, which provides analysis of air travel demand at different points in time up to 2020. Demand is given for 22 route groups, both domestic and international, by seat class. The forecast predicts worldwide aviation fleet composition based on the demand growth plus retirements, load factor, utilization, frequency/capacity, and aircraft model assignment assumptions. Retirements are handled by the empirical curves that were created to accurately capture the retirement of aircraft that are currently in-service. In order to

assign growth aircraft to different seat classes, the CAEP fleet forecast considers the existing schedule, operations frequency, average stage length, aircraft size, and utilization, and allocates passenger growth in each route group and seat class to a representative aircraft, which includes an associated operations and frequency set in each category. Specific vehicle models are then assigned in each category based on equal manufacturer/aircraft splits, as specified in IP13.[42]

A summary of the results for growth for each of the four discussed forecasts is presented in Figure 6.[6,7,8,38] The variation in results highlights the contribution that differences in baseline, assumptions, and scope have on the results of each study. While the goal of this current work is not to develop an independent forecast, the methodology that is presented must be flexible enough to incorporate elements of different forecasts as necessary and, as mentioned before, handle these distinctions consistently.

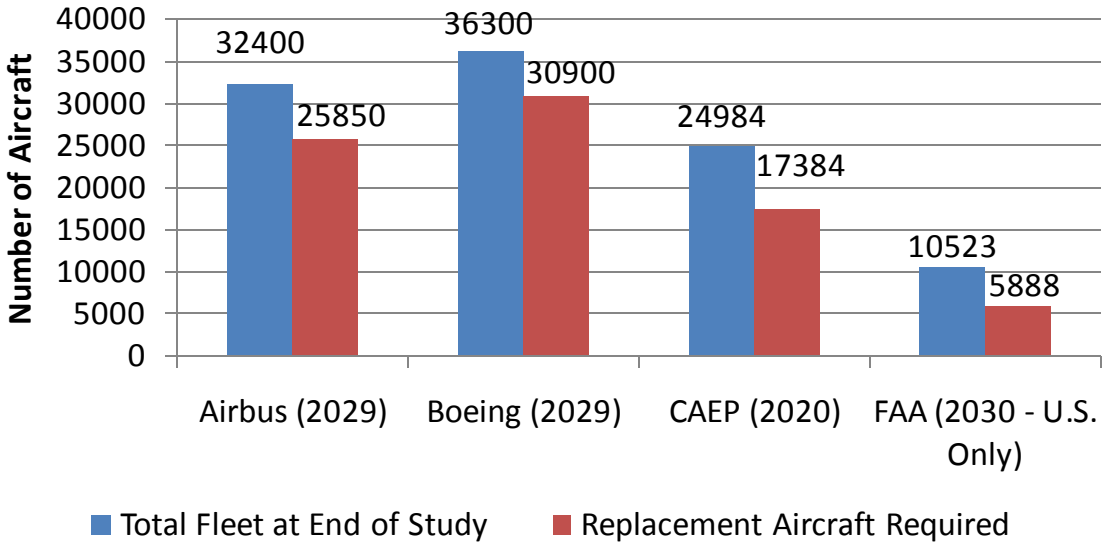

Figure 6. Fleet forecast growth results.

While Figure 6 shows the total number of aircraft to be added to the fleet at the end of each study, it does not illustrate fleet composition changes over time. To show an example of this aspect of a forecast, Figure 7 is provided from Boeing's Current Market

Outlook. As can be seen, at different points in time, the proportion of the fleet made up of retained aircraft, replacement aircraft, and growth aircraft changes. Comprehensive evaluation of the environmental impacts of aviation requires the ability to capture the performance of the aircraft that compose the commercial fleet; therefore any methodology meant to emulate fleet behaviors must be able to capture changes of the fleet's aircraft mix over time.

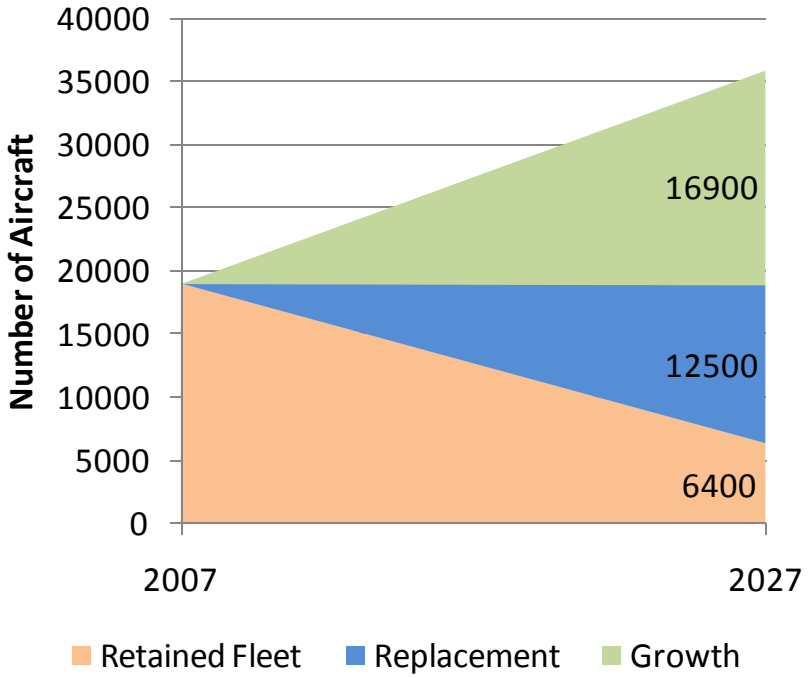

Figure 7. Fleet composition over time.

The Boeing data in Figure 7 can be further broken down by production status, as shown by the notional plot in Figure 8. The numbers of in-service aircraft that are out of production will tend to drop off based on retirement assumptions. In-service aircraft that are still in production will still be added to the fleet, but over time they will be replaced by aircraft that have undergone technology infusion. Over a longer timeframe, revolutionary aircraft, which may include concepts like geared turbofans, ducted fans, or truss braced wings, may enter the fleet. In addition to being able to capture the nuances of

Figure 7 in the form of retained aircraft, replacement aircraft, and growth, a methodology meant to model the fleet must also be able to capture the in-production status and applicability of technology to different aircraft in the fleet, as illustrated in Figure 8.

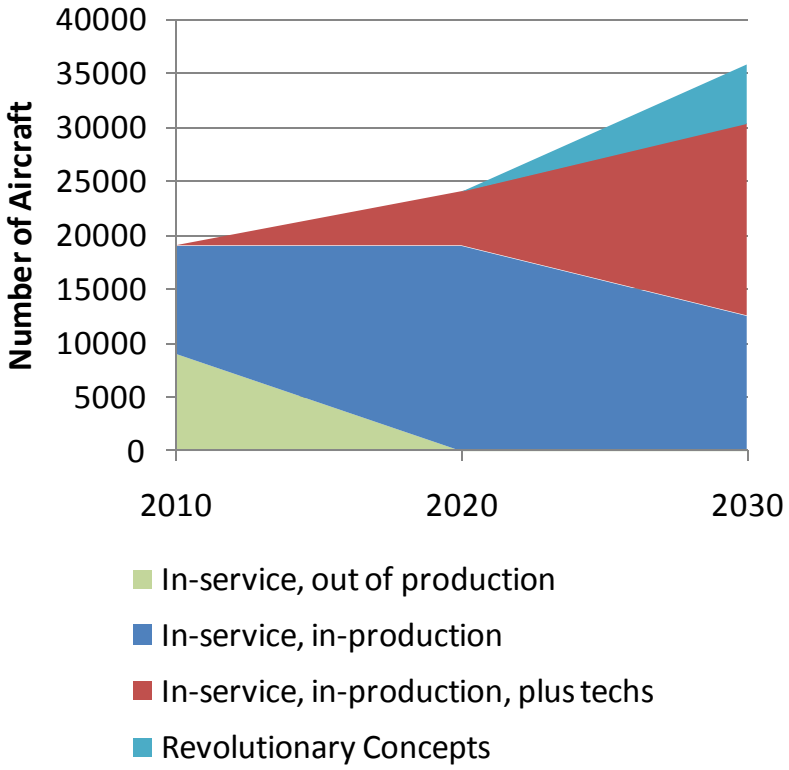

Figure 8. Notional breakdown of fleet by production status.

2.1.2 Modeling Operations

As noted in the description of the FAA and CAEP forecasting processes, different aircraft types, in terms of aircraft size or capability, must be assigned to different operations. In the real world, the assignment of aircraft to operations is carried out by airlines or other operators. Any attempt to model this assignment will involve simplifications or assumptions, which mean that the modeling will not equal reality. In the context of this work, it is not necessarily of greatest importance to create a more accurate forecast model. Future operational forecasts are dependent on economic and

schedule strategies for each individual airline, and the generation of model for such market dynamics is beyond the scope of this work. However, it is important to be able to incorporate different assumptions other entities may have, and to have enough understanding of what is lost when going from real world behavior to modeling capability.

When replacement occurs, newly produced aircraft replace retiring aircraft. Growth occurs as the number of aircraft in the fleet increases with introduction of newly produced aircraft. As manufacturers produce new engines and aircraft that must meet increasingly stringent standards, it is these in-production engines and aircraft that will receive a technology infusion or retrofit.[43] Categorizing aircraft that will receive technology means that the production status of each aircraft must be determined. One source for this information is the ICAO Growth and Replacements database;[44] however this is not publically available. Other, more encompassing aircraft databases exist that do not contain production status, but do represent a larger number of aircraft. These include the BACK and Campbell Hill databases of aircraft registrations, which are also not publically available. Identifying in-production aircraft from publically available sources may be done by searching manufacturers' websites or media outlets for reports of recent or pending deliveries.[45,46,47,48] An assumption is made that, while these delivery reports may not contain all in-service aircraft, they will contain all in-production aircraft. Therefore, any aircraft that are not identified in such a search are considered to be out of production. The specific aircraft that were used in this work and the manner in which they have been characterized is elaborated upon in Chapter 3.

Another available database is the movements database, which contains data for every commercial flight from over a certain period of time.[49] Each entry contains data for each flight's operator, flight number, departure and arrival airports, flight distance, aircraft type, engine code, and seat class. For a single day of flights, there can be on the order of 64,000 entries. For CAEP studies, data for flights from six different weeks in 2006 has been used to capture baseline fleet behavior for forecasting purposes, and the aircraft mix from this set of flights is illustrated in Figure 9. The aircraft mix for the entire year of flights from 2005 and 2006 is shown in Figure 10. As can be seen when comparing Figure 9 to Figure 10, the six weeks of flights is a good approximation for the proportion of operations undertaken over the course of an entire year, and these values do not change significantly over one single year.

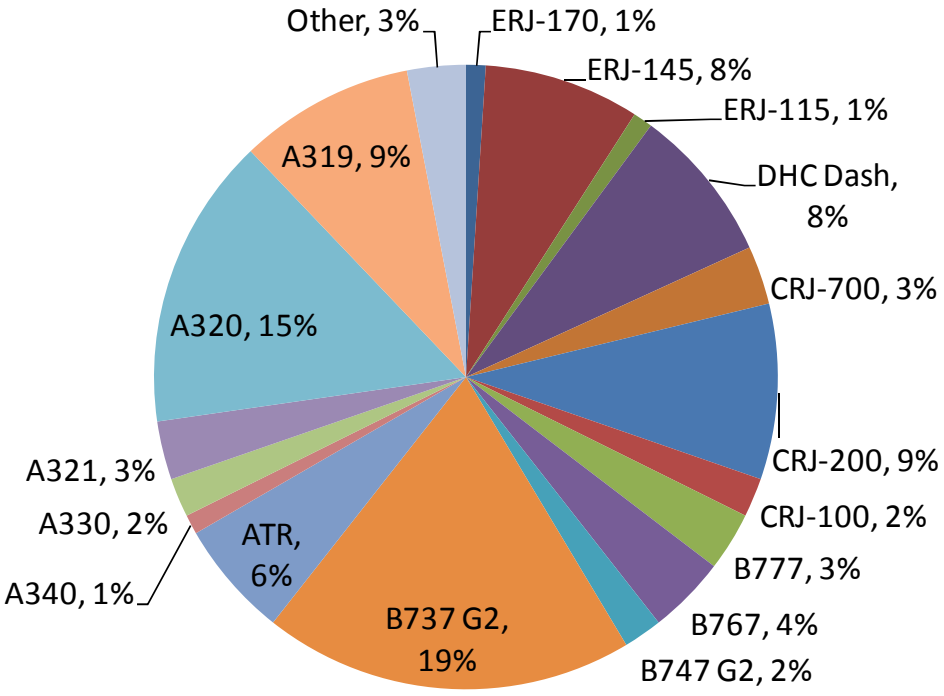

Figure 9. Aircraft mix for six weeks of 2006 flights.

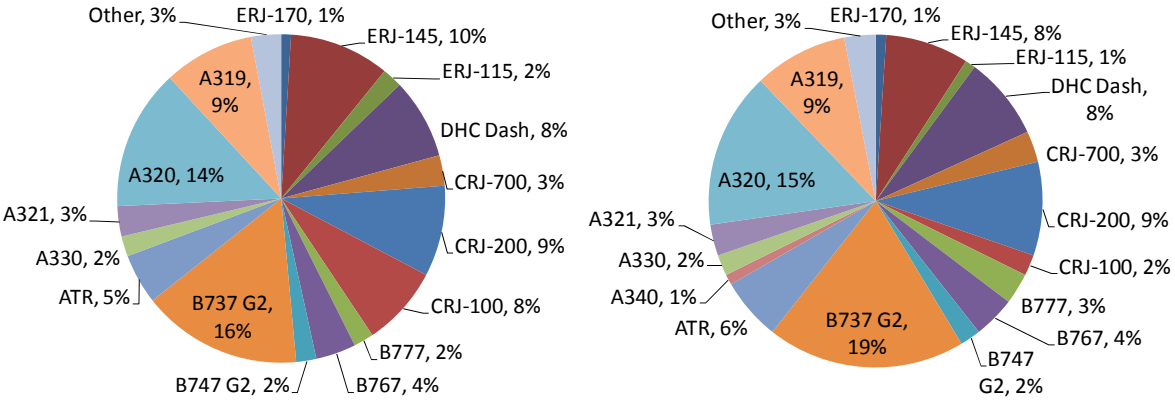

Figure 10. Aircraft mix for year of 2005 (left) and 2006 flights (right).

Identifying the aircraft mix of the current day fleet is indispensable to fleet analysis. However, going beyond the current day requires understanding how different entities create forecasts, and learning how to implement those forecast in a rapid tool for use in evaluating future scenarios. The process used by CAEP for fleet generation and forecasting, manifested in a tool known as the Fleet and Operations Module (FOM), is the most documented process that is available for review. The framework of the process is described in CAEP/8 Working Paper 10.[50]

The development process involved creating a basic input operational database, processing the database based on FESG input, modeling noise contours, and computation of the population exposed to noise contours. Additionally, because they were the basis of proposed noise stringency policy options, substantial development and validation resources were devoted to the software required for modeling fleet and operations changes according to input provided by other CAEP working groups, which became known as the FOM.[51] Using the FOM with the FESG forecast allows the user to predict the behavior of future operations. Forecasted growth rates for the different route groups lead to designation of aircraft to certain operations based on their size, as capacity

constraints are approached for each route. This designation is stage length dependent; therefore the output of the FESG forecasting process is a forecast based on route groups, which give an indication of origin and destination airports (OD pairs), stage length, which is a range of flight distance, and aircraft passenger capacity.

Required inputs to the FOM include a baseline set of operations and the retirement and replacement schedules that define the attrition rate of the each aircraft in the fleet. The first step in the FOM process involves calculating the number of operations that were designated as retired during the prior forecast period based on retirement curves designating percentage surviving aircraft as a function of age. Then for each forecast period, future demand may be predicted using the FESG forecast and is segmented by route group, stage length, and seat class. New operations may then be derived for each OD pair by seat class by using the forecasted demand and defined retirement schedule. Once operations are updated for retirement and new operations growth is estimated using the forecast, the seat class demand leads into designation of actual aircraft types for each route according to the replacement schedule, which allocates operations to specific aircraft based on the forecast year, aircraft size, and OD pair distance. The new operations may be assigned to either a current day aircraft from the existing forecast database, or to user defined aircraft according to the replacement schedule. Once completed, the baseline set of operations may be updated to reflect operations for the desired forecast year, and this new operations set is then used as the base set for the next forecast period. This process is repeated tens of thousands of times for every forecast period, resulting in a fairly high computational cost.

Some of the challenges in capturing the real life impact of different fleet forecasts arise due to unexpected changes that may occur over the duration of the forecast. Airlines often mix aircraft with different passenger and payload capabilities for operations based on traffic demand, impacting how aircraft retirement and replacement are represented in forecasts. One particular example of this is in how the Boeing 757 family of aircraft is treated. This family of aircraft has more payload capacity than the 737-700, 737-800, and 737-900, but less capacity than the Boeing 777 family, which represent the spectrum of aircraft that may replace it. When conducting long term fleet planning, an uncertainty of how airlines will handle replacement of 757s impacts the number of 737, 777, or later model aircraft that could be included in future forecasts.[52] Additionally, although the forecasts themselves are impacted by economics in the form of passenger and traffic demand predictions, economics may also result in changes to the number of available aircraft in any given year, as airlines may decide to delay retirement of old aircraft or delivery of new aircraft.[53] Thus, a need exists to not only be able to allow the study of different forecasts, but also allow stakeholders to vary them on the fly and quickly visualize their resulting impacts on policy scenarios.

In order to speed up the computationally expensive FOM, a faster forecasting method known as the surrogate operations approach has been developed that makes several simplifying assumptions in order to reduce computational time.[51] To reduce the number of OD pairs under consideration, the six weeks of 2006 flights described above and illustrated in Figure 9 is used to represent the entire year's operations. OD pairs are also aggregated so that departure and arrival airports are treated the same (i.e., LAX to JFK is the same as JFK to LAX). This halves the number of OD pairs, but is only a valid

assumptions when considering fuel burn and emissions, as future analyses which deal with noise considerations will require the ability to handle origin and destination airports individually. The number of operations types can be further reduced trimming the number of aircraft bins, which refer to the level of granularity of aircraft information contained in the model. For surrogate operations, the number of aircraft bins was reduced by grouping vehicles into aircraft families. Finally, new retirement curves were created for these aircraft families as a function of the original survival rate curves.

Categorization of the fleet is not only a significant contributor to how physics-based aircraft models may be applied in a fleet-level context to generate surrogate fleets, but it will also impact how any surrogate fleet will feed into forecasting tools that may be used for policy analysis. The importance of fleet categorization and forecasting in the current work is not trivial. Although the scope of this work does not fall within forecasting, the nature of forecasting must still be considered in the development and demonstration of the surrogate fleet methodology.

2.2 Approaches to Fleet Modeling

In recent years, there have been a several different efforts to evaluate fleet environmental metrics and/or assess the impact of technologies on the fleet. While described in the context of providing motivation in Chapter 1, they will be elaborated upon here to highlight elements of their implementation that may be useful in relation to developing hypotheses to answer the research questions.

2.2.1 CAEP Stringency Policy Analysis

The typical CAEP approach to emissions stringency analysis is presented in the AEDT NO_x Demonstration Analysis[54] and by Kirby et al,[34] was touched on in Chapter 1, and will be summarized here. A stringency analysis is the determination of the impact of a reduction in current emissions or noise standards on the commercial fleet, including the need for and impact of any new technology response, which is considered any modification required to comply with a new standard. All necessary disciplinary analyses for the stringency are performed in a manner similar to the method employed by working and support groups within CAEP composed of manufacturers and operators

The first step to be performed is to define aircraft seat classes, which includes the determination of number of aircraft by seat class and which engine families, including derated engine variants, are on each vehicle. The next step is to define potential stringency levels, or reductions from current standards, as well as potential future implementation dates. Following this, all engines that do not meet the new standards are documented, and for the purpose of the stringency analysis, all engines within a family are considered to require a technology response if any of the engines within the family fail.

The selection and determination of the qualitative impact of a technology response on a "failed" engine family is performed by the CAEP working groups. Existing technologies that have been proven to meet the stringency options are selected, and the required modifications to the engines in question are assumed for a reference certification condition and documented. These assumptions include possible performance degradation and costs of implementation, but lack the details of how the technology will be implemented on the engines, instead relying on post processing.

In order to assess the impact of technology response over time, a forecast must be generated from a baseline operations set. The baseline operations data for this demonstration were derived by combining a full year's worth of information from both the International Official Airline Guide (IOAG) schedule database and radar track data from the Enhanced Traffic Management System (ETMS), augmenting this with aircraft specific data from the Campbell Hill database, and processing them into an operations set that is FESG compatible format that may be used with FOM. The FOM is used, as described earlier, to provide estimates for future passenger and cargo demand, fleet operations evolution, and aircraft movements to create a forecast of the future fleet 20 to 30 years past the study start date.

Each aircraft determined to be in the current and future fleet is flown in the Aviation Environmental Design Tool (AEDT), which will be described in Section 2.4, for their associated movements, and, in the case of a NO_x stringency, terminal area and total missions emissions are calculated and aggregated for the entire fleet. A technology response would be required for each vehicle that did not meet the stringency level, necessitating the creation of a new replacement aircraft. Each potential technology response is applied through post-processing and is assigned a corresponding fuel burn penalty and cost as determined by ICCAIA, and so each stringency scenario can be evaluated by CAEP in terms of its environmental benefits and its costs.

The precursor of the replacement aircraft fleet databases is a "best practices" aircraft database that was used in conducting inventory analysis and noise stringency analysis with MAGENTA under CAEP/5. After modifications were made to use this database for emissions, the necessary future technology level designations required to meet each

stringency level were assigned to aircraft in it, resulting in multiple databases of replacement aircraft and engines, one for each of six potential stringency scenarios representing 5%, 10%, 15%, 20%, 25%, and 30% reductions in NO_x emissions below the CAEP/4 standard. Assigning a technology level involves selection of technologies to apply and then modifying performance based on NO_x improvement, fuel burn degradation, and cost as estimated by ICCAIA. The technology levels that end up being used are described in IP13 as follows:

- TL1 – Minor change that does not require a complete engine recertification.

  Such a change would be small enough that effects of the changes to the engine are within regulatory limits. Generally, a minor change would improve NO_x emissions by less than 5 percent.

- TL2 – Major change with scaled proven technology

  An already developed technology is applied within the existing combustor envelope, requiring full engine certification program and aircraft flight. NO_x reductions at this level might typically be in the 5 to 15 percent range.

- TL5 Category – New technology acquisition

  When a stringency level cannot be met with a TL2 change, the solution requires that a new technology be found or developed. The amount of development and certification that would be needed to introduce a new technology on an existing engine will vary depending on the characteristics of the new technology, leading to a further refinement of this category into TL5A and TL5B changes below.

  - TL5A – New technology using current industry best practice

Acquisition of available, existing technology by manufacturers of the noncompliant engine is necessary. Thus the TL5A solution becomes the equivalent of a TL2 solution plus the addition of applied research costs for technology acquisition.

- TL5B – New Technology (Beyond Current Best)

  No engine manufacturer has demonstrated technology that meets the required NO_x stringency for a noncompliant engine, and extensive technology acquisition with a full engine development program are required.

Assumptions around fuel burn degradation impact both the amount of fuel burned by a particular aircraft and a corresponding increase in takeoff gross weight that is required for the aircraft to maintain the same range/payload capability. Assumptions are made for how fuel burn penalties may be applied for each solution. The only fuel burn penalty that is applied to a technology level solution is for the TL5B solution, which requires development of new, unknown technologies, in contrast to examples of known technologies in this category like staged combustor engine designs. Fuel burn may be increased in staged combustors due to higher pressure loss (either the result of a longer or wider combustor configuration, or an intentional increase in pressure drop to improve fuel-air mixing) and/or non-standard temperature profile at the combustor exit, particularly during partial staging, that can affect turbine efficiency and cooling flow requirements. Empirical data available to ICCAIA from airline operations using dual annular combustor (DAC) engines confirm an increase in fuel consumption of approximately 2%. Thus, based on the performance of existing DAC designs, a two percent fuel penalty was assumed to be

a reasonable for TL5B solutions, while the TL1 through TL5A solutions are assumed to have no penalty. The reasoning behind this is that projected TL1 and TL5A solutions are assumed by the engine manufacturers to have fuel burn characteristics equivalent to currently implemented combustor technologies, which is justified by current performance of such in-service technologies, shown to have essentially 100% fuel efficiency. [42]

Technologies were assigned only to those engines in the "best practices" database that were designated as being in-production by FESG as part of the data used for the NO_x stringency work under CAEP/6, which assumes that it is not technically feasible and/or economically viable to retrofit older engines, even if they may currently be in service. The appropriate technology level was assigned to any in-production engine if its characteristic NO_x value was greater than the allowable NO_x value. The assigned technology levels are specific to the stringency level such that more advanced technologies were assigned to the higher stringency levels. Therefore, of the six replacement databases created for this work for each stringency level, the replacement database with the highest stringency level contained the most technology level assignments and the most advanced technologies. An example of how technology levels may be assigned to engine types is given in Table 2 for in-production CFM56 engine types.

Table 2. Example of technology level assignment.[42]

Engine Family	Combustor	NOx Reduction Level					
		-5%	-10%	-15%	-20%	-25%	-30%
CFM56-5B	SAC		TL2	TL5A	TL5A	TL5B	TL5B
CFM56-5B	DAC II			TL5A	TL5A	TL5B	TL5B
CFM56-5C	SAC	TL1	TL2	TL5A	TL5A	TL5B	TL5B
CFM56-7B	SAC	TL2	TL2	TL5B	TL5B	TL5B	TL5B
CFM56-7B	DAC II			TL5B	TL5B	TL5B	TL5B

As can be seen, there are only a few cases where an engine type is able to meet a stringency level without the application of technology, and most of these are engines with DACs, which already perform better than the singular annular combustors (SAC) in terms of NO_x. The majority of required technology levels are of the TL5B solution, which implies the development and application of new technologies. As will be shown in Chapter 3, studying the potential impacts of new technologies is best handled through a transparent, physics-based approach that is capable of addressing the uncertainties inherent to the process, which is not well captured by a post-processing approach.

Over the course of this approach, a number of elements emerged that reflect steps that are necessary in the development of a methodology to address the research questions. The commercial fleet was categorized based on seat class, investigated for technology adoption based on the ability of aircraft to meet stringencies over the course of future operations, and had that technology adoption modeled based on assumptions for amount of improvement necessary to meet stringencies. These elements point back to needs to for effective fleet categorization, modeling the fleet over variations in operations, and being able to capture the impact of aircraft technologies on fleet-level impacts transparently and in a physics-based manner.

2.2.2 Approach to Stringency Analysis Using EDS

Because of the drawbacks of the CAEP stringency analysis approach, Kirby et al. have proposed an approach to stringency analysis that leverages the physics-based capabilities of the Environmental Design Space (EDS) and AEDT,[34] which will be described in Sections 2.3 and 2.4. This approach will be summarized here. The parametric nature of EDS enables the development of physics-based trade spaces for each seat class

for which an EDS reference vehicle will be developed, and each trade space is represented by surrogate models of a given engine/airframe architecture to allow the exploration of the vehicle interdependencies under a given policy scenario. In order to be compatible for use within CAEP, an EDS model has already been developed for five of the seat classes defined by CAEP. The first step for trade space development would be to define the technologies to be implemented and the specific input variables and ranges that would be required to model them in EDS, analogous to how ICCAIA defines technology responses for CAEP. The difference is that the CAEP technology responses are applied through post-processing, which may not capture relevant interdependent effects. In contrast to a post-processing approach, the EDS approach determines the impact of technologies on input variables, and then allows the resulting changes in performance to fall out, with any resulting interdependencies having been captured in the physics-based modeling, rather than having been assumed as it is in the CAEP approach.

In order to demonstrate this approach and compare it to the traditional approach outlined above, a simplified notional stringency analysis was conducted by Kirby and Barros for a single aisle medium range and a twin aisle long-range aircraft and will be summarized here.[34] For each of these aircraft, a representative EDS model was used as the reference vehicle. For the purpose of generating surrogate models, a design of experiments (DOE) is executed on the EDS reference vehicle for each seat class included in the study to represent the technology response, and data to be regressed are compiled. The generated surrogates must then be validated for predictive capability and may then be used to investigate whether predicted trends are physical. Once the surrogates have been prepared, each technology response scenario can be investigated and constrained

based on limits that may exist and vary between seat classes. For each scenario, a series of candidate vehicles may be identified within the trade space that represents the Pareto efficient points to minimize NO_x, fuel burn, and cumulative noise within each seat class. A solution is defined to be a Pareto point if it is impossible to improve in one objective without degrading in another.[55] Because the Pareto points have been identified with the surrogate methods, each of them must be confirmed for optimality with the EDS. Engineering judgment may then be employed to down select to a single, best technology response solution for each stringency scenario. Finally, EDS generates the required input coefficients required by AEDT for fleet analysis.

This notional stringency analysis assumed levels of NO_x reduction from 0% to 20%, in increments of 5%, relative to the baseline aircraft rather than for specific CAEP certification levels. Additionally, the input values representing combustor modifications for the EDS approach to achieve any particular levels of NO_x reduction were estimates and have not been justified through interaction with technology developers, and the fleet analysis is based only on the two aircraft over a limited number of representative flight distances and frequencies for a single day of flights. Although this is not realistic for full fleet modeling, this assumption allows a comparison to be quickly made between the two approaches, which are likely to differ because the fuel burn and NO_x performance throughout the representative flights for the EDS approach are a result of the physical interdependencies captured in the modeling as opposed to the traditional CAEP post-processing approach.

The five NO_x reduction scenarios that were evaluated in this demonstration are provided in Table 3, along with their analogues in the traditional technology response.

The first difference to note between the two approaches is that in the traditional response, the fuel burn penalty is always assumed to be a constant value across the fleet and is determined in advance. In the EDS approach, it is allowed to be solved for as a result of physics-based modeling. Another difference may be noted in scenarios 3 through 5, and it is that the higher fidelity EDS approach allows for a technology response to be captured in multiple implementations with different implications for how much various engine components may be varied, in this case distinguishing between the combustor, fan, low pressure combustor, or even a redesign of the entire engine. In such cases, NO_x reduction does not take assumed values as it would in the tradition approach, and is instead a result of the physics based analysis. This type of fidelity is not available in a post-processing approach.

Table 3. Comparison of stringency scenarios.

Scenario #	% NOx Reduction	Traditional Technology Response	EDS Qualitative Response
1	5%	Slight combustor modification which has no other penalty (TL1)	Slight combustor modification, no changes in the rest of the engine
2	10%	Slight to moderate combustor modification and has no other penalty (TL2)	Moderate combustor modification, no changes in the rest of the engine
3	15%	Moderate combustor modification which results in a constant fuel burn penalty (TL5)	Aggressive combustor modification, no changes in the rest of the engine
4	20%	Aggressive combustor modification which results in a constant fuel burn penalty (TL5)	Fan and low pressure spool redesign with a moderate combustor modification, no changes in the rest of the engine
5	20%	Same as Scenario #4	New engine design with a moderate combustor modification

For the EDS technology response, each level of NO_x reduction was specified as a constraint for each candidate vehicle in the DOE runs, and the interdependencies that

result are quantified as a fall out. For the purpose of this demonstration, the combustor modifications were simulated in EDS by relating a reduction in NO_x to an assumed reduction in combustor efficiency and an assumed increase in pressure drop across the combustor relative to the reference vehicle, which would otherwise be provided through a higher fidelity physics-based chemical analysis or expert input. A key example of the importance of capturing interdependencies is that the typical CAEP approach assumes a reduction on the certification levels of NO_x and a corresponding fuel burn increase for the actual flight, while EDS applies the response on the functional form of NO_x such that if the cycle performance changes, the resulting NO_x for a given flight may not meet the percent reduction due to the NO_x interdependencies with fuel flow.

To assess each scenario on the pseudo fleet, AEDT was used to quantify the technology responses for the flight distances of three airport OD pairs selected to correspond to typical great circle flight distances of the two aircraft. For comparison's sake, the EDS single-aisle and large twin-aisle AEDT representations served as baselines for the traditional CAEP approach for a technology response. The pseudo fleet metrics for comparison include NO_x emissions and fuel burn below 3000 ft altitude and total mission NO_x emission and fuel burn. For each flight distance, AEDT flew the single-aisle or large twin-aisle missions, and the resulting NO_x and fuel burn data were extracted, multiplied by the associated number of flights, and summed for the fleet.

For EDS scenarios #1 through #3, only a single execution of EDS and AEDT was required along with the generation of fleet-level metrics described above. For scenarios #4 and #5, a comprehensive space exploration of 10,000 combinations within specified ranges of input variables relevant to the NO_x reduction technologies was conducted, and

surrogate models were generated for the fleet-level metrics of interest. Each combination of parameters for the trade space that resulted in violations of vehicle-specific constraints for results from the surrogate models were eliminated from further consideration. From the remaining combinations in the trade space, the NO_x, fuel burn, and cumulative noise were used as objectives to determine the Pareto frontier points. Each of the Pareto frontier points were reevaluated with EDS to confirm their metric values, and detailed information regarding the engine designs was extracted. Engineering judgment was utilized to down select to a single technology response for each stringency level and included consideration of the number of component stages, fan tip speed, spool speeds, and mechanical limits necessary for each potential design.

The results of the EDS stringency approach were very different from that of the traditional CAEP approach. Generally, the CAEP approach tended to underestimate the fuel burn penalty necessary to meet NO_x stringency. In addition, it was apparent from the EDS results that the change in total mission fuel burn and fuel burn below 3000 ft is not constant, which the CAEP approach assumes. These results underscore the importance of being able to capture interdependencies to correctly identify trends for future policy scenarios.

In contrast with the CAEP approach, modifying input coefficients to capture the change in performance that is associated with a technology response to the engine and aircraft improves upon the post-processing approach described previously. However, the calibration time in linking an EDS model with an AEDT model is very high and, as discovered during this study, the calibration itself is complicated by different assumptions that may exist between these two codes when modeling the reference aircraft, mainly due

to varying levels of fidelity in capturing the physics involved. Another issue is that although this approach addresses the drawbacks of the CAEP approach, it does have a drawback of its own: it reduces each seat class to a single vehicle without consideration how well that vehicle may capture the aggregate performance of each vehicle in the seat class.

In this approach, more elements emerged that reflect steps that are necessary in the development of a methodology to address the research questions. Aircraft were modeled using both aircraft and fleet-level modeling tools, they were evaluated over a limited number of operations, and were modeled using technology mapped to aircraft-level inputs. These elements point back to needs to for effective fleet categorization to make use of physics-based tools efficiently, rapidly modeling the fleet over a large number of variations in operations, and identifying how to map technologies onto a large number of aircraft in a physics-based manner.

2.2.3 JPDO NextGen Environmental Evaluation

As discussed in Chapter 1, JPDO has been tasked with evaluating what technologies and operational improvements will be critical to allow the sustained growth of commercial aviation over the next few decades while at the same time reducing its environmental impact. Within JPDO, the Interagency Portfolio and Systems Analysis Division has been given the role of analyzing potential future scenarios to assess overall system performance quantified in the form of various environmental metrics. An example of a typical study of the impact of future technologies and operations is given by Graham et al., and will be summarized here.[56]

The three primary goals of the sample study were to determine the impacts of NextGen on fuel burn, emissions, and noise; to determine how these impacts compare with potential environmental stringencies; and, finally, to determine the relative contributions of engine/airframe technology improvements versus procedural and avionics improvements to NextGen's ability to provide environmental sustainability. Evaluation of these goals is reliant upon the characterization of NextGen's future operational improvements, engine/airframe technology improvements, and future demand patterns.

The approach undertaken in the sample study is comprised of scenario development; and modeling of noise, air-quality, and fuel efficiency impacts. Future scenario development is dictated by traffic demand, the available capacity, projected fleet composition, and projected environmental technology improvements. Future demand was modeled using the FAA's Terminal Area Forecast, but also takes into account capacity constraints, which were assumed to improve through changes in infrastructure and operations including new runway construction, converging approaches, reduced separation restrictions, trajectory-based management, and continuous descent arrival. In order to evolve the fleet for future NextGen scenarios, a 2007-2035 U.S. fleet forecast developed by the MITRE Corporation was used as a reference starting point. Every aircraft with an entry in the schedule and the fleet forecast was assigned to its appropriate seat class, and then the proportion of each aircraft in each seat class was used to define the fleet mix for the forecast used to generate the NextGen scenario. The environmental impact of technologies beyond the current state of the art for fuel burn, emissions, and noise was modeled through post-processing by assuming that each of these areas is

aggressively improved based on two potential technology suites, termed N+1 and N+2, which correspond to corners of NASA's Subsonic Fixed Wing (SFW) Project trade space and are provided in Table 4.[57] Values are assumed for the technology suites implemented in this study and applied at the aircraft level, and no attempt is made to capture the physics of their implementation.[58]

Table 4. Technology assumptions corresponding to NASA SFW goals.

Metric	N+1	N+2
Fuel Burn	-33%	-40%
LTO NOx (relative to CAEP/6 Limit)	-60%	-75%
Noise (below Stage 4)	-32 db	-42 db

While these technologies were applied at the aircraft level, methods to generate fleet level fuel burn, emissions, and noise were required. Two approaches were used in this study to model fleet-level noise impacts. For the 34 major airports, which are considered to be Operational Evolution Partnership airports in the continental U.S., an approach requiring detailed LTO trajectories is used to capture the total number of population exposed to noise. Because such trajectories are often unavailable for smaller secondary airports, a contour-area approach is used to determine the area exposed to certain noise levels around these airports. Emissions modeling at the fleet-level is conducted by relating the value of fuel burned in each of several operational segments to estimate the mass of different pollutants that are generated, which may include CO, HC, NO_x, and SO_x. Below an altitude of 3000 feet, engine-specific ICAO fuel-flow rates and emissions indices are applied, while at altitudes exceeding 3000 feet, aircraft-specific fuel-flow factors are applied from the Base of Aircraft Data (BADA),[59] a set of coefficients developed by Eurocontrol to represent simplified performance characteristics of a large number of commercial aircraft.

Six potential future scenarios were evaluated in this study. The first was a 2006 baseline scenario representing domestic flights on a single day in July 2006. The next two were 2025 scenarios that include no new technologies or operational improvements, but have slightly different capacity limits. The next fourth and fifth cases were 2025 scenarios with operational improvements, but the fifth one also included N+1 technologies. The final one was a 2025 scenario that included operational improvements and N+2 technologies. Evaluating each one of these scenarios required the above approaches to be applied to roughly 100,000 flights each for the single day of flights.

As with the previous two approaches described, elements emerge that reflect steps that are necessary in the development of a methodology to address the research questions. Again, the commercial fleet was first categorized based on seat class, then evaluated for technology adoption over the course of five different scenarios. These elements point back to a need for effective fleet categorization, followed by a means through which to model the fleet rapidly over a large number variations in operations. This approach also points to potential future work that may be conducted in the form of contrasting the impact of aircraft technologies versus procedural improvements on fleet-level metrics.

2.2.4 Summary of Previous Approaches

As each approach was reviewed, elements were identified that are necessary in the development of a methodology to address the research questions. These approaches tended to categorize the commercial fleet simply based on seat class. When technology adoption was modeled based on post-processing assumptions, component-level impacts could not be considered. When aircraft were modeled using both aircraft and fleet-level modeling tools, component-level impacts were considered, but the fleet was evaluated over a limited

number of operations. These elements point back to needs to for effective fleet categorization to make use of physics-based tools efficiently, the ability to model the fleet over variations in operations, and the ability to capture the impact of aircraft technologies on fleet-level metrics transparently and in a physics-based manner.

The approaches that have been outlined above also lead into characteristics that an M&S environment chosen for this work should have. These characteristics are:

- Maturity/Acceptance
- Transparency
- Models component-level physics (for vehicle modeling)
- Translates vehicle-level results into fleet-level metrics (for fleet modeling)

The first two points relate to the applications that the methodology developed here could be considered for in the future. The approaches that have been examined are all real world problems; therefore they require codes that are mature, meaning in this case that they have gone through validation and acceptance by an organization like the FAA or CAEP. The next characteristic is transparency, which in the context of M&S for this work means that the tools used are not proprietary, and the data used is publically available. The next two points relate to capabilities that are desired for the methodology that is developed here to enhance previous approaches. In order to capture technology implementation without post-processing, the tools selected must be able to capture the physics of component-level impacts at the vehicle level and roll them up to the fleet level. At the vehicle level, this means that the tools must have the appropriate fidelity to independently generate performance results as a function of engine/airframe component parameters. At the fleet level, the tools must demonstrate the ability to translate vehicle-

level results that may change as a result of technology adoption into fleet-level metrics. These characteristics provide a filter of requirements through which the M&S tools must be viewed as they are surveyed in the next section.

2.3 Modeling and Simulation

Because the problem of interest necessitates capturing the impact of interdependencies that are rolled up at the fleet-level, any potential M&S environment must include accurate, physics-based computations for performance and emissions at the vehicle level and subsequently link them to fleet-level values, which include the effect of operations. Both vehicle-level and fleet-level modeling tools are required for this. A high-level framework of what such an M&S environment would need to look like is provided in Figure 11.

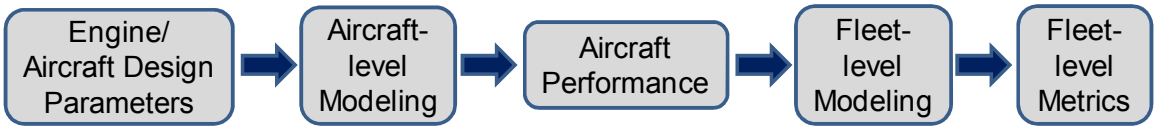

Figure 11. M&S framework.

In broad terms, the M&S environment should be able to link engine and aircraft design parameters up to fleet-level metrics. This reflects the desire to be able to enhance the capabilities of the NO_x demonstration problem in Section 2.2.1 by considering the physics of aircraft-level improvements. The intermediate tools for aircraft-level and fleet-level modeling will be described in this section.

Here it is important to define what is meant by the term physics-based. Because there is a desire to model the impact of aircraft technologies, doing so in a physics-based manner in the context of this work means that the physical inputs that are impacted by a new technology must be modeled at the level of engine and airframe components. A

comprehensive outline of what may be needed from a physics-based vehicle-level modeling tool in the context of developing fleet-level outputs was created during the development of an environmental design process by the Transportation Research Board of the National Academies.[60] In addition to evaluating aircraft that are representative of present-day designs and technology levels, the aircraft-level tool should have the ability to predict performance for future aircraft designs at the aircraft-level as a function of aircraft design parameters. The aircraft-level tool should be able to interact seamlessly with the fleet-level modeling tool by generating required inputs as a function of aircraft performance, whether for a present-day or future design. By providing such capabilities, the fleet-level assessment of future aircraft configurations and technology levels not in existence today is enabled.

2.3.1 Aircraft-level Modeling

In order to capture technology related interdependencies as a function of component-level input parameters, aircraft-level modeling must be multidisciplinary and consider the engine thermodynamic cycle, engine mechanical design, and aircraft. A sample of inputs and results for these disciplines is provided in Figure 12. Results for certain disciplinary analyses may serve as inputs to others. For example, an engine deck generated in engine cycle analysis may end up being used for aircraft design. Such usage will be described throughout this section. There are a number of tools that exist that can perform some or all of these analyses in an integrated fashion, and they will be reviewed in the following subsections.

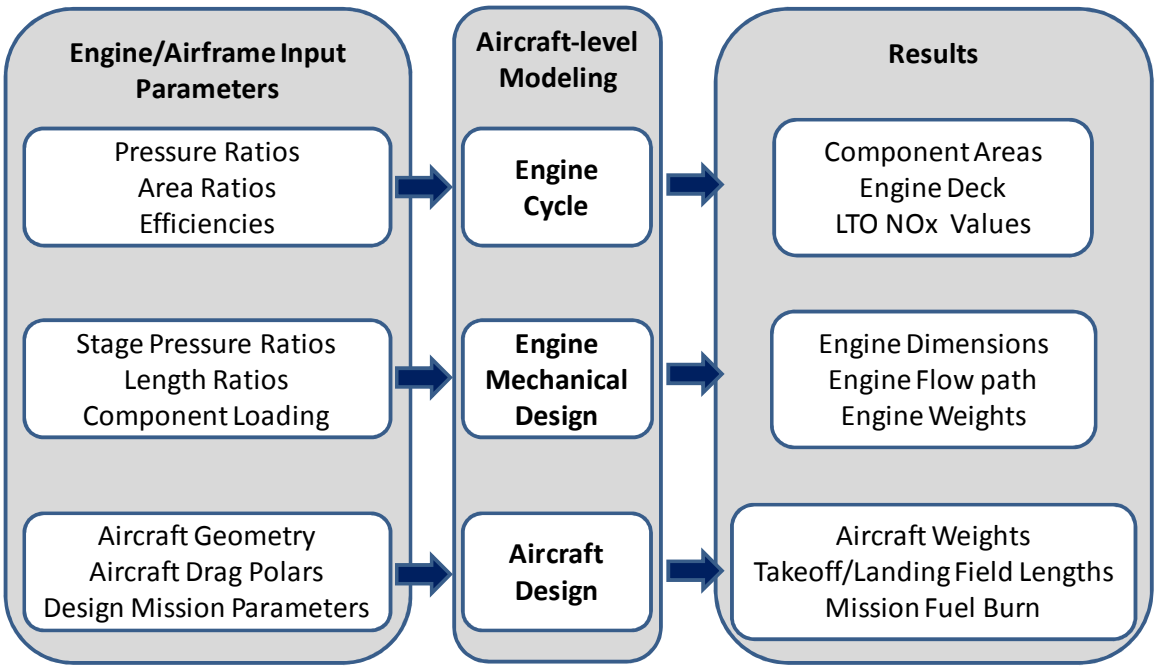

Figure 12. Aircraft-level M&S.

Defining the thermodynamic cycle of the engine is a critical first step in vehicle modeling. Because vehicle modeling is multidisciplinary in nature, the results of thermodynamic engine simulation program will feed forward and impact the results of the other disciplinary analyses. From the perspective of this study, results of interest that will be passed forward are those required to match the performance of aircraft in the current fleet, as well as those that indicate a technology level, whether current day or in the future. Examples of the former include inlet and exit areas of engine components, which are used for flow path design, while examples of the latter include temperatures and pressure ratios, which are used for materials selection and impact engine weight. The engine deck, which relates thrust and fuel consumption to altitude, Mach number, and throttle setting for aircraft sizing and mission analysis. The level of fidelity required to provide these types of outputs is relatively high, going beyond merely using a scaled engine deck and instead employing thermodynamic cycle analysis or design codes.

Mechanical design of the gas turbine engine is another critical part of vehicle preliminary design because it provides engine weight and dimensions, which are used for vehicle sizing and have significant impacts on fuel burn, vehicle gross weight, and cost. As with the engine cycle, the tools that are used for this function must be capable of matching engine parameters with those that are in use on aircraft of the current day fleet, which may include known quantities like blade radii or component length to width ratios, as well as those used in technology infused scenarios, such as turbine loadings or blade and vane solidity values. Just as the fidelity required for the engine cycle went beyond scaling engine decks, so too does the fidelity required for mechanical design go beyond scaling engine size.

In order to complete vehicle modeling, the engine design, generally represented in the form of an engine deck, which represents the thermodynamic cycle, and engine dimensions and weight, which represent the mechanical design, must be coupled with an airframe design for analysis. Analogous to the engine thermodynamic case and the mechanical design case, care must be taken to choose an airframe design code that has the fidelity to be capable of representing current day aircraft as well as future technology aircraft, so that any interdependencies that emerge may be rolled up to the fleet level. The primary available tools for modeling aircraft in such a physics-based manner will be reviewed here.

Tools have been developed to conduct conceptual or preliminary analysis of an aircraft design within each of the disciplines mentioned above. In order to complete a multidisciplinary conceptual or preliminary design of a complete aircraft design, these disciplines must be linked together. If such linkages are created with a user in the loop,

the outputs from each would need to be identified for each included code and then manually input to the next code, which would be time consuming and error prone, underscoring the need for an integrated environment. Proprietary tools for cycle analysis exist, such as GE Aviation's Preliminary Robust Design Analysis Tool for Evaluating customer Return (PREDATER)[61], but these tools are not available for this work and would not represent a transparent solution because of their proprietary nature. Other, more simplified tools have been developed from basic principles for use in academia as teaching. A good example of this is ONX/OFFX developed by Mattingly, which are well-suited to examining trends in early conceptual design; however tools of this nature may not be well suited to this work because of their simplified fidelity at the component level, e.g. they do not account for real gas effects, which can have a significant impact on performance.[62] Another program with a similar level of fidelity is ENGINE MAKER, developed with a limited number of inputs by Rolls-Royce for screening experiments in early conceptual design, but this is a proprietary code.[63]

Once an integrated environment has been created, it must be able to be calibrated to match the published characteristics of a variety of existing aircraft, verifying that the environment is able to capture the physics of different engine and airframe combinations. Public domain data is preferred over proprietary data, because transparency is a priority for the methodology developed here to be broadly applicable to future work. Using company specific codes or data could potentially bias the results, which would preclude their use in regulatory policy making.[64] This environment must be able to produce any set of inputs that may be required for fleet level analysis, which will be described in the next section. Because the inputs and analysis of such a unified environment would include

engine cycle parameters, engine mechanical design parameters, aircraft geometry and weights, and operations, parametric studies that capture the interdependencies between environmental metrics would be enabled.

An example of the framework of such an environment is given in Figure 13, adapted from Deluis's dissertation.[14]

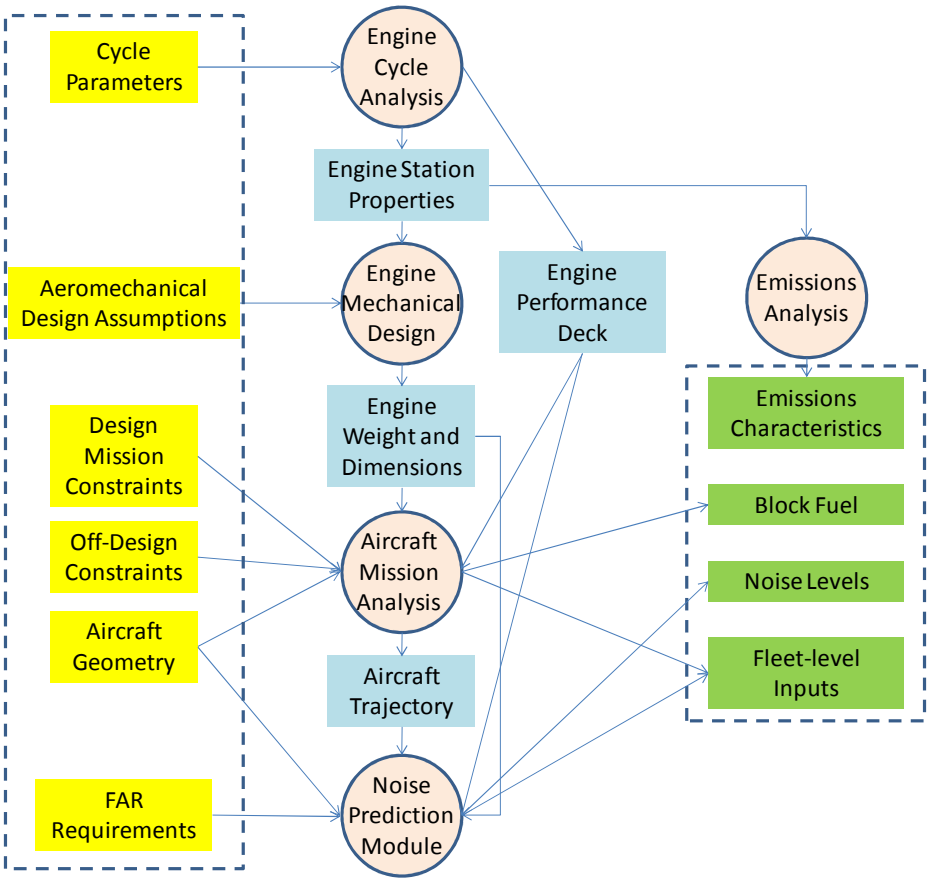

Figure 13. Aircraft M&S environment framework.

The engine thermodynamic cycle is the first code within the environment that is executed. Its results are passed to the engine mechanical design code, emissions correlation, and aircraft noise code in the form of flow station properties, and to the aircraft sizing code in the form of an engine performance deck. The engine mechanical design code passes its outputs to the aircraft sizing module and the aircraft noise module

in the form of engine dimensions and weight. The aircraft sizing code would pass aircraft trajectory information to the aircraft noise code.

There are a number of integrated engine/airframe design environments that are being developed that will be examined here. Generally, they tend to focus on one single aspect of the desired environmental framework, e.g. noise, trajectory, or aerodynamics. In the UK, Caves et al, at the Loughborough University, have developed an integrated environment that focuses on calculating noise characteristics of an aircraft during conceptual design.[65] The Integrated Wing Aerospace Technology Validation Programme (IWATVP), also centered in the UK but led by Airbus, has been set up to develop an integrated environment to assess different short to medium term wing technologies that could impact fuel consumption, noise, and emissions.[66] Within IWATVP, RETIVO (Requirements, Technology Impact, and Value Optimisation), a software package developed by QinetiQ with very basic and often empirically based modules for calculating engine and airframe performance, is used to model and assess the impact of technologies.[67] These tools, which are still under development, are not considered mature in the context of this work. Four tools that are more mature in terms of having been used by manufacturers and regulatory bodies will be described in the remainder of this section: Technology Evaluator, Piano, Pacelab and EDS.

2.3.1.1 Technology Evaluator

Technology Evaluator is a process being developed by Airbus, Snecma, and Rolls Royce that is meant to assess the environmental impacts of noise mitigation technologies in the context of other aircraft design constraints and economics as applied to a broad range of conventional engine/aircraft configurations.[68] Developed as part of the

European Commission's Clean Sky research and technology initiative, Technology Evaluator is meant to relate results of aircraft technology demonstrators up to quantitative environmental and economic impact at the fleet level.[69] The structure of the proposed methodology is depicted in Figure 14.

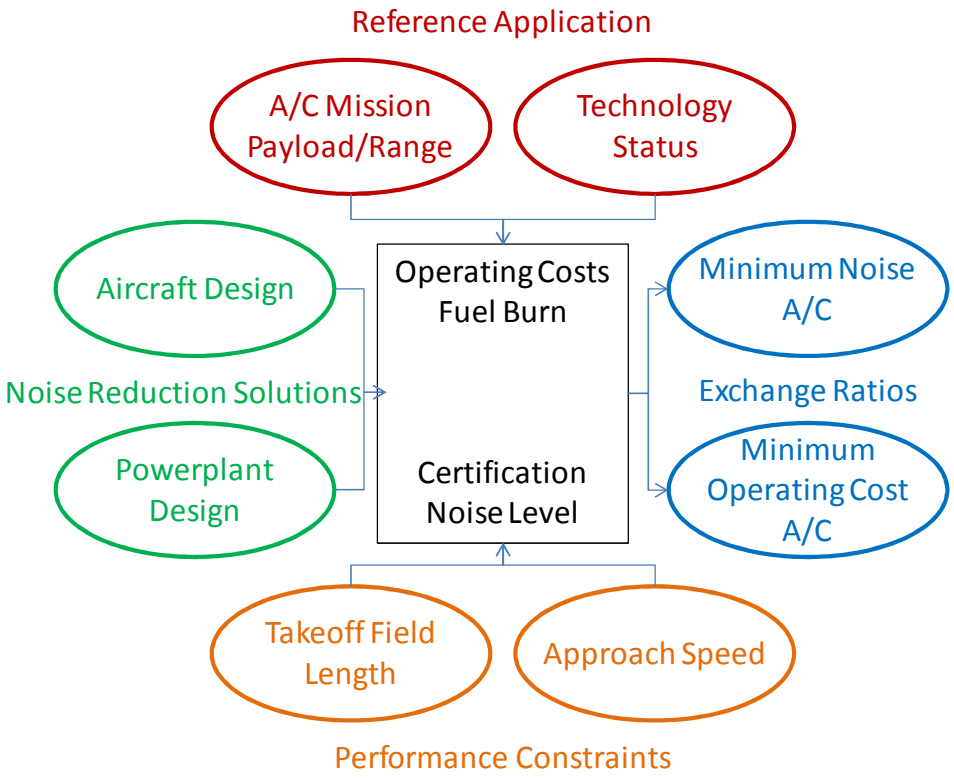

Figure 14. Proposed Technology Evaluator methodology.[68]

The engine and airframe manufacturers are responsible for defining virtual platforms to represent noise reduction solutions. Technology status and operational parameters are defined in the selection of a reference application, and operational constraints are applied to the problem. The airframer would then be responsible for conducting the acoustic and economics assessment, and Airbus plans to use TSOUR, their proprietary tool for certification noise level prediction, in this capacity. Technology Evaluator is focused on the noise metrics, and in the context of this work, it also has the added drawback of heavily relying on expert input, thereby not demonstrating transparency.

2.3.1.2 Project Interactive Analysis and Optimization (PIANO)

PIANO is a parametric aircraft design tool that is capable of conducting many of the analyses described in Figure 12. Documentation describing PIANO is provided by its developer, Lissys Ltd., and will be summarized here.[70] Existing and projected aircraft are modeled using roughly 260 parameters, and typical aircraft definition uses only around 50 to 60 parameters. PIANO-x is a database built by the developer that includes validated parameters for over 250 in-service commercial aircraft.[71] There are three basic types of parameters in Piano:

- Vital parameters (e.g. wing-area) – These are 15 parameters that are initially unassigned and constitute of the minimum level in a plane's definition.
- Default parameters (e.g. passenger weight) - Each of these has an assumed value, but may be overridden by the user.
- Calculated parameters (e.g. auxiliary power unit weight) – These are estimated with built-in equations in the absence of direct user input.

Engine performance characteristics are model as data matrices that are defined either by user input or by choosing from over 30 engines in the PIANO-x database. Thrust ratings and specific fuel consumption are represented as functions of altitude and Mach number. The performance of each engine may be modeled on different aircraft by scaling the data matrices to match specific SLS thrust, throttle ratings, and fuel efficiency. Independently, PIANO is not capable of generating this information from cycle analysis.

For airframe design, PIANO starts from basic inputs such as the wing area and aspect ratio, and calculates all other necessary geometric data, such as wetted areas and volumes. PIANO predicts the mass characteristics of each aircraft using both semi-

empirical and analytical equations calibrated against industry-derived data, including component mass breakdowns that are not generally available in the public domain. Technologies such as advanced materials are simulated through the use of factors applied within these equations. PIANO calculates the complete aerodynamic drag polar of an aircraft from its geometric description and allowing for various technology-level parameters.

Mission performance is calculated from first principles based on the engine, geometry, and aerodynamics characteristics. Climb, cruise and descent segments of a mission are analyzed through rigorous step-by-step techniques. Design missions or off-design missions (which correspond to specific takeoff weights or required block distances) may be analyzed.

Although PIANO is very capable of conducting aircraft design and performance analysis, it is not independently able to conduct engine cycle analysis, and its ability to evaluate engine weights and dimensions does not include component-level impacts. As technologies are applied, it would not by itself be able to generate engine decks that reflect their impacts on engine components. Therefore, this tool would be ill-suited to use in developing tests of Hypothesis 3.

2.3.1.3 Pacelab APD

Another software package with the capability to carry out conceptual vehicle modeling is Pacelab Aircraft Preliminary Design (APD). Pacelab APD is plugin that works with the original Pacelab Suite, a knowledge-based engineering environment that was created to conduct complex, interdisciplinary engineering analyses.[72,73] Pacelab APD enhances Pacelab Suite by providing tailored functionality for the modeling, synthesis

and analysis of aircraft configurations by including analyses for aircraft weights, aerodynamics, and flight performance. Pacelab APD numerically calculates the mission performance results based on the aircraft drag polars, engine performance decks, and weights primarily by using aircraft design methods and relationships derived by Torenbeek.[74,75] These analyses may be supplemented by integrating customer-specific tools or commercial analysis tools into the Pacelab environment.[73]

Pacelab APD contains an extensive collection of predefined aircraft components and configurations that may be used as inputs to set up new designs. This includes geometric definitions of standard aircraft bodies with aerodynamics and weight breakdowns, as well as a comprehensive database of existing aircraft (and their major components) with design and off-design flight performance.[73] Also within Pacelab are efficient techniques for comprehensive design space exploration and rapid design alternative evaluation, and includes PACE's aircraft performance computation module, which has been validated with all major aircraft manufacturers.[76] Pacelab is also capable of conducting mission analysis using performance data rather than conceptual engine/airframe design[77]

The drawbacks of Pacelab APD are very similar to those of PIANO. As with PIANO, Pacelab is very capable of conducting aircraft design and performance analysis, but is not independently able to conduct engine cycle analysis, and its ability to evaluate engine weights and dimensions does not include component-level impacts. As technologies are applied, Pacelab by itself would not be able to generate engine decks that reflect their impacts on engine components. Therefore, this tool would be ill-suited to use in developing tests of Hypothesis 3.

2.3.1.4 Environmental Design Space

At the Aerospace Systems Design Lab (ASDL) at the Georgia Institute of Technology, a physics-based vehicle design environment was developed to evaluate technologies for NASA's Ultra-Efficient Engine Technology program and Vehicle Systems Program, and this environment was later further evolved into the Environmental Design Space (EDS).[34] The FAA is developing EDS as part of a comprehensive suite of software tools that will enable thorough assessment of the environmental effects of aviation.[64] The other tools within the suite include the Aviation Environmental Portfolio Management Tool (APMT), and the Aviation Environmental Design Tool (AEDT). Together with EDS, these three tools provide the capability to perform aviation noise and environmental policy analysis that includes interdependencies.

The overarching goal of EDS is the development of a new capability that enables a more comprehensive assessment of the physical effects of aviation to inform national and international decision makers. One tangible product of this work is the EDS tool itself, which is capable of estimating source noise, exhaust emissions, and performance parameters for current day and future aircraft designs under different technological, operational, policy, market, and standards scenarios. Potential applications intended for EDS include assessment of existing and future advanced aircraft technologies that are being pursued under the FAA and NASA's research programs; assessing and communicating environmental effects, interrelationships, and economic consequences based on integrated analyses, as conducted by JPDO; and facilitating international agreements on standards, metrics, and mitigation options for international policy making as pursued by CAEP.[78,79] Thus, EDS does satisfy the conditions for maturity and

transparency set forth for this work. A framework of the structure of EDS is provided in Figure 15. The inputs to EDS can be a wide variety of engine and aircraft design variables and technology factors, which may include engine pressure ratios, efficiencies, geometry, drag polars, and suppression factors.

EDS begins by generating fan and compressor performance maps using CMGEN, a rapid, parametric compressor off-design performance calculator developed by General Electric on behalf of NASA.[80] The performance maps are fed forward to the engine cycle design code, which is Numerical Propulsion System Simulation (NPSS). NPSS was created to enhance the capabilities of previously developed codes such as NASA Engine Performance Program (NEPP).[81,82,83,84] by including the capability to handle multiple, simultaneous design points and their impact on the resulting design space.[85] The outputs of NPSS can include overall cycle characteristics, component characteristics, and flow station properties. Because it can simulate engine performance at different operating points, NPSS can also be used to generate engine decks for use in providing engine performance at different operating conditions in the flight envelope, which are passed to vehicle modeling.

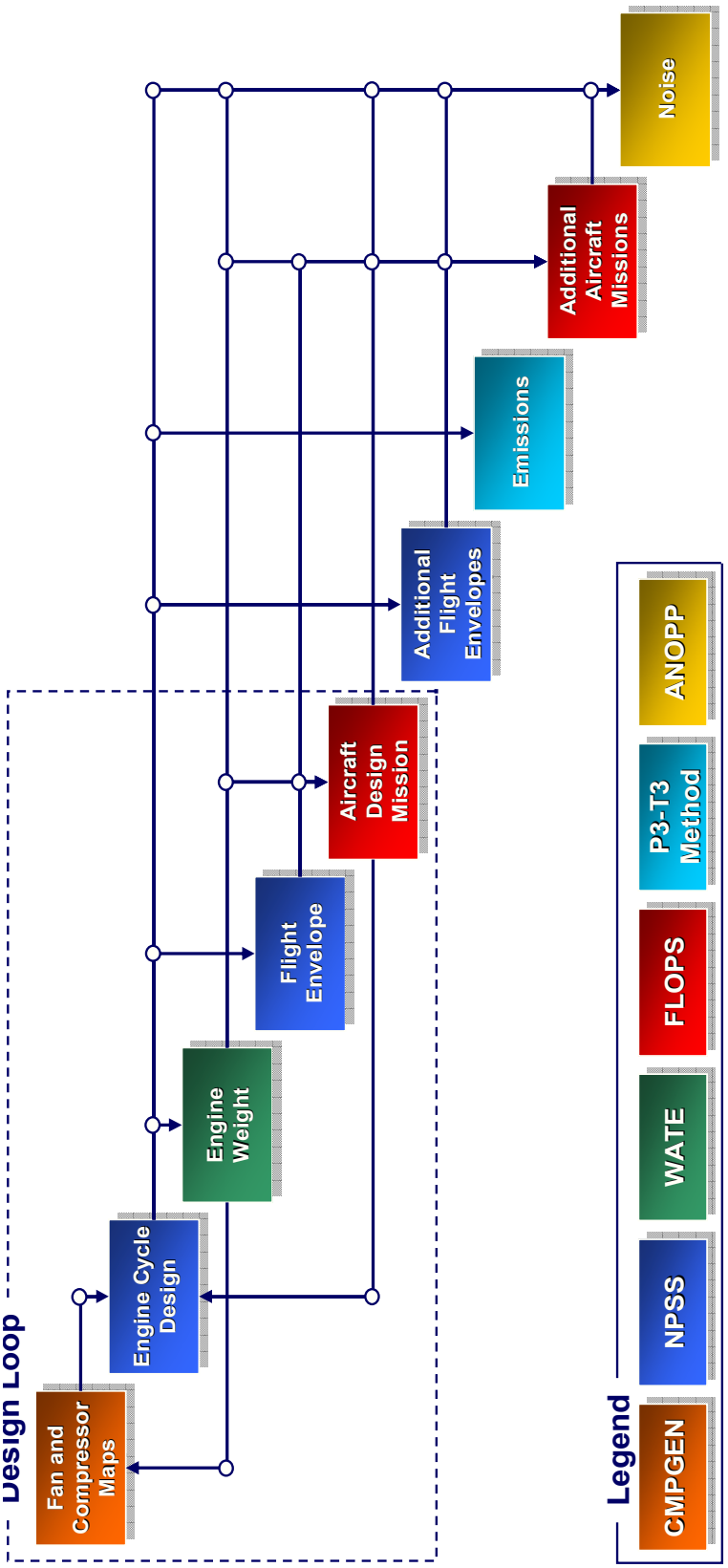

Figure 15. EDS Framework.[64]

Once WATE receives cycle information from NPSS, it calculates engine geometries, tip speeds of the rotational components, and component weights based on physical characteristics, such as mass flow rates and pressure ratios, geometric characteristics such as hub to tip ratios, and other component parameter information, such as material properties. The outputs of WATE include dimensions and weights for the inlet, fan, splitter, compressors, burner, turbines, nozzles, shafts, and ducts, along with a 2-D flow path and bare engine weight. These results may be fed back to CMGEN to generate more accurate component maps, requiring iteration back through to WATE. When this iteration is complete, WATE passes the engine weight and dimensions on to FLOPS, which can conduct aircraft sizing, design performance, and performance for off-design missions.

The inputs for FLOPS include airframe geometry, engine characteristics, payload, technology factors, and mission profile. Outputs can include range, fuel burn, airframe weights, mission segment breakdowns, detailed takeoff and landing profiles, and detailed noise profiles. At this point, everything within the dashed box is complete, but may be iterated upon to hit performance goals at different points within the flight envelope. Once engine and aircraft design and sizing have taken place, emissions results are calculated, followed by noise analysis within ANOPP, which requires engine exit temperature and pressures from NPSS and aircraft geometry and terminal area flight profiles from FLOPS.

All of the previously mentioned tools represent integrated environments that can capture, to a certain degree of fidelity, the interdependencies that exist between noise, emissions, and fuel burn. They can all map a set of inputs that define the engine and airframe to what should be a comparable set of results representing a single aircraft.

However, EDS is unique among them because it incorporates a cycle modeling tool, NPSS, to generate engine decks representative of physics-based cycles for use in airframe simulation, allowing the physical impacts of engine technologies to be modeled and propagated through to flight performance, emissions, and fuel burn results.

2.3.2 Modeling Vehicle Technologies

Because there is a desire to capture the impact of vehicle technologies at the fleet-level, the manner in which these technologies are modeled at the aircraft-level must be considered. The elements that are needed for this may be observed in existing approaches that use vehicle modeling tools to determine the impact of technologies. Capturing relevant elements from these techniques will enable the formulation of an approach to test the ability of the surrogate fleet to be used in technology evaluation. Examples of such techniques include Technology Identification, Evaluation, and Selection (TIES)[86,87,88,89] and Technology Impact Forecasting (TIF).[87,90]

These methods provide a good baseline of what elements are necessary to construct a framework to evaluate the impacts of technology implementation. There are numerous other existing technology implementation methods that will not be elaborated upon here, but the important factors that are required to undertake technology studies are highlighted by the notional illustration adapted from Patel[89] in Figure 16. Each of the actual technologies to be assessed, on the left, must be quantifiably mapped to the appropriate technology metrics that will physically characterize both their benefits and degradations to the baseline system, which is done through a technology auditing process. In turn, a mapping must then be created between the changes in technology metrics and the system objectives. This will typically require the use of a physics-based M&S environment,

which enables the thorough exploration of the design space through the variation of key input parameters.

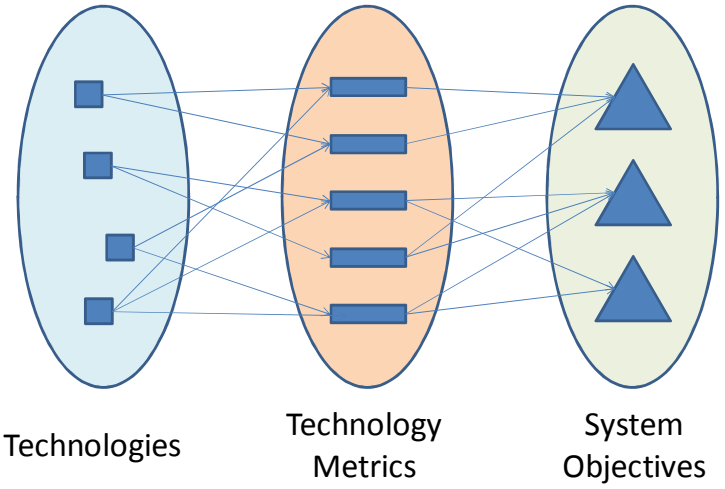

Figure 16. Notional technology evaluation framework.

M&S at the fleet-level involves mapping the physical impact of technologies to fleet-level metrics. As such, it fits into a technology evaluation framework by facilitating the mapping between the technology metric space and the system objective space shown in Figure 16. The sample problem used to evaluate the surrogate fleet approaches ability to capture the impacts of technologies will thus require a set of technologies that have been mapped to appropriate technology metrics. More details for how this is implemented will be provided in Chapter 4.

2.3.3 Fleet-level Modeling Tools

In the real world, aircraft do not operate alone in a vacuum, but rather they act in concert as part of a fleet, which may include multiple aircraft types and a multitude of different operations requiring varied missions profiles. The M&S needs in terms of the required input and outputs desired for the current work are illustrated in Figure 17. Inputs would be comprised of aircraft performance results generated from aircraft-level M&S,

as described in the previous section, along with information representing frequency of flights with different characteristics that are flown, which were described in the Section 2.1. Fleet-level analysis itself includes total mission and terminal area performance, and results include fuel burn and NO_x in these two areas.

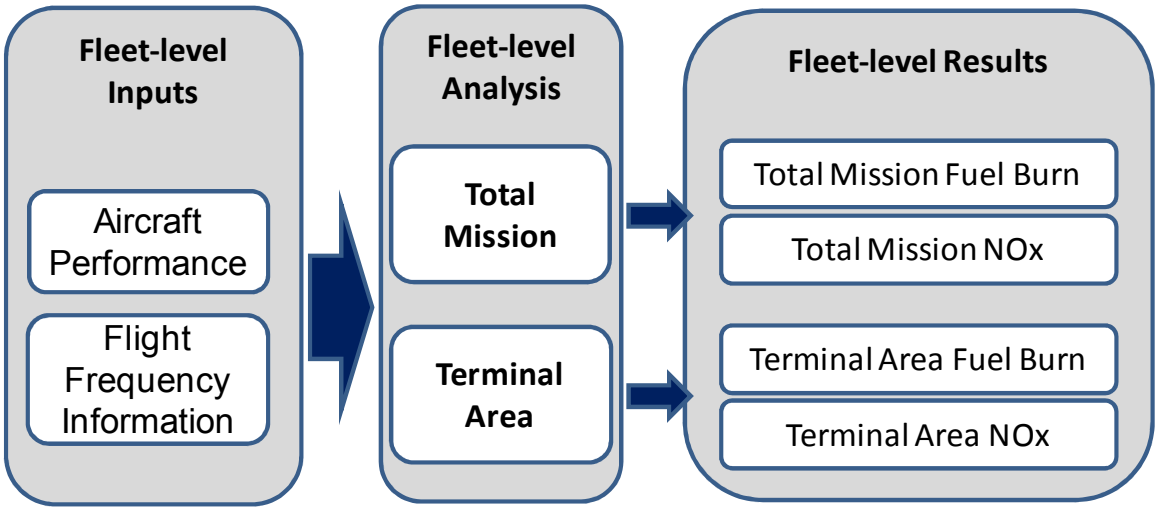

Figure 17. Fleet-level M&S.

Metrics of interest for this work include four fleet-level results: total mission fuel burn, total mission NO_x, terminal area fuel burn, and terminal area NO_x. Terminal area fuel burn and emissions in the local vicinity of airports are important drivers on local air quality. As their names suggest, total mission quantities for fuel burn and emissions contain the sum of these metrics over entire missions for aircraft in the fleet, which are important for consideration from both a fuel use standpoint and for potential global climate change impacts

There are a number of tools that are under development or already developed in the US and Europe that are capable of conducting fleet level analysis of vehicles to capture the performance of a fleet for a range of operations and fleet compositions in the form of fuel burn, emissions, and/or noise results. These tools are often used to conduct inventory analysis of the current fleet. The ability to assess the impact of different aircraft and

changes to those aircraft, which may be fed forward from the physics-based modeling at the aircraft-level described earlier in this chapter to the fleet-level, is critical to this work. Therefore, these tools will be reviewed here, with particular focus on the combined tool suites that are able to assess interdependencies by simultaneously calculating all four groups of fleet-level results listed in Figure 17.

2.3.3.1 AIM Project

The Institute for Aviation and the Environment at the University of Cambridge, in the UK, is coordinating the Aviation Integrated Modelling (AIM) project, which began in October 2006 and is tasked with developing a policy assessment tool to capture the environmental effects of aviation.[91] This tool is also composed of smaller modules that are currently under development, but when integrated together will provide a global view of the effects of aviation on the environment, and its framework is provided in Figure 18.

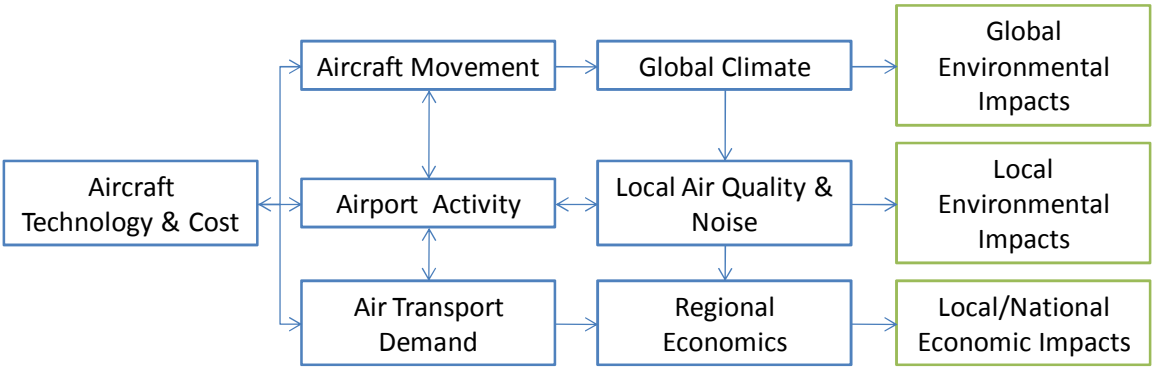

Figure 18. Structure of AIM.[91]

As can be seen from the framework, AIM focuses on emissions and economics, and each module's purpose will be described here.[92] Within the Aircraft Technology & Cost module, aircraft fuel burn, emissions and costs are calculated for various airframe/engine technology evolution scenarios. Aircraft performance may be represented in AIM through the use of BADA coefficients, which represent simplified performance

characteristics of commercial aircraft.[93] Impacts of technologies are modeled at the fleet level as functions of the cost and performance of the new technologies.[94] Results from this module are exchanged with the Aircraft Movement module, which generates trajectories between city-pairs; an Airport Activity module, which simulates terminal area operations near airports; and the Air Transport Demand module to predict future passenger demand between city pairs.

Results of the Aircraft Movement module are passed to the Global Climate module to calculate global environmental impacts of aircraft operations in the form of emissions and contrails. This information is passed along with Airport Activity results to the Local Air Quality & Noise module to investigate local environmental impacts from emissions and noise from LTO operations. Local environmental impact and air transport demand results are passed to the Regional Economics module to investigate positive and negative economic impacts of aviation, both locally and on a national scale.

Development of AIM began in 2006, and since then it has been used to conduct studies of aviation networks in Europe,[95] the U.S.,[96] and India.[97] Each of these studies modeled the fleet using representative models for a single aircraft within each seat class of the fleet considered. As such, the derivation of the inputs used by AIM and the analyses it conducts show transparency. However, it has not yet been accepted for use in CAEP analyses, and currently can only model technologies through post-processing.

2.3.3.3 AERO-MS

In 1994, the Dutch Civil Aviation Authority, with sponsorship through CAEP, developed the Aviation Emissions and Evaluation of Reduction Options – Modelling System (AERO-MS). As illustrated in Figure 19, AERO-MS consists of modules that are

organized into four large groupings: technology, economy, atmosphere, and environment, and each of them will be described here.[98] The Aircraft Technology module forecasts the future performance of aircraft in terms of changes to fuel burn and emissions indices. The Flights and Emissions module calculates emissions over the course of each mission.

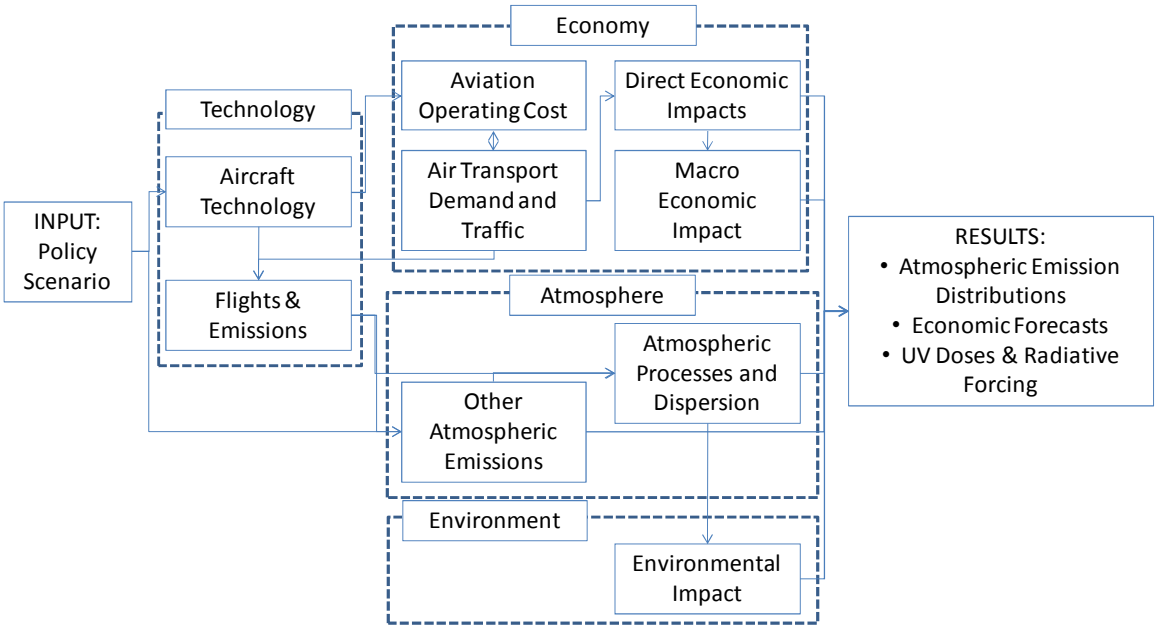

Figure 19. Framework of AERO-MS.

The Aviation Operating Cost module estimates costs of individual flights along cost increase resulting from mitigating measures. The Air Transport Demand and Traffic module forecasts traffic based future policy scenarios. The Macro Economic Impact module includes impacts of employment, income, and GDP on aviation. The Direct Economic Impacts module, calculates the direct financial and socioeconomic impacts for airlines, passengers, and governments at a global level. The Other Atmospheric Emissions module estimates atmospheric emissions from non-aviation sources. The Atmospheric Processes and Dispersion module calculates concentrations of CO_2, NO_x, and 0_3 from aviation and the non-aviation sources. Finally, the Environmental Impact model calculates the ultraviolet radiation based on CO_2 and O_3 concentrations. Together

these modules are capable of modeling aircraft technology development, air traffic demand, operating costs, direct economic effects, and aviation emissions.

Inputs for AERO-MS represent operational data and aircraft characteristics that are generated from a number of databases that are compiled for use within AERO-MS and will be briefly described here.[99] The Unified Database contains information on global air transport activity that has been compiled from four other sources: ICAO's database for international scheduled flights, the U.S. Department of Transportation's database for U.S. domestic scheduled flights, the Official Airline Guide's timetable for scheduled flights, and the ANCAT database for April 1992. Aircraft characteristics such as fuel-use and emissions are derived from flight data for aircraft classes that are grouped based on seat capacity, range bands, and technology levels. For each class, the characteristics of a generic aircraft within that class are calculated from the database of flight data to represent the entire class in fleet-level computations.

AERO-MS requires several economic related input assumptions to run, which include growth rates and real changes in fare levels.[100] Improvements in technology are modeled in AERO-MS through post-processing with industry input, rather than a physics-based approach,[101] and traffic demand is scaled proportionally to a base year of 1992, making it rather inflexible.[102] Although this tool is mature and transparent, it has not yet demonstrated the ability to roll up the results of technology implementation at the aircraft level to the fleet in a physics-based manner. AERO-MS also does not consider LTO operations in its analyses, instead focusing on en route operations.[94] Thus, in its current form, it is better suited to studies concerning the economic tradeoffs of policy analyses

rather than being used to satisfy the modeling requirements necessary to pursue the surrogate fleet methodology of this work.

2.3.3.4 AEDT

AEDT is an aircraft fleet analysis tool being developed by the FAA as part of a larger tool suite that includes EDS and APMT and is meant to facilitate decision making by CAEP. Its genesis occurred during the 2004 CAEP/6 meeting, at which CAEP members reinforced the need to capture interdependencies between noise, emissions, and fuel burn when modeling improvement in any of those areas.[103] The framework of AEDT is provided in Figure 20.[104]

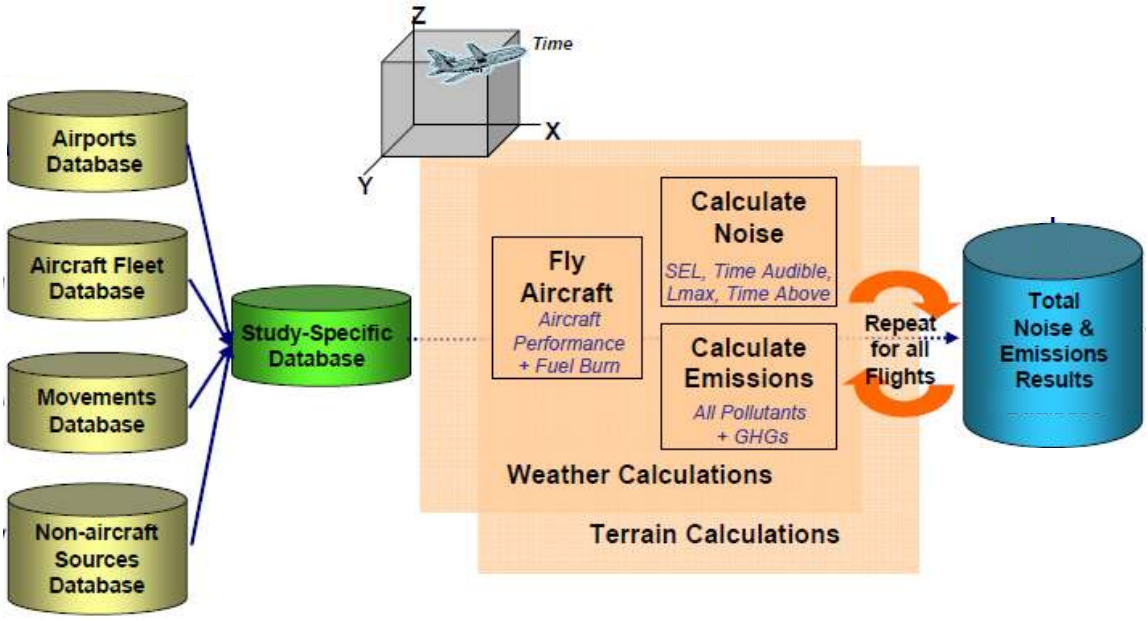

Figure 20. Framework of AEDT.

Inputs to AEDT consist of airport, aircraft, movement, and non-aircraft emissions source information that may be included in analyses based on the scope of the study involved.[105] Aircraft performance is calculated within the Aircraft Performance Module, which may include weather and terrain data based on analysis assumptions. Performance

results are passed to the noise and emissions calculations of AEDT, which are based on four previously existing tools that have been used by the FAA to calculate aircraft noise and emissions inventories, which makes it mature and transparent. Noise results are calculated within the Aviation Acoustics model,[106] which includes the Integrated Noise Module (INM), for local noise analysis, and the Model for Assessing Global Exposure from Noise of Transport Airplanes (MAGENTA), for global noise assessment. Emissions results are calculated within the Aviation Emissions Module, which includes the Emissions and Dispersion Modeling System (EDMS),[107] for local emissions analysis and the System for assessing Aviation's Global Emissions (SAGE)[25] for global emissions impacts. The significance of AEDT is that it brings these tools together in a consistent manner, giving it the ability to assess the interdependencies that can exist in the fleet-level responses.[108]

For each aircraft represented within AEDT, over 2000 coefficients are needed to define total mission and terminal area performance, emissions, and noise characteristics. These consist of BADA coefficients for en route operations, and coefficients presented in the Society of Automotive Engineers (SAE) Aerospace Information Report 1845[109] for LTO operations. AEDT is executed in conjunction with the aircraft represented by these coefficients, which have been compiled in databases populated by airframe manufacturers, to generate fleet level responses. Currently, there is no standard public domain documentation regarding how the coefficients are generated by the manufacturers, and they would also be unlikely to regenerate coefficients to represent different technology scenarios for entities that may wish to model them.[14]

2.3.4 Linking Aircraft and Fleet-Level Modeling

Because the inputs representing aircraft in each of the fleet-level tools reviewed here are coefficients from an industry supplied database, they independently could only be used to model the impact of future technologies through post-processing. Jorge de Luis's dissertation work focused on developing a connection between aircraft models and fleet modeling tools. Inputs to the fleet-level tools are derived from the previously mentioned databases, each with entries representing current or past engine and aircraft combinations.

While the information about each coefficient and how it may be used in a fleet-level tool, such as AEDT, is extensive, there is no clear explanation for the method by which they are calculated. DeLuis's work developed a methodology to calculate all the entries needed to run the AEDT for a single aircraft through the use of physics-based vehicle models developed from public domain data, which enabled the impact of technologies and their interdependencies to be captured independent of industry biases without the need for post-processing.[14]

The previously cited IP13 describes how each engine/aircraft combination considered for NO_x stringency studies is assumed to be characterized by a set of coefficients that, when used in conjunction with equations presented in the BADA and SAE 1845, represent noise, fuel burn, and emissions results for both en route and terminal area operations. BADA is comprised of a collection of aircraft performance and operation parameters, including data for roughly 300 aircraft types. As described in the BADA User's Manual, the underlying performance model is based on the use of the Total-Energy Model, which balances all of the forces acting on an aircraft as shown in

Eq. (1), where T is thrust, D is drag, m is aircraft mass, h is altitude, g is the gravitational constant, t is time, and V_{TAS} is true air speed.

$$(T - D)V_{TAS} = mg\frac{dh}{dt} + mV_{TAS}\frac{dV_{TAS}}{dt} \tag{1}$$

Using relations derived from this model, performance and operational information for each aircraft type is categorized into aircraft-specific coefficients. Lift and drag forces as well as thrust and fuel flow may be calculated with the coefficients prescribed by the data set. After all of the forces acting on an aircraft have determined, thrust-specific fuel consumption, fuel flow, and other performance characteristics may be calculated.

For the purpose of LTO mode aircraft performance modeling, the main underlying database primarily originates from SAE AIR 1845, which provides other parameterized equations to model aircraft performance in this mode. An example of one such equation is shown in Eq. (2) for jet engines, where Fn/δ is corrected thrust per engine, v is equivalent airspeed, h is altitude, T_c is ambient temperature, and E, F, G_A, G_B, and H are regression coefficients that are determined by engine power and temperature.

$$F_n / \delta = E + F \cdot v + G_A \cdot h + G_B \cdot h^2 + H \cdot T_C \tag{2}$$

This data is only valid for LTO modes, which are considered to extend up to 3,048 m (10,000 ft).[25] The cruise mode is not modeled, hence the use of BADA for en route modes.

The capability of this methodology was demonstrated by using EDS as the physics-based vehicle modeling tool, automating the generation of required AEDT fleet analysis

inputs from EDS output files, and using the EDS generated AEDT inputs to run AEDT and generate fleet-level responses for a reference vehicle, as depicted visually in Figure 21. Thus, this environment is not only mature and transparent, but it also demonstrated seamless integration between aircraft-level tools and fleet-level tools.

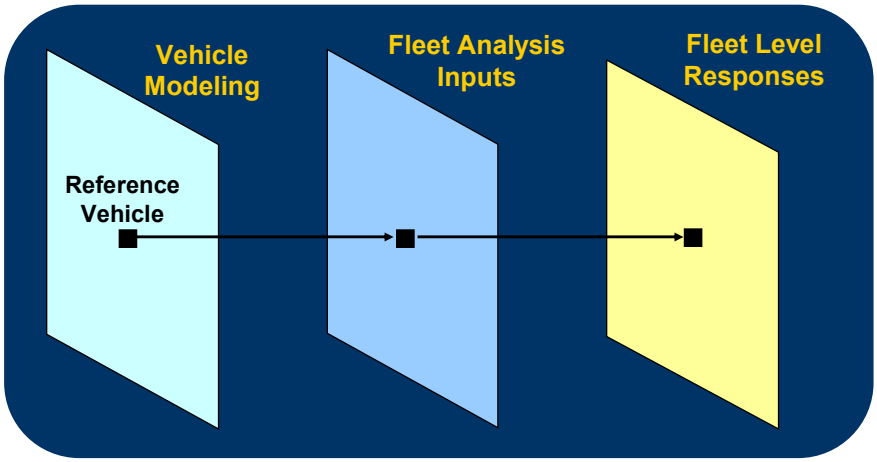

Figure 21. Linking aircraft and fleet analysis.

2.3.5 Summary of Modeling Tools

A survey of modeling tools shows that there are a number of options to consider using when developing an environment to link aircraft-level results to the fleet level as illustrated in Figure 11. Formal tool selection will not occur until experimental implementation is laid out in Chapter 4. However, a brief summary of how the tools compare to each other in relation to the desired M&S characteristics described in Section 2.2.4 is provided in Table 5 and Table 6. Positive characteristics are denoted with green checks, and negatives are in red crosses.

Table 5. Comparison of aircraft-level tools.

	Maturity	Transparency	Models Component-level Physics
Technology Evaluator	☑	☒	☑
PIANO	☑	☑	☒
Pacelab ADP	☒	☑	☒
EDS	☑	☑	☑

Table 6. Comparison of fleet-level tools.

	Maturity	Transparency	Translates Vehicle-level Results into Fleet-level Metrics
AIM	☒	☑	☒
AERO-MS	☑	☑	☒
AEDT	☑	☑	☑

Among the tools with drawbacks, the most common drawback is either in the ability of aircraft-level tools to independently model component-level physics, or in the demonstrated ability of fleet-level tools to translate vehicle-level results to the fleet. At the aircraft-level, both PIANO and Pacelab lack the ability to independently conduct cycle analysis, and at the fleet-level, both AIM and AERO-MS have been been set up to model technologies through post-processing.

2.4 Hypotheses

The literature review presented above provides insight on current methods of aircraft and fleet modeling and hint to how their capabilities could be improved. They lead into hypotheses that may be tested in an effort to answer the research questions in Chapter 1. The first research question related to identifying a method to rapidly generate environmental metrics for a fleet of aircraft:

Research Question 1: How can aggregate fuel burn and NO_x metrics be rapidly captured for a fleet of aircraft with a set of reference operations in a physics-based manner?

Because developing physics-based models for specific aircraft is very resource intensive, and only a limited set of them exist or may be created, the determination of the best use of these models to capture different portions of the fleet is important. The literature review showed the capabilities of aircraft and fleet modeling tools, the desired flow of information through them to link aircraft-level inputs to fleet-level outputs, and the importance played by the characterization of the fleet. These elements lead into the following hypothesis:

Hypothesis 1: Characterization of the commercial fleet into capability groups enables development of surrogate fleet approaches that use a limited number of aircraft models to rapidly capture environmental metrics within an acceptable level of accuracy.

Once the fleet has been grouped appropriately, the surrogate fleet approaches to using a physics-based vehicle model to represent each group must be addressed. By considering the capabilities of aircraft-level and fleet-level tools, along with the need for any surrogate fleet approach to be flexible to changes in operations, fleet mix, and technologies, three approaches have been brainstormed and will be described in detail in Chapter 4 along with the definition of acceptable levels of accuracy with respect to reference operations.

The second research question related to the change in the commercial fleet due to retirement of out-of-production aircraft, replacement and growth with in-production aircraft, and variations in flight frequency:

Research Question 2: How can the acceptability of surrogate fleet approaches be evaluated over wide variations of operations representing future fleet scenarios?

As was described in the review of the FOM and surrogate operations approaches, there are a wide range of operations that may be of interest for analysis. Surrogate fleet approaches must be rapidly evaluated over a wide range of operations, which leads into a need to employ an efficient mathematical representation for these potential operational variations. Research Question 2 is addressed by the following hypothesis:

Hypothesis 2: Parameterization of operations and use of design space exploration methods will quantify the ability of each surrogate fleet approach to capture wide variations of operations.

The assumptions entailed in the parameterization of operations will be discussed in the next chapter, along with the rationale behind using design space exploration methods to quickly represent a large number of operational scenarios. Surrogate fleet results over a significant range of operations may be compared to corresponding results of already existing fleet evaluation methods and judged for acceptance, criteria for which will be provided in Chapter 4. The outcome of hypothesis testing for Hypothesis 2 will not only enable the determination of acceptability of surrogate fleet approaches compared to current methods, but it will also allow comparisons to be made between the different approaches and the elimination of any inappropriate approaches.

The third research question related to evaluating technologies in conjunction with surrogate fleet approaches:

Research Question 3: How can the acceptability of surrogate fleet approaches be evaluated for implementation of technologies at the aircraft-level?

As described throughout the literature review, a limited number of calibrated physics-based vehicle models may be created to evaluate the impact of technologies on each individual aircraft. In order to test the ability of a surrogate fleet approach to capture technology implementation on a larger fleet of vehicles, the fleet may be examined for division into a virtual fleet of smaller, related groups based on aircraft families for modeling of technology trends that will each be modeled. Research Question 3 is addressed by the following hypothesis:

Hypothesis 3: The development of a physics-based virtual fleet quantifies each surrogate fleet approach's ability to capture technology infusion through a parallel technology implementation study.

Here again, acceptability is defined relative to current fleet evaluation methods and is further discussed in Chapter 4, along with more details on how the virtual fleet will be developed and the ensuing technology implementation study.

CHAPTER III

METHODOLOGY

In this chapter, a methodology is developed to provide the framework within which to evaluate the hypotheses presented at the end of the previous chapter. Tying together the needs and research questions presented in the previous chapter leads into the methodology illustrated in Figure 22. Specifically this methodology requires elements that will characterize the fleet, define reference vehicles to represent the fleet, include techniques that enable the use of physics-based models to rapidly represent the fleet, and test their ability to capture fleet evolution over time. This includes not only being able to capture the performance of a fleet of current technology aircraft, but to also do this for fleet of aircraft with varying future operations and potential technologies.

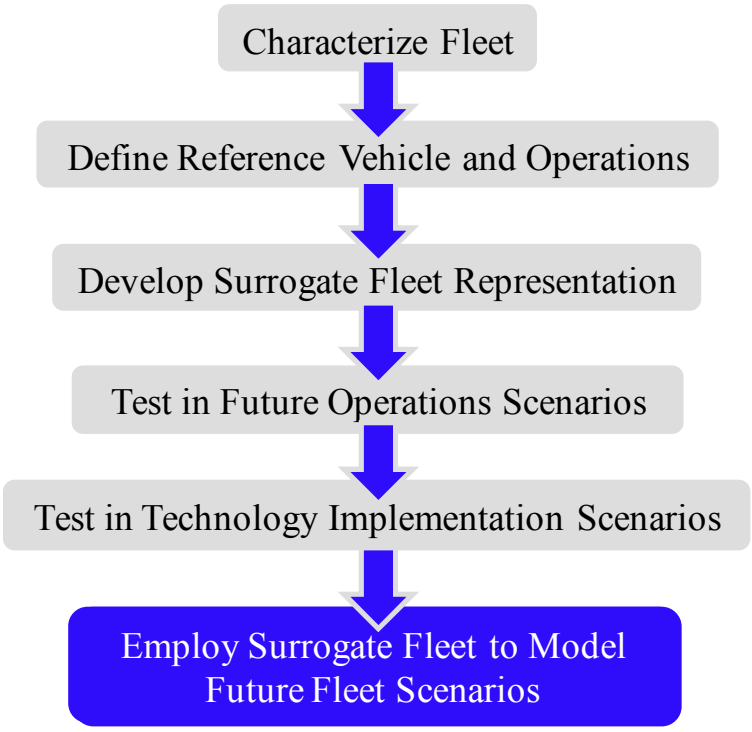

Figure 22. Framework of methodology.

Each of these elements will be described in this chapter. The end goal is to have a surrogate fleet that will represent a fleet of interest, enabling rapid evaluation of environmental metrics for future fleet scenarios, in which operations and/or technology levels may be varied from the present day.

3.1 Characterize the Fleet

The first step needed to develop a methodology to test the hypotheses is the formulation of a generalized approach to characterize the fleet. The approach outlined here is to categorize a fleet of vehicles based on a broader range of metrics than simply number of passengers, which varies based on changes to internal configuration without necessarily changing the performance of the vehicle. Steps for this categorization would be to:

- Identify a set of metrics that can be used as a basis to split the entire group of vehicles into smaller segments based on capability
- Collect values for these metrics for each vehicle in the fleet
- Examine trends across these multiple metrics to make a better judgment of where appropriate groupings within the fleet can be made

Characteristics to consider include intrinsic vehicle geometry and performance under specific operating conditions. Together, these will be referred to as capability. Geometry provides an indication of the size of a vehicle, which could thus be related to a metric like the capacity of number of passengers, but geometry itself would not change based on internal configuration. Likewise, if a performance metric is chosen at a specific operating condition, it also would not change based on internal configuration.

In applications where transparency is important, values for these types of metrics for each vehicle should be collected from publically available sources. For aircraft, these sources could include certification data or airport planning documents that are often available from manufacturers. After gathering this information, judgment of appropriate groupings may be conducted through data visualization to identify clusters or gaps between groups.

In the course of characterization, there may be vehicles that must be eliminated from consideration because they would not be eligible for a technology response. In the case of the commercial fleet, which is made up of the entire fleet of passenger aircraft operated for profit throughout the world, identification must be made of which aircraft may not be included within the fleet of interest, which will be the subset of the commercial fleet for which a surrogate fleet will be developed. The designation of whether these aircraft are in-production or out-of-production is important because aircraft that are currently out-of-production are unlikely to be competitive in a future market and future technologies may not be applied to them.[43] Their contribution to fleet-wide environmental effects will also continuously diminish as out-of-production aircraft are retired. In contrast, aircraft that are in-production today are likely to remain in the market for many years. These are the aircraft that will likely be upgraded with future technologies, contributing to changes in environmental metrics.

3.2 Define Reference Vehicle and Operations

In order for the physical interdependencies of a fleet of vehicles to be captured, a physics-based modeling tool must be employed. Once the capability groups have been defined, a reference vehicle within each group may be selected for physics-based

modeling, which will later be used as a baseline for creation of surrogate fleet approaches. Because of the resource intensive nature of physics-based modeling, the selection of what models must be developed or acquired must undertaken judiciously. If any physics-based models already exist, they may be examined to determine if they fall into any of the capability groups. Consideration must be given to which parts of the fleet of interest a model may be able to accurately represent. In order to be able to useful in studies involving changing technology levels, this reference vehicle must be one that would be included in a wide range of technology responses over time. Thus, it should be a relatively new in-production vehicle that is projected to be in service over time.

The selection of reference vehicles is followed by the compilation of data relevant to the environmental metrics of interest for each vehicle in the fleet of interest. The aggregate performance of this reference fleet will be used in conjunction with the models of the reference vehicles to build up the succeeding steps of the methodology. The performance of the reference fleet will be baselined over a certain set of operations over a certain timeframe for this purpose, creating a set of reference operations that allow for validation of the methodology.

Depending on what type of data is available for reference fleet metrics, baselining the reference fleet involves one of two options. The first option is in the case of having available fleet-level input files for each vehicle in the fleet of interest. Once the input files have been collected, fleet-level analysis may be conducted for each vehicle within the fleet of interest corresponding to flight distances representative of reference operations, and corresponding fleet level metrics for the reference fleet can be generated. The second option would be in the case of having access to actual flight data for the reference fleet

over the set of reference operations, along with the values for environmental metrics of interest for each flight.

3.3 Develop Surrogate Fleet Representation

Three potential surrogate approaches have been developed through brainstorming ways to employ physics-based modeling at the vehicle level to impact fleet-level results: the best-in-class replacement approach, which is the simplest of the three; and the parametric correction approach and average replacement approach, which build off of the best-in-class replacement approach.[110] The background and methods behind these three approaches will be developed here.

3.3.1 Best-in-Class Replacement Approach

As its name suggests, the best-in-class replacement approach proposes the use of a single physics-based reference vehicle model to capture the performance of an entire vehicle class. The origin of this approach is in the use of a single, best-in-class vehicle that has been employed to capture aircraft level technologies in the fleet-level sample problems.[34] This is a simple way of representing the fleet that only requires the development of a single vehicle. An overview of this method is provided in Figure 23.

The steps for the best-in-class replacement approach are as follows:

- Select the best-in-class vehicle model for each capability group from the fleet of interest
- Run through physics-based aircraft modeling to generate fleet-level inputs
- Generate fleet-level results for the best-in-class vehicle over the set of reference operations

- Compare results to the target of interest.

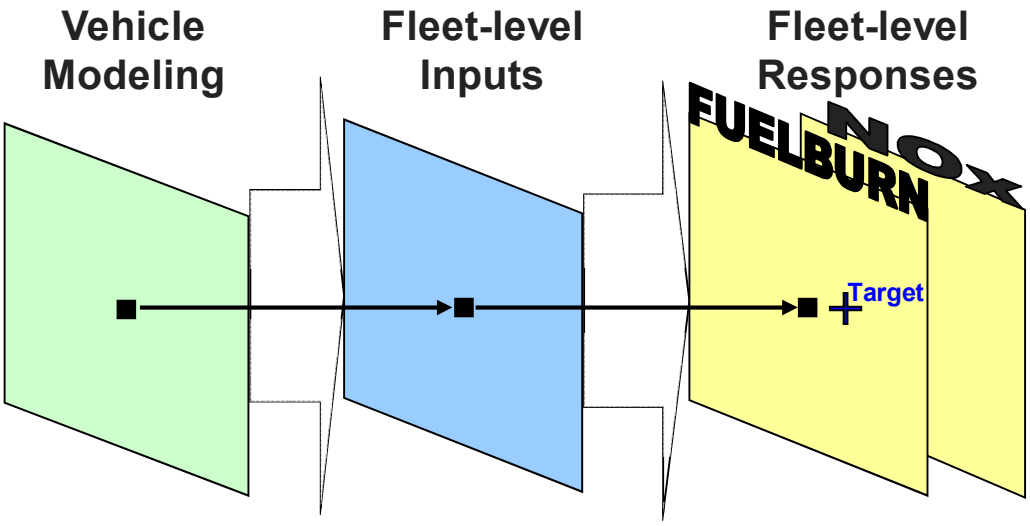

Figure 23. Best-in-class replacement approach overview.

Although this approach by its nature is not expected to be as accurate as the other two approaches that will be presented, it does provide a good source of control data because it is so similar to the JPDO analysis approach using EDS and will provide context for how much improvement the other two surrogate fleet approaches are able to achieve.

3.3.1.1 Aggregate Target Selection

The target for the existing vehicle represents the aggregate results of the fleet of interest, which must be calculated from the fleet-level responses of the fleet of interest and a given operations mix. This is akin to how a generic representation for each aircraft class is calculated in AERO-MS, as described in Chapter 2. The calculation used to generate these aggregate fleet metric targets is shown in Eq. (3). The vehicle results for each mission in the reference set of operations, $Y_{n,i}$, are multiplied by the number of operations for that particular mission, $N_{FD,i}$. By doing this, the impact of each mission is weighted in the target by its prevalence in the reference set of operations. This product is

calculated for each vehicle and summed over the total number of operations required to capture the mission profile of each vehicle.

$$Y_{AggregateFleet} = \sum_{n=1}^{NumAC} \left(\sum_{i=1}^{NumFD} \left(N_{FD,i} Y_{n,i} \right) \right) \tag{3}$$

Since operational distribution is a part of generating the aggregate target, as the operational mixes change, this target will shift. The impact of how the accuracy of an existing vehicle in capturing the fleet's performance as operations change is important to consider in order for this approach to be robust to these changes. This will be part of testing acceptability of Hypothesis 2. The ability of this approach to capture the application of technologies to aircraft in the fleet will also require the virtual fleet concept to be judged, which will be part of testing for Hypothesis 3.

3.3.2 Parametric Correction Factor Approach

The parametric correction approach is named as such because it involves the application of correction factors to fleet-level results of the reference vehicle model over a range of operational parameters to match the performance of other vehicles in the fleet. The genesis of this approach was simply through observation of parametric correction being used in applications such as remote sensing,[111] error correction of empirical data,[112] and compressibility correction,[113] followed by applying correction to the best-in-class replacement approaches. In these approaches, a true or ideal solution is known, and empirical results are modified through application of multipliers or scalars to match predicted behaviors. The parametric correction factor approach may thus be expected to be very accurate in capturing the performance of the fleet for a reference set of operations

and perhaps even for variations in operations. However, since all of the physical differences between the reference vehicles and the fleet aircraft are captured in a correction factor that is developed at a fixed technology condition, this may not be a good approach for technology evaluation.

An overview of how the correction factors will be generated and used in the context of the modeling flow illustrated in Figure 21 is provided in Figure 24.

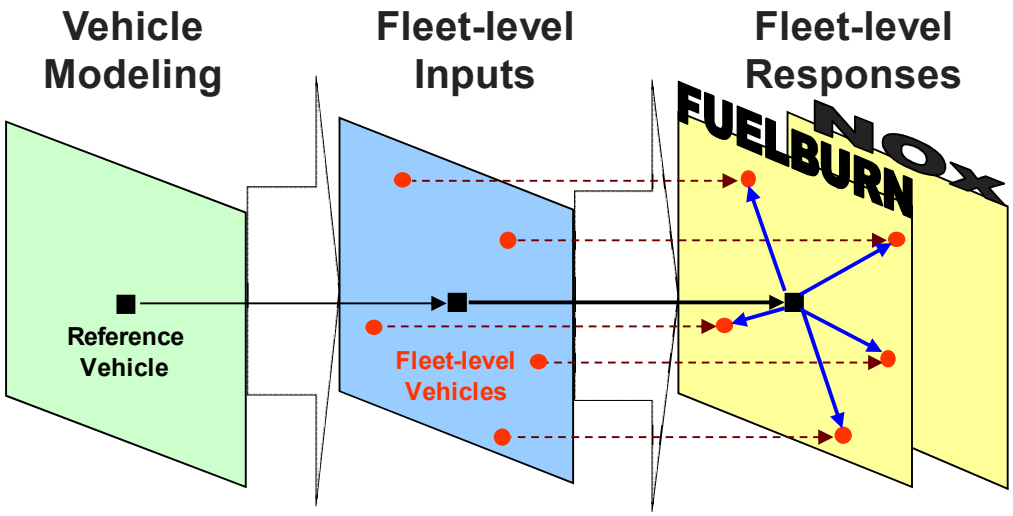

Figure 24. Parametric correction factor overview.

The steps are as follows:

- Execute the physics-based reference vehicle models for each capability group of the fleet of interest to generate fleet-level inputs
- Run these fleet-level coefficients are run through the fleet-level analysis tool using the same distribution of operations that were used to run the fleet-level vehicle models in the first method for generating a reference fleet (Section 3.4.1)
- Calculate correction factors (represented by blue arrows in the fleet-level response space) for each of the fleet metrics of interest for each vehicle as a

function of significant operational parameters, which will be described in more detail below.

The correction factors thus allow the single physics-based vehicle model to represent each vehicle in the fleet of interest as a physics-based surrogate.

The approach for the calculation of the correction factors is illustrated in Figure 25.

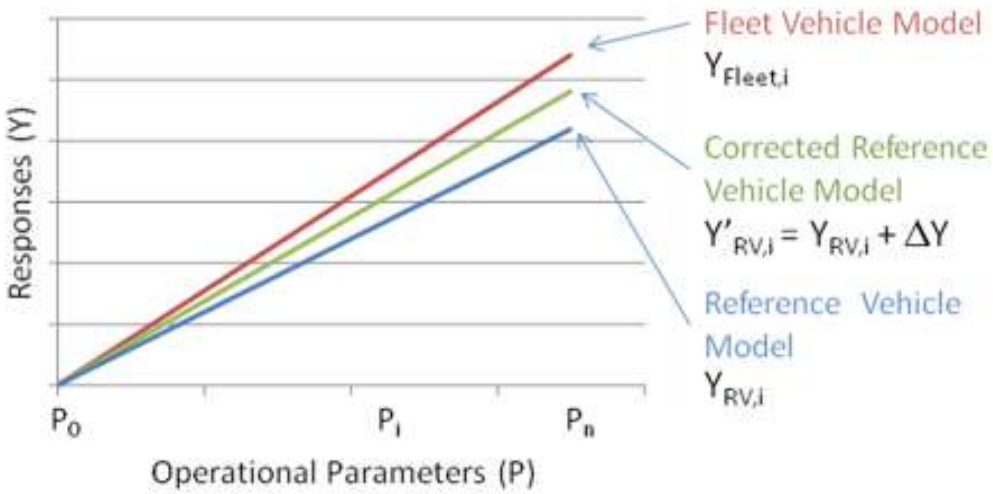

Figure 25. Calculating parametric correction factors.

The steps are as follows:

- Using a screening test, determine the functional form for the correction factor ΔY as a parametric function of the significant operational parameters that are primary drivers of the fleet-level metrics of interest.
- Solve for the parameters of correction factor ΔY to minimize the sum of squares error between corrected physics-based vehicle responses and the fleet-level vehicle responses over the entire range of operational parameters, given in Eq. (4)

$$Sum\ of\ squares\ error = \sum \left(Y_{Fleet,i} - Y'_{RV,i} \right)^2 \tag{4}$$

- Parametrically correct each response of interest generated for the physics-based generic vehicle model, $Y_{GV,i}$, by adding the correction term ΔY to form the corrected generic vehicle response, $Y'_{GV,i,}$
- Use the corrected vehicle response to approximate the fleet-level response is represented by Eq. (5).

$$Y_{Fleet,i} \approx Y'_{GV,i} = Y_{GV,i} + \Delta Y \tag{5}$$

An example of the process through which the functional form of the correction factor ΔY may be developed for a specific problem will be discussed in Chapter 4.

3.3.3 Average Replacement Approach

The final approach covered in this work is the average replacement approach, the goal of which is to create a single physics-based vehicle model that, when flown through the same aggregate operations mix as the fleet of interest, will result in the same aggregate results as the fleet of interest. The starting point for developing this vehicle model is in the same reference vehicle model of the best-in-class replacement approach. The concept of using an average vehicle to capture environmental performance of a larger group has been used in prior work conducting analysis of annual automobile emissions data in the context of Corporate Average Fuel Economy regulations by the EPA.[114] The work presented here will move beyond merely grouping data into an average, but instead calibrating a potentially predictive model to hit an average target.

The average replacement approach is illustrated in Figure 26, and is analogous to calibrating a physics-based model to a target representing a particular engine/airframe combination. The steps are as follows:

- Conduct effect screening to determine which input parameters are in fact the most influential on the relevant fleet-level metrics
- Calculate a target representing the aggregate performance of the fleet for each metric of interest using Eq. (3)
- Vary the key input parameters from effect screening around the reference vehicle to generate engine cycle and airframe geometry combinations for design space exploration.
- Conduct thorough design space exploration identify the best option for an averaged vehicle that hits the aggregate targets calculated for the entire fleet for each environmental metric

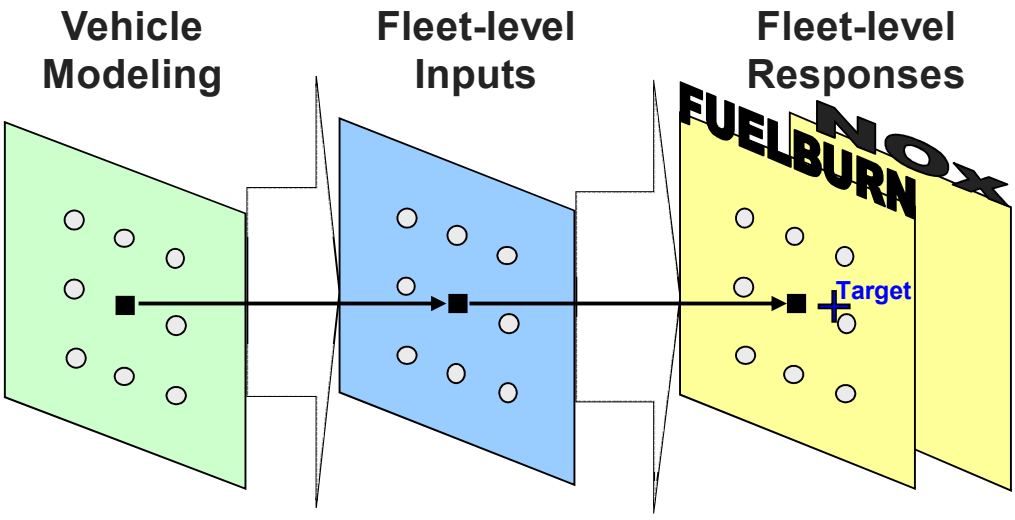

Figure 26. Average vehicle replacement overview.

Because of the large number of input parameters that may be varied in a physics-based vehicle model, screening tests must be conducted to determine which ones may

have significant impact on fleet-level responses. Common methods for conducting effect screening are reviewed in Appendix A. Once these variables have been identified, a DOE may be executed around the reference vehicle in order to generate candidates for average replacement, which will finally be selected using the aggregate target.

3.3.3.1 Vehicle Selection

Once the DOE has been executed and an average target has been calculated, the next step is to identify an aircraft design from the DOE results that best represents the aggregate fleet. At this point, the problem is one of inverse design, described as such because any variable in the system, including metrics that are traditionally outputs, may be handled almost like an independent variable. Constraints may be applied to the aggregate fleet-level metrics and used to calculate the corresponding traditional inputs analytically using their relationships through the physics-based environment. When appropriate, the use of surrogate models or probability theory allows inverse design to be applied to a wide range of problems in the M&S community.[115]

Selecting an average vehicle from the DOE results is similar to probabilistic calibration approach outlined for EDS calibration, which makes use of probabilistic exploration of the design space and filtering because of the absence of large amounts of calibration data.[116] Using these techniques to calibrate other environmental models in the presences of sparse data is well established[117,118,119] and generally implemented through filtering.[120] Filtering can be used as an approach to reject model simulation results that fail to meet established performance goals, thus being useful to objectively establishing estimates for parameter values, and can be described in three key steps:[121]

- Use of available information to define acceptable model behavior

- Application of random variation of input parameters to generate corresponding model predictions
- Classification of each prediction as acceptable or unacceptable based on pre-specified definition

The definition of acceptable model behavior for the average vehicle approach is set through the calculation of the aggregate fleet target, representing the results of the fleet of interest, which must be calculated from the fleet-level output files of the fleet of interest and a given operations mix. Like the best-in-class replacement approach, flight distance distribution is a part of generating the aggregate target for the average replacement vehicle. Therefore as the aircraft and operations mixes change, the target will shift. The accuracy of the average vehicle's ability to capture a fleet undergoing such changes may be directly tested through comparison with the reference models for the fleet of interest, which will be part of testing for Hypothesis 2.

3.4 Testing Surrogate Fleet for Variations in Operations

Once a surrogate fleet has been developed for the fleet of interest for the baseline set of operations, it must be tested for robustness towards variation of the fleet operations to be useful for scenarios away from the baseline case. This will allow confidence in using the surrogate fleet approaches with a wide range of potential future forecasts to be quantified. Comparisons may be made between the aggregate fleet results for fuel burn and NO_x calculated through the surrogate fleet methods and those of the AEDT fleet of interest. The operational data from the six weeks of 2006 CAEP flights[49] can be used as the baseline for the aircraft in the fleet of interest. A sample distribution of flight distances for single-aisle operations from those six weeks is shown in Figure 27. As can

be seen in the figure, the distribution of flights is bounded by flight distances of 0 nm and a maximum flight distance, and also appears to be multimodal in the sense that there are multiple local maxima.

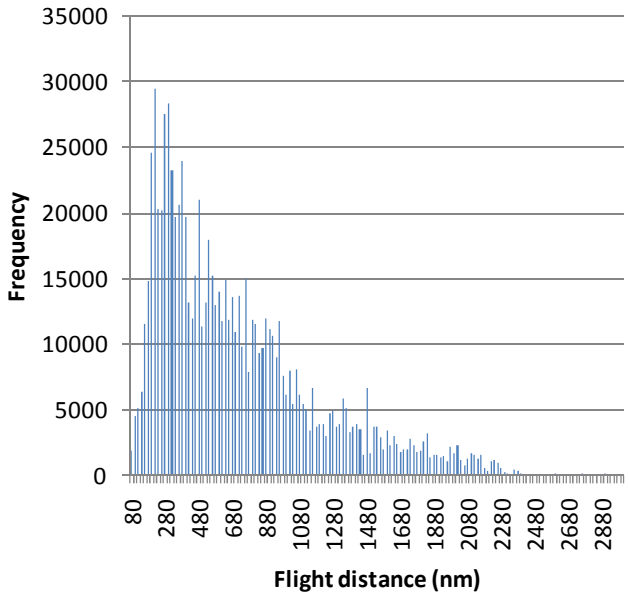

Figure 27. Sample distribution of flights from six weeks of 2006 flights.

3.4.1 Representing Future Operational Distributions

In order to quickly generate potential future operational distributions for surrogate fleet evaluation, three potential approaches employing composite probability distributions were considered. Composite probability distributions, which are sums of multiple probability distributions, were used in an attempt to capture the multimodal nature of operational distributions as seen in Figure 27. There are multiple choices of well-known continuous probability distributions that may be considered, but for this application a distribution with bounded intervals is desired, since this is also the form taken by the actual distribution of flights. Potentially appropriate bounded continuous probability distributions from which to choose from for this application include the beta distribution

and the truncated normal distribution, which are described in depth in Appendix B. Thousands of potential operations mixes can be quickly generated by varying the handful of parameters that define each distribution. Multiple distributions also allow multimodal fleet performance in terms of potential future operational scenarios can be calculated for both the reference fleet and each surrogate fleet approach, and their results may be evaluated to determine the suitability of each method in terms of its ability to capture these types of variations.

The first approach considered was to directly substitute sums of continuous probability distributions to represent future scenarios. This is illustrated with a composite distribution of three constituent distributions in Figure 28.

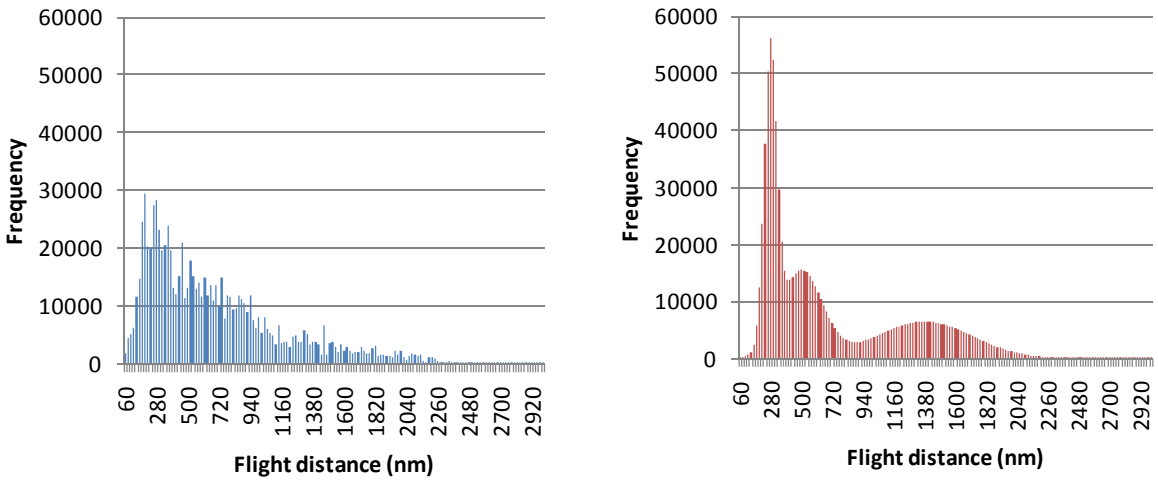

Figure 28. Original distribution (left) and substituted composite distribution (right).

The steps for this approach are as follows:

- Generate individual distributions of frequencies across range of operations
- Construct future operational distributions for each capability group by summing these individual distributions
- Use value of resulting sum as the frequency within each operational bin

One drawback of using this first approach is that the number of modes that a composite probability distribution may capture is limited to the number of individual distributions contained therein. Multimodality of the distributions of reference operations may not be completely captured. This leads into the second drawback: matching the original reference distribution exactly would require a large number of constituent distributions.

The second method to rapidly generate future operational distributions is to generate sample distributions by using the composite continuous probability distributions to generate a distribution of scalars across the range of flight distance. The steps are as follows:

- Generate individual distributions across the range of operations
- Use sum of values of distributions at each bin to generate values for scalars across the range of operational distributions
- Scalars are multiplied by the reference fleet's distribution of operations within each operational bin
- Resulting product is used as the frequency within each operational bin to generate potential future operational distributions for each capability group

A distribution of scalars is illustrated on the left side of Figure 29 along with a product of that distribution with the original distribution of Figure 27 on the right. The range of scaling for any particular flight was chosen to vary by a factor of between ½ and 2 for this illustration. In this situation, the tendency of the truncated normal distribution to form peaks can tend to leave large portions of the flight distribution unchanged. The composite beta distributions provide varying levels of scaling across the entire flight range. Another benefit of the beta distributions is that they may form a uniform

distribution easily, meaning that they will reproduce the reference fleet operations as a result of setting each parameter to unity, and then allow variations away from that case. Thus, in contrast to the first method, in this second method of varying operations, the composite beta distribution is superior to the composite truncated normal distribution.

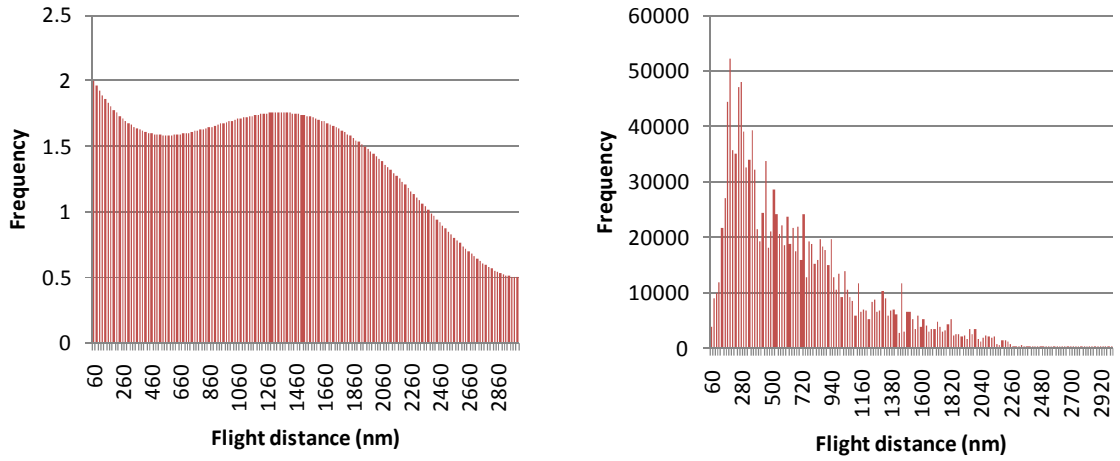

Figure 29. Composite distribution of scalars (left) and scaled distribution (right).

As with the use of composite probability distributions to directly represent the distributions, this second method also allows thousands of potential operations mixes to be quickly generated by varying the handful of parameters that define each distribution. However, in this method, the multimodal characteristics of fleet performance can be scaled from that of the original operations distribution, rather than having to be applied through the distributions themselves. By scaling the original distribution, the resulting distribution has a sense of realism to it, because this would be akin to expanding frequency of flights between given sets of OD pairs at specific distances. Matching the original distribution of reference operations is also made possible when uniform distributions are used as constituent distributions.

The third method considered to rapidly generate future operational distributions is to simply employ distributions of random numbers to represent flight frequency across the

range of operations. These random numbers may represent the distribution itself, as in the first method, or they may represent scalars to be applied to the original distribution, as in the second method. The first approach is illustrated in Figure 30 and the second approach is illustrated in Figure 31 for a range of scalars again between ½ and 2. Because the scalars are randomly chosen across flight distance, it is very possible that if none of the higher frequency operations were scaled up significantly, high frequency counts may not be achieved. Indeed, comparing Figure 31 with Figure 29 reveals a significantly lower maximum frequency for the distribution with random scalars. This would imply that potential future operational scenarios would not be captured by using the random approach.

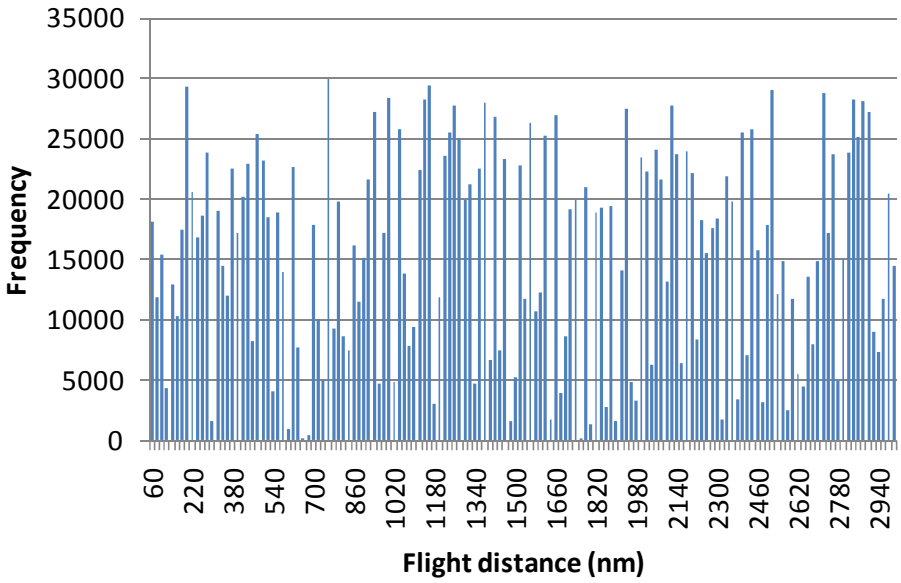

Figure 30. Random distribution of flights.

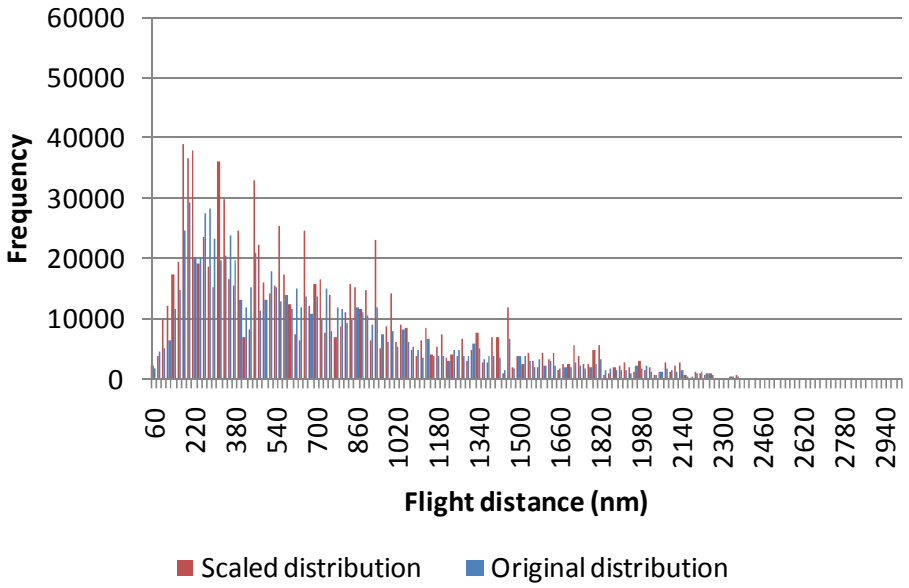

Figure 31. Random scaled distribution of flights.

After examining the options presented in this section, the two best approaches to varying the operations mix to simulate distributions of actual operations are to use the composite truncated normal distribution to represent potential flight distributions, or to use the composite beta distribution to generate potential flight distributions through scaling of the reference distribution. The latter option was selected for this work. The ability to match the reference distribution with this option, allowing variations to be made away from it, along with the more realistic distribution shapes that result from scaling the reference distribution, proved to be the deciding factors.

While techniques to vary operations for the surrogate fleet methods are outlined above, attention must also be given to how they will be varied to accomplish assessment of the surrogate fleet methods. The design space exploration approach considered here has similarities to the Monte Carlo approach, but unlike pure Monte Carlo sampling, which is random, a space filling DOE is used to determine values of input parameters for the composite distributions in each case. The impact of using the space filling DOE is

that the potential space of future fleet scenarios is covered.[122] The output of the DOE will still be a distribution of points that, for the purpose of this work, would be examined for its minimum and maximum values to determine the ability of the surrogate fleet to capture operation variations at their extremes.

3.5 Testing in Technology Implementation Scenarios

Capturing the impact of technologies using the surrogate fleet approaches presents different challenges for each approach, which will be outlined here. A simple notional illustration of technology infusion is presented in Figure 32 for a generic vehicle, represented by the black square, and other vehicles that it may represent in the fleet of interest: AC1, AC2, and AC3.

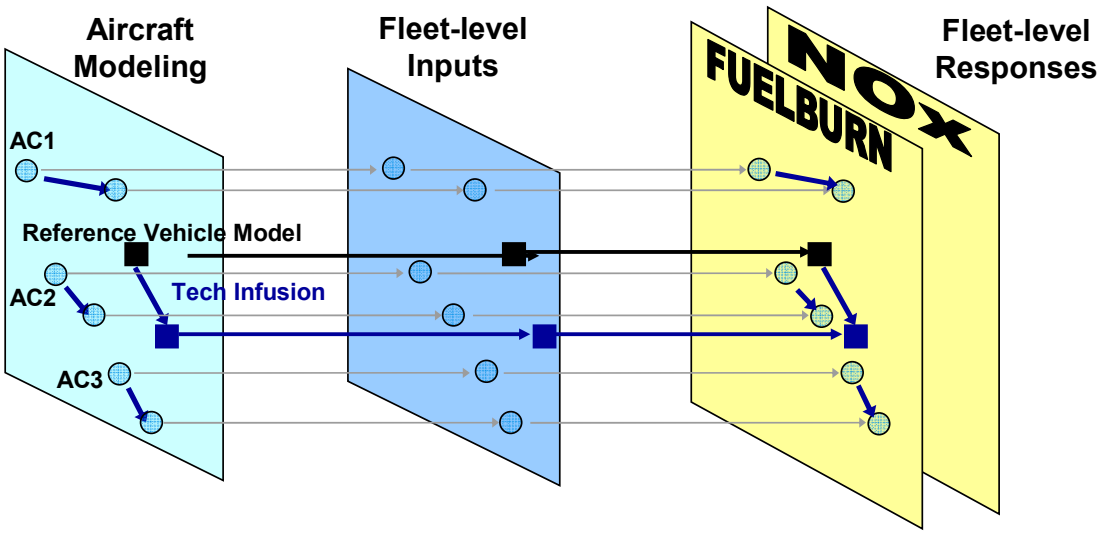

Figure 32. Technology infusion.

When the reference vehicle has technologies applied to it in the physics-based modeling space, its fleet-level inputs and outputs for fuel burn and NO_x will shift; however, while shifts may also be expected for AC1, AC2, and AC3, their shifts may be in different directions and of different magnitudes than for the reference vehicle. In order to prove the applicability of the surrogate fleet approaches to capturing technology implementation,

the ability of a generic vehicle to capture such shifts caused by technology on a larger group of aircraft must be demonstrated.

This scenario is further complicated by the fact that the impact of technology infusion on AC1, AC2, and AC3 cannot be directly modeled in a physics-based fashion in the fleet-level input space alone; this would require the creation of three new physics-based aircraft models to represent each one and generate appropriate fleet-level coefficients after technology infusion. Although this may be relatively easy to do for a small number of aircraft, it would be cost-prohibitive to do for every vehicle in the fleet.

If parametric correction factors that were developed to relate the reference vehicle to the baseline fleet of interest, they would most likely be different than those required to relate a technology infused reference vehicle to a technology infused fleet of interest because of different aircraft specific behaviors in response to technology infusion. A similar quandary also exists for the average replacement and best-in-class replacement approaches. Because all of the aircraft within the fleet of interest may not respond in exactly the same manner to implementation of a particular technology, the target for these approaches may also shift unpredictably when conducting technology evaluation on the fleet. Again, this could be modeled in a physics-based fashion by developing models for each vehicle in the fleet, but would be cost-prohibitive to do.

The method developed here to circumvent the need to develop validated physics-based models for each vehicle in the fleet is to leverage the parametric nature of a physics-based aircraft modeling to generate a virtual fleet of aircraft that spans and captures the performance of the fleet of interest. The conception of using a virtual fleet to quickly simulate behavior of the larger fleet in this work came from observations of the

application of similar ideas in structural analysis[123] and fishery studies.[124] In those applications, rapid models that spanned the potential behavior of the aircraft or fishing fleet that were being studied were developed to enable probabilistic analysis. The virtual fleet approach for this work is aimed at developing physics-based models to represent the behavior of aircraft families within each capability group and function as a reference fleet for evaluation of the ability of the surrogate fleet methodology to capture technology response.

The virtual fleet concept is illustrated in Figure 33.

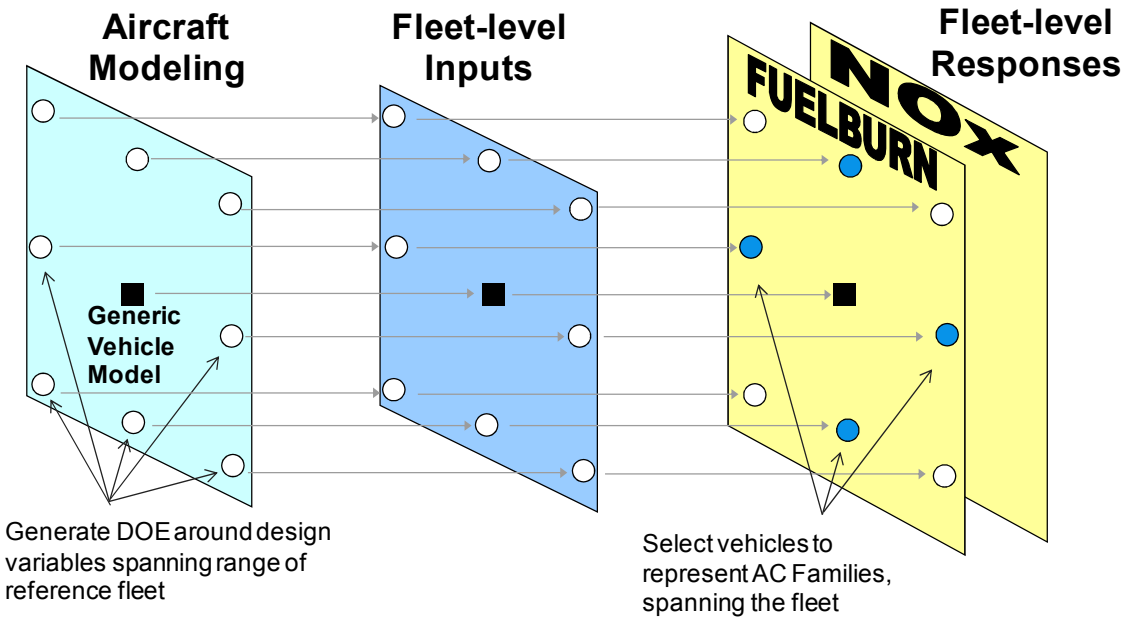

Figure 33. Virtual fleet overview.

First a DOE is generated around the design variables of the generic vehicle model spanning the ranges represented by aircraft within its capability group. The DOE is run, and once fleet-level responses have been generated, vehicles are intelligently selected to match fleet-level performance of aggregate aircraft families within the reference fleet, rather than the performance or geometry of any specific individual aircraft. This will

allow the surrogate fleet approaches to be tested in their ability to capture performance shifts caused by technology infusion by determining how well a single generic aircraft can capture that shift of a larger group of aircraft.

Because selection of a vehicle is very similar to the model calibration and average vehicle selection, the selection of a vehicle from the DOE results can be done for each aircraft family in the reference fleet through the use of filtering, which has been previously described. The difference between this case and the average vehicle case is in the target that is used to judge the acceptability of each candidate virtual vehicle. Instead of an aggregate fleet target, the target for the virtual fleet vehicles is based on the closeness of the performance of each candidate vehicle across the distribution of missions for the reference operations to the performance of each corresponding vehicle family.

Once the virtual fleet has been created, it can be used in conjunction with the parametric correction factor as notionally illustrated in Figure 34.

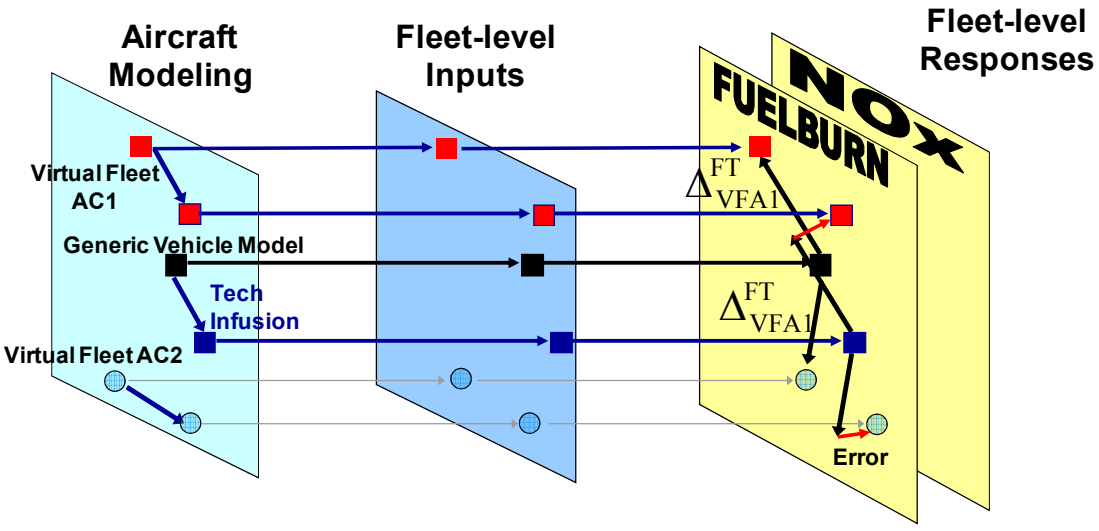

Figure 34. Notional use of the virtual fleet with parametric correction approach.

For each vehicle in the virtual fleet, the correction factors for the baseline aircraft without technologies, Δ_{VFAi}, may be calculated, signified by the black arrows in the figure. These

may then be applied to the vehicles after technologies have been implemented on their physics-based models. The error between the technology infused virtual aircraft results and the sum of the technology infused generic vehicle model plus the parametric correction factor, signified by the red arrows, may then be calculated. In such a manner, the virtual fleet is an enabler to evaluate the parametric correction factor approach for use in modeling the impact of technologies.

The virtual fleet may also be used in conjunction with the average vehicle approach, as illustrated notionally in Figure 35.

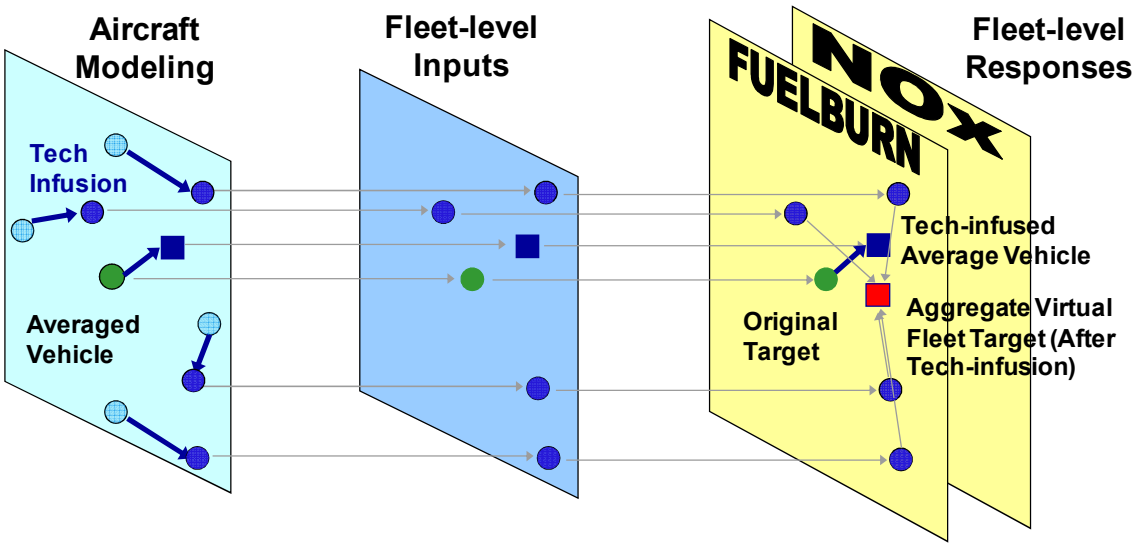

Figure 35. Notional use of the virtual fleet with average vehicle approach.

As technologies are applied to the vehicles of the fleet of interest, represented by the light blue circles in the aircraft modeling space, the aggregate virtual fleet target after tech infusion, represented by the red square in the fleet-level response space, will likely move away from the original target, the green circle in the fleet-level response space. At the same time the performance of the average vehicle with technologies applied will also move away from the original target, from the green circle to the blue square in the fleet-level response space. The difference between the fleet-level responses for the technology

infused average vehicle and the aggregate fleet target after technology infusion may or may not be significant, and must be evaluated. By using a virtual fleet of physics-based models to capture the impact of technologies at the aircraft level, assessment of the ability of the average vehicle approach to accurately capture the impact of technologies is made possible.

A similar approach may be employed to evaluate the best-in-class replacement approach, illustrated notionally in Figure 36.

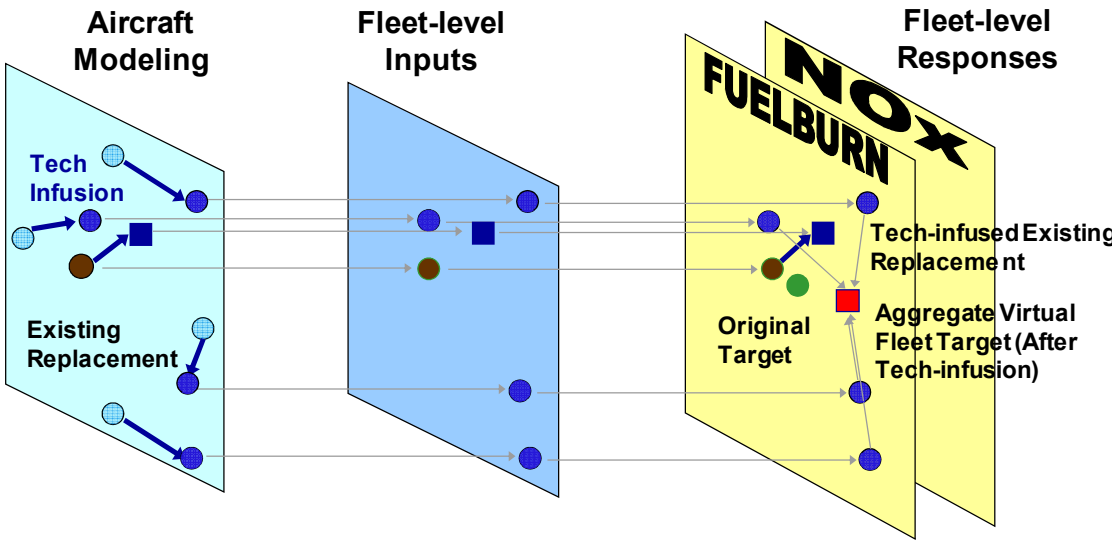

Figure 36. Notional use of the virtual fleet with best-in-class replacement approach.

As technologies are applied to the vehicles of the fleet of interest, again represented by the light blue circles in the aircraft modeling space, the aggregate virtual fleet target after tech infusion, represented by the red square in the fleet-level response space, will likely move away from the original target, the green circle in the fleet-level response space. Concurrently the performance of the best-in-class replacement vehicle with technologies applied will also move away from the original target, from the brown circle to the blue square in the fleet-level response space. The resulting difference between the fleet-level responses for the technology infused best-in-class replacement vehicle and the aggregate

fleet target after technology infusion must be evaluated. By using a virtual fleet of physics-based models to capture the impact of technologies at the aircraft level, assessment of the ability of the best-in-class replacement approach to accurately capture the impact of technologies is made possible.

The approaches developed in this chapter represent elements of a methodology that allows rapid evaluation of potential future fleet scenarios. This capability includes being able to capture the fleet as it is today, the fleet as its operations change, and the fleet as new technologies are introduced. Together, each element that has been introduced here allows the hypotheses posed in Chapter 2 to be evaluated for acceptance. The next step, which is the goal of Chapter 4, is to implement this method on a relevant sample problem.

CHAPTER IV

IMPLEMENTATION

In order to meet the research objectives, experiments have been constructed and executed to test the hypotheses presented in Chapter 2. The surrogate fleet methods that have been devised were applied to a set aircraft of the commercial fleet, which will be specifically defined for the purposes of this work later in this chapter. The aircraft that compose this fleet span a wide range of geometric, weight, and performance characteristics. As such, it provides ideal test problems for the surrogate fleet approaches in their ability to rapidly capture a very diverse group of aircraft, for the reference case and across different scenarios that involve changes to operations, fleet mix, and technology levels.

4.1 Tool Selection

In order to construct and conduct experiments, appropriate tools must be selected. For the purposes of this work, a tool or set of tools capable of generating fleet-level fuel burn and NO_x performance while at the same time retaining the ability to capture physical impacts at the aircraft-level are desired. A summary of the tools surveyed in Chapter 2 that possess these characteristics are given in Table 7. It would be possible to stitch together different combinations of the codes listed in Table 7 to achieve this purpose. However, as was seen in Chapter 2, a mature, transparent tool suite that has been developed in conjunction with the FAA and provides the capabilities needed for this work is already available.. This tool suite is EDS run in conjunction with AEDT, and this is the tool suite of choice for this work.

Table 7. Summary of potential tools.

Aircraft Level	Fleet Level
Technology Evaluator (Airbus, Snecma, Rolls Royce)	Aviation Integrated Modelling (Cambridge)
PIANO (Lissys Ltd)	AERO-MS (Dutch CAA)
Pacelab (Pace)	AEDT (FAA)
EDS (FAA)	

As previously stated, in order for the physical interdependencies of the aircraft to be captured, a physics-based aircraft modeling tool must be used to model aircraft, and at least one EDS model for each aircraft capability group has already been developed. Calibrating such a model to the public domain data that is available for a particular aircraft is a resource intensive process, but EDS models for the Bombardier CRJ900, the Boeing 737-800, Boeing 767, and Boeing 777-200ER now exist, some of which have gone through extensive review by the manufacturers. The EDS models are capable of generating the complete set of input files required to run AEDT. The fleet metrics that are of interest for the scope of this work are terminal area fuel burn, terminal area NO_x emissions, total mission fuel burn, and total mission NOx emissions, and AEDT is capable of generating all of these results.

4.2 Assumptions

The goal of this methodology is to employ techniques for rapidly capturing fleet metrics, and it is important to now consider what assumptions will be made and their implications. The first assumption made is that the available AEDT data, in the form of AEDT vehicle models and the results of the six weeks of 2006 flights, are considered the gold standard of data for this work and will be used as the reference fleet. The reasoning behind this originates in the well-established acceptance of the legacy codes which contributed to the capability of AEDT and its intended use by both the FAA domestically

and CAEP internationally. More on how this assumption impacts experimental accuracy requirements will be discussed in section 4.3. Running AEDT to generate the data for each flight of these six weeks, representing over 2.8 million flight operations. Designing a surrogate fleet of aircraft to fly these missions individually would be cost prohibitive. Therefore, other assumptions have been made in this work to simplify the number of operations for this set of data and are described below.

4.2.1 OD Pair Assumptions

The first assumption made in simplifying the number of operations is the consideration of each unique OD pair as any other operation of the same flight distance without regard to specific airport location. This also does not include airport altitude effects. An example of this would be treating a flight from Brussels, Belgium, to Newark, New Jersey, which has a great circle flight distance of approximately 3198 nm, the same as a flight from Atlanta to a destination 3198 nm away. A simple experiment was conducted with AEDT to test the implications of this assumption. Notional flights were generated for a representative large twin-aisle aircraft originating from locations representing Atlanta's Hartsfield-Jackson International Airport, Moscow's Sheremetyevo International Airport, Sydney's Kingford Smith Airport, and the Ministro Pistarini International Airport in Buenos Aires, each positioned in a different quadrant of the Earth's surface. The flight distances themselves were chosen as the midpoints of different stage lengths, and the direction of the final destination for each one of them was randomly selected. The results for total mission fuel burn, total mission NO_x, terminal area fuel burn, and terminal area NO_x are given in Figure 37.

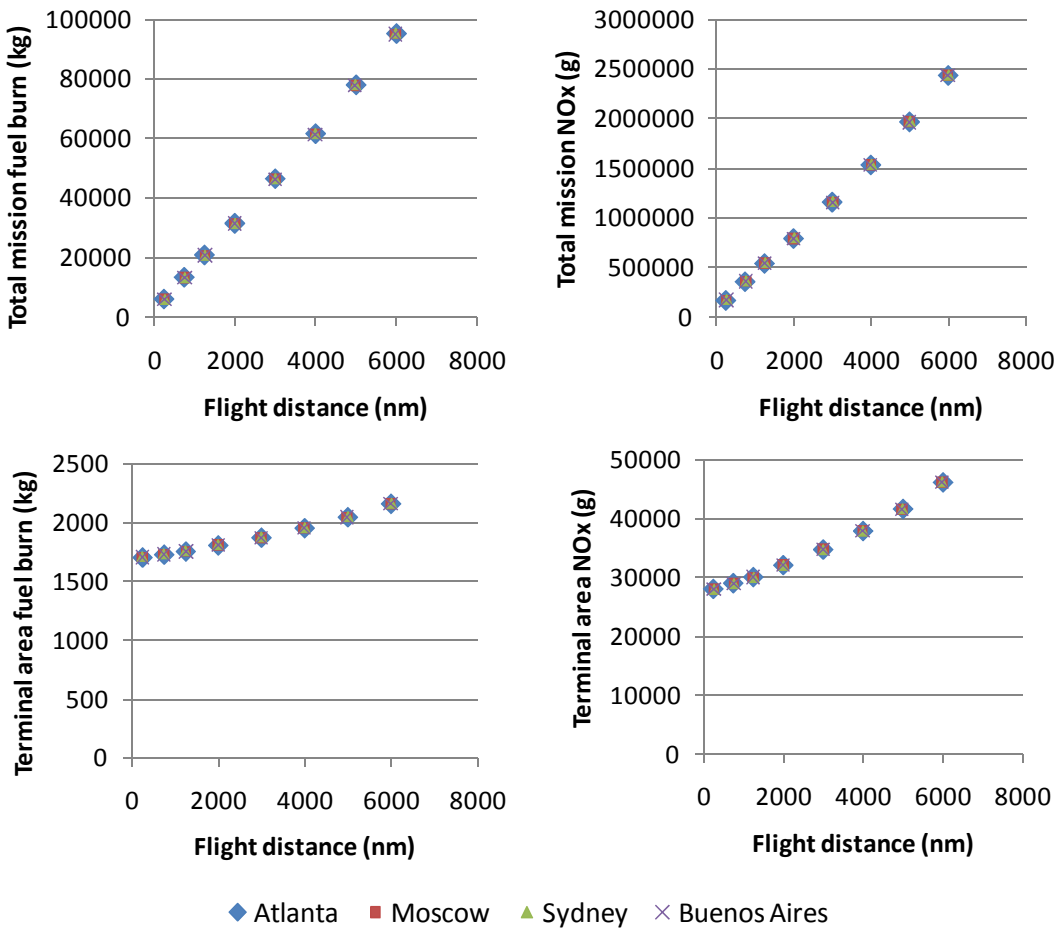

Figure 37. Comparison of metrics with respect to departure/arrival location.

The results for these metrics do appear to be independent of origin and destination location, as Figure 37 shows. Indeed, the maximum percentage difference between any of origin airports for any of the metrics is 0.31%, and the average is 0.08%. Thus, the assumption that any unique OD pair can be represented by an operation of the same flight distance without regard to specific airport location is considered reasonable for the purposes of this work.

4.2.2 Flight Distance Bins

Once the assumption of considering OD pairs based on flight distance rather than unique combinations was made, the set of operations for the six weeks of 2006 flights

may be further simplified as a function of flight distance by grouping, or binning, the entire distribution of flights by range of flight distance. For instance, if all flights were binned into 20 nm increments, then flights between 0 nm and 20 nm would be in a bin, all the flights between 20 nm and 40 nm would be in a bin, and so on. Combined with the OD pair assumption, the advantage in binning the frequency distributions is that instead of having to handle each of these flights for any particular vehicle group, potentially only one flight needs to be handled for each bin, of which there may only need to be on the order of a few hundred. This raises two points that will be covered in this section: is anything lost by not directly modeling flight level details; and what size should the bins be to render the differences between a single representative flight within the bin and any other flight within the bin insignificant.

In contrast to the inventory analyses that are conducted on a tail number basis, flight level details are not directly modeled in order to improve run time in this work. Because the purpose of this method is more focused on investigating trends related to technology forecasting rather than changes in operations, flight level details are not directly modeled. These include weather impacts, airport specific factors (such as altitude and ambient conditions), and flight delay related factors on individual flights. Although these are not directly modeled, their aggregate effects are still accounted for in the methodology because they are still captured in the targets used to generate the surrogate fleet, which are the results of the six weeks of actual operations mentioned in Chapter 2. The test of how valid this treatment is will occur when the surrogate fleet approaches are tested for changes to the operations mix, which will exaggerate the impact of any flight differences as the frequency of certain flights is increased or decreased.

Another simple experiment was conducted within AEDT to shed light on this assumption. Again, a notional representation of a large twin-aisle aircraft was flown through a series of flights for each stage length representing where flights would occur around a representative flight for each bin size. An example of what this would look like for the four bin sizes as they would project around a flight distance of 750 nm is given in Table 8, along with the number of flights that would be required to cover the number of bins for each flight distance.

Table 8. Representative flights for bin sizes around 750 nm.

Projected bin size	Bin range	Representative flight within bin	Number of flights to cover range of flight distance
10 nm	741 nm - 750 nm	745 nm	836
20 nm	741 nm - 760 nm	750 nm	418
40 nm	720 nm - 760 nm	740 nm	209
100 nm	700 nm - 800 nm	750 nm	84

For each bin size, a representative flight in the center of the bin is flown. For this experiment, the difference in metrics between this representative flight and flights at the edges of the bin range are evaluated. The results of this experiment are illustrated in Figure 38. Note the difference in scale between the total mission metrics and the terminal area metrics. As can be seen, all percentage differences between metrics are fairly close to zero, with the exception of total mission fuel burn and total mission NO_x at 250 nm, which is still within a reasonable 3% for the 10 nm and 20 nm bins. This is almost to be expected because of the relatively low magnitude of these metrics at such low flight distances; in fact the raw difference in total mission fuel burn for the 20 nm bin around 250 nm is only 166 kg. As bin size increases to 40 nm and 100 nm, differences at 250 nm double and become more significant, and these options for bin size would not make good assumptions.

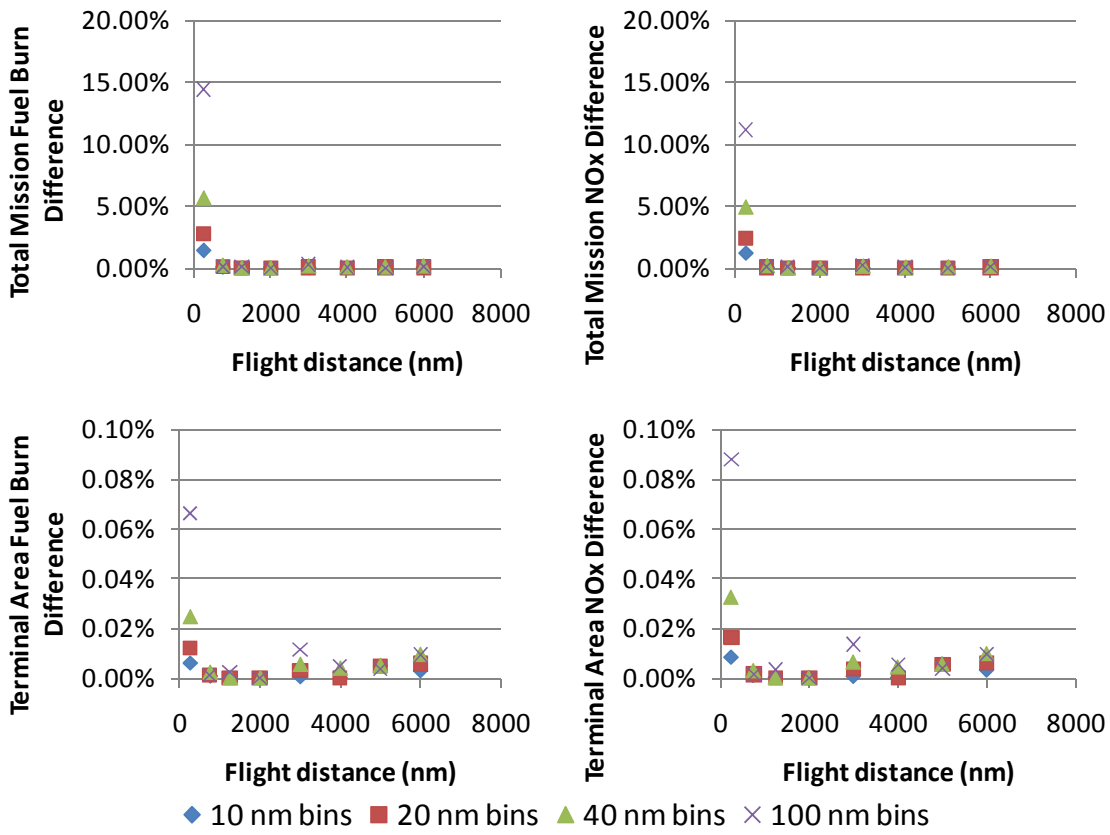

Figure 38. Comparison of bin size effects on metrics.

For the purpose of this work, the 20 nm bin size was chosen because of its reasonable accuracy and the fact that it requires half the number of flights to cover the entire spectrum of flight distances when compared to the 10 nm bin size. Thus, the roughly 50,000 flights for a particular capability group are now reduced to 418 flights. This is significant, because potential vehicle designs, of which there may be tens of thousands in any particular DOE, will need to be run through this set of operations.

4.3 Accuracy Requirements

In order to define acceptance criteria for this work and the experimental results herein, accuracy requirements must be discussed in the context of current fleet evaluation techniques. Because of the assumption designating AEDT as the "gold standard" for this

work, the assessment process that has been undertaken to validate that tool and the legacy tools that led to its development provides informed guidance on the level of accuracy that must be attained here. AEDT was developed with the desire to be able to accommodate a wide range of potential applications with different accuracy requirements. Thus, depending on the fidelity of inputs used for it, the level of accuracy may change. An example of such a change that may be expected is in how the detail of results of a preliminary technology assessment may vary from that of an inventory analysis. The most recent description of the assessment of AEDT was given by Noel et al.,[125] and will be reviewed here. Assessment of AEDT has been pursued through a number of different avenues, including examination of sample problem trends, comparison to benchmark data, expert review, and sensitivity analysis.

One way of assessing AEDT and the legacy codes that form its backbone is through comparison with benchmark operational data, which may include empirically gathered information like computer flight data recorder information and airline reported fuel burn for emissions, as was done for SAGE when validated by CAEP,[126] and through comparisons with data conducted by SAE for INM and EDMS.[121] However, such data may also be proprietary in certain cases and not available for incorporation into analytical models, which is why multiple avenues for assessment are being pursued.

Because of its potential to have a broad range of applicability, review by multiple groups of experts both domestically and internationally has provided another forum for the assessment of AEDT throughout the course of its development. The customer requirements that provided the impetus for the development of AEDT itself was in the form of an expert review conducted by the National Academy's Transportation Research

Board in 2004.[60] Two more expert review groups have guided the development of AEDT since that time: the Design Review Group, which is comprised of an international collection of members of government, industry, and academia who refine AEDT's requirements and design, and CAEP. Review by CAEP occurs in three phases, which are a thorough documentation of model capabilities to assess AEDT's ability to conduct anticipated CAEP analyses; comparison of AEDT results with benchmark data; and the execution and analysis of sample problems of interest. As part of documentation of modeling capabilities for international acceptance, CAEP verifies that AEDT results are compliant with the European Civil Aviation Conference's standards on a flight segment basis. Finally, parametric sensitivity and uncertainty analyses of AEDT are conducting to develop a rank ordering of the most important assumptions and limitations and to quantify uncertainty, resulting in an assessment report that can guide future AEDT enhancements by providing a measurable approach on which to base future model investment.

As described, AEDT has been very thoroughly evaluated for accuracy. For the purpose of the current work, which focuses on rapid evaluation of fleet-level environmental metrics and uses AEDT as the gold standard, the accuracy of AEDT in calculating fleet level metrics is looked to for the purpose of determining an acceptable amount of accuracy. The accuracy of AEDT and its backbone legacy tools in calculating aggregate fleet-level metrics when using a current day forecast in comparison to the actual fleet has been documented to be on the order of ±3-6%.[25,127]

In choosing acceptance criteria for the surrogate fleet methodology, there are tradeoffs between accuracy, speed, and the ability to model variations in operations mix

and technology. In the case of varying both operations and technologies simultaneously, which could represent the least accurate case, the acceptance criteria should still be within the bounds of the accuracy of the AEDT fleet. This would be the scenario for testing Hypothesis 3. However, when testing the methodology for matching the reference fleet with reference operations or the reference fleet with changes in operations, which should be "simpler," the methodology would be expected to be more accurate. This would be the scenario for Hypotheses 1 and 2. Because the surrogate fleet methodology represents an approximation of modeling the entire fleet, a ±1% difference between its fleet-level metrics and those of AEDT is assumed to be acceptable for matching reference operations in testing Hypothesis 1. When using a future forecast to simulate potential future scenarios to test Hypothesis 2, which introduces more potential uncertainties, the acceptable bound of accuracy for the surrogate fleet is increased to ±3%. When evaluating the impact of future technologies for Hypothesis 3, this accuracy bound is retained between the surrogate fleet approaches and the AEDT results of a validation fleet that will be described later in this chapter. Finally, when evaluating future technologies with a simultaneous variation in operations, the acceptable bound of accuracy is assumed to be ±4%. With these assumed bounds, the error between the surrogate fleet and the actual fleet should always be within ±5% of the AEDT fleet. These measures of accuracy are assumed to be adequate to provide exit criteria when evaluating the experimental results of the surrogate fleet methodology. The benefit of making this tradeoff to construct a surrogate fleet will be shown to be a markedly decreased in development time and runtime compared to traditional methods.

4.4 Experimentation

Because vehicles exist across a different range of capabilities, the commercial fleet will be segmented into fleets of interest for each capability grouping. As a starting point, all of the in-production, in-service airframes of the reference fleet studied in this work, which include aircraft with greater than 50 passengers, were gathered[45,46,47,48] and are shown in Table 9.

Table 9. In-production, in-service airframes.

CRJ700	ERJ190	A321-2	B767-3	A340-6
CRJ700-ER	A318	B737-600	B767-3ER	B777-2
CRJ700-LR	A319-1	B737-700	A330-2	B777-2ER
CRJ900	A320-1	B737-800	A330-3	B777-2LR
ERJ170	A320-2	B767-2	A340-2	B777-3
ERJ170-LR	A321-1	B767-2ER	A340-3	B777-3ER

An initial example of how the reference fleet of in-production aircraft may be grouped by capability is given in Figure 39. The points on the plot represent the maximum payload for each airframe within the reference fleet, along with the maximum range with that payload, which is also known as the R1 point for a particular aircraft. These metrics were chosen for this plot because they provide a visualization analogous to a payload-range diagram.

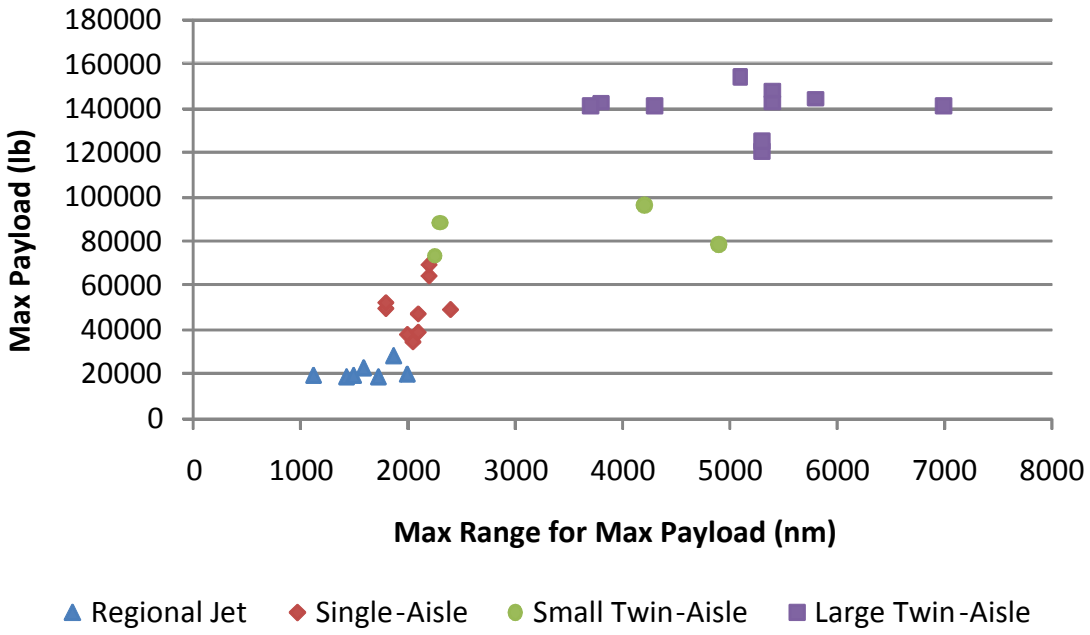

Figure 39. Reference fleet visualized in two metrics.

As can be seen in the plot, there do seem to be natural groupings within the fleet that may be leveraged when selecting a physics-based vehicle to represent portions of the fleet, and in Figure 39, the fleet has indeed been segmented into four groups: regional jets, single-aisle, small twin-aisle, and large twin-aisle. The two small twin-aisle airframes closest to the large twin-aisle group represent the Boeing 767-200ER and Boeing 767-300ER, and the justification for their inclusion in the large twin-aisle group is discussed with Figure 40 below. A similar justification will be illustrated for the two small twin aisle airframes closest to the single-aisle group, the Boeing 767-200 and Boeing 767-300. However, it is clear that examination of only two metrics alone will not provide sufficient information with which to characterize the fleet into capability groups.

Only a visualization of the capability of the aircraft represented by two metrics is presented in Figure 39. In order to judge whether the selected capability groups are appropriate, other metrics descriptive of the geometry and performance must be

compared among these aircraft. A line plot that compares normalized values of eight performance and geometry metrics compiled with data from available airport planning documents for the reference fleet is provided in Figure 40.

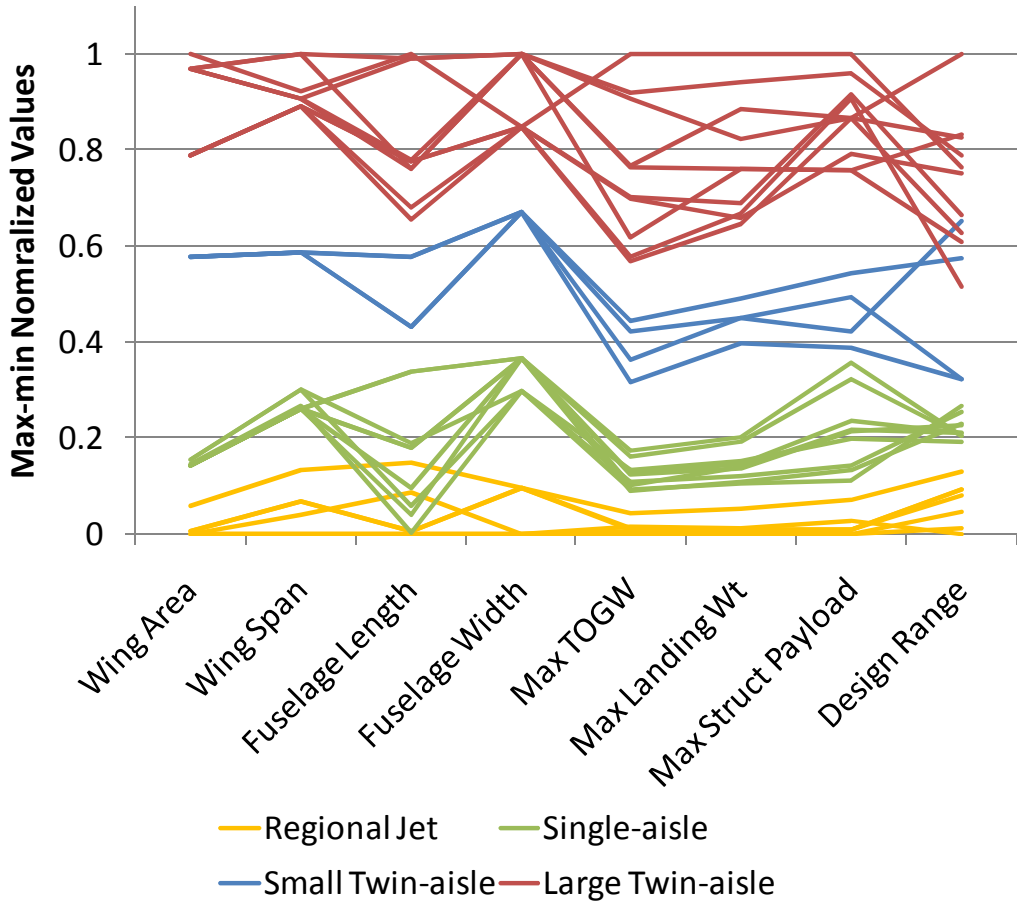

Figure 40. Metric comparison among reference fleet aircraft.

As can be seen in this figure, there again is clear segmentation that is captured by the groups across most of the metrics, and the overlapping that does exist in metrics across the capability groups may be explained. The largest regional jets, the CRJ900 and the ERJ190, have slightly longer fuselage lengths than the smallest single-aisle aircraft, the A318 and Boeing 737-600; however the regional jets are still clearly smaller when looking at weight and wing area.

As was seen with the range at R1 illustrated in Figure 39, the design ranges of the small twin-aisle group also overlap with those of the large twin-aisle group. Both of these points will be addressed here and clarified with the data in Figure 40. In Figure 39, it is apparent that although the ranges at R1 for two of the extended range versions of the small twin-aisle aircraft, the Boeing 767-200ER and Boeing 767-300ER, are comparable to those of the large twin-aisle group, their maximum payloads and geometric dimensions, as illustrated in Figure 40 are significantly smaller, necessitating inclusion in a small twin-aisle group. Similarly, the other small twin-aisle aircraft have ranges at R1 comparable with those of the single-aisle group; however they clearly have much higher design range, payload capacity, weights, and dimensions, which create a clear distinction between the two groups.

The reference fleet aircraft from Table 9 are listed in Table 10, but this time they are categorized by differences visualized in Figure 39 and Figure 40, and they are listed with their engine derivatives. Thus, they include 21 unique in-production and in service (as of 2006) engine/airframe combinations for the regional jet class, 54 for the single-aisle group, 35 for the small twin-aisle group, and 71 for the large twin-aisle group. By considering the in-production vehicles of these classes, the entire in-production reference fleet is spanned, and the generality of the method's ability to cover all aircraft in the fleet may be evaluated.

Table 10. Categorized in-production reference fleet aircraft.

Regional Jet					
CRJ700	CF34-8C1	CF34-8C1 Block 1			
CRJ700-ER	CF34-8C1	CF34-8C1 Block 1			
CRJ700-LR	CF34-8C5				
CRJ900	CF34-8C5	CF34-8C5			
ERJ170	CF34-8E5	CF34-8E5			
ERJ170-LR	CF34-8E5				
ERJ190	CF34-10E5	CF34-10E5A1	CF34-10E6		
Single Aisle					
A318	CFM56-5B8/P				
A319-1	V2527-A5	CFM56-5B6/2	CFM56-5B6/2P	CFM56-5B5/P	CFM56-5B6/P
	V2522-A5	V2524-A5	CFM56-5A4	CFM56-5A5	CFM56-5B7/P
A320-1	CFM56-5-A1				
A320-2	CFM56-5-A1	CFM56-5A3	V2500-A1	V2527-A5	CFM56-5B4
	CFM56-5B4/2	CFM56-5B4/P	CFM56-5B4/2P		
A321-1	V2530-A5	CFM56-5B2	CFM56-5B1/2	CFM56-5B1/P	CFM56-5B2/P
	CFM56-5B1/2P				
A321-2	V2530-A5	CFM56-5B1/P	CFM56-5B3/P	V2533-A5	CFM56-5B3/2P
B737-600	CFM56-7B20	CFM56-7B22	CFM56-7B20/2		
B737-700	CFM56-7B20	CFM56-7B24	CFM56-7B22	CFM56-7B26	
B737-800	CFM56-7B26	CFM56-7B24	CFM56-7B27	CFM56-7B26	
Small Twin Aisle					
B767-2	CF6-80A	CF6-80A2	CF6-80C2B2F		
B767-2ER	CF6-80A2	CF6-80C2B2	CF6-80C2B2F	CF6-80C2B4	CF6-80C2B4F
	PW4056	PW4060			
B767-3	CF6-80A2	CF6-80C2B2	CF6-80C2B2F	CF6-80C2B4F	CF6-80C2B2F
	CF6-80C2B7F	PW4056	PW4060		
B767-3ER	CF6-80C2B2F	CF6-80C2B4	CF6-80C2B6	CF6-80C2B6F	CF6-80C2B6
	CF6-80C2B2F	CF6-80C2B6F	CF6-80C2B7F	CF6-80C2B7F	PW4056
	PW4060	PW4x52	PW4x62	RB211-524H	
Large Twin Aisle					
A330-2	CF6-80E1A2	CF6-80E1A4	CF6-80E1A3	PW4168A	PW4168A
	Trent 772				
A330-3	CF6-80E1A2	CF6-80E1A2	CF6-80E1A4	CF6-80E1A3	PW4164
	PW4168	PW4168A	PW4168A	Trent 772	Trent 768
	Trent 772				
A340-2	CFM56-5C2	CFM56-5C3			
A340-3	CFM56-5C2	CFM56-5C3	CFM56-5C4	CFM56-5C4/P	
A340-6	Trent 556-61				
B777-2	GE90-76B	GE90-85B	PW4074	PW4077	PW4090
	Trent 875	Trent 877	Trent 884	GE90-76B	
B777-2ER	GE90-85B	GE90-90B	GE90-85B	GE90-90B	GE90-92B
	PW4090	Trent 884	Trent 892	Trent 895	GE90-90B
B777-2LR	GE90-110B1				
B777-3	Trent 892	PW4090	PW4098		
B777-3ER	GE90-115B				

The experiments that were conducted are outlined here and their detailed descriptions follow. The acceptability of Hypothesis 1 is evaluated through the results of Experiment 1, which involves the implementation of each of the surrogate fleet methods proposed in Hypothesis 1 on the fleet of interest for the parametric correction factor approach, the average replacement approach, and the best-in-class approach, respectively. Experiment 2 will test Hypothesis 2 by evaluating the performance of the acceptable (in the context of the reference operations of Hypothesis 1) surrogate fleet approaches across large variations of operations mixes to simulate potential future fleet scenarios. Experiment 3 will test Hypothesis 3 by determining the ability of each acceptable surrogate fleet approach to capture the impact of a technology suite infusion.

4.4.1 Experiment 1 – Surrogate Fleet Approaches with Reference Operations

Experiment 1 is the application of each of the surrogate fleet approaches to the reference fleet as it is described and categorized into the capability groups of Table 10: the regional jets, single-aisle aircraft, small twin-aisle aircraft, and large twin-aisle aircraft. The ability of each surrogate fleet approach to match the performance of the aggregate performance of the aircraft in each capability group is evaluated through comparison with the reference fleet, composed of the actual operations and performance of the AEDT fleet through six weeks of 2006 flights. The exit criteria for success in this experiment are to match the aggregate performance of the reference fleet within an acceptable difference of ±1% for each capability group for each of the metrics of interest, which is based on observations of the acceptable accuracy of current fleet evaluation approaches.

4.4.1.1 Parametric Correction Factor Approach

The first experiment to be described here is the parametric correction approach, an overview of which was provided in Figure 24. The steps of conducting Experiment 1 with the parametric correction factor approach are as follows:

- Collect the AEDT database input files for each engine/airframe combination given in Table 10
- Generate results for total mission and terminal area fuel burn and emissions for each aircraft across the entire span of reference operations using AEDT
- Choose a reference vehicle model within each capability group from within already developed and validated EDS models and generate total mission and terminal area fuel burn and emissions across span of reference operations
- With this data and a reference vehicle for each capability group, identify form of parametric correction factors as a function of operational parameters
- Generate database of parametric correction factors for each aircraft in Table 10
- Use the parametric correction factors in conjunction with the reference set of operations to attempt to match results of the reference fleet.

One exception to this procedure was made for the regional jet group. The available regional jet models in the AEDT database for specific engine/airframe combinations did not match up well with the listed operations for the six weeks of 2006 flights, i.e. there were aircraft in the six weeks of flights that lacked a corresponding AEDT model, and there were AEDT database models that had no operations. For this capability group, instead of attempting to develop the correction factors to correct the results of the EDS

model to those of database model, they were corrected to the six weeks' results. The selected EDS models for each seat class are provided in Table 11.

Table 11. Reference EDS models.

Capability Group	Reference Airframe/Engine Model
Regional Jet	CRJ 900 / CF34-8C5
Single-aisle	Boeing 737-800 / CFM56-7B26
Small Twin-aisle	Boeing 767-300ER / CF6-80C2
Large Twin-aisle	Boeing 777-200ER / GE90-94B

4.4.1.1.1 Developing Correction Factor Form

After the AEDT database results and the AEDT results for each reference EDS vehicle have been generated, they may be related to each other through the development of parametric correction factors that are functions of operational metrics, represented by ΔY in Figure 25. Developing the form of these factors required careful consideration of what the operational input parameters are available within AEDT and the mathematical form of the parametric correction factors.

The operational factors that are available to vary in AEDT for the purpose of creating a parametric correction factor are cruise altitude, flight distance, and takeoff gross weight. However, these three factors are not completely independent. In AEDT, the takeoff gross weights for a particular aircraft over a set of operations are assumed to be functions of the stage lengths of the missions, an example of which is given in Table 12 for a large twin-aisle aircraft. As can be seen in this table, because TOGW is assumed to vary with stage length, it may also be considered to be dependent on the flight distance.

The distribution of operational cruise altitudes is also heavily dependent on flight distance. An illustration of how the distributions of potential flight altitudes for ranges of flight distances shift is provided in Figure 41. As flight distance increases, the altitude distributions shift toward higher cruise altitudes.

Table 12. TOGW versus stage length for a large twin-aisle aircraft.

Stage Length	Range of Flight Distance (nm)	Assumed TOGW (lb)
1	0-500	410289
2	501-1000	424966
3	1001-1500	440182
4	1501-2500	467227
5	2501-3500	500718
6	3501-4500	536411
7	4501-5500	574678
8	5501-6500	615266
9	>6500	679901

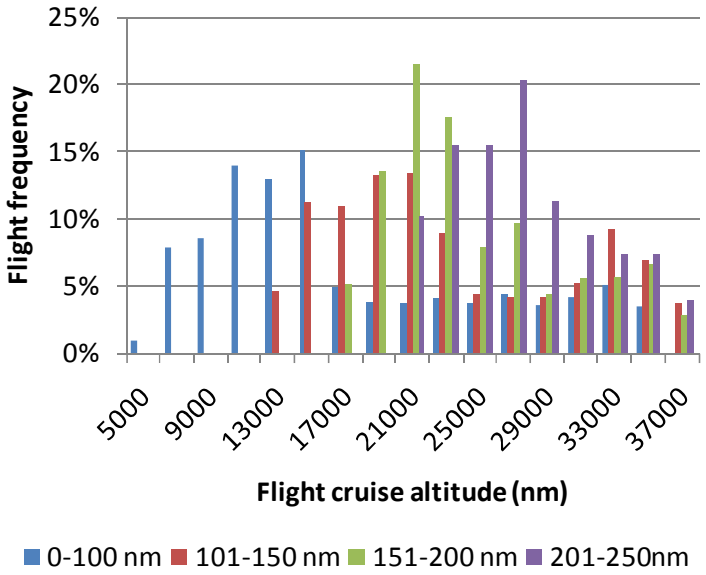

Figure 41. Distribution of flight altitudes for selected flight distances.

Because flight distance causes variations in the other two operational parameters, it is clearly the most important factor around which to formulate a parametric correction factor among the three AEDT operational parameters that may be varied.

Next, the mathematical form of the parametric correction factor must be developed. As a first step, linear statistical regressions of varying order were considered because of their simplicity to develop these factors to correct the results of the EDS reference vehicle to match those of each aircraft in the AEDT fleet as a function of flight distance. Their

appropriateness for this task was evaluated by observing how well they are able to match the aggregated fuel burn and emissions results of each vehicle for a simple uniform operational distribution across the entire range of flight distances. This wellness is defined as being able to capture the aggregate results within the aforementioned 1%, and because multiple regressions may be able to capture the aggregate results within this accuracy, the sum of squares error, as given previously in Eq. (3) may also be compared across regressions of different orders to determine how well they are capturing values across the entire distribution of flight distances.

First and second order linear models were constructed to determine their adequacy for this task. The forms of these equations, which represent the corrected shift in metrics ΔY previously given in Eq. (4), are provided in Eq. (6) and Eq. (7), respectively, were R is the flight distance and a_i represent the correction factors themselves.

$$\Delta Y = a_0 + a_1 \cdot R \tag{6}$$

$$\Delta Y = a_0 + a_1 \cdot R + a_2 \cdot R^2 \tag{7}$$

An example of how these two forms were evaluated that is representative of their behavior across all aircraft in the fleet of interest will be described here. In this example, the fuel burn and emissions results of the EDS reference vehicle for the single-aisle category group are being matched to those of the AEDT database model of the Boeing 737-600 airframe with CFM56-7B20 engines across a range of flight distances representing their range of operations. Doing so results in a set of coefficients representing the correction factor for each of the four metrics of interest: eight for the

first order and 12 for the second order. After applying both the first order and second order linear models of Eq. (6) and Eq. (7) to each of the total mission and terminal area fuel burn and emissions, their respective abilities to correct the reference vehicle results to minimize differences with the AEDT database model were evaluated and are quantified in Table 13. In terms of the raw percentage difference in aggregate values, the first order models performed better than the second order models, but they were both well within the acceptable error of ±1%. However, in terms of the sum of squares error, the second order models performed better than the first order models, particularly for the total mission metrics, which is expected because these account for differences across a broader range of operations. Based on these results, the second order models of the type shown in Eq. (7) were used as the form of the parametric correction factors for this work.

Table 13. Evaluation of first and second order linear models.

	First order		Second order	
	Difference in Aggregate Values (%)	**Sum of Squares Error**	**Difference in Aggregate Values (%)**	**Sum of Squares Error**
Total Mission Fuel Burn	-2.66E-06	1300 lb	-5.11E-03	816 lb
Total Mission NOx	4.20E-06	45510 g	-2.04E-04	28173 g
Terminal Area Fuel Burn	-4.71E-06	22 lb	-1.72E-02	21 lb
Terminal Area NOx	-1.16E-05	857 g	-1.29E-03	850 g

4.4.1.1.2 Calculating Correction Factors

As described in Chapter 3 and above, the Parametric Correction Factor approach was applied to all four capability groups, using the EDS reference aircraft listed in Table 11 as the baseline vehicles. As a representative example of the parametric correction factor results for a single vehicle, Figure 42 shows the total mission fuel burn results for the EDS reference vehicle for the single-aisle capability group with correction factors applied to match the AEDT 737-600 airframe with CFM56-7B20 engines. The fact that the

parametric correction factor approach is capable of creating a much closer match of the EDS results with the AEDT results than when uncorrected is shown by the data graphed in Figure 42, particularly at longer flight distances, where discrepancies in fuel burn are more apparent between the original EDS model and the AEDT model.

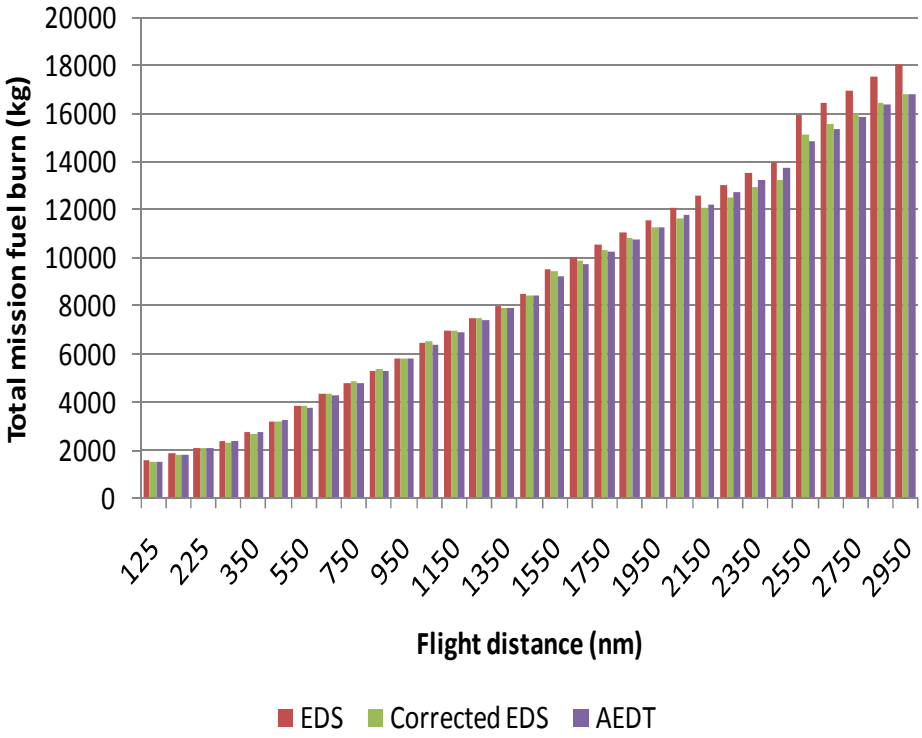

Figure 42. Total mission fuel burn result for single vehicle in fleet of interest.

The process of generating parametric correction factors is conducted for all four fleet metrics of interest for every aircraft in the fleet of interest. The result of this is a database of coefficients a_0, a_1, and a_2 corresponding to the correction factor ΔY previously given in Eq. (7) for each metric of interest for each vehicle in the reference fleet, to be used in conjunction with the appropriate reference vehicle in each capability group. These have been created using the vehicles in the AEDT reference fleet, and they may be validated through comparison with the six weeks of 2006 flights.

4.4.1.1.3 Results

Once correction factors for all aircraft and fleet metrics have been generated, it is then possible to examine how well this approach is able to capture the actual results of the six weeks of 2006 flights. The results for this set of reference operations are given in Figure 43 for the four fleet-level metrics of interest. The values for the differences in terminal area fuel burn and terminal area NO_x for the regional jet group are higher than for any other metric, yet still within 1%. As explained above, the procedure for the regional jets represented a deviation from the approach for the other capability groups in that the correction factors for this group were created using operational data instead of model data. The higher magnitude of difference may then have been caused by the fact that the operational data is sparser and less smooth over the entire range of flight distance when compared to the model data, leading in this case to a slightly poorer fit.

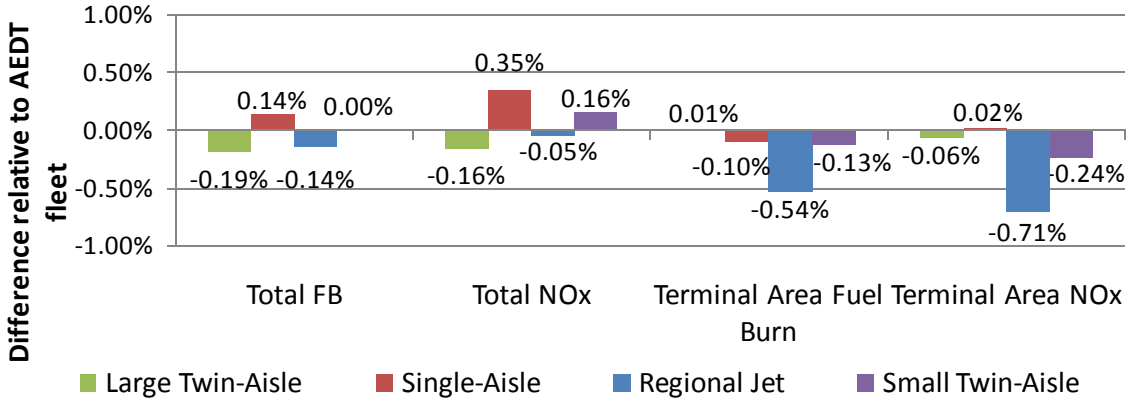

Figure 43. Parametric correction factor results for reference operations.

At this point, the performance of the surrogate fleet can be compared to that of the AEDT reference fleet across the range of reference operations and evaluated for acceptability, leading to acceptance or rejection of Hypothesis 1 for the parametric correction factor approach. As Figure 43 shows, using the parametric correction factor approach, the aggregate performance of the reference fleet is matched within 1% for all

capability groups and metrics of interest using the EDS reference vehicles. Therefore it may be concluded that this approach does satisfy acceptance of Hypothesis 1.

4.4.1.2 Average Replacement Approach

For the average vehicle approach, an overview of which was illustrated in Figure 26, the goal is to generate a single physics-based vehicle model that matches the aggregate results for the four fleet-level metrics of interest over the six weeks of 2006 flights for the capability groups of aircraft listed in Table 10. The steps of Experiment 1 for this approach are as follows:

- Choose a reference vehicle model within each capability group from within already developed and validated EDS models
- Use reference fleet data for aircraft in Table 10 to generate total mission and terminal area fuel burn and NO_x emissions targets for each capability group
- Conduct variable screening to identify input parameters with the greatest impact on total mission and terminal area fuel burn and NO_x emissions
- Execute a DOE to vary the significant input parameters
- Filter results to choose an average replacement vehicle closest to the fuel burn and emissions targets from DOE results
- Apply operational distribution of the entire capability group to the average vehicle
- Compare average vehicle results for fuel burn and NO_x emissions with aggregate results for the entire capability group

As with the parametric correction factor approach, the baseline models used for this approach are the same EDS reference vehicles given in Table 11. Target selection was

conducted for each capability group as presented in section 3.3.2.1. The next few sections provide details on the remainder of the experimental steps and the results.

4.4.1.2.1 Variable Screening

Prior to executing the larger design space exploration DOE to filter an average vehicle for each particular capability group, variable screening was executed to determine the input parameters with greatest influence on the fleet-level metrics. In this case, a two-level fractional factorial screening DOE was executed around each EDS reference vehicle to determine what input variables contribute most significantly to the variability of aggregate fleet metrics generated by the EDS vehicles in each capability group. The variables selected to vary in this exercise represented a wide range of 74 engine and airframe design variables. These variables are provided in Table 14. Note that the engine of the regional jet reference aircraft does not have an LPC. Therefore, there are ten variables that do not need to be considered for the regional jet, and there are two more whose definitions change slightly. These are also indicated in Table 14. The ranges for all input variables are provided in Appendix D.

Once ranges for these variables were appropriately defined for each DOE, corresponding to a capability group with baseline reference vehicle, the screening DOEs were executed in the M&S environment. The DOE results were collected and the inputs were evaluated for effect significance as described in Chapter 3 and Appendix B. Variable screening was conducted across each of the four output metrics of interest to include the significant variables relating to each output, forming a single subset of variables for each capability group. Exclusion of a major variable after screening across each of the four output metrics and including all significant parameters is improbable. For

the purpose of effect screening in this work, orthogonalized parameter estimates were employed to identify the potentially significant input parameters for each capability group because of their ease of implementation and interpretation of variable selection for DOE creation. This variable selection does not preclude the need to observe and possibly tweak other variables to tune the average vehicle's behavior as necessary. Selected variables were then varied as part of a larger design space exploration to generate potential average replacement vehicle for evaluation against fleet-level targets.

Table 14. Input parameters varied for screening.

SLS Thrust	HPC Max 1st Stage PR	LPT Flow Coefficient
Burner Time	HPC Stall Margin	LPT Loading
Customer Bleed	HPC Specific Flow	LPT Exit Mach Number
Burner Pressure Drop	HPC Pressure Ratio	LPT Nonchargeable Cooling
Burner Efficiency	HPT Chargeable Cooling	LPT Radius Ratio
Bypass Nozzle Pressure Drop	HPT Efficiency	LPT Solidity Factor
HPT-LPT Duct Pressure Drop	HPT Flow Coefficient	Core Nozzle Plug Length Ratio
HPT-LPT Duct Length/Height	HPT Loading	Design Reynolds Number
LPC-HPC Duct Pressure Drop†	HPT Exit Mach Number	Design HPC Reynolds Number
LPC-HPC Duct Length/Height†	HPT Nonchargeable Efficiency	Maximum T4
LPT-Core Nozzle Duct Pressure Drop	HPT Solidity Factor	Horizontal Tail Thickness to Chord
LPT-Core Nozzle Duct Length/Height	Horsepower Extraction	Vertical Tail Thickness to Chord
Splitter-LPC Duct Pressure Drop*	Bypass Nozzle Area	Takeoff Thrust
Splitter-LPC Duct Length/Height*	Core Nozzle Area	Top of Climb Thrust
Extraction Ratio	Engine Weight Factor	Ratio of Top of Climb and Design Engine Flow
Fan Efficiency	LPC Area Ratio*	Wing Aspect Ratio
Fan Tip Speed	LPC Efficiency*	Wing Sweep
Fan Stall Margin	LPC Max First Stage PR*	Wing Area
Fan Specific Flow	LPC Hub to Tip Ratio*	Wing Glove Area
Lift Dependent Drag Factor	LPC Stall Margin*	Wing Break Location
Lift Independent Drag Factor	LPC Solidity Factor*	Wing Taper Ratio
Fan Pressure Ratio	LPC Specific Flow*	Wing Average Thickness to Chord
HPC Area Ratio	LPC Pressure Ratio*	Number of Passengers
HPC Efficiency	LPT Chargeable Cooling	Passenger Cabin Length
HPC Tip Speed	LPT Efficiency	

*Not included in Regional Jet †Splitter-HPC in Regional Jet

For visualization purposes, Pareto charts for each metric that contributes to the highest 80% of cumulative orthogonalized parameter estimates for each capability group are provided in Appendix E. Because each reference vehicle represents different engine architectures, differences exist between each vehicle; however, there are a number of

interesting trends that may be observed from these results. As would be expected, component efficiencies are very prevalent in the set of significant inputs for all metrics, as are vehicle parameters related to weight and drag, which include number of passengers, thickness to cord ratios of the wing and tails, and the aerodynamic drag factors. Additionally, the NO_x results tend to show the high significance of factors that impact T3, the temperature at the combustor entrance, most notably among them being the pressure ratios of the compression elements. After the significance of the entire set of potential input factors has been evaluated, a single set of input parameters for each capability group may be identified by including the significant factors through all four metrics to create a design space exploration DOE. These include 44 variables for the regional jet, 53 variables for the single-aisle, 40 variables for the small twin-aisle, and 46 variables for the large twin-aisle. Listings of each of these sets of input parameters are provided in Appendix F. The effect screening may be considered successful because the original list of 74 variables has been reduced, allowing design space exploration to be conducted more thoroughly.

4.4.1.2.2 Design Space Exploration

A space-filling Latin Hypercube DOE was selected to thoroughly cover the design space.[122] A set of 10,000 cases was run using each EDS reference vehicle as the baseline, varying engine and airframe design variables for each capability group as given in Appendix D to generate potential average replacement vehicles. The fuel burn results for each DOE case of a single-aisle group are presented in the context of their errors from the calculated fleet level targets in Figure 44. It is clear that through filtering, a point very close to zero error from the targets for both of the fuel burn metrics may be selected.

Filtering was conducted with the results to determine the vehicle that is closest to the aggregate results for the six weeks of 2006 flights for the aircraft in Table 10. In order to hit the targets for the NO_x metrics, a separate 1,000 case space-filling DOE was run using the best fuel burn case from the 10,000 case DOE and varying its NO_x correlation based on the bounds defined by the fleet of interest.

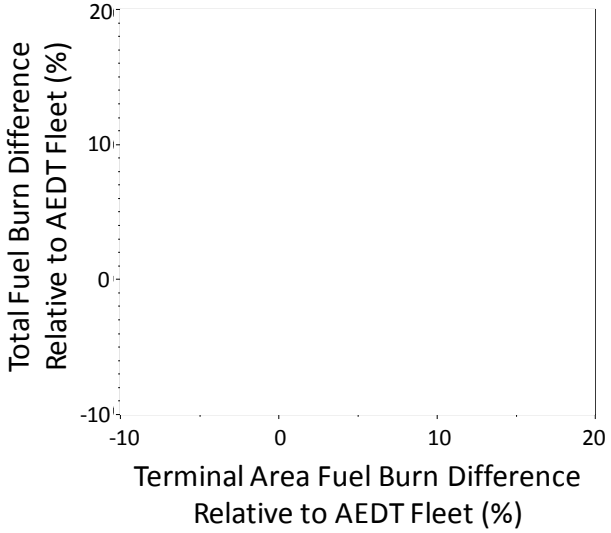

Figure 44. Fuel burn results from average vehicle DOE.

4.4.1.2.3 Results

The performance of these vehicles in reproducing the results of the reference operations was compared to the AEDT reference fleet and evaluated for their accuracy in comparison to the AEDT for reference operations, leading to acceptance or rejection of Hypothesis 1 for the average replacement approach. The results for all the fleet metrics in relation to the target for the fleet of interest are presented in Figure 45. The differences are generally higher than were seen in the same results for the parametric correction factor approach illustrated in Figure 43; however, all of the errors are within roughly 1%, demonstrating that the average replacement approach is capable of representing the baseline fleet of interest within the previously defined acceptable range of accuracy.

Therefore, the average replacement approach also satisfies the requirements to accept Hypothesis 1.

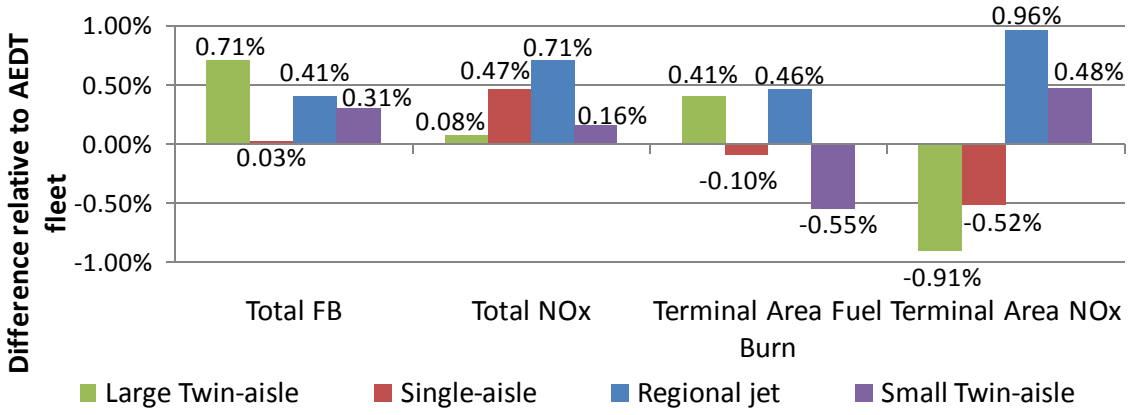

Figure 45. Average replacement results for reference operations.

4.4.1.3 Best-in-Class Replacement Approach

The best-in-class replacement approach is essentially a simplified form of the average replacement approach in which baseline vehicles, in this case the EDS reference vehicles, are selected to represent each capability group. The experimental steps for this approach are as follows:

- Choose a reference vehicle model within each capability group from within already developed and validated EDS models
- Use reference fleet data for aircraft in Table 10 to generate total mission and terminal area fuel burn and NO_x emissions targets for each capability group
- Apply operational distribution of each entire capability group to the reference vehicle
- Compare reference vehicle results for fuel burn and NO_x emissions with aggregate results for the entire capability group

The same fleet target for the best-in-class replacement approach was generated using the AEDT results for the aircraft in Table 10 for each aircraft across the entire span of reference operations. The result of this approach, in terms of error from the fleet of interest targets, is presented in Figure 46.

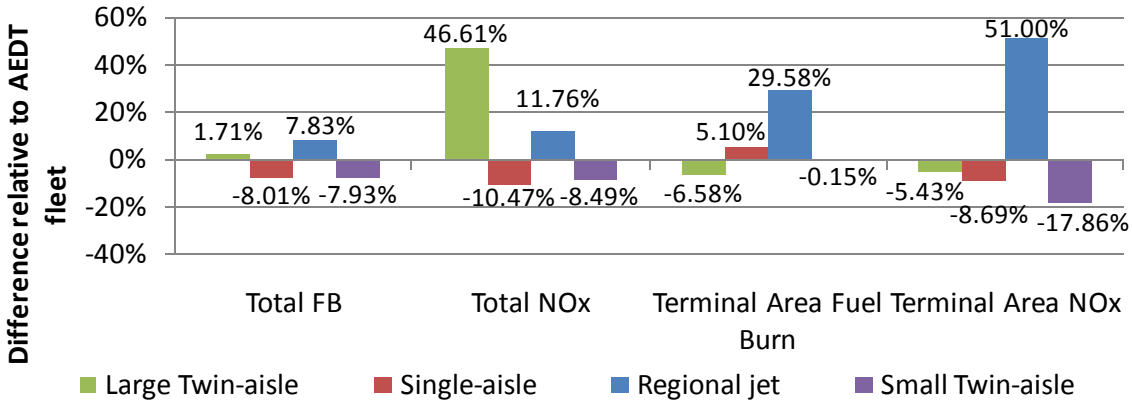

Figure 46. Best-in-class replacement approach results for reference operations.

Note the change in magnitude of the vertical axis in relation to Figure 43 and Figure 45. As is clear from the results, this approach has significantly higher errors compared to the fleet of interest than the other two approaches. In fact, of the four metrics for the four capability groups, only one of them, the terminal area fuel burn for the small twin-aisle group, is within the acceptable ±1% bounds of accuracy. There may be certain applications for which the simplicity of this approach outweighs capturing the fleet of interest with higher accuracy; however, it on its own would clearly result in rejection of Hypothesis 1.

Before wrapping up Experiment 1, a quick examination of how sensitive these results are to changes in operational distributions was conducted. The single-aisle average replacement results were evaluated for the reference operations and two other operational distributions: one in which the frequency of all flights below 510 nm were doubled, and

another in which the frequency of all flights above 510 nm were doubled. The value of 510 nm was chosen for this examination for two reasons: as Figure 47 shows, a large cluster of local minima occurs below 510 nm in the distribution of single-aisle flights from the set of reference operations, and secondly, flight bin distances are defined in intervals of 20 nm beginning at a value of 50 nm.

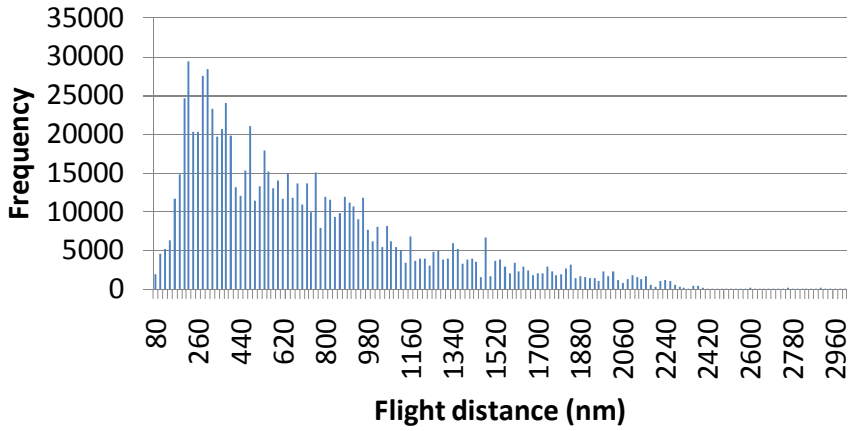

Figure 47. Distribution of single-aisle flights from the set of reference operations.

These results of this examination are provided in Figure 48. The results computed with the two variations are different from the results computed with reference variations; however, only the result for total NO_x for the doubled frequency of flights below 510 nm was greater than 1%. The changes in magnitude of results is caused by the fact that the average replacement vehicles are developed to match results for reference operations, and underscores the need to determine the effectiveness of this approach in capturing variations in operations, which will be done in Experiment 2.

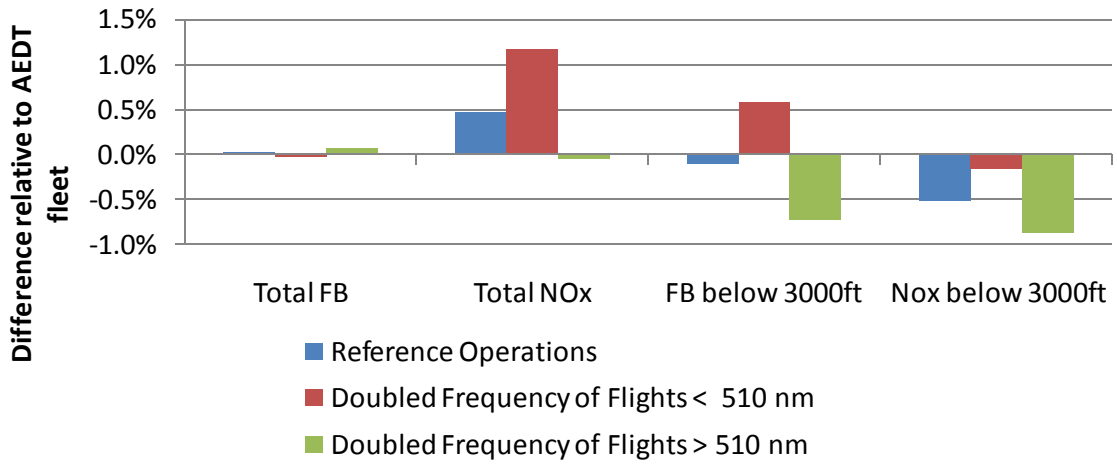

Figure 48. Sensitivity of single-aisle average replacement to variations in operations.

4.4.1.4 Experiment 1 Results Summary

The results of Experiment 1 are significant because they shows that the parametric correction factor approach and the average replacement approach are capable of representing a fleet of interest with a limited number of physics-based aircraft within an acceptable range of accuracy, thereby each leading to acceptance of Hypothesis 1. Indeed, they performed significantly better than the "control" experiment of the best-in-class replacement approach, the results of which were significant because they were shown to not be within an acceptable range of accuracy. In addition to accuracy, the execution time that was required to achieve the results in this experiment is also of note. Generating parametric correction factors for each aircraft in the fleet of interest using the methods developed here requires roughly an hour, at which point they may be queried to produce fleet-level results in a matter of seconds. Once matured, development of an average replacement vehicle for any given capability group required on the order of a month to complete. However, once created, each average replacement vehicle may easily be incorporated into rapid scenario generation through the use of surrogate models, such

as regression equations, which again can be queried to produce fleet-level results within seconds and will be discussed in the methodology demonstration experiment later in this work. The parametric correction factor approach and the average replacement approach are therefore well suited to be used in applications that require close to real-time analysis.

4.4.2 Experiment 2 – Surrogate Fleet Approaches Away from Reference Operations

Once the surrogate fleet approaches were generated and validated for the reference set of operations, the performance of the developed models away from that reference set must be evaluated to accept or reject Hypothesis 2. The development of the parameterized operations described in Chapter 3 allows a structured, space filling DOE to be used to create large numbers of sample distributions by varying the scalar values that are applied to the baseline set of operations. The experimental steps for this are as follows:

- Composite beta distributions are generated to represent the scalars applied to reference fleet operations
    - Three component beta distributions are used to ensure sensitivity in the low, middle, and upper ranges of flight distances
    - The magnitude of the scalar for each flight bin are allowed to vary between 0.5 and 2, representing a halving or doubling of flight frequency at each flight distance bin (explained in paragraph below)
    - Space-filling Latin hypercube DOE is used to vary the parameters α and β of each component distribution
    - The ranges for the α and β parameters for operations variation are between 0.5 and 5, which, while difficult to illustrate visually,

effectively covers a wide range of flight distances for potential future fleet scenarios, which may be observed in Figure 67 of Appendix A

- Each surrogate fleet approach is used to generate environmental metrics for a single flight within each operational bin for each capability group
- Results for each operational distribution are generated by summing the product of the scalars and the environmental metrics at each operational bin for each approach
- DOE results are compared to the AEDT reference fleet values for the same corresponding operational distributions
- Comparing these results allow the distribution of percentage difference between the surrogate fleet approaches and the AEDT reference fleet to be generated in order to accept or reject Hypothesis 2

The range of variation of the scalar of each flight bin was chosen based on traffic growth rates forecasted by manufacturers.[6,7] At an upper bound of 5% annual growth, after 20 years the traffic will have doubled. Although traffic is not forecast to decline globally, 0.5 was selected as a minimum bound to determine robustness to decreasing operations. The minima and maxima of the distributions of percentage difference are of interest because they define the bounds of the difference between the surrogate fleet approaches and the AEDT fleet across all of the potential operation distributions. For display purposes, these resulting extremes will be represented by error bars superimposed on the results for the reference operations. This is depicted notionally in Figure 49, with a distribution of error difference on the left represented as a set of error bars on the right. In the interest of completeness, the full set of actual distributions is provided in Appendix E.

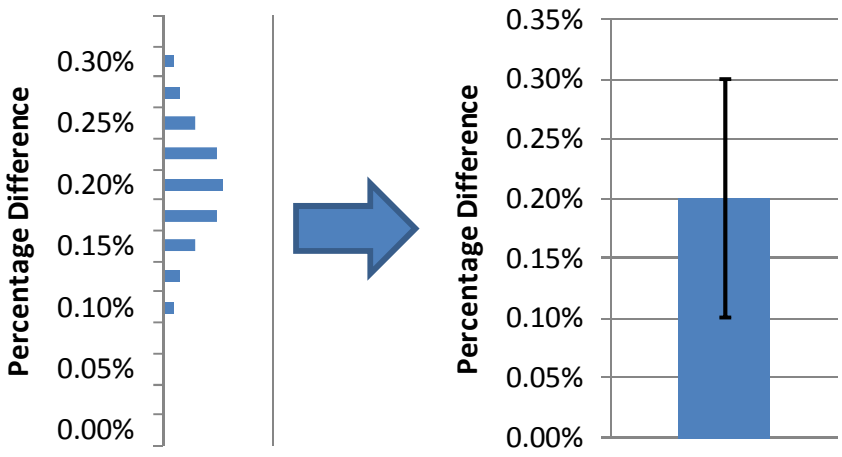

Figure 49. Representing results as error bars.

Results for the parametric correction factor approach are shown in Figure 51. It is clear from the figure that even with variations in operations, the resulting magnitudes of difference relative to the AEDT fleet are within 1%. Thus, this approach meets the criteria necessary to accept Hypothesis 2. It is interesting to note that the difference in total NO_x between the surrogate fleet with parametric correction and the AEDT fleet for the single-aisle group is significantly higher than for the other groups. The differences between results for each capability group lie in how well or poorly the fits of the correction factors compare from group to group.

Results for the average replacement approach are illustrated in Figure 51; note the difference in scale when compared to Figure 50. As this would foreshadow, the magnitudes of difference relative to the AEDT fleet are higher than for the parametric correction factor approach, this time roughly within ±2%. The underlying cause of this increase in magnitudes is that in the parametric correction factor approach, each vehicle is represented with its own set of coefficients, so the scaling of the operations is applied to each unique vehicle representation. Contrastingly, in the average replacement approach, the reference operations are inherently part of the performance target that it hits

when it is originally developed. While this results in a noticeably higher difference than the parametric correction factor approach, it is still within the bounds of acceptability for this experiment. Thus, it may be concluded that the average replacement approach also meets the acceptability criteria for Hypothesis 2.

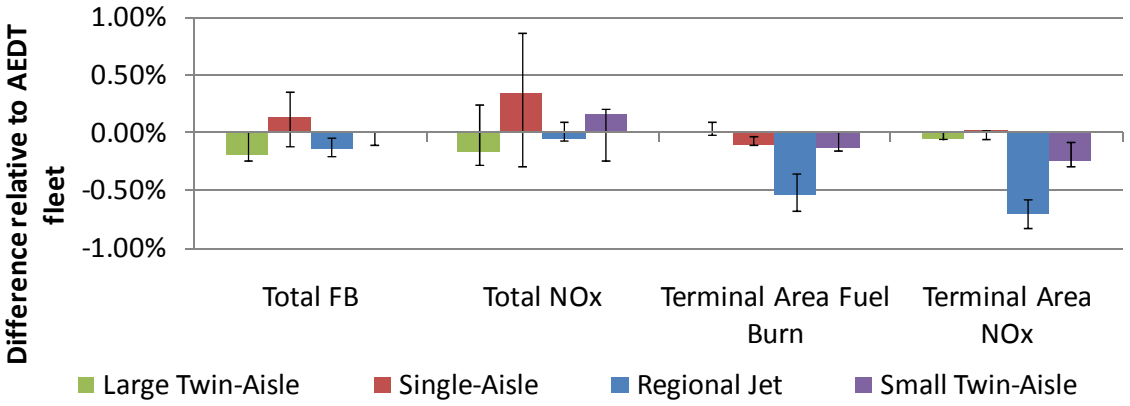

Figure 50. Parametric correction factor results for variations in operations.

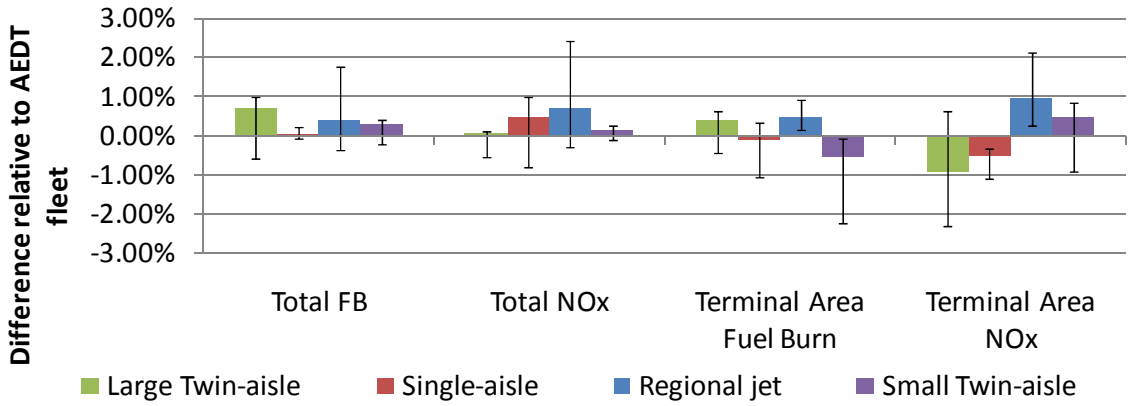

Figure 51. Average replacement results for variations in operations.

Finally, Figure 52 provides the results of Experiment 2 for the best-in-class replacement approach. Again, note the difference in axis scale, which in this case is still indicative of the high errors of this approach for representative operations. While not obvious because of the change in axis scale, the magnitudes of difference relative to the AEDT fleet for operational variations themselves are roughly of the same order as seen in

the average replacement approach. However, because of the large magnitude of errors when compared to reference operations, they still end up well outside of the acceptability criteria for Hypothesis 2.

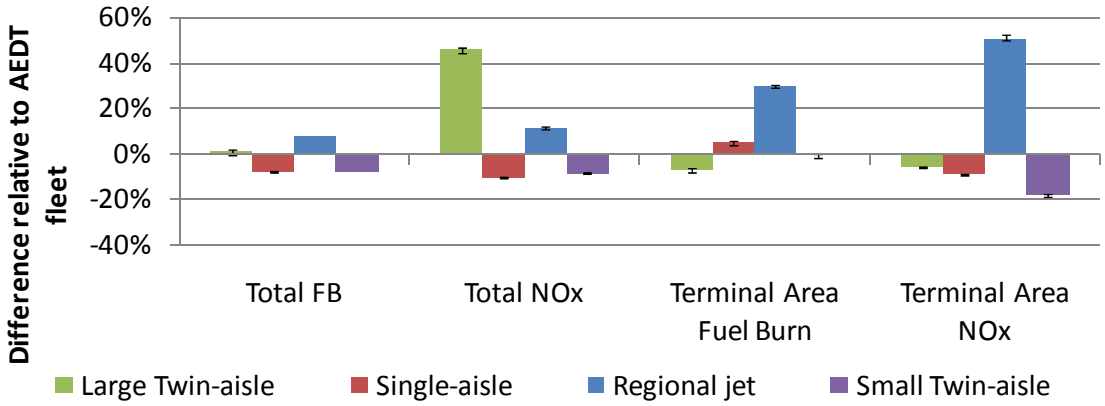

Figure 52. Best-in-class replacement approach for variation in operations.

In a manner analogous to the results for Experiment 1, Experiment 2 shows that the parametric correction factor and the average replacement approaches are able meet acceptability criteria for Hypothesis 2, while the best-in-class replacement approach does not. Now it is also possible to discuss the advantages in computational time with these two approaches. For both approaches, once they have been developed, potential future operational distributions, represented by each single case in the MCS, may be evaluated within a matter of seconds.

4.4.3 Experiment 3 – Surrogate Fleet Approaches with Technology Implementation

After the surrogate fleet approaches were evaluated for their ability to capture variations in operations, they then need testing to determine their suitability for use in studies of technology implementation. The ability of the surrogate fleet approaches to be robust in capture technology responses is critical to its utility for modeling potential future fleet scenarios. In order to prove the validity of the approaches while minimizing

computation burden of developing a virtual fleet for every aircraft, two groups were selected for virtual fleet implementation out of the four. Experiment 3 itself revolves around development of a virtual fleet to study the impact of technology implementation on the single-aisle and large twin-aisle groups, thereby evaluating acceptability of Hypothesis 3. Evaluation of the virtual fleet concept over these two groups was deemed to be appropriate for the following reasons: they cover a wide range of the capabilities of entire fleet of interest, as evidenced by Figure 39 and Figure 40; they also include the largest numbers of aircraft and aircraft families, as seen in Table 10, meaning that they are most conservative because they would be the hardest for a single vehicle to capture their aggregate behavior; and finally the results of the previous two experiments do not show a marked difference in surrogate fleet acceptability across the capability groups.

The steps of Experiment 3 are as follows:

- Develop a virtual fleet composed of aircraft models representing each aircraft family within the capability groups
- Identify representative aircraft technology sets with different impacts on environmental metrics to highlight interdependencies
- Apply technologies to the virtual fleet and to surrogate fleet representations of each capability group
- Map technologies to appropriate component level inputs to EDS
- Compare resulting environmental metrics to determine suitability of surrogate fleet approaches to capture the performance of the larger group for both reference operations and variations in operations
- Verify surrogate fleet approaches'' ability to capture interdependent effects

4.4.3.1 Virtual Fleet Development

In order to generate a virtual fleet, engine cycle and airframe parameters were varied around their values for the average replacement within ranges that span that of the reference fleet to generate potential virtual fleet vehicles. These parameters were selected because, within an aircraft family, often the only changes are minor cycle changes and adding or removing fuselage length. In a manner analogous to the average replacement approach, an EDS vehicle model was selected to represent each aircraft family in the capability group to match their aggregate environmental performance, and these vehicles collectively make up the virtual fleet. The DOE settings for the engine cycle and airframe parameters that were varied for each of these vehicles are given in Appendix H. It is important to note that each virtual fleet model does not necessarily represent the specific performance or geometry of any particular aircraft in the real fleet. Instead they exist for the purpose of providing a physics-based control group that spans the behavior of the real fleet for the purpose of determining the suitability of the surrogate fleet approaches in technology implementation.

The ability of these virtual fleet models to capture the aggregate performance of the fleet for reference operations with no technology infusion is a critical prerequisite to using them to observe changes as technologies are implemented. The differences between each vehicle that constitutes the virtual fleet for the large twin-aisle group and the single-aisle group are shown in Figure 53 and Figure 54, respectively, when compared to the AEDT fleet results for each aircraft family for the four fleet-level metric of interest over the distribution of reference operations. The key point to be drawn from these figures is that the virtual fleet aircraft are able to match the aggregate performance of each aircraft

family to within ±1%. These figures also include the resulting difference between their aggregate performance as a group with the entire capability group, shown as "Composite." As would be expected, their magnitudes are also well within ±1%. Therefore, it may be concluded that the virtual fleet vehicles do indeed capture the impact of the reference fleet prior to implementation of technologies.

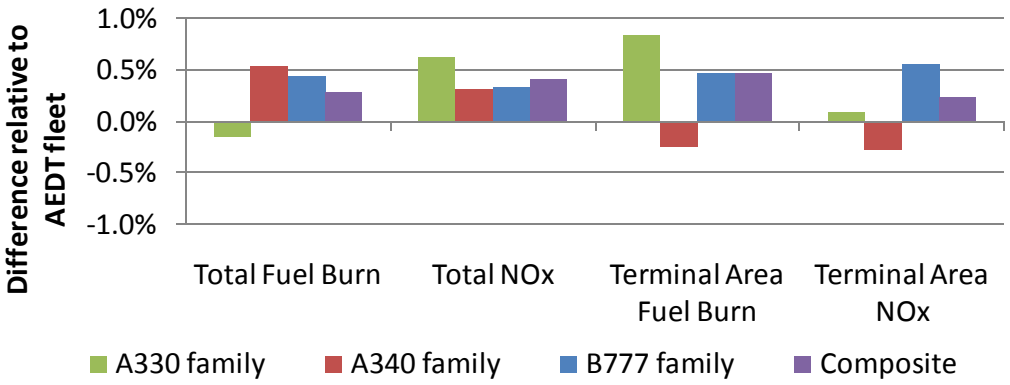

Figure 53. Results for constituent models of large twin-aisle virtual fleet.

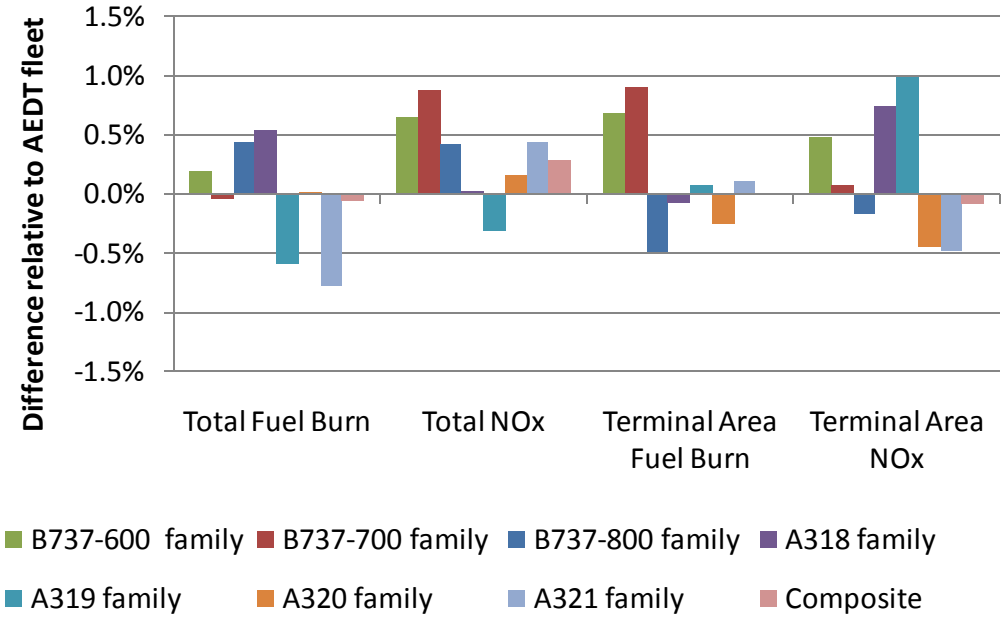

Figure 54. Results for constituent models of single-aisle virtual fleet.

4.4.3.2 Technology Selection

As described in Chapter 3, the surrogate fleet's role in a technology implementation study is to provide a M&S linkage between technology metrics and system objectives, which in this case are the four fleet-level metrics of interest. As such, a portfolio of technologies must be chosen that has already been mapped to technology metrics, which function as inputs to the M&S environment. For Experiment 3, a representative technology portfolio developed for application to civil subsonic aircraft to facilitate NextGen goals of expanding airspace system capacity while simultaneously reducing emissions impacts was selected. The specific goals of this representative portfolio are similar to those of NASA's SFW program given in Table 4 and are as follows[128]:

- Develop aircraft technology to reduce fuel burn by 33% compared to current technology
- Develop engine technology to reduce LTO NO_x emissions by 60%, at an engine pressure ratio of 30, below the ICAO CAEP\6 standard
- Develop aircraft technology to reduce levels by a cumulative 32 EPNLdB relative to Stage 4 standards

Selection of this portfolio for this problem is advantageous for a number of reasons. Technology assessment for programs with similar standards is a relevant example of current work, as described in Chapter 2, and is an application for which a methodology such as the surrogate fleet would be extremely useful in terms of allowing technologies to be rapidly assessed over a wide range of future scenarios. The portfolio of potential technologies includes both engine and airframe technologies, provided a good opportunity to test the physics-based nature of the surrogate fleet approaches, including

their ability to capture interdependencies. Finally, the representative potential technologies that are outlined here have already been mapped to EDS input variables as part of research undertaken by the EDS team. Descriptions of each technology are provided here, and their mappings to EDS input variables, both positive and negative, are available and provided in Appendix G.[129]

- Aspirated Blades – Employ flow control to highly load the compressor blades, resulting in one of two outcomes. Stage counts may be reduced by achieving more work per blade row, reducing engine weight and potentially leading to fuel savings. Or, highly loaded blades can rotate more slowly, thereby reducing fuel burn through increased component efficiency.
- Active Clearance Control (ACC) – Continually monitors and minimizes the clearance between the turbine blades and end wall in real time. Minimizing clearance, and the ensuing amount of air that may spill from the high pressure side to the suction side of each turbine blade, increases efficiency, resulting in lower fuel burn.
- Ceramic Matrix Composite (CMC) and Thermal Barrier Coatings (TBC) – When placed in the hot gas path, these high temperature materials can significantly reduce required cooling flows, which increases engine thermal efficiency and reduces fuel burn.
- Hybrid Laminar Flow Control (HLFC) – Employs engine bleed air to create suction along the wing span, which prolongs a laminar boundary layer and delays the transition to turbulence. In nonseparated regions, laminar boundary layers produce less drag and reduce fuel burn.

- Twin Annular Premixing Swirler (TAPS) combustor – Lean premixing combustor that employs a concentric pilot flame for low power emissions and operability, resulting in reduced NO_x formation.
- Lean Direct Injection (LDI) – Employs many small fuel injectors to achieve a lean fuel-air mixture, lowering flame temperature and resulting in reduced NO_x formation.
- Soft Vane – Reduces the unsteady pressure response on the fan stator surface and absorbs energy that would eventually become sound radiating from the stator, reducing fan noise.
- Over the Rotor Foam – Places Haynes 25 high temperature metal forward and aft of the fan rotor, absorbing sound and reducing fan noise.

The mapping of each technology to EDS inputs that was conducted at a physics-based subsystem level is provided in the form of technology impact matrices in Appendix I. Since the EDS framework is flexible and physics based, interdependencies between technologies may be captured and also fed forward to AEDT in order to evaluate fleet-level implications. Technologies were also grouped the above technologies into packages weighted for different outcomes: minimum total mission fuel burn, minimum terminal area NO_x, and equal weighting to minimize both metrics simultaneously. The resulting technology packages are shown in Table 15 for the single-aisle group and Table 16 for the large-twin aisle group.

Table 15. Technologies included for single-aisle group.

Technology	Minimum Fuel Burn	Minimum NOx	Equal Weighting
ACC	☑	☑	☑
Aspirated Blades (weight)	☑		☑
Aspirated Blades (efficiency)		☑	
CMC	☑	☑	☑
Advanced TBC	☑	☑	☑
Over the Rotor Foam			☑
Soft Vanes			☑
TAPS	☑		
LDI		☑	☑
HLFC	☑		☑

Table 16. Technologies included for large twin-aisle group.

Technology	Minimum Fuel Burn	Minimum NOx	Equal Weighting
ACC		☑	☑
Aspirated Blades (weight)			
Aspirated Blades (efficiency)	☑	☑	☑
CMC	☑	☑	☑
Advanced TBC	☑	☑	☑
Over the Rotor Foam			☑
Soft Vanes			☑
TAPS			
LDI		☑	☑
HLFC	☑	☑	☑

The differences in technology selection between the two capability groups highlight the need for the groups themselves, as was pointed out in Chapter 3. The technologies selected for a certain application for the large twin-aisle may not be appropriate or may not lead to the same effect as for the single-aisle. A good example of this is seen with the combustor technology applied to the single-aisle, TAPS. The combustors used in large twin-aisle aircraft today already incorporate technologies with similar impacts; therefore these technologies would not be appropriate to include for them.

4.4.3.3 Parametric Correction Factor

As described in Chapter 3, the virtual fleet was used to evaluate the performance of the parametric correction factor approach by:

- Determining the impact of aircraft technologies on fleet-level results for EDS models of the virtual fleet
- Determining the impact of aircraft technologies on EDS reference models
- Correcting EDS reference model results with the parametric correction factors developed in Experiment 1 to match the virtual fleet results prior to technology infusion
- Comparing results to determine acceptability of this approach in the context of Hypothesis 3

The resulting differences between the virtual fleet and the parametrically corrected surrogate fleet for the three technology packages for the large twin-aisle group and the single-aisle group, respectively, are shown in

Min FB Min NOx Equal Weight

Figure 55 and Figure 56. The magnitude of the differences is very large and well beyond the acceptability criteria that were defined. Even the fuel burn results for the large twin aisle, which are comparatively smaller than the other differences, are still on the order of 3%.

The reason for the large magnitude of these differences lies in the fact that the parametric correction factors were developed with the fixed technology reference fleet. As fleet performance changes due to the physics of adding technologies, the magnitude of these factors does not change. In fact, because the technologies packages work to

minimize fuel burn and NO_x, the scale of the correction factors begins to outweigh the scale of the actual results, leading to extremely high percentage errors as seen in

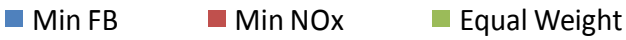

Figure 55 and Figure 56. This effect is highly pronounced in the NO_x results for both vehicles, because the magnitude of NO_x, measured in grams, is higher than the magnitude of fuel burn, measured in kilograms. The correction factors for NO_x are of a greater magnitude than for fuel burn, and when technologies drastically reduce the magnitude of NO_x production, the results show ridiculously large differences of up to roughly 100% between performance predicted by the parametrically corrected fleet and the virtual fleet. Using the parametric correction factor approach to capture the performance of a fleet with technologies added would clearly be highly inappropriate. From these results, the parametric correction factor approach would not lead to acceptance of Hypothesis 3.

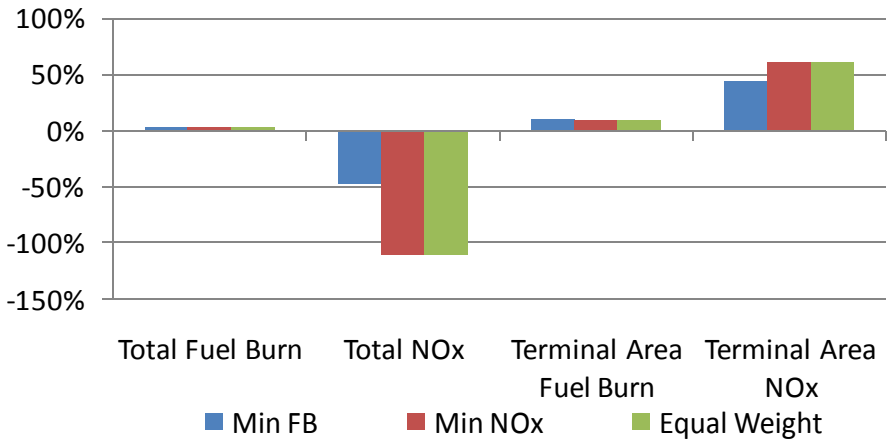

Figure 55. Large twin-aisle technology results for parametric correction factor.

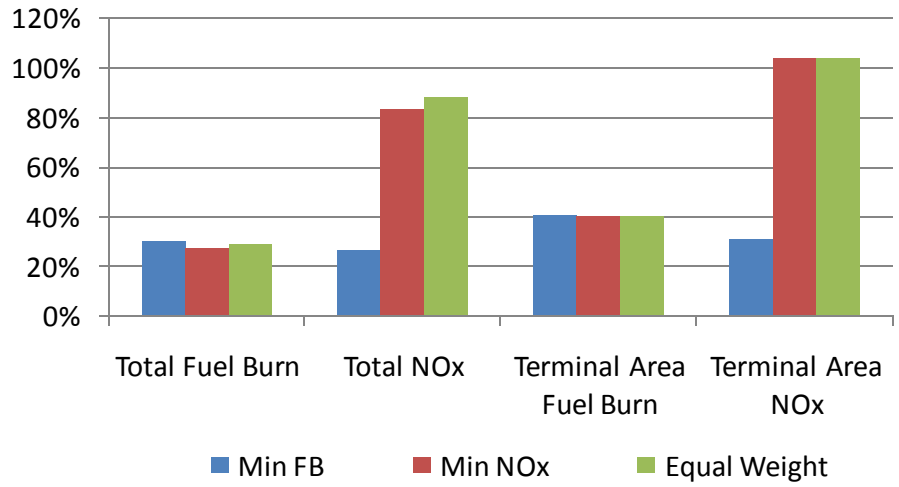

Figure 56. Single-aisle technology results for parametric correction factor approach.

4.4.3.4 Average Replacement

The virtual fleet was also used to evaluate the performance of the average vehicle approach through the following steps:

- Determine the impact of aircraft technologies on fleet-level results for EDS models of the virtual fleet
- Determine the impact of aircraft technologies on fleet-level results for the average vehicle models
- Compare results to determine acceptability of approach in the context of Hypothesis 3

The resulting differences between the virtual fleet and the average replacement approach for the three technology packages for the large twin-aisle group and the single-aisle group, respectively, in Figure 57 and Figure 58. Here the magnitudes of the differences are much smaller than for the parametric correction factor approach, within roughly ±1.5%, which does satisfy the acceptability criteria set forth for technology implementation.

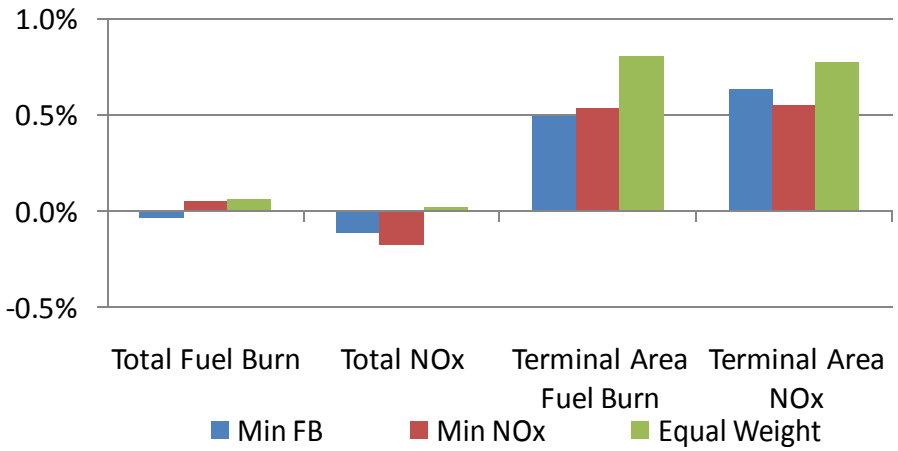

Figure 57. Large twin-aisle technology results for average replacement approach.

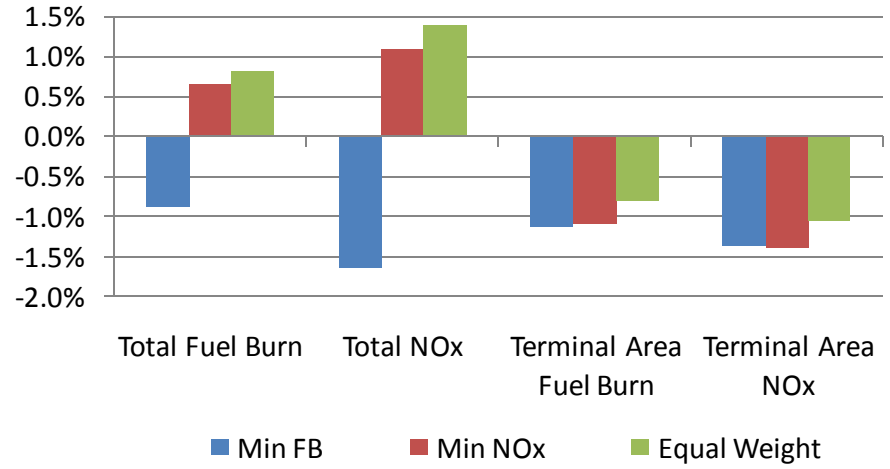

Figure 58. Single-aisle technology results for average replacement approach.

The magnitudes for the single-aisle differences tend to be larger than the magnitudes for the large twin-aisle results. This may be attributed to the fact that the single-aisle group has more aircraft families to be matched, and when comparing the performance of these families, there is more of a relative difference between the smallest and the largest aircraft in the group. Therefore, if these families behave slightly differently as technologies are added, a greater difference between their aggregate result and that of the average replacement may be observed, which is seen when contrasting Figure 57 and

Figure 58. However, for the fleet of interest in this problem, the single-aisle has the greatest number of aircraft families, and it is still within the defined acceptability criteria. Therefore, the average replacement approach satisfies acceptance of Hypothesis 3.

4.4.3.5 Best-in-class replacement

In a manner similar to that of the average replacement approach, the virtual fleet was also used to evaluate the performance of the best-in-class replacement approach through the following steps:

- Determine the impact of aircraft technologies on fleet-level results for EDS models of the virtual fleet
- Determine the impact of aircraft technologies on fleet-level results for the best-in-class replacement models
- Compare results to determine acceptability of approach in the context of Hypothesis 3

The resulting differences between the virtual fleet and the best-in-class replacement approach for the three technology packages for the large twin-aisle group and the single-aisle group, respectively, in Figure 59 and Figure 60.

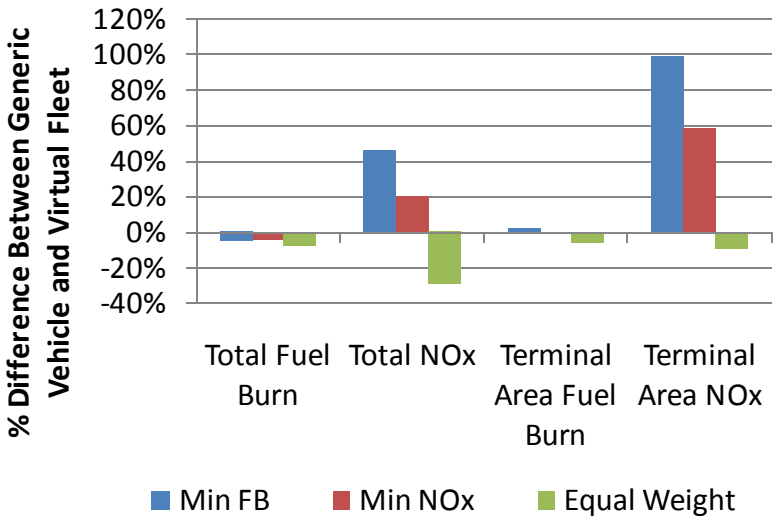

Figure 59. Large twin-aisle technology results for best-in-class replacement approach.

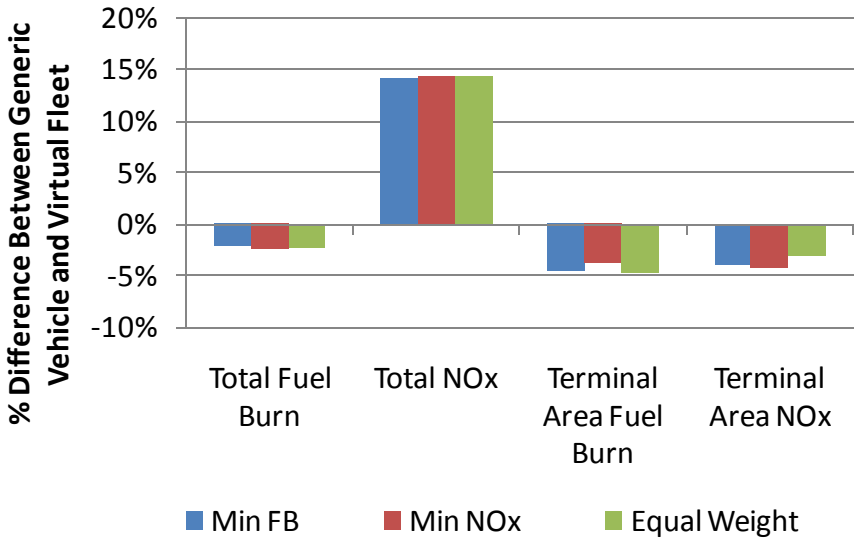

Figure 60. Single-aisle technology results for best-in-class replacement approach.

As might be expected, the magnitude of their differences is roughly of the same order as seen when the best-in-class replacement approach was used to capture the reference fleet as illustrated in Figure 46. The differences in terminal area fuel burn metrics for the minimum fuel burn and minimum NO_x packages applied to the large twin-aisle group, the total fuel burn metrics for all packages on the single-aisle group, and the terminal area fuel burn metrics for the minimum noise package on the single-aisle group

are the only results that fell within 3%. Interestingly, the magnitude of the NO_x differences are markedly higher than the fuel burn differences, which highlights the difficulty of using an already existing vehicle to capture the performance of a larger and diverse group of aircraft. From the results, it is clear that the best-in-class replacement approach does not satisfy the criteria necessary to accept Hypothesis 3.

4.4.3.6 Average Replacement with Operational Variations

Because the average replacement approach was the only one that was able to demonstrate criteria leading to acceptance of Hypothesis 3, simultaneous variation of technologies and operations was pursued with this approach.

- Determine the impact of aircraft technologies on fleet-level results for EDS models of the virtual fleet
- Determine the impact of aircraft technologies on fleet-level results for the average vehicle models
- Vary operations for both the virtual fleet and average vehicle models as described in Experiment 2
- Compare results to determine acceptability of approach in the context of Hypothesis 3

The resulting differences between the virtual fleet and the best-in-class replacement approach for the four technology packages for the large twin-aisle group and the single-aisle group in Figure 61 and Figure 62, respectively.

They are presented in the same form as the Experiment 2 results in Figure 50 through Figure 52, with error bars representing the minimum and maximum extent of the resulting distributions of the operational distributions. Here again the differences for the

single-aisle group tend to be higher than for the large twin-aisle group, which may be attributed to the greater number of constituent aircraft that make up the group. However, all of the differences are within 4%, which confirm the acceptability of the average replacement approach for this application.

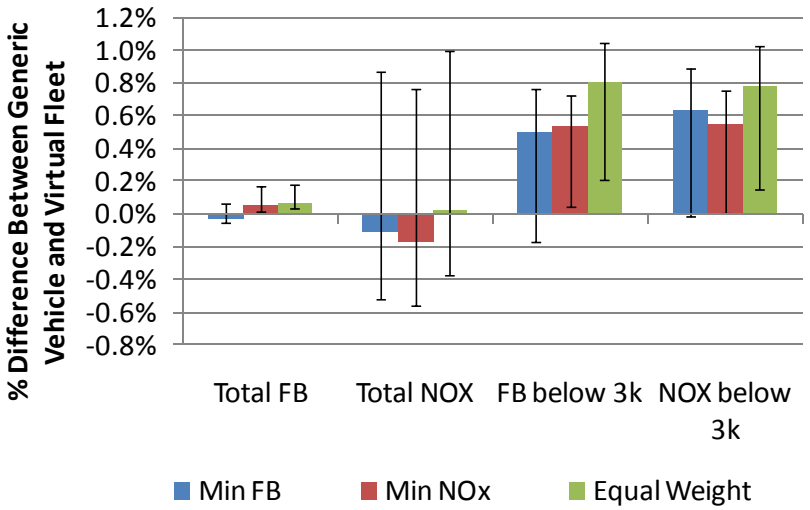

Figure 61. Variation of technologies and operations for large twin-aisle group.

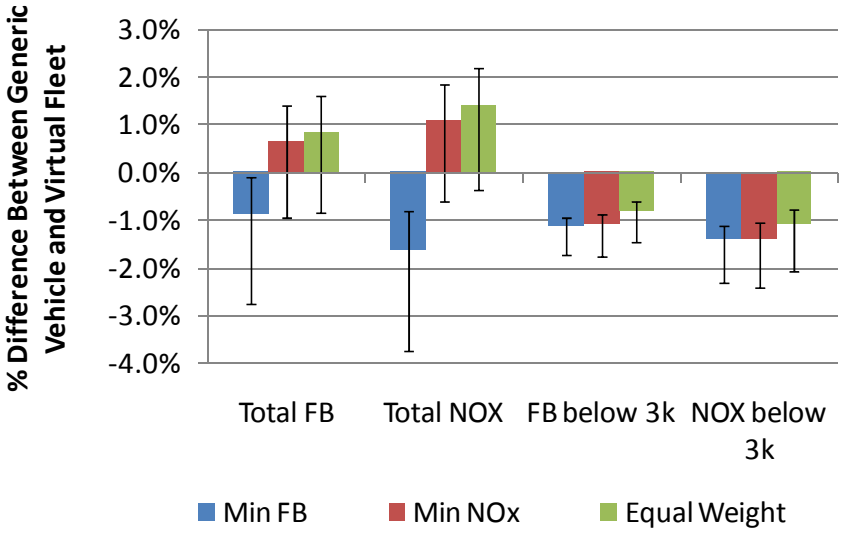

Figure 62. Variation of technologies and operations for single-aisle group.

4.4.3.7 Observing Technology Impacts Relative to Fixed Technology Case

One final observation of the results for all four metrics for the Min FB and Min NO_x packages for both vehicles was conducted to examine the magnitude of differences between vehicles that was captured by the average replacement approach. When conducting technology evaluation, one benefit of using a physics-based approach is that it captures the impact of interdependent effects that may arise between different metrics, such as fuel burn and NO_x emissions, and this may be observed as well. The results, relative to the fixed technology reference set of operations, are provided for the large twin-aisle and the single-aisle groups in Figure 63 and Figure 64. The fixed technology points are at the origin, and the application of technology packages results in movement away from the origin. Single aisle results are plotted as dashed lines, large twin aisle results are plotted as solid lines, fuel burn results are in blue squares and NO_x results are in blue diamonds.

Again, it is important to note that the differences in magnitudes between the single aisle and large twin aisle results highlights the importance of segmenting the fleet into relevant capability groups as it shows different sensitivities to the technology packages. The single-aisle group has much greater improvements in fuel burn than the large twin aisle because of the difference in the technology packages for the single-aisle, which include new combustors.

Looking at the values for total and terminal area fuel burn, the greatest amount of decrease occurs for the minimum fuel burn package for both vehicles, which is expected. However, the effect of decreasing fuel burn is not as great for the minimum NO_x package. The corresponding effect may be seen simultaneously in the NO_x results as

well. There is a tradeoff that may be observed between minimizing fuel burn or minimizing NO_x. Upon examination of the data, it is clear that impacts of interdependencies have been captured. These interdependencies are the nuances that may be overlooked when modeling a technology through post-processing, but they are captured in this physics-based approach.

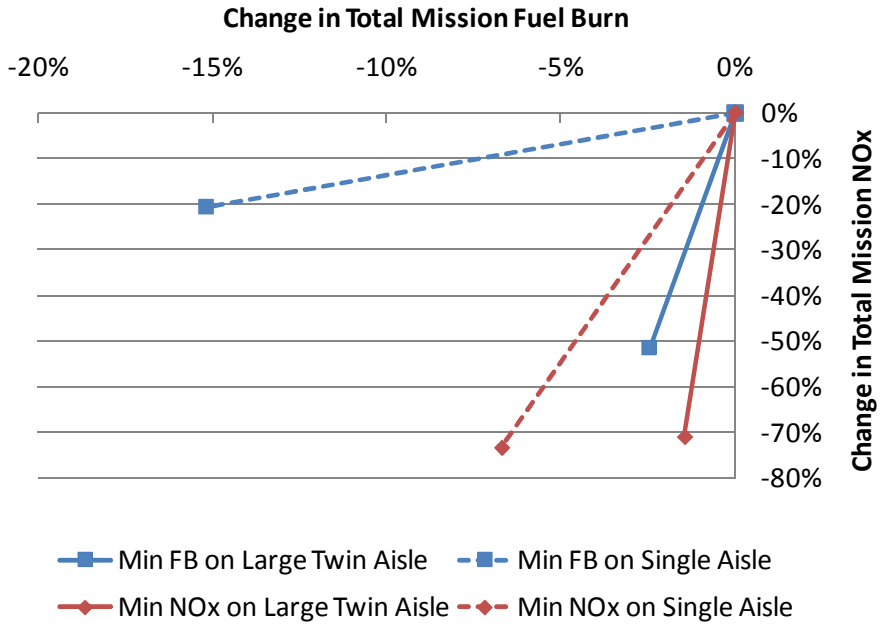

Figure 63. Effect of technology packages on total mission metrics.

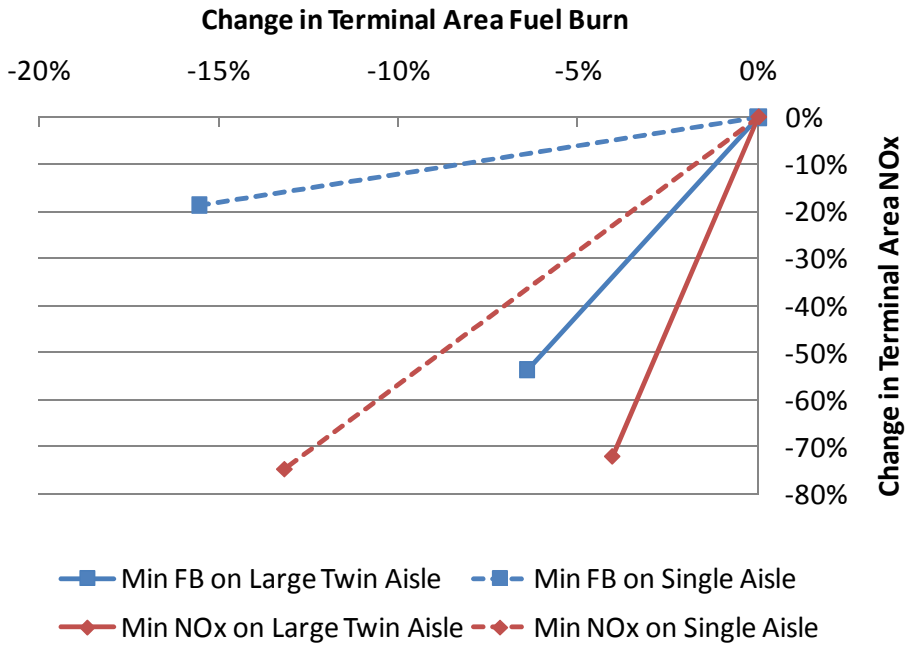

Figure 64. Effect of technology packages on terminal area metrics.

4.4.3.8 Summary

The implications of the results of Experiment 3 for the average replacement approach cannot be overstated. With this approach, the response of an entire group of aircraft to a technology package may be physically modeled through one aircraft. The entire fleet may be modeled with just a handful of aircraft models, instead of requiring one for each aircraft in the fleet. In the context of runtime, once the technology has been mapped to the appropriate input variables, physics-based aggregate fleet performance for the capability groups in Table 9 may be generated in the amount of time required to run four models through EDS and AEDT, which is on the order of thirty minutes total, and surrogate equations may then be developed around these models. Using this approach, technologies may also be modeled in a transparent and physics-based manner at the component level in real time, which is not possible when using AEDT alone. This allows for the realities of interdependent effects to be captured, which was illustrated by the

comparison between results of the technology packages and is important to show the different trends among metrics if they are to be individually optimized.

4.5 Experimental Summary

The significance of the success of the surrogate fleet approaches is that they enable rapid evaluation of fleet-level metrics for the experiments in which they satisfied acceptance criteria for the corresponding hypotheses. The maximum magnitude of the difference between results for each approach with the reference fleet is provided in Table 17. The maximum magnitude is used to demonstrate whether the worst performing case within each experiment was able to satisfy acceptance criteria for the corresponding hypothesis. Those that were within accuracy bounds are denoted by green fields, while those which failed are denoted by red fields.

Table 17. Summary of worst-case experimental results by approach and experiment.

	Parametric Correction Factor	Average Replacement	Best-in-Class Replacement
Experiment 1 - Capturing Reference Operations	0.71%	0.96%	51.00%
Experiment 2 - Capturing Variations in Operations	0.87%	2.42%	52.73%
Experiment 3 - Capturing Technology Implementation	110.91%	3.73%	

The average replacement approach was the only one that satisfied acceptance for all three experiments: reference operations, variations in operations, and technology implementation. The parametric correction factor approach was successful in capturing

reference operations and variations in operations, but failed to capture technology implementation. This may still be a useful approach for applications that do not require technology implementation. Finally, the best-in-class replacement approach failed for capturing reference operations and variations in operations, and because of these failures was not tested for technology implementation.

The implications of these results lie in the fact that there is now a physics-based methodology that satisfies the research objectives presented in Chapter 1. A methodology now exists that captures the physical interdependencies that emerge at the aircraft level when evaluating different future fleet scenarios, does so quickly, and does so within acceptable bounds of accuracy when compared to current global fleet analysis methods. By meeting the research objectives, this methodology is now available for use in informing decision makers of the effect of a wide range of policy scenarios involving commercial fleet operations and technologies in a transparent and rapid manner.

CHAPTER V

CONCLUSIONS

Over the past few decades, commercial aviation has undergone tremendous growth, which shows no indication of slowing down over the years to come. While that expansion has allowed aviation to become a significant contributor to social and economic development globally, it has concurrently led to several negative consequences. Among these are fuel burn demand, greenhouse gas emissions at cruise altitudes, and increasing capacity demand that impinges on physical limits at airports. In an effort to mitigate these negative consequences while at the same time enabling further growth of commercial aviations, there are a number of entities, both domestic and international, that are interested in setting new environmental regulations, developing new technologies, and implementing new operational procedures, which together comprise different potential future scenarios.

Evaluation of these potential future scenarios is a capability in which the accuracy and run time of the evaluation approach must be considered, particularly in the context of methods that already exist. Examples of already existing methods include inventory analyses, in which the performance of each aircraft over the course of an entire year are considered, and single aircraft trade studies, in which the impact of technologies is evaluated for a particular representative aircraft. In the former, any attempt to study technologies may only be conducted through post-processing, which may not capture the physical interdependencies of the technologies. In methods such as the latter, the impact of technologies is thoroughly studied, but only on a single aircraft, which may not

accurately capture aggregate fleet-level trends. These techniques therefore require enhancements to be able to capture technology impacts in a physics-based manner.

5.1 Review of Research Questions and Hypotheses

The desire to model potential future fleet scenarios under the projected growth of commercial aviation to inform decision makers and policy makers has thus led to a need for a rapid, physics-based analysis capability for fleet environmental metrics. As presented in this document, the objective of the research conducted here was to develop such a methodology by utilizing physics-based aircraft models to construct surrogate fleets that provide an avenue to rapidly evaluate environmental metrics under varying conditions, including application of aircraft technologies and the interdependencies that may emerge therein. Out of this research objective, three research questions were formulated, and three hypotheses were formulated to address these research questions. In order to test the hypotheses, a framework representing the roadmap to create a surrogate fleet was formulated, as provided in Figure 22. Here each research question and hypothesis will be presented, along with the experimental results that addressed them.

The first research question and hypothesis are as follows:

> **Research Question 1**: How can aggregate fuel burn and NO_x metrics be rapidly captured for a fleet of aircraft with a set of reference operations in a physics-based manner?
>
> **Hypothesis 1:** Characterization of the commercial fleet into capability groups enables development of surrogate fleet approaches that use a limited number of aircraft models to rapidly capture environmental metrics within an acceptable level of accuracy.

In order to test this hypothesis, the entire fleet of interest, composed of in-production aircraft, was segmented into groups based on geometry and performance. Next, three surrogate fleet approaches, the parametric correction factor approach, the average vehicle approach, and the best-in-class replacement approach, were developed and applied to the reference fleet under a set of reference operations to observe how well each one was able to reproduce the aggregate fleet metrics for total mission fuel burn and NO_x emissions and terminal area fuel burn and NO_x emissions. Results of Experiment 1 showed that the parametric correction factor approach and the average replacement approach were able to reproduce the aggregate fleet metrics within a range of accuracy that allowed for the acceptance of Hypothesis 1. Both of these approaches reduce the entire fleet of interest to just a few physics-based models, significantly reducing runtime. It is just as important of a result that the performance of the best-in-class replacement approach as a surrogate fleet led to rejection of its acceptance for this hypothesis.

The second research question and hypothesis are as follows:

> **Research Question 2:** How can the acceptability of surrogate fleet approaches be evaluated over wide variations of operations representing future fleet scenarios?
>
> **Hypothesis 2:** Parameterization of operations and use of design space exploration methods will quantify the ability of each surrogate fleet approach to capture wide variations of operations.

To test this hypothesis, the reference set of operations was probabilistically varied in order to simulate potential future fleet scenarios and evaluate the ability of the surrogate fleet approach to match that of accepted models for the fleet of interest under these conditions. These probabilistic variations were chosen in an attempt to thoroughly

capture a realistic set of potential future operations. Here again, results showed that the parametric correction factor approach and the average replacement approach were able to reproduce the aggregate fleet metrics within a range of accuracy, allowing for the acceptance of Hypothesis 2. Additionally, it must be noted that the best-in-class replacement approach did not meet the criteria for acceptance of Hypothesis 2.

The third research question and hypothesis are as follows:

> **Research Question 3:** How can the acceptability of surrogate fleet approaches be evaluated for implementation of technologies at the aircraft-level?
>
> **Hypothesis 3:** The development of a physics-based virtual fleet quantifies each surrogate fleet approach's ability to capture technology infusion through a parallel technology implementation study.

Finally, the ability of the surrogate fleet approaches to capture the physical impact of technologies was evaluated. The virtual fleet concept of using physics-based aircraft model to represent different constituent aircraft families in each capability group was developed for the purposes of investigating technology impacts on the fleet. Using the virtual fleet, the results of technology package implementation could be observed for both the surrogate fleet approaches and aircraft that constitute the larger groups that they represent. Results demonstrated that the average replacement approach was the only one that was able to produce the same results of the virtual fleet within an acceptable range of accuracy, providing necessary criteria for the acceptance of Hypothesis 3. Furthermore, the average replacement approach was also validated against simultaneous changes in technologies and operations, and its results also were used to confirm the impact of

interdependencies. The other two approaches were unsuccessful in meeting the acceptance criteria for Hypothesis 3.

5.2 Contributions

The desire to model potential future fleet scenarios under the projected growth of commercial aviation to inform decision makers and policy makers has thus led to a need for a rapid, physics-based analysis capability for fleet environmental metrics. As presented in this document, the objective of the research conducted here was to develop such a methodology by utilizing physics-based aircraft models to construct surrogate fleets that provide an avenue to rapidly evaluate environmental metrics under varying conditions. Out of this research objective, three research questions were formulated. Three hypotheses were formulated to address these research questions.

In order to show the utility of the surrogate fleet, specifically the average replacement approach, the replacement vehicles representing the single-aisle and large twin-aisle groups for multiple technology packages were integrated into a demonstration tool that calculates and visualized different future fuel burn scenarios. This tool allows the parameters of potential future scenarios, including operations and technology packages, to be varied by policy makers and then analyzed in real time, on the order of minutes. Because of this short run time, many different policy scenarios may be comprehensively considered, leading to more informed decision making.

With the completion of this work, a number of significant tangible contributions have been made. The methodology itself may serve as a roadmap for the development of surrogate fleets across any aircraft categories that may be of interest. As a result of the experimentation done in this work, surrogate fleet frameworks already exist for defined

in-production capability groups representing the regional jet, single-aisle, small twin-aisle, and large twin-aisle aircraft categories. These surrogate fleets exist in the form of the parametric correction factors to be used with EDS models of the reference vehicles of each capability group and the EDS models for average replacement vehicles developed for each group. They are ready for use in evaluation of the current reference fleet and operations or for variations in operations. In addition, the average replacement vehicles have been shown to be able to capture technology responses in conjunction with a future fleet forecast and defined technology suites.

As the fleet evolves from the current fleet to the future fleet, changes will occur to operations and technology levels. The value of the surrogate fleet approach, specifically the average replacement approach, is that it may itself be used to construct surrogate equations that quickly provide the values of fuel burn and emissions. Sample coefficients and goodness of fit metrics for these regressions are provided for the single-aisle and large twin-aisle vehicles in Appendix J. These surrogate equations can enable seamless integration of vehicle and fleet behavior with other operational forecasting capabilities to create an environment in which to rapidly analyze potential scenarios and provide meaningful visualization of the results to policy makers. In addition, by utilizing the surrogate fleet information from the average vehicle approach, the impact physics-based modeling of technologies at the component level is also included within the demonstrated levels of accuracy, which was not possible in previous post-processing approaches. Many different combinations of technologies and operations may therefore be rapidly queried in real time, allowing thorough exploration of potential future scenarios, which is invaluable in decision making.

The benefits of the surrogate fleet approach has been shown to be the ability to rapidly evaluate fleet metrics for a wide range of future scenarios, which is an enabler for more intelligent decision making when evaluating operational changes or technology implementation. Potential applications of this capability include evaluation of technology suites, such as that done for the Continuous Lower Energy, Emissions and Noise (CLEEN) technologies by FAA, rapid assessment of changes in operations and fleet mix, such as that done by JPDO, and development of a CO_2 emissions metric, as being pursued by CAEP.

5.3 Future Work

Because of the scope of the work conducted in this thesis and the assumptions that have been made herein, there are a number of elements that may be identified to pursue for future work. These elements will be described here and include developing capabilities to calculate noise impacts, airport-level impacts, and procedural changes. Adding these capabilities would enable the surrogate fleet approaches to be applied to a broader range of real world problem.

5.3.1 Adding Noise Capability

The work that has been completed here was focused on fuel burn and emissions. Therefore, a reasonable next step in surrogate fleet development is to create a method that provides the same capability for noise metrics. One factor that makes this a challenging problem is that, unlike fuel burn and emission, noise production from single aircraft events such as departure or approach is not physically additive. Despite this fact, there are numbers that attempt to create noise metrics around airports through averaging, such as day night levels (DNL), which can indicate the areas subjected to an hourly average at or

above certain prescribed noise levels, over the course of an entire day, with a 10 dB penalty assessed on noise generated between 10 pm and 7 am. Metrics like DNL contours may lend themselves to a surrogate fleet approach for noise.

Another factor is that noise performance is very airport specific due to a number of different reasons. Because noise is not in the scope of the current work, airport specific characteristics were not assumed to be important. However, any future work that does consider noise must take into account the fact that the same aircraft may have different noise performance at different airports, depending on its altitude and the location of potential noise observers. The impact of aircraft noise on people living near airports depends on the layout of the airport, terminal area trajectories, and the relative location of neighborhoods around the airport, which is illustrated by the sample DNL contours for two airports in Figure 65 and Figure 66.[130] As is clear, the contours are very different, both in their shapes and the amount of land that may be impacted around them. The cumulative impact of noise at a particular airport will also depend on the specific mix of aircraft that originate from, or are destined for, it.

Adding the ability to quantify noise with a surrogate fleet approach is a complex problem, but would be powerful because it would completely cover all of the environmental metrics that have been targeted for regulation by CAEP in the past and that are therefore of great interest to other regulatory bodies, operators, manufacturers, and government agencies. Its significance would also be seen in the ability to capture interdependencies in all three metrics simultaneously. Together with the ability to rapidly quantify fuel burn and emissions, thorough examination of the impact of operations and technologies on future fleet scenarios would be completely enabled.

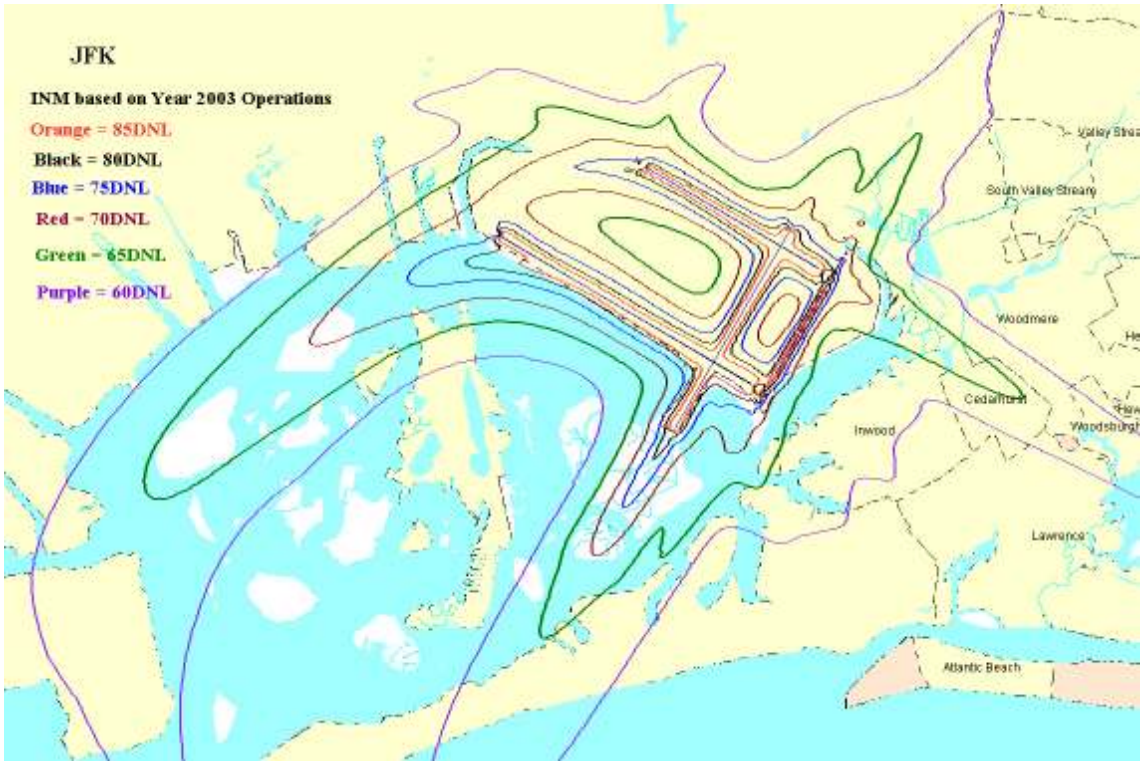

Figure 65. Example DNL noise contours for John F. Kennedy International Airport.

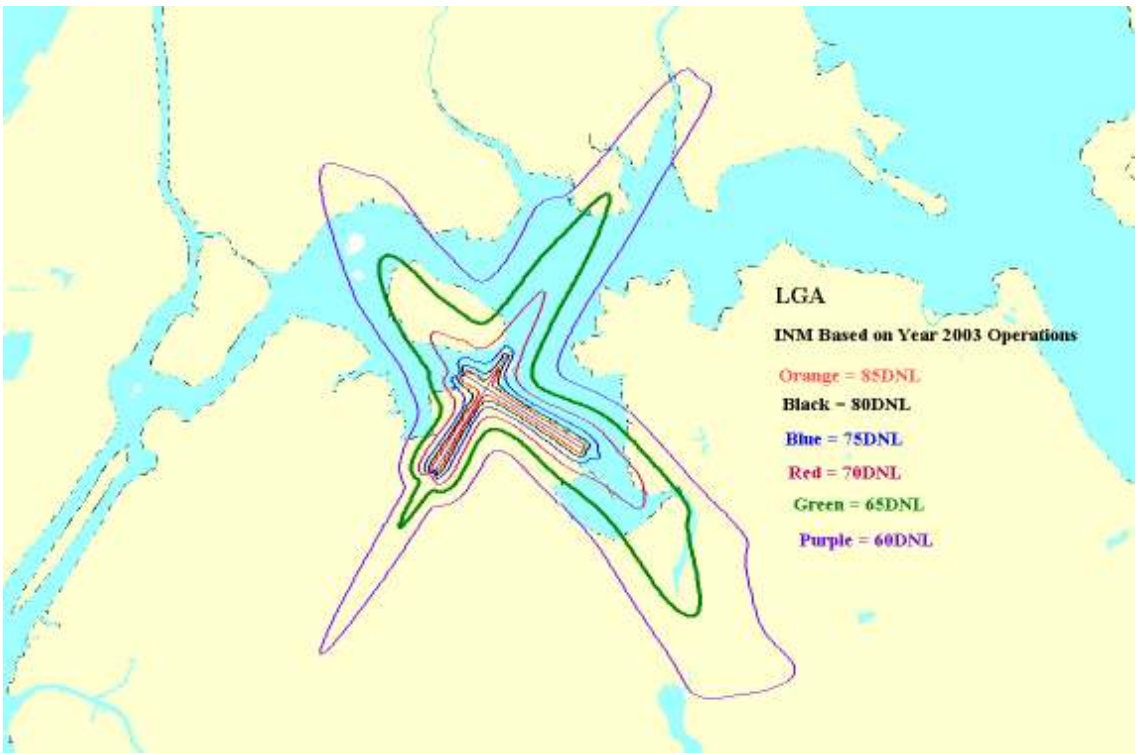

Figure 66. Example DNL noise contours for LaGuardia Airport.

5.3.2 Capturing Airport Level Metrics

The work in this thesis focused on developing surrogate fleet approaches to capture the environmental metrics of a large fleet. At the same time, there is also a need to evaluate environmental metrics of the smaller groups of aircraft operating at specific airports, including scenarios with potential technology implementation. The need to increase traffic and capacity at airports must be balanced with mitigation of local environmental impacts in the neighborhood of these airports, which make up a significant portion of total mission impacts.[131] As previously mentioned in the noise section, operations at each individual airport have unique features and a unique mix of aircraft operating out of it.

One suggested area of future work is to determine how well the surrogate fleet approaches developed to capture the larger fleet are able to capture performance at a specific airport. Depending on what level of accuracy is desired, this may be an acceptable approach. Another suggested approach would be to determine the utility of generating surrogate fleet models to capture fuel burn and NO_x emissions performance at specific airports. Because this would need to be done for each airport of interest, development time would increase as number of airports considered increases.

5.3.3 Capturing Procedural Changes

The work in this thesis focused on developing surrogate fleet approaches to capture the impacts of aircraft technologies on a large fleet of aircraft. Outside of aircraft technologies, optimizing aspects of aircraft procedures also show potential to significantly reduce fleet-level environmental impacts.[132] Thus, there is a need for a similar approach to capture the impacts of procedural changes on a large fleet of aircraft,

which would contribute to completing the ability to model the elements in Figure 4 in Chapter I. Procedural improvements include techniques such as reduced vertical separation and continuous descent approach, which impact the trajectories of individual flights.

Again, determining how well the current surrogate fleet approaches capture procedural changes would be an interesting starting point for future work in this area. If this proves to be unsatisfactory, new techniques will be needed to expand the capability of the surrogate fleet approaches. In the context of M&S, these will most likely include developing the ability to capture such changes in trajectories within the aircraft modeling tool.

5.3.4 Other Improvements in Surrogate Fleet Approach

Besides adding capabilities to the surrogate fleet, there are potential areas to improve the surrogate fleet methodology itself. One of them would be to increase the number of reference vehicles within each capability group. An avenue for accomplishing this would be to take a more in depth look at the metrics used to segment the groups, identify whether there are smaller subgroups that may emerge within the capability groups, and create reference vehicle models for these subgroups. Because each vehicle model could then be used as an approximation for a smaller number of vehicles in the fleet, this may potentially improve the parametric correction factor approach's performance for technology implementation, and the best-in-class replacement approach for all applications.

Another potential improvement would be to completely automate average replacement target generation and vehicle selection. Doing so would make the

methodology more dynamic by allowing even more rapid surrogate fleet generation for multiple sets of reference operations to observe how vehicle behavior changes over time. This would also be an enabler to create reference vehicle models for subgroups within capability groups mentioned in the previous paragraph. This type of automation could be accomplished through construction of a wrapper script around the aircraft and fleet modeling tools, and the model parameters and reference data that are used as inputs. Such a script could be designed to calculate aggregate targets and intelligently vary model parameters to hit those targets using inverse design techniques.

Finally, a third improvement would be to develop specific scenarios to use for modeling operational variations. In this work, a wide range of mathematically generated operations were used to simulate variations, but their range could be so wide that the resulting errors when evaluating the surrogate fleet approaches are inflated. In order to improve this, the set of potential future operations could be examined, and those that may not represent realistic future scenarios may be eliminated, e.g. flights for aircraft within capability groups at distances they are unlikely to fly. This could be done in concert with expert feedback to create an accepted set of operations and technology parameters for use in simulating future scenarios.

APPENDIX A

PROBABILITY DISTRIBUTIONS FOR OPERATIONAL VARIATIONS

This appendix describes the mathematics behind the probability distributions that were used to rapidly generate distributions of future operations. These distributions are all finite, meaning each one ends at a maximum specified flight distance, and they are a function of shape parameters, which allows for quick generation of multiple distributions. Because they are all capable being used to thoroughly query the space of potential future scenarios, selecting which one to use is a choice based on ease of implementation and how well they may represent actual flight operations.

The generalized form of the probability density function for a beta distribution is given in Eq. (8), scaled for $0 \leq x \leq 1$ with shape parameters α and β:

$$f(x;\alpha,\beta) = \frac{\Gamma(\alpha+\beta)}{\Gamma(\alpha)\Gamma(\beta)} x^{a-1}(1-x)^{\beta-1} \tag{8}$$

where

$$\Gamma(k) = \int_0^\infty x^{k-1} e^{-x} dx \tag{9}$$

Although the form of this distribution may outwardly seem very complex, it is generally readily available in most statistical and spreadsheet software packages. Samples of single beta distributions are provided in Figure 67. The reasons that beta distributions are good candidates to represent operations were that, as illustrated in Figure 67, It also shows that

a wide spectrum of possible distributions may be attained simply by varying α and β between 0 and 5.

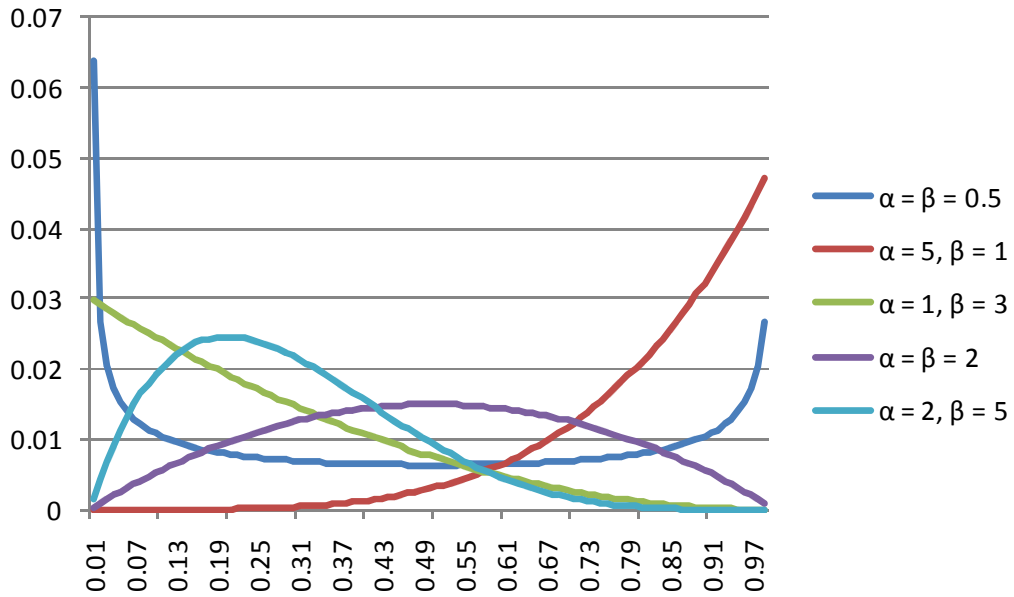

Figure 67. Sample beta distributions.

The Kumaraswamy distribution, originally developed to fit hydrological variables, is similar to the beta distribution, but its probability density function may be expressed in closed form with two shape parameters α and β as given in Eq. (10)[133]:

$$f(x;\alpha,\beta) = \alpha\beta x^{\alpha-1}\left(1-x^{\alpha}\right)^{\beta-1} \tag{10}$$

Figure 68 is an illustration of Kumaraswamy distributions for the same values of α and β as the beta distributions in Figure 67. These distributions take very similar forms; indeed any Kumaraswamy distribution with parameters α and β is in fact the α^{th} root of a beta distribution with α = 1 and the same β.[134] Forms of this distribution are typically not included in statistical and spreadsheet packages, and while they would be easy to code, they would essentially be a simplification of already available Beta distributions.

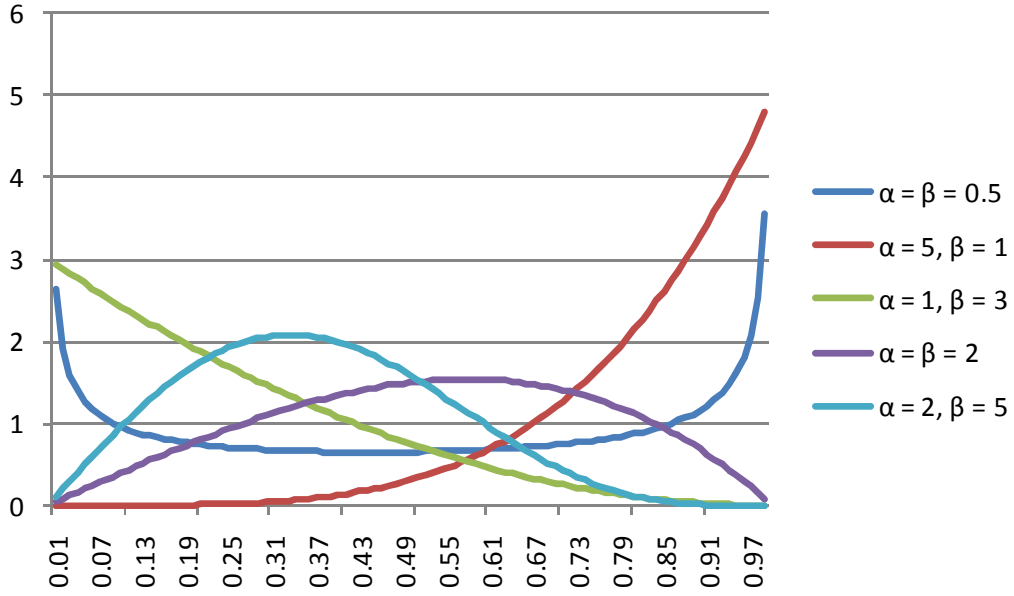

Figure 68. Sample Kumaraswamy distributions.

The truncated normal distribution behaves simply as a bounded normal distribution, and its probability density function in a region bounded by $0 \leq x \leq 1$ is given by Eq. (11):

$$f(x;\mu,\sigma) = \frac{\frac{1}{\sigma}\phi\left(\frac{x-\mu}{\sigma}\right)}{\Phi\left(\frac{1-\mu}{\sigma}\right) - \Phi\left(\frac{-\mu}{\sigma}\right)} \tag{11}$$

where $\varphi(x;\mu,\sigma)$ represents the standard normal probability density function given by Eq. (12)

$$\phi(x;\mu,\sigma) = \frac{1}{\sqrt{2\pi\sigma^2}} e^{-\left(x-\mu^2\right)/(2\sigma)^2} \tag{12}$$

and $\Phi(x)$ represents the standard normal cumulative distribution function given by Eq. (13)

$$\Phi(x) = \frac{1}{\sqrt{2\pi}} \int_{-\infty}^{x} e^{-t^2/2} dt \tag{13}$$

One advantage of the truncated normal distribution is that its two parameters, μ and σ, represent the mean and standard deviation, respectively, of the distribution, making visualization of the distribution very intuitive relative to the parameters α and β of the other two distributions considered. Sample truncated normal distributions are given in Figure 69. As the figure shows, these distributions are extremely sensitive to changes in σ; a change from 0.1 to 0.5 is the difference between a very flat and a very peaked distribution. Because these parameters will be varied in generating future fleet scenarios, the fact that they are so sensitive means that caution must be exercised in choosing their ranges when attempting to comprehensively evaluate the design space.

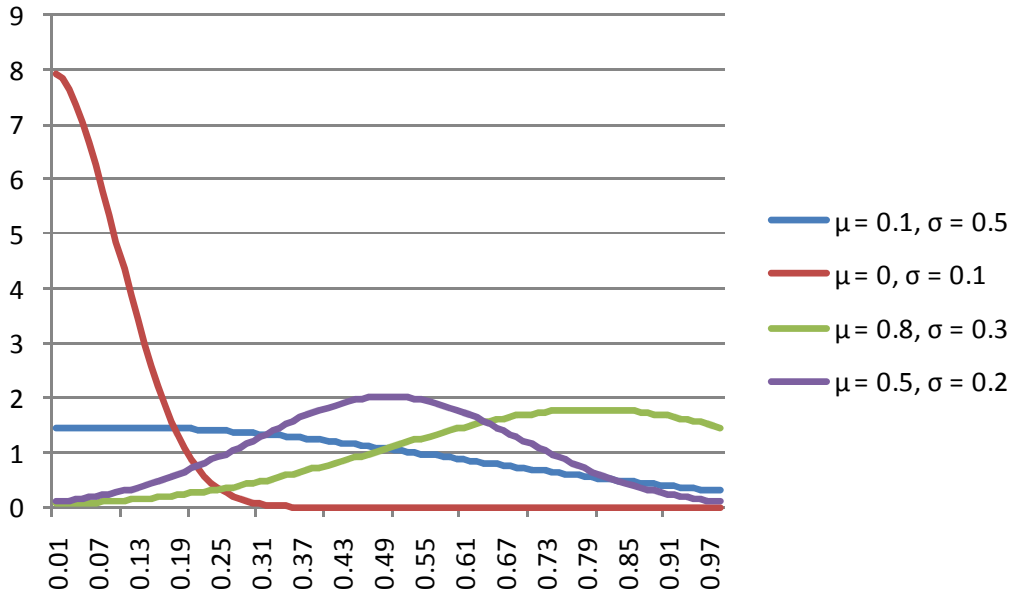

Figure 69. Sample truncated normal distributions.

The ability of each approach to simulate realistic flight distributions must be evaluated to choose the best one for this first approach. Samples of beta distributions and

truncated normal distributions which may be considered indicative of their general behaviors are provided in Figure 70.

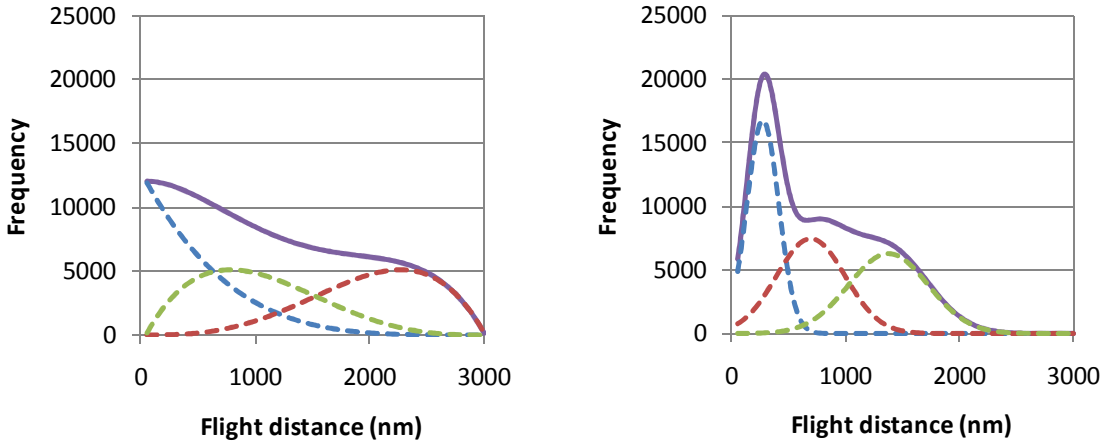

Figure 70. Sample composite beta distribution (left) and sample composite truncated normal distribution (right).

Kumaraswamy distributions were not included due to their similarities with the beta distribution. In each figure, the constituent distributions are represented by dashed lines, and the composite distributions are represented by solid lines. Each composite distribution represents the same number of flights and the same range of flight distance as presented in Figure 27, however it is also easy to see that the actual flight frequencies represented by Figure 27 are much less smooth because these two figures do not constrained by having to represent actual OD pairs. Although each of these distributions is easy to implement as functions of two parameters, it is clear from examination of these two distributions, the composite truncated normal distribution is able to capture the shape of the actual flight distribution better. The sensitivity of the peakedness of the normal distributions is actually a benefit in terms of generating multimodal segments analogous to those of the actual flight distribution. Thus, for this first approach of using a

composite, continuous probability distribution to represent an actual distribution of flight frequency, the composite truncated normal distribution would be more appropriate.

APPENDIX B

DESIGNS OF EXPERIMENTS FOR SCREENING AND DESIGN SPACE EXPLORATION

This appendix describes the use of DOEs for screening tests and design space exploration. A screening test may be conducted with a full factorial DOE, and fractional factorial DOE, a random balance DOE, or a Plackett-Burman DOE. A full factorial DOE will contain every combination of every level of every design variable that is considered in the DOE. Assuming two levels for each DOE, the number of cases run for this is 2^n, where n represents the number of variables considered. An example of a two level, full factorial DOE for three variables A, B, and C is given in Table 18, where + and – represent the two levels of each variable. For only three input variables, a full factorial requires 2^3 runs, or 8 runs.

Table 18. Two level, full factorial DOE.

Run	A	B	C
1	-	-	-
2	+	-	-
3	-	+	-
4	+	+	-
5	-	-	+
6	+	-	+
7	-	+	+
8	+	+	+

For large numbers of variables, this quickly becomes very computationally expensive. In cases where the total number of variables n is large, but only a subset are expected to be significant, designs which are fractional factorial in the n variables may be chosen, meaning that the design contains full factorials for any subset of a certain smaller amount

of input variables. Building off of the full factorial example of Table 18, Table 19 illustrates a two level, fractional factorial DOE for four input variables. The fractional factorial DOE still contains a full factorial for any three of the input variables, but, in this instance, the fourth variable is always confounded with, or equivalent to, the sum of the settings of, the other three. As can be seen, the number of runs to screen the effects of four variables with a fractional factorial DOE is still eight, as opposed to the 16 runs that would have required with a full factorial DOE. In general, the number of runs required for a fractional factorial is 2^{n-p}, where n is the total number of variables, and p represents the fraction of number of full factorial runs that the design represents, equivalent to the exponent of $\left(\frac{1}{2}\right)^{p}$ multiplied by the number of full factorial runs.[135]

Table 19. Two level, fractional factorial DOE.

Run	A	B	C	D
1	-	-	-	-
2	+	-	-	+
3	-	+	-	+
4	+	+	-	-
5	-	-	+	+
6	+	-	+	-
7	-	+	+	-
8	+	+	+	+

Another efficient DOE for screening is the Plackett-Burman design. This design significantly reduces the number of runs by focusing only on the impact of main effects and neglecting the impact of interactions. As shown in Table 20, for the same eight runs as a the previous full or fractional factorial examples, the Plackett-Burman DOE can screen up to seven variables, or one less than the number of cases. The drawbacks of this design are that by assuming no interactions, there is significant compounding of main

effects with two factor interactions, e.g. it would be impossible to distinguish between the impact of A and the impact of the product of D and E.[136]

Table 20. Two level, Plackett-Burman DOE.

Run	A	B	C	D	E	F	G
1	-	-	+	-	+	+	-
2	+	-	-	-	-	+	+
3	-	+	-	-	+	-	+
4	+	+	+	-	-	-	-
5	-	-	+	+	-	-	+
6	+	-	-	+	+	-	-
7	-	+	-	+	-	+	-
8	+	+	+	+	+	+	+

Each of these different types of designs may be further characterized by their resolution, which specifies what effects may be confounded. The Plackett-Burman design is Resolution III, meaning that main effects are not confounded with any other main effect; they are confounded with two-factor interactions as described in the relationship between A and the product of D and E above. A fractional factorial design is Resolution IV, meaning that no main effects are confounded with each other or with two-factor interactions, but also that two-factor interactions are confounded with one another. A full factorial design is considered to be Resolution V, which means that no main effect or two-factor interactions are confounded with any other main effect or two-factor interaction. However, two factor interactions are confounded with three factor interactions. For the purpose of screening variables for this work, a fractional factorial design is well suited because of its resolution and efficiency.

After the effect screening DOE has been evaluated through the M&S environment with appropriate ranges for each of the input effects, there are a number of techniques available to study the behavior of the outputs and make inferences as to the significance

of each of the inputs. One of the most commonly accepted techniques is the use of a statistical process chart known as the Pareto chart, which is considered one of the seven basic quality tools.[137] Developed to illustrate the Pareto principle, which was the observation in 1906 by Italian economist Vilfredo Pareto that 80% of Italy's wealth was distributed among the richest 20% of its people, the Pareto chart visually displays the relative significance of several input effects by ranking them in order of decreasing importance, allowing the calculation of their cumulative impact on the outputs.[138] Since that time, the Pareto principle itself has become an accepted rule of thumb for determining the impact of known variables on the results of a problem.[139]

A number of statistical methods exist to analyze the results of a factorial design for effect screening. The impact of an input parameter may be calculated as the difference between the mean value of all outputs at the maximum setting of, and the mean value of all outputs at the minimum setting of, the input parameter. Significance of an input may also be determined by examining the parameter estimates of a linear model representing the output. The more significant input factors will tend to have larger parameter estimates in this model; however, caution must be exercised because the scale of the input factors may also influence the magnitude of parameter estimates. In order to circumvent this, the estimates may be orthogonalized, which allows the estimates to be compared objectively.[140]

Another method is Analysis of Variance (ANOVA), which decomposes the total variability of the outputs, which is measured by the sum of the squared deviations from the total mean sum of squares, into contributions by each of the input parameters and an error term. The impact of each input on the variability of the output can be compared to

each other, as in the Pareto principle, or they may be used to generate statistics for evaluation of significance using probability testing.[141] Other methods include t-testing, which also uses probability to evaluate statistical significance, and scaled estimates, in which the aforementioned parameter estimates assigned to input factors are scaled to a mean of 0 and a range of 2, allowing direct comparison to be made on effect sizes between factors.[140] Although these approaches could also be applied to this work, the choice of approach is not particularly important here because the goal of effect screening here is not to provide a restricted or definitive list of variables to vary. The goal is purely to be able to observe what variables may contribute significantly to each of the output metrics, thereby creating a structured process for variable selection in Chapter 4.

The nature of the random variation of the input parameters is the second key point of interest for the filtering approach, and ties back in with DOE selection mentioned earlier. In pure Monte Carlo approaches, the nature of input variation is not structured, but purely random. However, for this application, exploration of the complete design space is a priority to identify potential average replacement vehicles. In the second DOE that is run around the most significant input parameters, each DOE case represents a potential average replacement model, and the physics-based aircraft model generates fleet-level inputs for each one of them, allowing them to be run through fleet-level analysis to generate their responses for fuel burn and NO_x. In contrast with the screening DOE, the goal of which is to determine significant input parameters based on the trends of outputs, the DOE that is selected for use in determining the average replacement model must be capable of spanning the design space of the significant input parameters. Classical DOEs, such as the Box Behnken and Central Composite Design, were developed assuming the

existence of experimental error in the results, and therefore focus on sampling the edges of the design space in an attempt to minimize the impact of these errors.

More recent DOEs, developed for use with repeatable computer codes, differ from classical DOEs by focusing on the interior portions of the design space to minimize any bias between the approximation model and mathematical function. These DOEs are known as space-filling designs and generally rely on one of two approaches: covering the entire design space as much as possible or to distribute them evenly across the space.[142] The simplest approach is pure random sampling of the set of input parameters X from their input ranges and distributions. An example of such a stochastic sampling method is known as Monte Carlo sampling, which employs a pseudo random number generator to sample different bins in each dimension. As the number of samples increase, the frequency distributions of samples taken in each dimension approach a uniform distribution.[143] Stratified sampling, or importance sampling, breaks the space of the input parameters into distinct groups. The input parameters are then randomly sampled from each group. This guarantees that all areas of the input space are captured by the sampling, but it adds the added complexity of having to predetermine the bounds of each strata; however the disadvantage is that characteristics of the space must be well known in order to predetermine the bounds of each strata.[144]

Other methods exist to extend the stratified sampling method by splitting the range of each input variable x_i is split into a predetermined number of intervals, and values for x_i are chosen with equal probability from each interval. These space-filling methods combine the advantages of random sampling, which requires no complex predetermination of interval boundaries, with stratified sampling, which guarantees

complete coverage of the input space. Common examples of space-filling designs are the sphere packing design, the uniform design, the Latin hypercube design, the minimum potential design, the minimum entropy design, and the integrated mean square optimal design, and they will be described here as defined in a user guide from the statistical software package JMP.[145] The benefits and drawbacks of each will be illustrated with a figures representing two factor, eight run DOEs. The sphere packing design maximizes the minimum distance between each pair of design points to spread the points out as much as possible inside the design region As shown in Figure 71; however, as the figure shows, the design space is not necessarily uniformly sampled for each factor, leading to potential gaps in the design space.

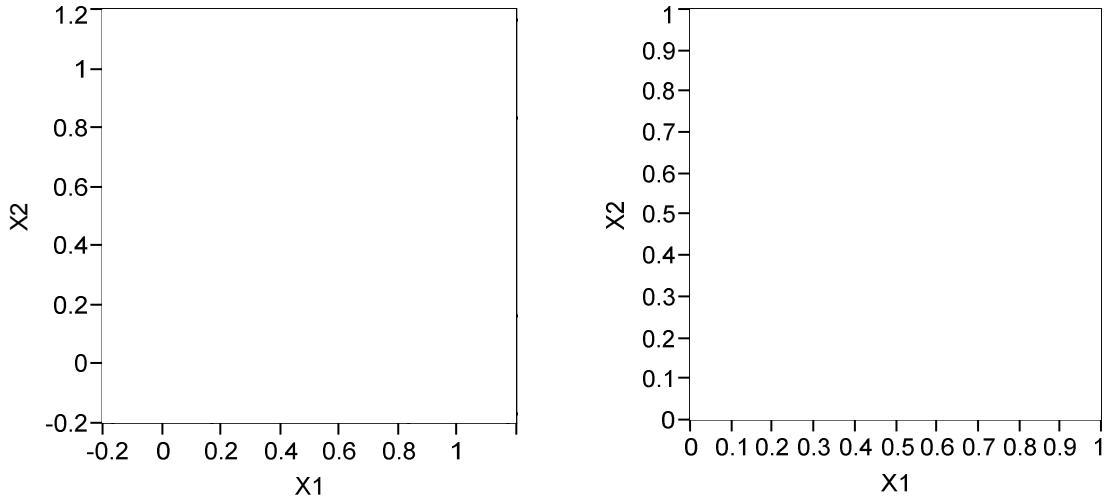

Figure 71. Two factor sphere packing DOE (left) and two factor uniform DOE (right).

. Contrastingly, the uniform design positions the design points to mimic a uniform distribution for each factor. As illustrated by the gaps in certain areas of the design space in Figure 71 with large distance between points, because that distance between points is not considered, this design may require more points to cover all areas of the design space.

In a Latin hypercube design, each factor has as many levels as there are runs in the design. Like the uniform design, levels are evenly spaced between each factor's lower bound and upper bound. Like the sphere-packing method, the Latin hypercube method chooses points to maximize the minimum distance between design points, but with a constraint that maintains even spacing between factor levels. As can be seen in Figure 72, this design has very good coverage of the interior of the design space; however, it does have gaps at the edges of the design space.

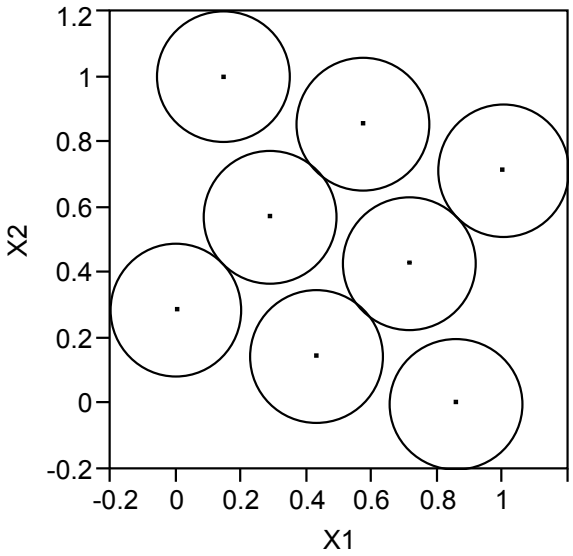

Figure 72. Two factor Latin hypercube DOE.

The minimum potential design spreads points out within a sphere by optimizing their positions based on a notional potential energy. This energy is calculated based on values of attraction and repulsion calculated as functions of distance between points, and is then minimized for the system. The resulting spherical design is illustrated in Figure 73. Because of its spherical nature, it may not capture intermediate range points or points at the corners.

The maximum entropy design deploys points by maximizing a measure of the amount of information contained in the system of points, calculated as a sum of weighted squared differences between point positions. This design has good overall coverage of the design space as shown in Figure 73, but may be sparse in the center. The integrated mean square optimal design minimizes the sum of a mean squared error calculated as a weighted function of each point's position within the experimental region.[146] The result is similar to that of the sphere packing design, as can be seen in Figure 74, and it is rather sparse in the interior of the design space.

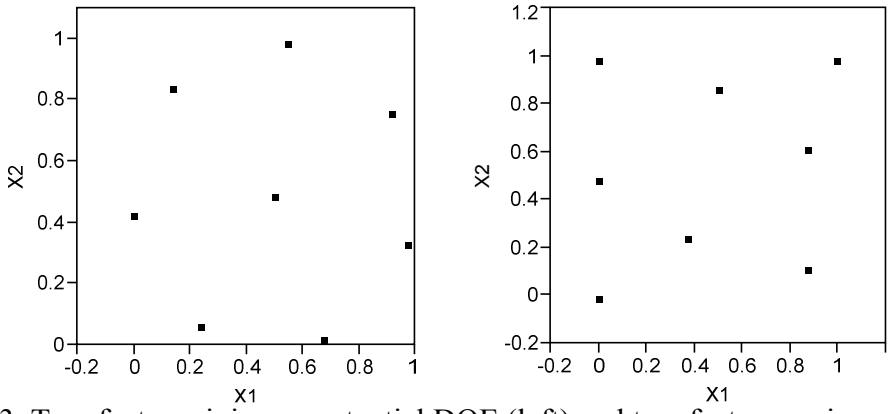

Figure 73. Two factor minimum potential DOE (left) and two factor maximum entropy DOE (right).

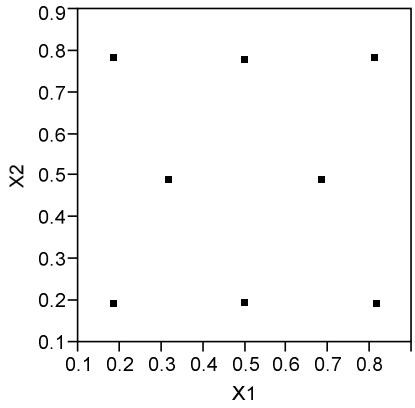

Figure 74. Integrated mean squared error DOE.

The advantages and disadvantages of these designs must be considered when selecting a DOE to use for average replacement selection. The ranges of the DOE will

encompass known values for factors from each aircraft within each capability group. It is desirable to query these ranges uniformly and also have good coverage of the interior of the design space, because by their nature, the average replacement vehicles themselves will most likely lie in that region. Thus, for this work, the DOE that makes the most sense to use is the Latin hypercube design.

The final step of the filtering approach is to classify each DOE result for each prediction as acceptable or unacceptable based on how well it captures the target. This will result in one final average vehicle to represent the capability group. If multiple vehicles capture the aggregate target within an acceptable level of accuracy, the sum of squares error may be used to compare how well they may capture the environmental metrics of interest over the entire range of flight distance. Beyond this, engineering judgment may be used to if multiple vehicles comparably capture the targets. In this scenario, engineering judgment would rule out vehicles with characteristics that are either unlikely to exist in an actual production aircraft, or that would render a vehicle insensitive to the application of technologies. Examples of the former would include high stage counts in the HPC, or high combustor inlet temperature, while examples of the latter include low cooling requirements or a design Mach number much greater than the cruise Mach number.

APPENDIX C

PARAMETRIC CORRECTION FACTOR COEFFICIENTS

On the following pages, tables of the parametric correction factors developed for each environmental metric study are provided for all four capability groups. These equations take the form of Eq. (14) as follows:

$$Y = a_2(FD)^2 + a_1(FD) + a_0 \tag{14}$$

where Y is the particular environmental metric and FD is the flight distance.

Table 21. Parametric correction factors for regional jet total mission fuel burn.

Airframe	Engine	a_2	a_1	a_0
CRJ7	CF34-8C1	-7.011E-04	1.221E-01	-3.195E+02
CRJ7	CF34-8C1 Block 1	-3.267E-04	-4.339E-01	-1.566E+02
CRJ7-ER	CF34-8C1	-4.996E-04	-2.444E-01	-1.938E+02
CRJ7-ER	CF34-8C1 Block 1	-2.918E-04	-3.780E-01	-1.856E+02
CRJ7-LR	CF34-8C5	-3.208E-04	-3.465E-01	-2.287E+02
CRJ9	CF34-8C5	-1.238E-03	6.267E-01	-4.378E+02
CRJ9	CF34-8C5	-2.943E-04	6.568E-01	-3.281E+01
ERJ170	CF34-8E5	-1.695E-04	4.194E-01	-8.971E+01
ERJ170	CF34-8E5	-6.040E-04	9.022E-01	-7.064E+01
ERJ170-LR	CF34-8E5	6.865E-04	3.414E-01	7.818E+01
ERJ190	CF34-10E5	1.971E-03	3.977E-05	2.485E-06
ERJ190	CF34-10E5A1	2.811E-04	-6.193E-02	2.951E+02
ERJ190	CF34-10E6	-1.338E-04	8.696E-01	2.181E+02

Table 22. Parametric correction factors for regional jet total mission NO_x.

Airframe	Engine	a_2	a_1	a_0
CRJ7	CF34-8C1	-9.253E-03	2.439E+00	-4.486E+03
CRJ7	CF34-8C1 Block 1	-3.610E-03	-8.145E+00	-2.479E+03
CRJ7-ER	CF34-8C1	-5.051E-03	-4.099E+00	-2.497E+03
CRJ7-ER	CF34-8C1 Block 1	-3.823E-03	-6.697E+00	-3.026E+03
CRJ7-LR	CF34-8C5	-3.557E-03	-5.539E+00	-2.901E+03
CRJ9	CF34-8C5	-1.416E-02	4.920E+00	-5.221E+03
CRJ9	CF34-8C5	-3.617E-03	8.929E+00	-5.101E+02
ERJ170	CF34-8E5	-5.350E-04	5.125E+00	-1.119E+03
ERJ170	CF34-8E5	-9.025E-03	1.480E+01	-8.723E+02
ERJ170-LR	CF34-8E5	7.123E-03	8.355E+00	7.646E+02
ERJ190	CF34-10E5	1.600E-02	3.637E-05	-1.575E-05
ERJ190	CF34-10E5A1	2.699E-04	1.962E+00	1.727E+03
ERJ190	CF34-10E6	-2.072E-03	7.257E+00	1.898E+03

Table 23. Parametric correction factors for regional jet terminal area fuel burn.

Airframe	Engine	a_2	a_1	a_0
CRJ7	CF34-8C1	-2.292E-05	3.049E-03	-1.498E+02
CRJ7	CF34-8C1 Block 1	-1.932E-05	1.112E-02	-1.476E+02
CRJ7-ER	CF34-8C1	-1.142E-04	1.218E-01	-1.670E+02
CRJ7-ER	CF34-8C1 Block 1	-8.823E-06	2.230E-02	-1.515E+02
CRJ7-LR	CF34-8C5	-4.831E-05	2.924E-02	-1.714E+02
CRJ9	CF34-8C5	-8.150E-06	-7.002E-03	-1.939E+02
CRJ9	CF34-8C5	-2.429E-05	-1.404E-03	-1.054E+02
ERJ170	CF34-8E5	5.688E-05	-4.187E-02	-7.215E+01
ERJ170	CF34-8E5	-4.155E-05	4.092E-02	-4.923E+01
ERJ170-LR	CF34-8E5	6.456E-05	-2.094E-02	-1.908E+00
ERJ190	CF34-10E5	-3.458E-04	-7.859E-07	-1.786E-09
ERJ190	CF34-10E5A1	4.913E-06	-2.669E-02	-5.288E+01
ERJ190	CF34-10E6	1.993E-05	-7.417E-02	6.293E+01

Table 24. Parametric correction factors for regional jet terminal area NO_x.

Airframe	Engine	a_2	a_1	a_0
CRJ7	CF34-8C1	-2.904E-04	9.416E-02	-1.968E+03
CRJ7	CF34-8C1 Block 1	-1.703E-04	-4.889E-02	-2.028E+03
CRJ7-ER	CF34-8C1	-6.444E-04	4.849E-01	-1.985E+03
CRJ7-ER	CF34-8C1 Block 1	-1.436E-04	1.384E-02	-2.058E+03
CRJ7-LR	CF34-8C5	-3.874E-04	8.817E-02	-1.940E+03
CRJ9	CF34-8C5	1.807E-04	-3.292E-01	-2.227E+03
CRJ9	CF34-8C5	-2.421E-04	2.495E-02	-1.129E+03
ERJ170	CF34-8E5	4.553E-04	-5.234E-01	-5.146E+02
ERJ170	CF34-8E5	-5.089E-04	2.921E-01	-9.628E+01
ERJ170-LR	CF34-8E5	-7.979E-06	4.698E-01	4.660E+02
ERJ190	CF34-10E5	-5.695E-03	5.394E-06	2.476E-08
ERJ190	CF34-10E5A1	9.890E-05	-5.178E-01	-7.082E+02
ERJ190	CF34-10E6	3.231E-04	-9.689E-01	7.749E+01

Table 25. Parametric correction factors for single-aisle total mission fuel burn.

Airframe	Engine	a_2	a_1	a_0
B737-6	CFM56-7B22	-9.913E-05	-2.505E-01	5.204E+01
B737-6	CFM56-7B20/2	-5.591E-05	-1.481E-01	1.478E+02
B737-6	CFM56-7B20	-5.458E-05	-1.525E-01	1.405E+02
B737-7	CFM56-7B22	-3.987E-05	-1.054E-01	6.294E+01
B737-7	CFM56-7B24	-4.061E-05	-1.029E-01	7.732E+01
B737-7	CFM56-7B27	-4.072E-05	-1.027E-01	9.009E+01
B737-7	CFM56-7B26	-3.895E-05	-1.093E-01	1.163E+02
B737-7	CFM56-7B24	3.072E-05	8.797E+00	1.324E+03
B737-8	CFM56-7B27	-8.627E-05	5.143E-01	1.088E+02
B737-8	CFM56-7B26	-8.625E-05	5.141E-01	1.312E+02
B737-8	CFM56-5B8/P	3.072E-05	8.797E+00	1.324E+03
A318-1	V2527-A5	2.063E-05	-3.611E-01	6.739E+01
A319-1	CFM56-5B6/2	2.000E-05	-3.583E-01	1.710E+02
A319-1	CFM56-5B6/2P	2.039E-05	-3.597E-01	1.186E+02
A319-1	CFM56-5B5/P	2.042E-05	-3.598E-01	1.156E+02
A319-1	CFM56-5B6/P	2.063E-05	-3.611E-01	6.739E+01
A319-1	V2522-A5	2.055E-05	-3.604E-01	7.571E+01
A319-1	V2524-A5	2.004E-05	-3.585E-01	1.400E+02
A319-1	CFM56-5A4	1.984E-05	-3.578E-01	1.552E+02
A319-1	CFM56-5A5	2.063E-05	-3.609E-01	7.009E+01
A319-1	CFM56-5B7/P	2.034E-05	-3.598E-01	7.869E+01
A319-1	CFM56-5-A1	2.058E-05	-3.606E-01	9.777E+01
A320-2	CFM56-5A3	-1.892E-04	6.828E-01	-6.531E+01
A320-2	V2500-A1	-1.896E-04	6.840E-01	-5.559E+01
A320-2	V2527-A5	-1.343E-04	5.420E-01	1.223E+01
A320-2	V2527-A5	-1.338E-04	5.398E-01	2.792E+01
A320-2	CFM56-5B4	-1.338E-04	5.398E-01	2.792E+01
A320-2	CFM56-5B4/2	-1.894E-04	6.833E-01	-4.715E+01
A320-2	V2530-A5	-1.887E-04	6.801E-01	-4.354E-02
A321-1	CFM56-5B2	2.757E-04	5.825E-01	4.002E+02
A321-1	CFM56-5B1/2	2.758E-04	5.819E-01	3.413E+02
A321-1	V2530-A5	2.757E-04	5.823E-01	3.722E+02
A321-2	CFM56-5B1/P	2.757E-04	5.825E-01	4.002E+02
A321-2	CFM56-5B3/P	2.759E-04	5.819E-01	3.130E+02
A321-2	V2533-A5	2.758E-04	5.819E-01	3.289E+02
A321-2	CFM56-5B3/2P	2.757E-04	5.825E-01	3.949E+02
A321-2	CFM56-5B3	2.757E-04	5.824E-01	3.753E+02

Table 26. Parametric correction factors for single-aisle total mission NO_x.

Airframe	Engine	a_2	a_1	a_0
B737-6	CFM56-7B22	-3.462E-03	-7.091E+00	-1.202E+02
B737-6	CFM56-7B20/2	-1.842E-03	-6.061E+00	3.752E+03
B737-6	CFM56-7B20	-1.999E-03	-2.448E+01	-3.097E+03
B737-7	CFM56-7B22	-1.652E-03	-6.187E+00	1.068E+03
B737-7	CFM56-7B24	-1.640E-03	-4.776E+00	2.879E+03
B737-7	CFM56-7B27	-1.611E-03	-4.368E+00	3.518E+03
B737-7	CFM56-7B26	-1.560E-03	-2.308E+00	3.820E+03
B737-7	CFM56-7B24	4.569E-04	7.194E+01	2.495E+04
B737-8	CFM56-7B27	-2.590E-03	8.691E+00	5.313E+03
B737-8	CFM56-7B26	-2.591E-03	1.169E+01	6.518E+03
B737-8	CFM56-5B8/P	4.569E-04	7.194E+01	2.495E+04
A318-1	V2527-A5	-2.783E-04	-1.415E+01	2.585E+03
A319-1	CFM56-5B6/2	1.342E-04	-1.120E+01	7.032E+03
A319-1	CFM56-5B6/2P	-1.132E-03	-2.665E+01	-3.937E+03
A319-1	CFM56-5B5/P	-1.033E-03	-2.839E+01	-2.861E+03
A319-1	CFM56-5B6/P	-1.000E-04	-9.772E+00	4.464E+03
A319-1	V2522-A5	-9.016E-05	-8.897E+00	5.031E+03
A319-1	V2524-A5	3.264E-05	-1.116E+01	6.593E+03
A319-1	CFM56-5A4	1.283E-04	-1.162E+01	6.980E+03
A319-1	CFM56-5A5	-1.167E-05	-8.834E+00	5.224E+03
A319-1	CFM56-5B7/P	-3.286E-05	-8.721E+00	5.916E+03
A319-1	CFM56-5-A1	1.313E-04	-7.700E+00	5.892E+03
A320-2	CFM56-5A3	-4.540E-03	7.112E+00	4.668E+03
A320-2	V2500-A1	-4.584E-03	7.615E+00	5.016E+03
A320-2	V2527-A5	-3.851E-03	3.956E+01	1.398E+04
A320-2	V2527-A5	-3.499E-03	1.032E+01	7.165E+03
A320-2	CFM56-5B4	-3.499E-03	1.032E+01	7.165E+03
A320-2	CFM56-5B4/2	-4.714E-03	1.494E+01	6.138E+03
A320-2	V2530-A5	-3.398E-03	-2.234E+01	-1.798E+03
A321-1	CFM56-5B2	8.347E-03	1.081E+01	2.121E+04
A321-1	CFM56-5B1/2	8.257E-03	1.384E+01	2.094E+04
A321-1	V2530-A5	3.815E-03	-1.960E+01	8.327E+03
A321-2	CFM56-5B1/P	8.347E-03	1.081E+01	2.121E+04
A321-2	CFM56-5B3/P	8.170E-03	1.519E+01	1.964E+04
A321-2	V2533-A5	8.386E-03	1.607E+01	2.101E+04
A321-2	CFM56-5B3/2P	8.355E-03	1.240E+01	2.170E+04
A321-2	CFM56-5B3	4.814E-03	-1.380E+01	1.140E+04

Table 27. Parametric correction factors for single-aisle terminal area fuel burn.

Airframe	Engine	a_2	a_1	a_0
B737-6	CFM56-7B22	-2.631E-07	-1.635E-02	-1.255E+02
B737-6	CFM56-7B20/2	-6.404E-07	-7.732E-03	-6.178E+01
B737-6	CFM56-7B20	-6.369E-07	-7.748E-03	-7.113E+01
B737-7	CFM56-7B22	-6.580E-07	-7.710E-03	-7.743E+01
B737-7	CFM56-7B24	-6.753E-07	-7.672E-03	-6.175E+01
B737-7	CFM56-7B27	-1.380E-06	-5.319E-03	-5.027E+01
B737-7	CFM56-7B26	-1.709E-06	-4.215E-03	-2.889E+01
B737-7	CFM56-7B24	-8.496E-06	8.940E-02	1.010E+03
B737-8	CFM56-7B27	-3.456E-06	2.073E-03	3.377E+01
B737-8	CFM56-7B26	-3.613E-06	2.643E-03	5.527E+01
B737-8	CFM56-5B8/P	-8.496E-06	8.940E-02	1.010E+03
A318-1	V2527-A5	1.260E-06	-1.362E-02	-1.176E+02
A319-1	CFM56-5B6/2	1.183E-06	-1.361E-02	-1.084E+01
A319-1	CFM56-5B6/2P	7.214E-07	-1.193E-02	-6.506E+01
A319-1	CFM56-5B5/P	7.408E-07	-1.196E-02	-6.824E+01
A319-1	CFM56-5B6/P	1.260E-06	-1.362E-02	-1.176E+02
A319-1	V2522-A5	1.060E-06	-1.286E-02	-1.088E+02
A319-1	V2524-A5	6.315E-07	-1.199E-02	-4.231E+01
A319-1	CFM56-5A4	4.645E-07	-1.076E-02	-2.851E+01
A319-1	CFM56-5A5	1.232E-06	-1.350E-02	-1.146E+02
A319-1	CFM56-5B7/P	1.174E-06	-1.322E-02	-1.055E+02
A319-1	CFM56-5-A1	1.221E-06	-1.326E-02	-8.686E+01
A320-2	CFM56-5A3	-1.828E-06	1.800E-03	2.548E+01
A320-2	V2500-A1	-9.019E-07	-1.545E-03	3.774E+01
A320-2	V2527-A5	2.255E-06	-1.085E-02	6.185E+01
A320-2	V2527-A5	2.117E-06	-1.017E-02	7.320E+01
A320-2	CFM56-5B4	2.117E-06	-1.017E-02	7.320E+01
A320-2	CFM56-5B4/2	-1.917E-06	1.963E-03	4.390E+01
A320-2	V2530-A5	-8.068E-07	-2.069E-03	9.000E+01
A321-1	CFM56-5B2	1.902E-06	-3.534E-03	1.328E+02
A321-1	CFM56-5B1/2	2.527E-06	-6.027E-03	7.548E+01
A321-1	V2530-A5	2.018E-06	-4.150E-03	1.055E+02
A321-2	CFM56-5B1/P	1.902E-06	-3.534E-03	1.328E+02
A321-2	CFM56-5B3/P	2.765E-06	-7.065E-03	4.838E+01
A321-2	V2533-A5	1.882E-06	-3.802E-03	6.188E+01
A321-2	CFM56-5B3/2P	1.894E-06	-3.501E-03	1.275E+02
A321-2	CFM56-5B3	1.978E-06	-3.918E-03	1.083E+02

Table 28. Parametric correction factors for single-aisle terminal area NO_x.

Airframe	Engine	a_2	a_1	a_0
B737-6	CFM56-7B22	-4.326E-06	-4.460E-01	-1.562E+03
B737-6	CFM56-7B20/2	-4.259E-06	-2.188E-01	-4.740E+02
B737-6	CFM56-7B20	1.818E-06	-4.924E-01	-2.615E+03
B737-7	CFM56-7B22	-2.799E-06	-2.923E-01	-1.063E+03
B737-7	CFM56-7B24	-4.927E-06	-2.181E-01	-4.723E+02
B737-7	CFM56-7B27	-6.063E-06	-1.635E-01	-1.804E+02
B737-7	CFM56-7B26	-5.814E-06	-1.596E-01	9.526E+01
B737-7	CFM56-7B24	-1.092E-04	1.431E+00	8.429E+03
B737-8	CFM56-7B27	-6.252E-05	3.937E-02	1.408E+03
B737-8	CFM56-7B26	-7.690E-05	1.935E-01	2.622E+03
B737-8	CFM56-5B8/P	-1.092E-04	1.431E+00	8.429E+03
A318-1	V2527-A5	4.120E-05	-4.423E-01	-1.744E+03
A319-1	CFM56-5B6/2	4.501E-05	-3.211E-01	6.211E+01
A319-1	CFM56-5B6/2P	3.232E-05	-5.911E-01	-2.668E+03
A319-1	CFM56-5B5/P	3.462E-05	-5.724E-01	-2.740E+03
A319-1	CFM56-5B6/P	4.638E-05	-3.959E-01	-1.179E+03
A319-1	V2522-A5	4.745E-05	-3.638E-01	-8.234E+02
A319-1	V2524-A5	4.718E-05	-3.399E-01	-3.250E+02
A319-1	CFM56-5A4	4.652E-05	-3.282E-01	-2.009E+01
A319-1	CFM56-5A5	4.705E-05	-3.794E-01	-9.754E+02
A319-1	CFM56-5B7/P	4.865E-05	-3.382E-01	-5.396E+02
A319-1	CFM56-5-A1	4.505E-05	-3.335E-01	-3.795E+02
A320-2	CFM56-5A3	-2.171E-05	1.822E-02	1.481E+03
A320-2	V2500-A1	-2.427E-05	7.657E-02	1.947E+03
A320-2	V2527-A5	7.781E-05	1.307E-01	5.857E+03
A320-2	V2527-A5	6.017E-05	-1.517E-01	2.359E+03
A320-2	CFM56-5B4	6.017E-05	-1.517E-01	2.359E+03
A320-2	CFM56-5B4/2	-2.610E-05	1.491E-01	2.771E+03
A320-2	V2530-A5	-8.099E-06	-2.927E-01	-5.746E+02
A321-1	CFM56-5B2	6.687E-05	1.901E-01	5.210E+03
A321-1	CFM56-5B1/2	6.049E-05	3.163E-01	5.735E+03
A321-1	V2530-A5	4.007E-05	-2.973E-02	2.545E+03
A321-2	CFM56-5B1/P	6.687E-05	1.901E-01	5.210E+03
A321-2	CFM56-5B3/P	6.623E-05	1.679E-01	4.566E+03
A321-2	V2533-A5	6.209E-05	3.014E-01	5.640E+03
A321-2	CFM56-5B3/2P	6.310E-05	2.755E-01	5.907E+03
A321-2	CFM56-5B3	3.984E-05	1.192E-01	3.463E+03

Table 29. Parametric correction factors for small twin-aisle total mission fuel burn.

Airframe	Engine	a_2	a_1	a_0
B767-2	CF6-80A	-1.524E-04	-1.379E-01	-9.756E+02
B767-2	CF6-80A2	-1.524E-04	-1.379E-01	-9.756E+02
B767-2	CF6-80C2B2F	-1.520E-04	-1.403E-01	-8.635E+02
B767-2ER	CF6-80A2	-1.784E-04	1.282E+00	-6.936E+02
B767-2ER	CF6-80C2B2	-1.778E-04	1.279E+00	-5.601E+02
B767-2ER	CF6-80C2B2F	-1.781E-04	1.281E+00	-5.824E+02
B767-2ER	CF6-80C2B4	-1.775E-04	1.278E+00	-5.388E+02
B767-2ER	PW4056	-1.778E-04	1.280E+00	-5.114E+02
B767-2ER	PW4060	-1.776E-04	1.279E+00	-4.955E+02
B767-2ER	CF6-80C2B4F	-1.775E-04	1.278E+00	-5.388E+02
B767-3	CF6-80A2	-1.540E-04	9.144E-01	-2.809E+02
B767-3	CF6-80C2B2	-1.532E-04	9.107E-01	-1.489E+02
B767-3	CF6-80C2B2F	-1.528E-04	9.085E-01	-1.672E+02
B767-3	CF6-80C2B4F	-1.532E-04	9.106E-01	-1.469E+02
B767-3	PW4056	-1.523E-04	9.055E-01	-9.212E+01
B767-3	PW4060	-1.539E-04	9.145E-01	-8.672E+01
B767-3	CF6-80C2B2F	-1.530E-04	9.093E-01	-1.595E+02
B767-3	CF6-80C2B7F	-1.540E-04	9.139E-01	-1.135E+02
B767-3ER	CF6-80C2B2F	-1.534E-04	9.123E-01	-1.722E+02
B767-3ER	CF6-80C2B4	-1.521E-04	9.038E-01	-1.178E+02
B767-3ER	CF6-80C2B6	-1.529E-04	9.100E-01	-1.027E+02
B767-3ER	CF6-80C2B6F	-1.527E-04	9.066E-01	-1.268E+02
B767-3ER	PW4056	-1.531E-04	9.112E-01	-1.007E+02
B767-3ER	PW4060	-1.528E-04	9.073E-01	-7.528E+01
B767-3ER	PW4x52	-1.522E-04	9.042E-01	-1.204E+02
B767-3ER	PW4x56	-1.531E-04	9.112E-01	-1.007E+02
B767-3ER	PW4x60	-1.538E-04	9.143E-01	-7.085E+01
B767-3ER	PW4x62	-1.535E-04	9.127E-01	-7.361E+01
B767-3ER	PW4x62	-1.524E-04	9.060E-01	-4.766E+01
B767-3ER	RB211-524H	-1.530E-04	9.104E-01	6.323E+01
B767-3ER	CF6-80C2B6	-1.526E-04	9.075E-01	-1.063E+02
B767-3ER	CF6-80C2B2F	-1.536E-04	9.135E-01	-1.642E+02
B767-3ER	CF6-80C2B6F	-1.523E-04	9.058E-01	-1.101E+02
B767-3ER	CF6-80C2B7F	-1.527E-04	9.066E-01	-1.268E+02
B767-3ER	CF6-80C2B7F	-1.523E-04	9.058E-01	-1.101E+02

Table 30. Parametric correction factors for small twin-aisle total mission NO_x.

Airframe	Engine	a_2	a_1	a_0
B767-2	CF6-80A	-2.686E-03	-1.143E-01	-1.367E+04
B767-2	CF6-80A2	-2.712E-03	5.806E-01	-1.377E+04
B767-2	CF6-80C2B2F	-3.901E-03	-1.959E+01	-1.717E+04
B767-2ER	CF6-80A2	-2.957E-03	3.544E+01	1.328E+01
B767-2ER	CF6-80C2B2	-3.844E-03	5.638E+00	-4.346E+03
B767-2ER	CF6-80C2B2F	-3.957E-03	6.378E+00	-4.417E+03
B767-2ER	CF6-80C2B4	-3.594E-03	5.273E+00	-1.863E+03
B767-2ER	PW4056	-3.206E-03	2.560E+01	-9.498E+02
B767-2ER	PW4060	-3.195E-03	2.669E+01	6.226E+02
B767-2ER	CF6-80C2B4F	-3.486E-03	1.865E+01	-4.281E+03
B767-3	CF6-80A2	-2.100E-03	2.394E+01	8.028E+03
B767-3	CF6-80C2B2	-3.612E-03	-1.569E+00	1.715E+03
B767-3	CF6-80C2B2F	-3.621E-03	-1.324E+00	1.698E+03
B767-3	CF6-80C2B4F	-3.303E-03	1.094E+00	3.890E+03
B767-3	PW4056	-2.783E-03	1.725E+01	5.748E+03
B767-3	PW4060	-2.692E-03	1.796E+01	7.224E+03
B767-3	CF6-80C2B2F	-3.563E-03	9.446E+00	2.162E-02
B767-3	CF6-80C2B7F	-3.219E-03	1.426E+01	2.082E+03
B767-3ER	CF6-80C2B2F	-3.483E-03	-1.926E+00	2.127E+03
B767-3ER	CF6-80C2B4	-3.331E-03	-2.060E+00	3.622E+03
B767-3ER	CF6-80C2B6	-3.332E-03	-2.853E+00	4.006E+03
B767-3ER	CF6-80C2B6F	-3.196E-03	1.852E+00	5.062E+03
B767-3ER	PW4056	-2.855E-03	1.756E+01	5.524E+03
B767-3ER	PW4060	-2.797E-03	1.842E+01	6.900E+03
B767-3ER	PW4x52	-2.697E-03	2.349E+01	5.714E+03
B767-3ER	PW4x56	-2.613E-03	2.508E+01	6.801E+03
B767-3ER	PW4x60	-2.522E-03	2.711E+01	8.127E+03
B767-3ER	PW4x62	-2.773E-03	1.897E+01	7.465E+03
B767-3ER	PW4x62	-2.492E-03	2.796E+01	8.873E+03
B767-3ER	RB211-524H	-1.416E-03	4.258E+01	3.241E+04
B767-3ER	CF6-80C2B6	-3.037E-03	1.562E+01	3.248E+03
B767-3ER	CF6-80C2B2F	-3.356E-03	8.524E+00	6.808E+02
B767-3ER	CF6-80C2B6F	-3.118E-03	1.382E+01	2.391E+03
B767-3ER	CF6-80C2B7F	-3.196E-03	1.852E+00	5.062E+03
B767-3ER	CF6-80C2B7F	-3.118E-03	1.382E+01	2.391E+03

Table 31. Parametric correction factors for small twin-aisle terminal area fuel burn.

Airframe	Engine	a_2	a_1	a_0
B767-2	CF6-80A	-3.797E-06	3.396E-03	-3.887E+02
B767-2	CF6-80A2	-3.797E-06	3.396E-03	-3.887E+02
B767-2	CF6-80C2B2F	-4.675E-06	8.392E-03	-2.837E+02
B767-2ER	CF6-80A2	-5.467E-06	2.375E-02	-1.188E+02
B767-2ER	CF6-80C2B2	-6.765E-06	3.247E-02	2.806E-01
B767-2ER	CF6-80C2B2F	-5.823E-06	2.540E-02	-9.615E+00
B767-2ER	CF6-80C2B4	-6.768E-06	3.216E-02	2.355E+01
B767-2ER	PW4056	-5.364E-06	2.335E-02	6.245E+01
B767-2ER	PW4060	-5.336E-06	2.298E-02	7.853E+01
B767-2ER	CF6-80C2B4F	-6.768E-06	3.216E-02	2.355E+01
B767-3	CF6-80A2	-5.772E-06	2.553E-02	-1.207E+02
B767-3	CF6-80C2B2	-6.762E-06	3.234E-02	5.343E-01
B767-3	CF6-80C2B2F	-5.931E-06	2.603E-02	-1.030E+01
B767-3	CF6-80C2B4F	-6.967E-06	3.361E-02	7.865E-01
B767-3	PW4056	-5.151E-06	2.238E-02	6.287E+01
B767-3	PW4060	-5.613E-06	2.479E-02	7.667E+01
B767-3	CF6-80C2B2F	-5.269E-06	2.309E-02	-3.236E-01
B767-3	CF6-80C2B7F	-5.150E-06	2.222E-02	4.736E+01
B767-3ER	CF6-80C2B2F	-5.850E-06	2.587E-02	-1.008E+01
B767-3ER	CF6-80C2B4	-6.792E-06	3.223E-02	2.386E+01
B767-3ER	CF6-80C2B6	-5.466E-06	2.424E-02	5.833E+01
B767-3ER	CF6-80C2B6F	-6.382E-06	3.067E-02	1.488E+01
B767-3ER	PW4056	-5.291E-06	2.329E-02	6.234E+01
B767-3ER	PW4060	-5.256E-06	2.290E-02	7.835E+01
B767-3ER	PW4x52	-6.793E-06	3.225E-02	2.068E+01
B767-3ER	PW4x56	-5.291E-06	2.329E-02	6.234E+01
B767-3ER	PW4x60	-5.054E-06	2.233E-02	9.312E+01
B767-3ER	PW4x62	-5.661E-06	2.501E-02	8.944E+01
B767-3ER	PW4x62	-5.364E-06	2.338E-02	1.098E+02
B767-3ER	RB211-524H	-5.709E-06	2.601E-02	2.202E+02
B767-3ER	CF6-80C2B6	-6.019E-06	2.746E-02	4.878E+01
B767-3ER	CF6-80C2B2F	-5.809E-06	2.620E-02	4.704E+01
B767-3ER	CF6-80C2B6F	-5.598E-06	2.493E-02	4.530E+01
B767-3ER	CF6-80C2B7F	-6.382E-06	3.067E-02	1.488E+01
B767-3ER	CF6-80C2B7F	-5.598E-06	2.493E-02	4.530E+01

Table 32. Parametric correction factors for small twin-aisle terminal area NO_x.

Airframe	Engine	a_2	a_1	a_0
B767-2	CF6-80A	-7.558E-05	1.663E-01	-4.783E+03
B767-2	CF6-80A2	-7.567E-05	1.653E-01	-4.780E+03
B767-2	CF6-80C2B2F	-7.596E-05	-5.663E-02	-5.821E+03
B767-2ER	CF6-80A2	-1.190E-04	9.602E-01	2.914E+03
B767-2ER	CF6-80C2B2	-1.046E-04	6.134E-01	9.976E+02
B767-2ER	CF6-80C2B2F	-1.046E-04	5.978E-01	7.435E+02
B767-2ER	CF6-80C2B4	-1.115E-04	8.378E-01	2.375E+03
B767-2ER	PW4056	-1.164E-04	8.424E-01	3.728E+03
B767-2ER	PW4060	-1.232E-04	1.030E+00	5.013E+03
B767-2ER	CF6-80C2B4F	-1.116E-04	6.439E-01	2.400E+03
B767-3	CF6-80A2	-1.108E-04	9.296E-01	2.936E+03
B767-3	CF6-80C2B2	-1.028E-04	6.097E-01	1.000E+03
B767-3	CF6-80C2B2F	-1.036E-04	5.965E-01	7.472E+02
B767-3	CF6-80C2B4F	-1.061E-04	8.156E-01	2.413E+03
B767-3	PW4056	-1.102E-04	8.204E-01	3.744E+03
B767-3	PW4060	-1.124E-04	9.862E-01	5.047E+03
B767-3	CF6-80C2B2F	-1.042E-04	4.942E-01	1.200E+03
B767-3	CF6-80C2B7F	-1.102E-04	7.214E-01	3.018E+03
B767-3ER	CF6-80C2B2F	-1.047E-04	6.024E-01	7.407E+02
B767-3ER	CF6-80C2B4	-1.111E-04	8.393E-01	2.375E+03
B767-3ER	CF6-80C2B6	-1.130E-04	8.932E-01	2.825E+03
B767-3ER	CF6-80C2B6F	-1.167E-04	9.786E-01	3.314E+03
B767-3ER	PW4056	-1.161E-04	8.461E-01	3.726E+03
B767-3ER	PW4060	-1.227E-04	1.032E+00	5.015E+03
B767-3ER	PW4x52	-1.171E-04	8.344E-01	2.954E+03
B767-3ER	PW4x56	-1.239E-04	9.943E-01	4.093E+03
B767-3ER	PW4x60	-1.289E-04	1.163E+00	5.381E+03
B767-3ER	PW4x62	-1.238E-04	1.097E+00	5.405E+03
B767-3ER	PW4x62	-1.328E-04	1.263E+00	5.957E+03
B767-3ER	RB211-524H	-1.731E-04	2.729E+00	1.657E+04
B767-3ER	CF6-80C2B6	-1.167E-04	8.049E-01	3.431E+03
B767-3ER	CF6-80C2B2F	-1.048E-04	4.974E-01	1.198E+03
B767-3ER	CF6-80C2B6F	-1.139E-04	7.368E-01	3.008E+03
B767-3ER	CF6-80C2B7F	-1.167E-04	9.786E-01	3.314E+03
B767-3ER	CF6-80C2B7F	-1.139E-04	7.368E-01	3.008E+03

Table 33. Parametric correction factors for large twin-aisle total mission fuel burn.

Airframe	Engine	a_2	a_1	a_0
A330-2	CF6-80E1A2	2.110E-05	-2.426E+00	-6.072E+02
A330-2	Trent 772	2.766E-04	-3.394E+00	2.509E+02
A330-2	CF6-80E1A4	2.110E-05	-2.426E+00	-6.102E+02
A330-2	PW4168A	2.690E-04	-3.346E+00	2.857E+00
A330-2	CF6-80E1A3	2.110E-05	-2.426E+00	-6.102E+02
A330-2	PW4168A	2.783E-04	-3.404E+00	1.646E+02
A330-3	CF6-80E1A2	1.980E-05	-3.718E+00	-9.270E+01
A330-3	PW4164	2.399E-04	-4.556E+00	4.642E+02
A330-3	PW4168	2.398E-04	-4.555E+00	4.980E+02
A330-3	CF6-80E1A2	1.980E-05	-3.718E+00	-9.270E+01
A330-3	Trent 772	2.391E-04	-4.553E+00	6.520E+02
A330-3	Trent 768	2.391E-04	-4.553E+00	6.520E+02
A330-3	Trent 772	2.391E-04	-4.553E+00	6.834E+02
A330-3	CF6-80E1A4	2.113E-05	-3.725E+00	-8.720E+01
A330-3	PW4168A	2.398E-04	-4.555E+00	4.980E+02
A330-3	CF6-80E1A3	2.113E-05	-3.725E+00	-8.720E+01
A330-3	PW4168A	2.392E-04	-4.553E+00	5.878E+02
A340-2	CFM56-5C2	8.165E-04	-4.615E+00	1.444E+03
A340-2	CFM56-5C3	8.165E-04	-4.615E+00	1.461E+03
A340-3	CFM56-5C2	8.165E-04	-4.615E+00	1.444E+03
A340-3	CFM56-5C3	8.165E-04	-4.615E+00	1.461E+03
A340-3	CFM56-5C4	8.164E-04	-4.614E+00	1.483E+03
A340-3	CFM56-5C4/P	8.159E-04	-4.612E+00	1.425E+03
A340-6	Trent 556-61	8.167E-04	-4.616E+00	2.146E+03
B777-2	GE90-76B	-8.120E-05	3.997E-01	-8.737E+02
B777-2	GE90-85B	-8.120E-05	3.997E-01	-8.737E+02
B777-2	PW4074	-7.816E-05	3.820E-01	-1.090E+03
B777-2	PW4077	-7.822E-05	3.819E-01	-1.076E+03
B777-2	Trent 875	-8.028E-05	3.936E-01	-9.291E+02
B777-2	Trent 877	-8.028E-05	3.936E-01	-9.291E+02
B777-2	Trent 884	-8.203E-05	4.052E-01	-8.474E+02
B777-2	GE90-76B	-8.028E-05	3.936E-01	-9.291E+02
B777-2	PW4090	-7.985E-05	3.907E-01	-9.628E+02
B777-2ER	GE90-85B	-8.120E-05	3.997E-01	-8.737E+02
B777-2ER	Trent 884	-8.203E-05	4.052E-01	-8.474E+02
B777-2ER	Trent 892	-8.120E-05	3.997E-01	-8.737E+02
B777-2ER	GE90-90B	-8.167E-05	4.037E-01	-8.401E+02
B777-2ER	GE90-85B	-8.082E-05	3.971E-01	-8.959E+02
B777-2ER	GE90-90B	-8.120E-05	3.997E-01	-8.737E+02
B777-2ER	GE90-92B	-8.137E-05	4.008E-01	-8.627E+02
B777-2ER	PW4090	-7.985E-05	3.907E-01	-9.628E+02
B777-2ER	Trent 895	-8.250E-05	4.094E-01	-7.968E+02
B777-2ER	GE90-90B	-8.077E-05	3.968E-01	-8.986E+02
B777-2LR	GE90-110B1	-8.557E-05	4.327E-01	-7.029E+02
B777-3	Trent 892	5.820E-04	-1.942E+00	1.262E+03
B777-3	PW4090	5.819E-04	-1.941E+00	1.161E+03
B777-3	PW4098	5.820E-04	-1.941E+00	1.326E+03
B777-3ER	GE90-115B	5.829E-04	-1.945E+00	1.511E+03

Table 34. Parametric correction factors for large twin-aisle total mission NO_x.

Airframe	Engine	a_2	a_1	a_0
A330-2	CF6-80E1A2	-3.337E-03	-1.619E+02	-5.213E+04
A330-2	Trent 772	3.300E-03	-2.052E+02	-2.597E+04
A330-2	CF6-80E1A4	-3.149E-03	-1.591E+02	-4.986E+04
A330-2	PW4168A	8.233E-03	-1.501E+02	-2.240E-01
A330-2	CF6-80E1A3	-2.279E-03	-1.502E+02	-2.628E+04
A330-2	PW4168A	1.553E-03	-1.991E+02	-4.183E+04
A330-3	CF6-80E1A2	-3.416E-03	-1.871E+02	-9.331E+03
A330-3	PW4164	5.148E-03	-1.809E+02	1.242E+04
A330-3	PW4168	5.496E-03	-1.805E+02	1.778E+04
A330-3	CF6-80E1A2	-3.709E-03	-1.875E+02	-3.521E+04
A330-3	Trent 772	3.132E-03	-2.174E+02	9.943E+03
A330-3	Trent 768	1.222E-03	-2.264E+02	-1.632E+04
A330-3	Trent 772	1.333E-03	-2.268E+02	-1.351E+04
A330-3	CF6-80E1A4	-3.553E-03	-1.858E+02	-3.265E+04
A330-3	PW4168A	5.496E-03	-1.805E+02	1.778E+04
A330-3	CF6-80E1A3	-3.165E-03	-1.833E+02	-3.511E+03
A330-3	PW4168A	2.277E-04	-2.177E+02	-3.021E+04
A340-2	CFM56-5C2	2.250E-02	-2.363E+02	2.464E+04
A340-2	CFM56-5C3	2.292E-02	-2.363E+02	2.737E+04
A340-3	CFM56-5C2	2.250E-02	-2.363E+02	2.464E+04
A340-3	CFM56-5C3	2.292E-02	-2.363E+02	2.737E+04
A340-3	CFM56-5C4	2.377E-02	-2.378E+02	3.135E+04
A340-3	CFM56-5C4/P	2.222E-02	-2.407E+02	2.410E+04
A340-6	Trent 556-61	1.562E-02	-2.639E+02	6.202E+03
B777-2	GE90-76B	-4.331E-04	-3.046E+01	-2.090E+04
B777-2	GE90-85B	3.221E-03	-8.157E+01	7.396E+03
B777-2	PW4074	4.818E-03	-1.137E+02	1.265E+04
B777-2	PW4077	4.831E-03	-1.138E+02	1.314E+04
B777-2	Trent 875	1.099E-02	-2.161E+02	6.204E+04
B777-2	Trent 877	1.093E-02	-2.149E+02	6.178E+04
B777-2	Trent 884	1.081E-02	-2.123E+02	6.307E+04
B777-2	GE90-76B	-5.301E-05	-4.468E+01	-1.685E+04
B777-2	PW4090	3.268E-03	-8.679E+01	5.184E+03
B777-2ER	GE90-85B	3.221E-03	-8.157E+01	7.396E+03
B777-2ER	Trent 884	1.081E-02	-2.123E+02	6.307E+04
B777-2ER	Trent 892	1.034E-02	-2.047E+02	5.992E+04
B777-2ER	GE90-90B	3.146E-03	-7.989E+01	8.855E+03
B777-2ER	GE90-85B	-1.290E-03	-2.234E+01	-3.018E+04
B777-2ER	GE90-90B	-2.226E-03	-6.003E+00	-3.705E+04
B777-2ER	GE90-92B	-2.574E-03	-1.204E-01	-3.895E+04
B777-2ER	PW4090	3.268E-03	-8.679E+01	5.184E+03
B777-2ER	Trent 895	1.128E-02	-2.189E+02	6.759E+04
B777-2ER	GE90-90B	-2.442E-03	-1.730E+00	-3.889E+04
B777-2LR	GE90-110B1	7.033E-03	-1.569E+02	3.244E+04
B777-3	Trent 892	1.728E-02	-1.743E+02	1.495E+04
B777-3	PW4090	2.559E-02	-1.389E+02	5.112E+04
B777-3	PW4098	1.898E-02	-1.489E+02	2.438E+04
B777-3ER	GE90-115B	1.692E-02	-1.431E+02	9.206E+03

Table 35. Parametric correction factors for large twin-aisle terminal area fuel burn.

Airframe	Engine	a_2	a_1	a_0
A330-2	CF6-80E1A2	-6.532E-06	1.413E-02	-7.372E+01
A330-2	Trent 772	-5.071E-07	-8.160E-03	1.343E+02
A330-2	CF6-80E1A4	-6.449E-06	1.358E-02	-7.608E+01
A330-2	PW4168A	-1.199E-06	-2.894E-03	-5.894E+01
A330-2	CF6-80E1A3	-6.449E-06	1.358E-02	-7.608E+01
A330-2	PW4168A	-7.211E-07	-6.061E-03	3.592E+01
A330-3	CF6-80E1A2	-7.831E-06	2.531E-02	-1.921E-03
A330-3	PW4164	-2.013E-07	-5.215E-03	-5.829E-01
A330-3	PW4168	-9.184E-07	-2.110E-03	3.310E+01
A330-3	CF6-80E1A2	-7.831E-06	2.531E-02	-1.921E-03
A330-3	Trent 772	4.059E-08	-6.205E-03	1.863E+02
A330-3	Trent 768	4.059E-08	-6.205E-03	1.863E+02
A330-3	Trent 772	-1.123E-07	-5.511E-03	2.167E+02
A330-3	CF6-80E1A4	-7.255E-06	2.202E-02	-6.497E-02
A330-3	PW4168A	-9.184E-07	-2.110E-03	3.310E+01
A330-3	CF6-80E1A3	-7.255E-06	2.202E-02	-6.497E-02
A330-3	PW4168A	9.593E-08	-6.658E-03	1.248E+02
A340-2	CFM56-5C2	1.409E-05	-4.565E-02	1.796E+02
A340-2	CFM56-5C3	1.405E-05	-4.575E-02	1.980E+02
A340-3	CFM56-5C2	1.409E-05	-4.565E-02	1.796E+02
A340-3	CFM56-5C3	1.405E-05	-4.575E-02	1.980E+02
A340-3	CFM56-5C4	1.428E-05	-4.735E-02	2.236E+02
A340-3	CFM56-5C4/P	1.426E-05	-4.652E-02	1.644E+02
A340-6	Trent 556-61	1.340E-05	-4.140E-02	8.764E+02
B777-2	GE90-76B	-7.677E-06	3.202E-02	1.957E+02
B777-2	GE90-85B	-7.677E-06	3.202E-02	1.957E+02
B777-2	PW4074	-3.967E-06	6.512E-03	-1.948E-01
B777-2	PW4077	-4.763E-06	1.361E-02	-2.180E-02
B777-2	Trent 875	-6.663E-06	2.569E-02	1.384E+02
B777-2	Trent 877	-6.663E-06	2.569E-02	1.384E+02
B777-2	Trent 884	-7.993E-06	3.336E-02	2.289E+02
B777-2	GE90-76B	-6.663E-06	2.569E-02	1.384E+02
B777-2	PW4090	-6.629E-06	2.625E-02	9.852E+01
B777-2ER	GE90-85B	-7.677E-06	3.202E-02	1.957E+02
B777-2ER	Trent 884	-7.993E-06	3.336E-02	2.289E+02
B777-2ER	Trent 892	-7.677E-06	3.202E-02	1.957E+02
B777-2ER	GE90-90B	-8.104E-06	3.398E-02	2.377E+02
B777-2ER	GE90-85B	-7.291E-06	2.980E-02	1.724E+02
B777-2ER	GE90-90B	-7.677E-06	3.202E-02	1.957E+02
B777-2ER	GE90-92B	-7.834E-06	3.289E-02	2.085E+02
B777-2ER	PW4090	-6.629E-06	2.625E-02	9.852E+01
B777-2ER	Trent 895	-8.956E-06	4.016E-02	2.826E+02
B777-2ER	GE90-90B	-7.315E-06	2.962E-02	1.715E+02
B777-2LR	GE90-110B1	-9.738E-06	4.380E-02	4.031E+02
B777-3	Trent 892	6.637E-06	-1.813E-02	3.676E+02
B777-3	PW4090	7.062E-06	-2.095E-02	2.717E+02
B777-3	PW4098	6.830E-06	-1.942E-02	4.349E+02
B777-3ER	GE90-115B	6.098E-06	-1.496E-02	6.139E+02

Table 36. Parametric correction factors for large twin-aisle terminal area NO_x.

Airframe	Engine	a_2	a_1	a_0
A330-2	CF6-80E1A2	-2.173E-04	-2.584E-01	-3.896E+03
A330-2	Trent 772	-3.621E-05	-6.722E-01	1.268E+02
A330-2	CF6-80E1A4	-2.248E-04	-1.175E-01	-2.791E+03
A330-2	PW4168A	-5.803E-06	-2.996E-01	5.473E+03
A330-2	CF6-80E1A3	-2.655E-04	7.466E-01	4.479E+03
A330-2	PW4168A	-5.119E-05	-9.772E-01	-3.594E+03
A330-3	CF6-80E1A2	-2.612E-04	6.672E-01	4.320E+03
A330-3	PW4164	-3.950E-06	-3.169E-01	6.136E+03
A330-3	PW4168	7.774E-06	-1.372E-01	8.867E+03
A330-3	CF6-80E1A2	-2.262E-04	-7.923E-02	-1.554E+03
A330-3	Trent 772	2.318E-06	-1.256E-01	9.869E+03
A330-3	Trent 768	-3.032E-05	-6.717E-01	7.166E+02
A330-3	Trent 772	-2.376E-05	-5.540E-01	2.751E+03
A330-3	CF6-80E1A4	-2.339E-04	7.341E-02	-3.236E+02
A330-3	PW4168A	7.774E-06	-1.372E-01	8.867E+03
A330-3	CF6-80E1A3	-2.784E-04	1.024E+00	7.844E+03
A330-3	PW4168A	-4.143E-05	-8.750E-01	-1.331E+03
A340-2	CFM56-5C2	4.564E-04	-2.002E+00	4.135E+03
A340-2	CFM56-5C3	4.937E-04	-1.992E+00	5.896E+03
A340-3	CFM56-5C2	4.564E-04	-2.002E+00	4.135E+03
A340-3	CFM56-5C3	4.937E-04	-1.992E+00	5.896E+03
A340-3	CFM56-5C4	5.341E-04	-1.987E+00	7.977E+03
A340-3	CFM56-5C4/P	4.833E-04	-2.017E+00	5.018E+03
A340-6	Trent 556-61	3.873E-04	-1.970E+00	7.699E+03
B777-2	GE90-76B	-2.367E-04	8.968E-01	5.934E+03
B777-2	GE90-85B	-2.789E-04	1.422E+00	6.553E+03
B777-2	PW4074	-1.060E-04	-3.247E-01	3.249E+00
B777-2	PW4077	-1.045E-04	-3.272E-01	7.771E+02
B777-2	Trent 875	-4.807E-06	-1.429E+00	-1.714E+03
B777-2	Trent 877	-1.776E-05	-1.289E+00	-1.269E+03
B777-2	Trent 884	-7.770E-05	-6.811E-01	5.870E+02
B777-2	GE90-76B	-1.721E-04	1.887E-01	4.234E+03
B777-2	PW4090	-2.573E-04	1.308E+00	5.052E+03
B777-2ER	GE90-85B	-2.789E-04	1.422E+00	6.553E+03
B777-2ER	Trent 884	-7.770E-05	-6.811E-01	5.870E+02
B777-2ER	Trent 892	-9.180E-05	-5.390E-01	1.050E+03
B777-2ER	GE90-90B	-3.320E-04	1.982E+00	8.101E+03
B777-2ER	GE90-85B	-2.374E-04	8.621E-01	6.331E+03
B777-2ER	GE90-90B	-3.002E-04	1.532E+00	8.097E+03
B777-2ER	GE90-92B	-3.277E-04	1.827E+00	8.859E+03
B777-2ER	PW4090	-2.573E-04	1.308E+00	5.052E+03
B777-2ER	Trent 895	-8.841E-05	-5.772E-01	1.011E+03
B777-2ER	GE90-90B	-2.983E-04	1.512E+00	8.037E+03
B777-2LR	GE90-110B1	-6.779E-05	-8.982E-01	1.149E+03
B777-3	Trent 892	2.629E-04	-9.352E-01	7.264E+03
B777-3	PW4090	3.943E-04	-5.404E-01	1.495E+04
B777-3	PW4098	2.807E-04	-8.742E-01	1.245E+04
B777-3ER	GE90-115B	2.270E-04	-1.046E+00	7.117E+03

APPENDIX D

RANGES FOR SCREENING DESIGNS OF EXPERIMENTS

Here, the maximum and minimum values used for each input in each screening DOE are provided, along with the corresponding values of the reference vehicle model used as the baseline.

Table 37. Screening DOE ranges for the regional jet group (1 of 2).

	Min	Base	Max
SLS Thrust (lbf)	12000	14506	15000
Burner Time (s)	0.007	0.0086	0.009
Customer Bleed (lb/sec)	0	0	1
Burner Pressure Drop (%)	5	5.25265	5.5
Burner Efficiency	0.985	0.989761	0.99
Bypass Nozzle Pressure Drop (%)	1.3	1.37133	1.4
HPT-LPT Duct Pressure Drop (%)	0.4	0.545609	0.7
HPT-LPT Duct Length/Height	1.8	2.2	2.6
Splitter-HPC Duct Pressure Drop (%)	0.6	0.717346	0.8
Splitter-HPC Duct Length/Height	2.5	2.948	3.5
LPT-Core Nozzle Duct Pressure Drop (%)	0.85	0.997116	1.2
LPT-Core Nozzle Duct Length/Height	0.15	0.216	0.5
Extraction Ratio	0.55	0.655	0.8
Fan Efficiency	-0.01	0.00108	0.01
Fan Tip Speed Adder (ft/s)	340	389.52	430
Fan Stall Margin	20	24.345	30
Fan Specific Flow ($lb/s/ft^2$)	42.1	42.6124	43.5
Lift Dependent Drag Factor	0.85	0.897	0.95
Lift Independent Drag Factor	0.95	0.985	1.05
Fan Pressure Ratio	1.58	1.62876	1.66
HPC Area Ratio	0.196365	0.2067	0.217035
HPC Efficiency	-0.001	0.0009	0.001
HPC Tip Speed Adder (ft/s)	170	220	270
HPC Max 1st Stage PR	1.4	1.529	1.56
HPC Stall Margin	20	24.0273	28
HPC Specific Flow ($lb/s/ft^2$)	37	39.82	41
HPC Pressure Ratio	25	27.5	32
HPT Chargeable Cooling Factor	0.5	0.850744	1.2
HPT Efficiency	0.86	0.882237	0.893
HPT Flow Coefficient	1.8	2.1	2.5
HPT Loading	0.4	0.6	0.8
HPT Exit Mach Number	0.4	0.4469	0.46
HPT Nonchargeable Cooling Factor	1.2	1.52572	1.8
HPT Solidity Factor	0.92	0.98	1.08
Horsepower Extraction (hp)	50	75	125
Bypass Nozzle Area Ratio	0.8	0.847574	0.9
Core Nozzle Area Ratio	0.9	0.924355	0.98
Engine Weight Factor	1.3	1.3	1.6

Table 38. Screening DOE ranges for the regional jet group (2 of 2).

	Min	Base	Max
LPT Chargeable Cooling Factor	0.65	0.864028	1.05
LPT Efficiency	0.87	0.878717	0.9
LPT Flow Coefficient	5.4	5.9	6.4
LPT Loading	1.05	1.2	1.4
LPT Exit Mach Number	0.25	0.3	0.35
LPT Nonchargeable Cooling Factor	1	1.105	1.4
LPT Radius Ratio	0.9	0.9	1.1
LPT Solidity Factor	0.95	1	1.05
Core Nozzle Plug Length Ratio	3.8	4	4.2
Design Reynolds Number	300000	325465.7	350000
Design HPC Reynolds Number	325000	367580.8	375000
Maximum T4 (K)	3150	3170	3250
Horizontal Tail Thickness to Chord	0.09	0.0939	0.12
Vertical Tail Thickness to Chord	0.09	0.0942	0.12
Takeoff Thrust (lbf)	11000	12400	12800
Thrust to Weight Ratio	0.315	0.32068	0.325
Wing Loading	113.5	114.1693	114.5
Top of Climb Thrust (lbf)	3200	3550	3650
Ratio of Top of Climb and Design Engine Flow	1.001	1.003	1.03
Wing Aspect Ratio	8	8.29	8.8
Wing Sweep (deg)	25	27	28
Wing Area (ft^2)	520	752.8	760
Wing Glove Area (ft^2)	0.07	0.07663	0.08
Wing Break Location	0.35	0.41	0.42
Wing Taper Ratio	0.26	0.28	0.3
Wing Average Thickness to Chord	0.1	0.12	0.14
Number of Passengers	50	86	90
Passenger Cabin Length (ft)	50.16	86.27	90.28

Table 39. Screening DOE ranges for the single-aisle group (1 of 2).

	Min	Base	Max
SLS Thrust (lbf)	26000	27300	27500
Burner Time (s)	0.007	0.0095	0.013
Customer Bleed (lb/s)	2	2.35	3.5
Burner Pressure Drop (%)	0.044	0.05402	0.064
Buner Efficiency	0.979	0.982745	0.99
Bypass Nozzle Pressure Drop (%)	1.3	1.4892	1.8
HPT-LPT Duct Pressure Drop (%)	0.3	0.5055	1
HPT-LPT Duct Length/Height	0.5	0.75	1
LPC-HPC Duct Pressure Drop (%)	0.9	1.0125	1.3
LPC-HPC Duct Length/Height	4.6	4.9	5.5
LPT-Core Nozzle Duct Pressure Drop (%)	0.85	1.0685	1.4
LPT-Core Nozzle Duct Length/Height	0.25	0.05	0.75
Splitter-LPC Duct Pressure Drop (%)	0.3	0.4825	0.8
Splitter-LPC Duct Length/Height	0.05	0.07	0.1
Extraction Ratio	0.92	0.9437	1.15
Fan Efficiency	-0.02	-0.010198	-0.005
Fan Tip Speed Adder (ft/s)	20	61.63	100
Fan Stall Margin	25	30.89	35
Fan Specific Flow (lb/sec/ft^2)	43	43.9	44
Lift Dependent Drag Factor	0.97	1	1.1
Lift Independent Drag Factor	0.99	1	1.17
Fan Pressure Ratio	1.65	1.68511	1.69
HPC Area Ratio	0.179398	0.18884	0.198282
HPC Efficiency	-0.03	-0.016226	-0.01
HPC Tip Speed Adder (ft/sec)	220	270.98	320
HPC Max 1st Stage PR	1.38	1.42	1.46
HPC Stall Margin	14	15.05	20
HPC Specific Flow (lb/sec/ft^2)	29	28.1852	33
HPC Pressure Ratio	27	30.094	32
HPT Chargeable Cooling Factor	1.7	2.03237	2.3
HPT Efficiency	0.86	0.88882	0.895
HPT Flow Coefficient	0.94	0.973	1
HPT Loading	0.9	0.925	0.97
HPT Exit Mach Number	0.34	0.365	0.39
HPT Nonchargeable Cooling Factor	0.6	0.757	0.9
HPT Solidity Factor	0.92	1	1.08
Horsepower Extraction (hp)	200	250	400
Bypass Nozzle Area Ratio	1.65	1.7723	1.9

Table 40. Screening DOE ranges for the single-aisle group (2 of 2).

	Min	Base	Max
Core Nozzle Area Ratio	1.25	1.3593	1.45
Engine Weight Factor	1.55	1.6	1.7
LPC Area Ratio	0.5	0.5828	0.65
LPC Efficiency	0.02	0.04844	0.05
LPC Max First Stage PR	1.15	1.21	1.3
LPC Hub to Tip Ratio	0.7	0.745	0.85
LPC Stall Margin	12	13.69	20
LPC Solidity Factor	0.9	1	1.1
LPC Specific Flow (lb/sec/ft2)	24	25.1518	28
LPC Pressure Ratio	1.8	1.935	2.1
LPT Chargeable Cooling Factor	0.7	0.776	0.85
LPT Efficiency	0.87	0.89963	0.9
LPT Flow Coefficient	6.5	7.21	7.5
LPT Loading	1.55	1.58	1.77
LPT Exit Mach Number	0.38	0.4127	0.42
LPT Nonchargeable Cooling Factor	1.7	1.82563	1.9
LPT Radius Ratio	1.25	1.3423	1.4
LPT Solidity Factor	0.95	1	1.05
Core Nozzle Plug Length Ratio	3.8	4	4.2
Design Reynolds Number	350000	399125	450000
Design HPC Reynolds Number	450000	507300	550000
Maximum T4 (K)	3250	3300	3350
Horizontal Tail Thickness to Chord	0.1	0.112051	0.14
Vertical Tail Thickness to Chord	0.11	0.1179773	0.14
Takeoff Thrust (lbf)	22000	22782.9	23500
Thrust to Weight Ratio	0.31	0.31594	0.32
Wing Loading	124	124.8141	126
Top of Climb Thrust (lbf)	5600	5962	6000
Ratio of Top of Climb and Design Engine Flow	1.01	1.01906	1.03
Wing Aspect Ratio	9	9.56	9.8
Wing Sweep (deg)	20	25.33	26
Wing Area (ft^2)	1300	1384.6	1400
Wing Glove Area (ft^2)	0.05	0.05984	0.07
Wing Break Location	0.25	0.3	0.35
Wing Taper Ratio	0.2	0.27	0.3
Wing Average Thickness to Chord	0.1	0.1208	0.14
Number of Passengers	150	162	170
Passenger Cabin Length (ft)	95.27	102.89	107.97

Table 41. Screening DOE ranges for the small twin-aisle group (1 of 2).

	Min	Base	Max
SLS Thrust (lbf)	58000	61267	64000
Burner Time (s)	0.00905	0.01	0.0105
Customer Bleed (lb/s)	2	3.93	3.93
Burner Pressure Drop (%)	2	2.35321	2.5
Buner Efficiency	0.99	0.99643	0.997
Bypass Nozzle Pressure Drop (%)	1.9	1.994	2.05
HPT-LPT Duct Pressure Drop (%)	1.3	1.36002	1.4
HPT-LPT Duct Length/Height	0.5	0.7	0.8
LPC-HPC Duct Pressure Drop (%)	0.45	0.50364	0.55
LPC-HPC Duct Length/Height	3.25	3.75	4.5
LPT-Core Nozzle Duct Pressure Drop (%)	0.85	0.90993	1.05
LPT-Core Nozzle Duct Length/Height	0.08	0.1	0.12
Splitter-LPC Duct Pressure Drop (%)	0.4	0.50409	0.55
Splitter-LPC Duct Length/Height	0.03	0.05	0.07
Extraction Ratio	0.87	0.9197	0.95
Fan Efficiency	-0.005	0.00118	0.01
Fan Tip Speed Adder (ft/s)	-100	-47.89	50
Fan Stall Margin	20	24.8284	30
Fan Specific Flow (lb/sec/ft^2)	43.4	43.9322	43.95
Lift Dependent Drag Factor	0.9	1	1.1
Lift Independent Drag Factor	0.9	1	1.1
Fan Pressure Ratio	1.62	1.6427	1.66
HPC Area Ratio	0.19652	0.20259	0.21272
HPC Efficiency	0	0.01041	0.02
HPC Tip Speed Adder (ft/sec)	300	357.83	400
HPC Max 1st Stage PR	1.2	1.3	1.35
HPC Stall Margin	20	23.3963	28
HPC Specific Flow (lb/sec/ft^2)	37	37.295	38
HPC Pressure Ratio	27	30.32	34
HPT Chargeable Cooling Factor	0.2	0.48	0.75
HPT Efficiency	0.87	0.90184	0.905
HPT Flow Coefficient	0.9	0.975	1.1
HPT Loading	0.4	0.6	0.8
HPT Exit Mach Number	0.37	0.3735	0.38
HPT Nonchargeable Cooling Factor	4.5	4.82	5
HPT Solidity Factor	0.95	1	1.08
Horsepower Extraction (hp)	50	250	275
Bypass Nozzle Area Ratio	2	2.16712	2.3

Table 42. Screening DOE ranges for the small twin-aisle group (2 of 2).

	Min	Base	Max
Core Nozzle Area Ratio	1.1	1.32695	1.5
Engine Weight Factor	1	1	1.3
LPC Area Ratio	0.45	0.54253	0.65
LPC Efficiency	0.02	0.0274	0.03
LPC Max First Stage PR	1.1	1.12	1.17
LPC Hub to Tip Ratio	0.7	0.79103	0.85
LPC Stall Margin	18	20.5726	25
LPC Solidity Factor	0.95	1	1.05
LPC Specific Flow (lb/sec/ft^2)	25	28.3948	31
LPC Pressure Ratio	1.4	1.48036	1.55
LPT Chargeable Cooling Factor	1.5	2.05	2.5
LPT Efficiency	0.895	0.912	0.915
LPT Flow Coefficient	3.5	3.635	3.8
LPT Loading	2	2.2	2.3
LPT Exit Mach Number	0.32	0.3503	0.37
LPT Nonchargeable Cooling Factor	3	3.53	4
LPT Radius Ratio	0.9	1.05	1.1
LPT Solidity Factor	0.95	1	1.05
Core Nozzle Plug Length Ratio	3.8	4	4.2
Design Reynolds Number	375000	396348	450000
Design HPC Reynolds Number	375000	445654	500000
Maximum T4 (K)	3375	3425.2	3550
Horizontal Tail Thickness to Chord	0.09	0.105	0.12
Vertical Tail Thickness to Chord	0.09	0.095	0.12
Takeoff Thrust (lbf)	48500	50219	55000
Thrust to Weight Ratio	0.315	0.32	0.325
Wing Loading	113.5	114	114.5
Top of Climb Thrust (lbf)	10900	11927	12500
Ratio of Top of Climb and Design Engine Flow	1.01	1.01833	1.03
Wing Aspect Ratio	8	8.05	8.8
Wing Sweep (deg)	27	30.8	33
Wing Area (ft^2)	3000	3187.6	3300
Wing Glove Area (ft^2)	0.5	0.06	0.7
Wing Break Location	0.25	0.29	0.35
Wing Taper Ratio	0.2	0.23	0.27
Wing Average Thickness to Chord	0.1	0.11167	0.14
Number of Passengers	120	150	180
Passenger Cabin Length (ft)	117	146.25	175.5

Table 43. Screening DOE ranges for the large twin-aisle group (1 of 2).

	Min	Base	Max
SLS Thrust (lbf)	96000	97300	99000
Burner Time (s)	0.007	0.009	0.013
Customer Bleed (lb/s)	3.7	3.93	4.2
Burner Pressure Drop (%)	3	3.9872	5
Buner Efficiency	0.985	0.997	0.997
Bypass Nozzle Pressure Drop (%)	1.6	1.8	2
HPT-LPT Duct Pressure Drop (%)	0.3	0.9459	1
HPT-LPT Duct Length/Height	2.5	2.96852	3.5
LPC-HPC Duct Pressure Drop (%)	0.3	0.8299	1
LPC-HPC Duct Length/Height	2.5	2.82209	3.2
LPT-Core Nozzle Duct Pressure Drop (%)	0.5	0.7858	1
LPT-Core Nozzle Duct Length/Height	0.15	0.216	0.25
Splitter-LPC Duct Pressure Drop (%)	0.8	1.02	1.5
Splitter-LPC Duct Length/Height	0.05	0.07821	0.1
Extraction Ratio	1.05	1.08198	1.3
Fan Efficiency	-0.0035	-0.00318	-0.0025
Fan Tip Speed Adder (ft/s)	0	35.57	100
Fan Stall Margin	22	27.9243	28
Fan Specific Flow (lb/sec/ft^2)	42	42.7519	43
Lift Dependent Drag Factor	1.12	1.18242	1.2
Lift Independent Drag Factor	0.85	0.804	0.75
Fan Pressure Ratio	1.5	1.58	1.65
HPC Area Ratio	0.10289	0.1083	0.11372
HPC Efficiency	0	0.01663	0.02
HPC Tip Speed Adder (ft/sec)	-130	-64.32	-30
HPC Max 1st Stage PR	1.55	1.582	1.59
HPC Stall Margin	14	17.6001	20
HPC Specific Flow (lb/sec/ft^2)	29	31.3692	33
HPC Pressure Ratio	35	40.539	42
HPT Chargeable Cooling Factor	0.35	0.40954	0.45
HPT Efficiency	0.89	0.92508	0.93
HPT Flow Coefficient	1.05	1.1157	1.2
HPT Loading	0.87	0.93	0.99
HPT Exit Mach Number	0.28	0.3079	0.32
HPT Nonchargeable Cooling Factor	1.82	1.8651	1.9
HPT Solidity Factor	0.92	0.98	1.05
Horsepower Extraction (hp)	200	250	400
Bypass Nozzle Area Ratio	1.05	1.21	1.3

Table 44. Screening DOE ranges for the large twin-aisle group (2 of 2).

	Min	Base	Max
Core Nozzle Area Ratio	1.05	1.22461	1.25
Engine Weight Factor	1.3	1.3	1.5
LPC Area Ratio	0.73	0.74568	0.76
LPC Efficiency	0.0171	0.01769	0.0181
LPC Max First Stage PR	1.1	1.12	1.2
LPC Hub to Tip Ratio	0.75	0.805	0.85
LPC Stall Margin	25	33.3025	34
LPC Solidity Factor	0.9	1	1.1
LPC Specific Flow (lb/sec/ft^2)	24	26.3073	28
LPC Pressure Ratio	1.2	1.2603	1.8
LPT Chargeable Cooling Factor	0.8	0.8838	0.95
LPT Efficiency	0.9	0.93758	0.9376
LPT Flow Coefficient	5.1	5.448	5.75
LPT Loading	1.6	1.7	1.77
LPT Exit Mach Number	0.29	0.2977	0.305
LPT Nonchargeable Cooling Factor	1.35	1.43	1.47
LPT Radius Ratio	0.75	0.8	1.25
LPT Solidity Factor	0.85	0.944	1
Core Nozzle Plug Length Ratio	3.8	4	4.2
Design Reynolds Number	350000	388967	410000
Design HPC Reynolds Number	280000	311926	340000
Maximum T4 (K)	3400	3450	3475
Horizontal Tail Thickness to Chord	0.08	0.089	0.1
Vertical Tail Thickness to Chord	0.08	0.09226	0.1
Takeoff Thrust (lbf)	76000	78400	79400
Thrust to Weight Ratio	0.295	0.29573	0.296
Wing Loading	130	133.198	140
Top of Climb Thrust (lbf)	19200	19600	20000
Ratio of Top of Climb and Design Engine Flow	1.01	1.03558	1.04
Wing Aspect Ratio	8.5	8.85431	9.5
Wing Sweep (deg)	32	30.84	27
Wing Area (ft^2)	5100	4940.27	4800
Wing Glove Area (ft^2)	0.07	0.0861	0.09
Wing Break Location	0.3	0.3585	0.36
Wing Taper Ratio	0.14	0.17589	0.18
Wing Average Thickness to Chord	0.1	0.12998	0.14
Number of Passengers	260	271	280
Passenger Cabin Length (ft)	154.54	161.08	166.43

APPENDIX E

VIZUALIZATION OF SCREENING RESULTS

On the following pages, a total of sixteen Pareto charts, one for each output metric that contributes to the top 80% of cumulative orthogonal parameter estimates for each capability group, are provided. These charts, which for this application facilitated the evaluation of the significance of up to 74 input parameters to the physics-based M&S environment, are the result of the effect screening that was described in Chapter 3 and implemented in Chapter 4.

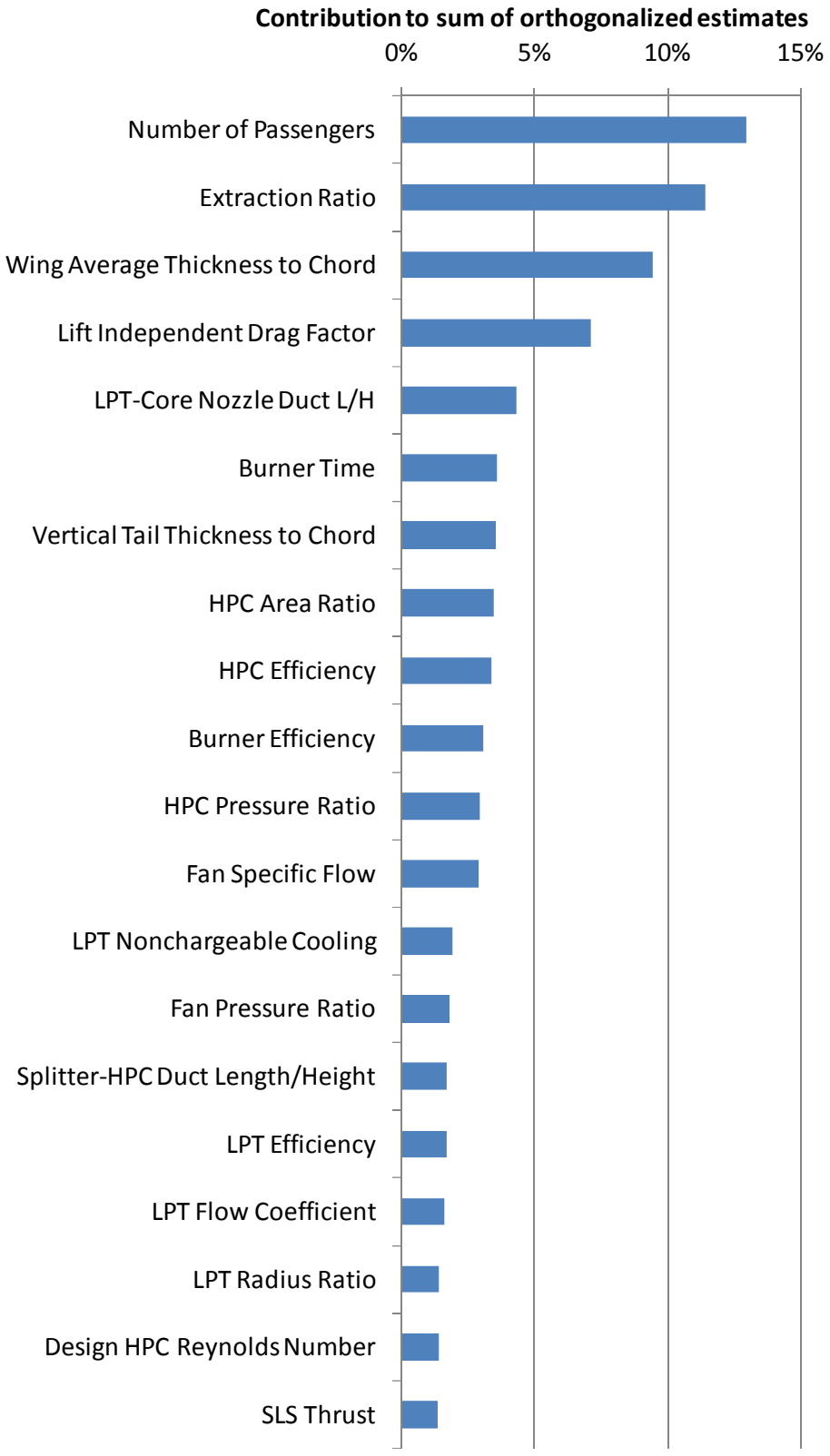

Figure 75. Pareto chart for total mission fuel burn for regional jet reference vehicle.

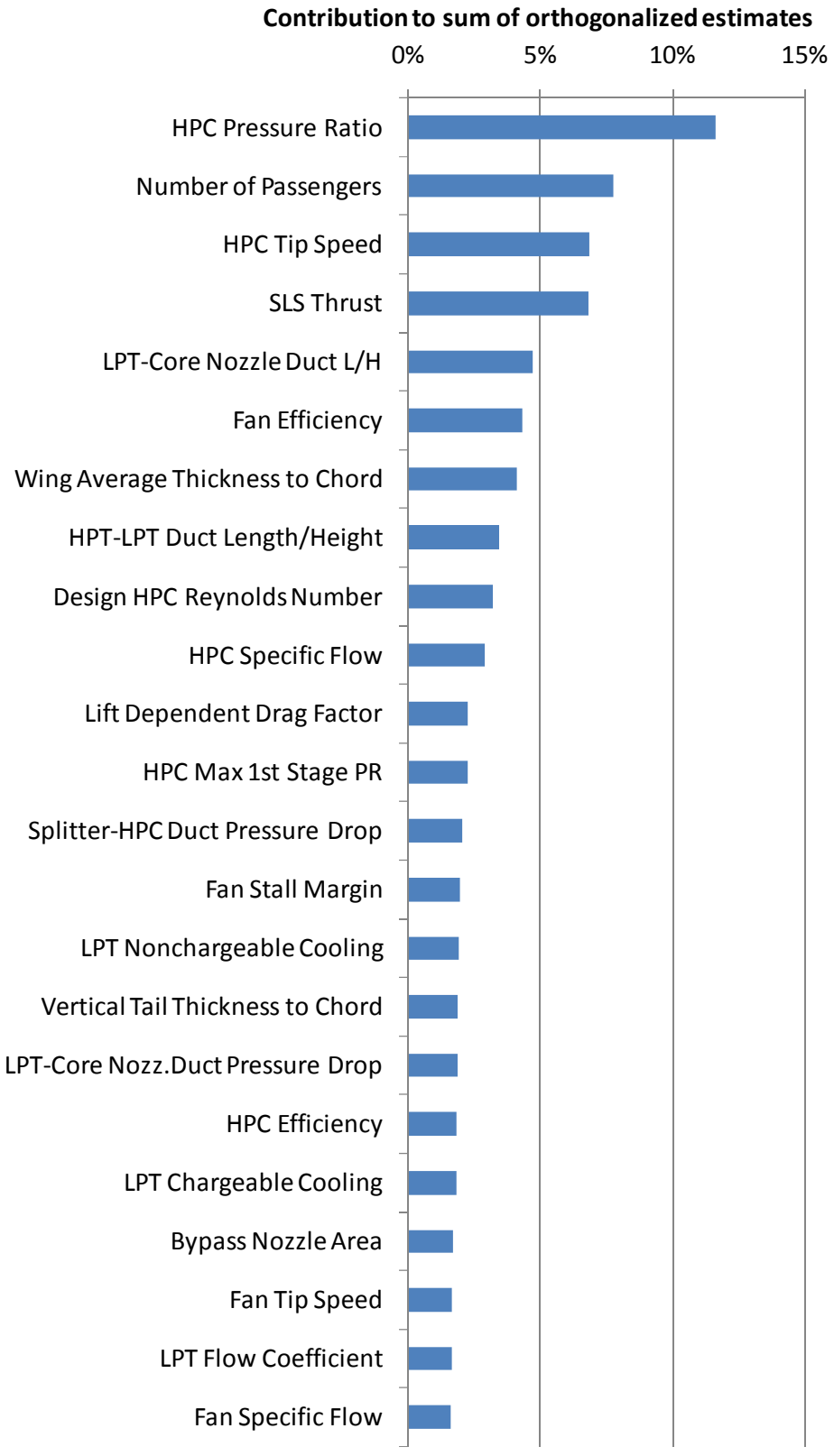

Figure 76. Pareto chart for total mission NO_x for regional jet reference vehicle.

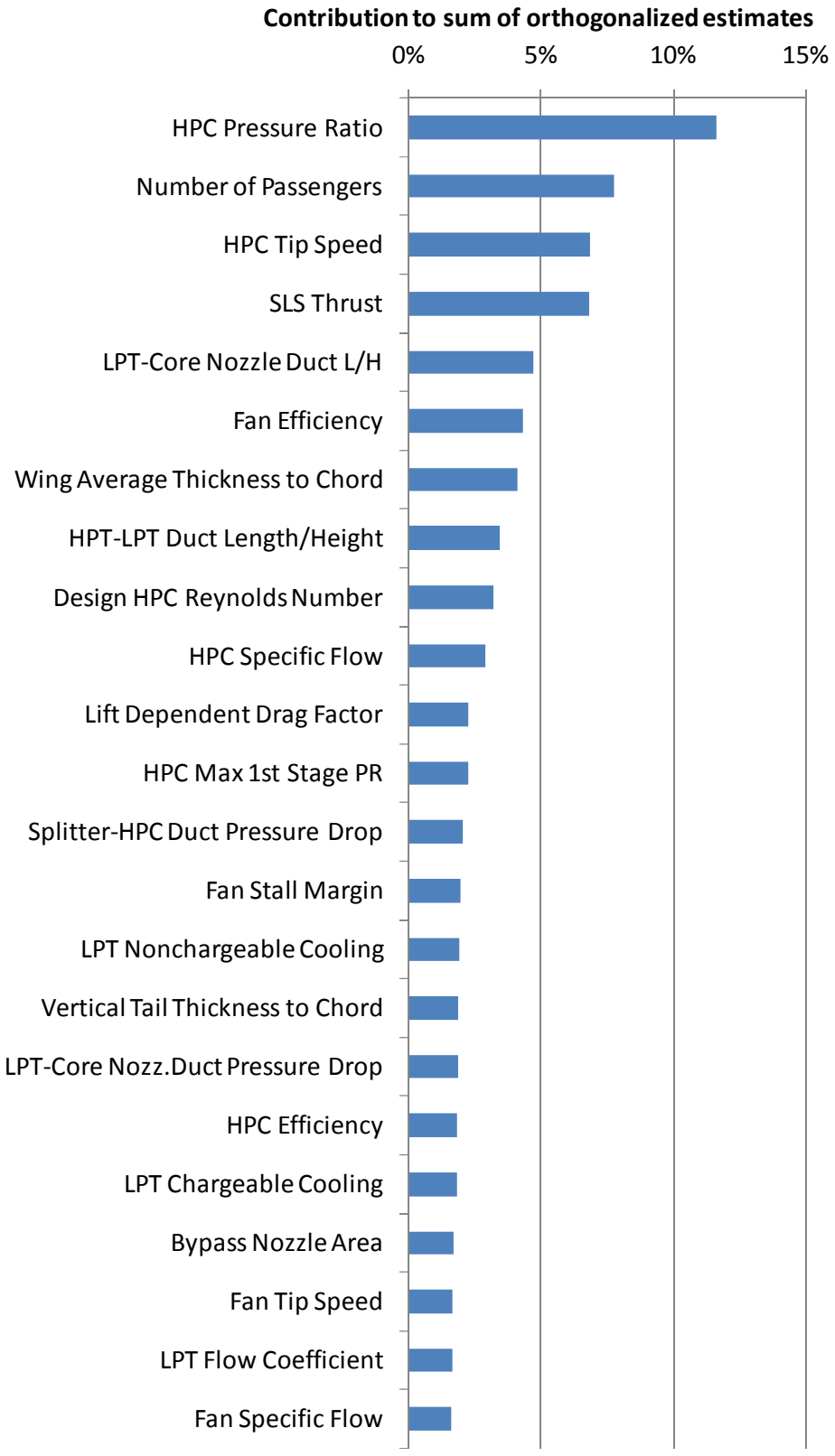

Figure 77. Pareto chart for terminal area fuel burn for regional jet reference vehicle

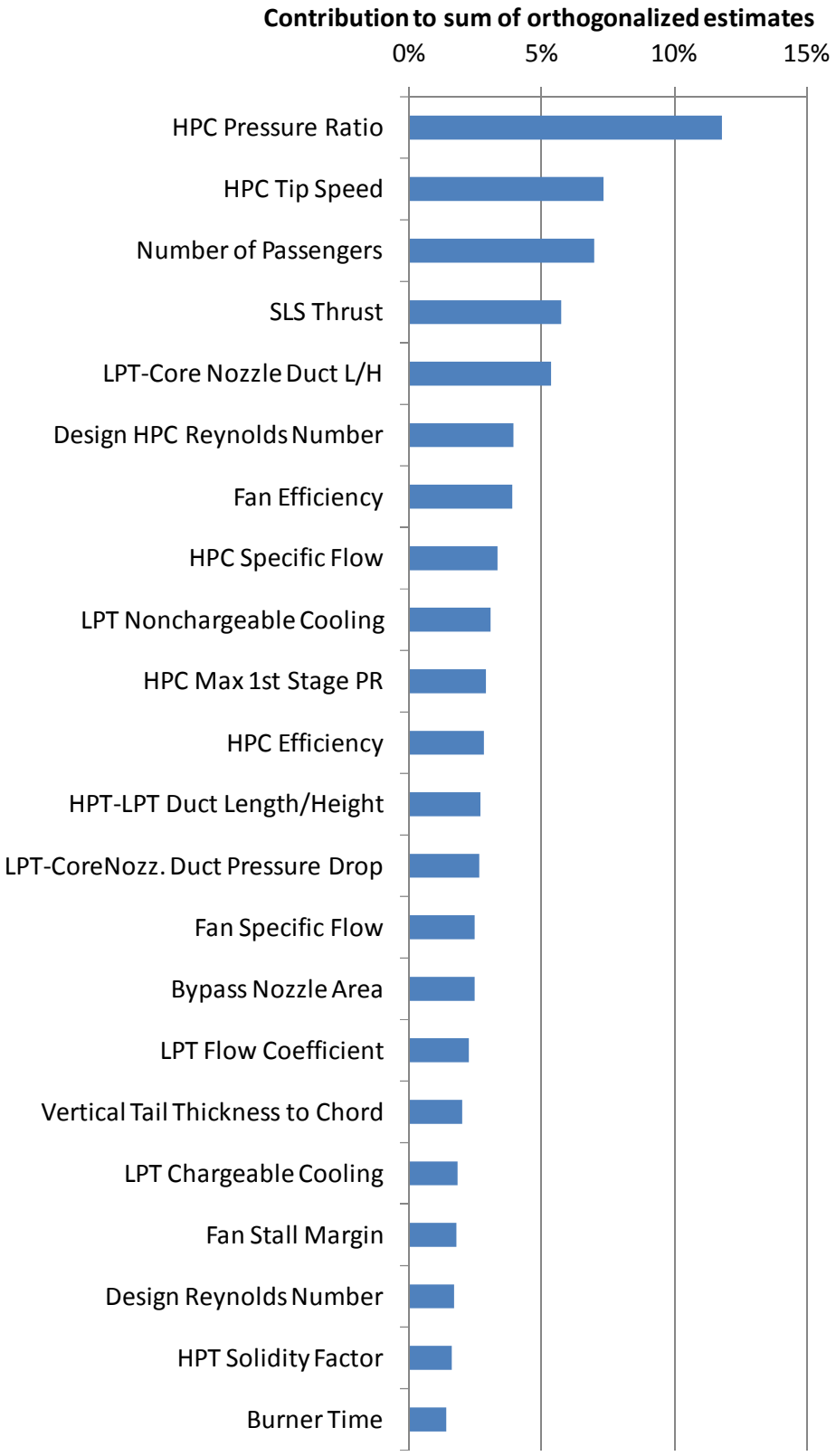

Figure 78. Pareto chart for terminal area NO_x for regional jet reference vehicle.

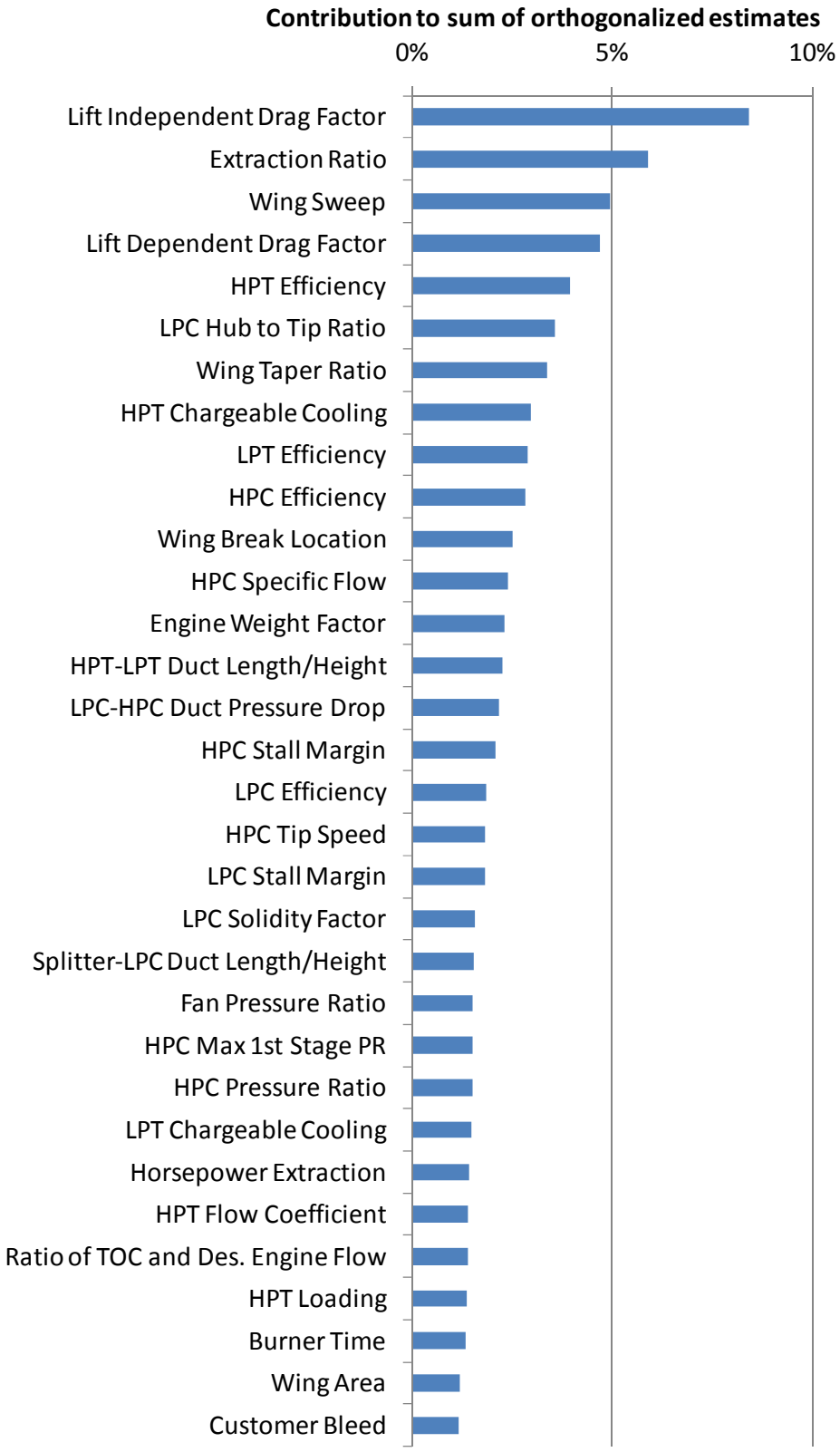

Figure 79. Pareto chart for total mission fuel burn for single-aisle reference vehicle.

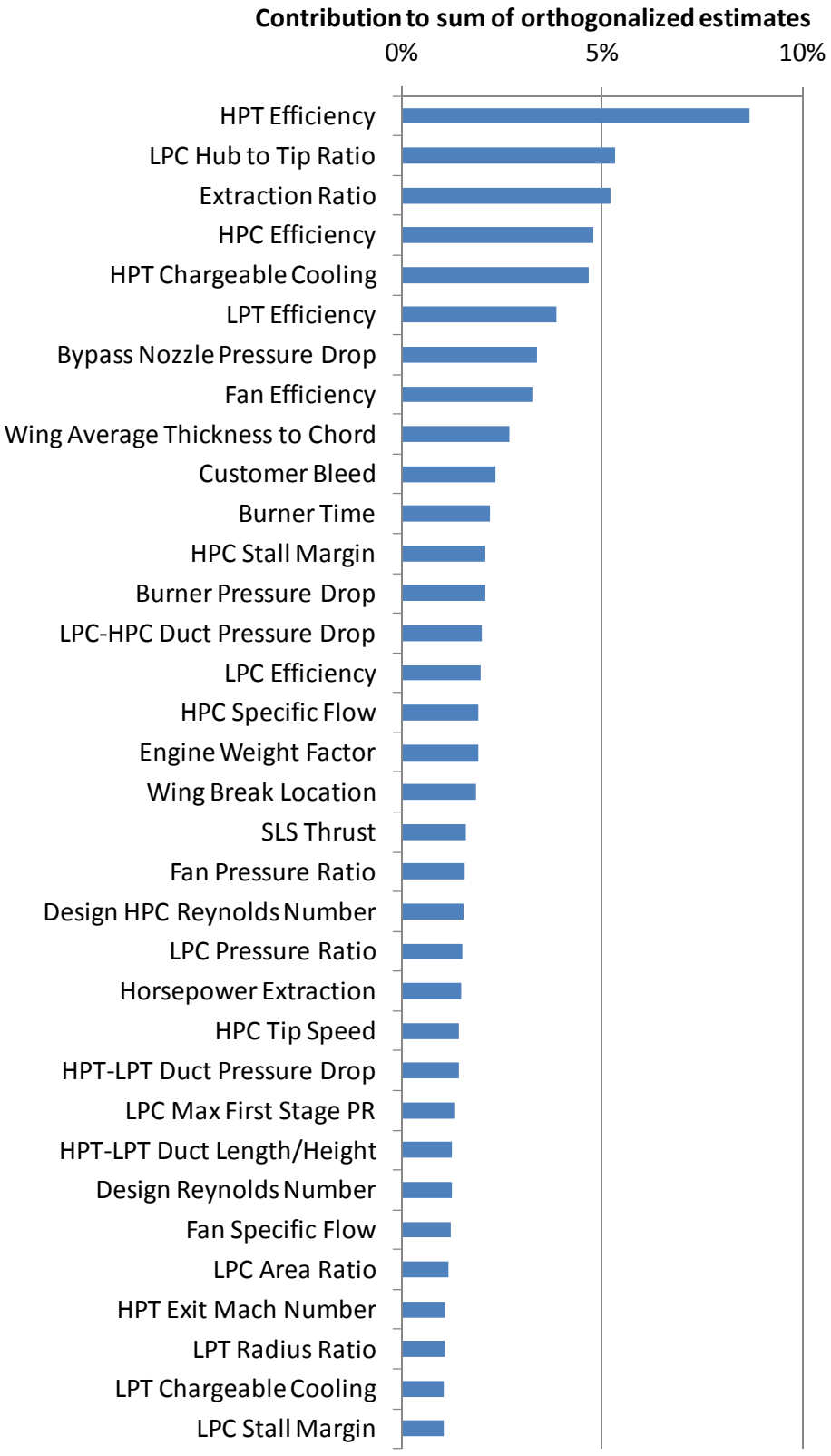

Figure 80. Pareto chart for terminal area fuel burn for single-aisle reference vehicle.

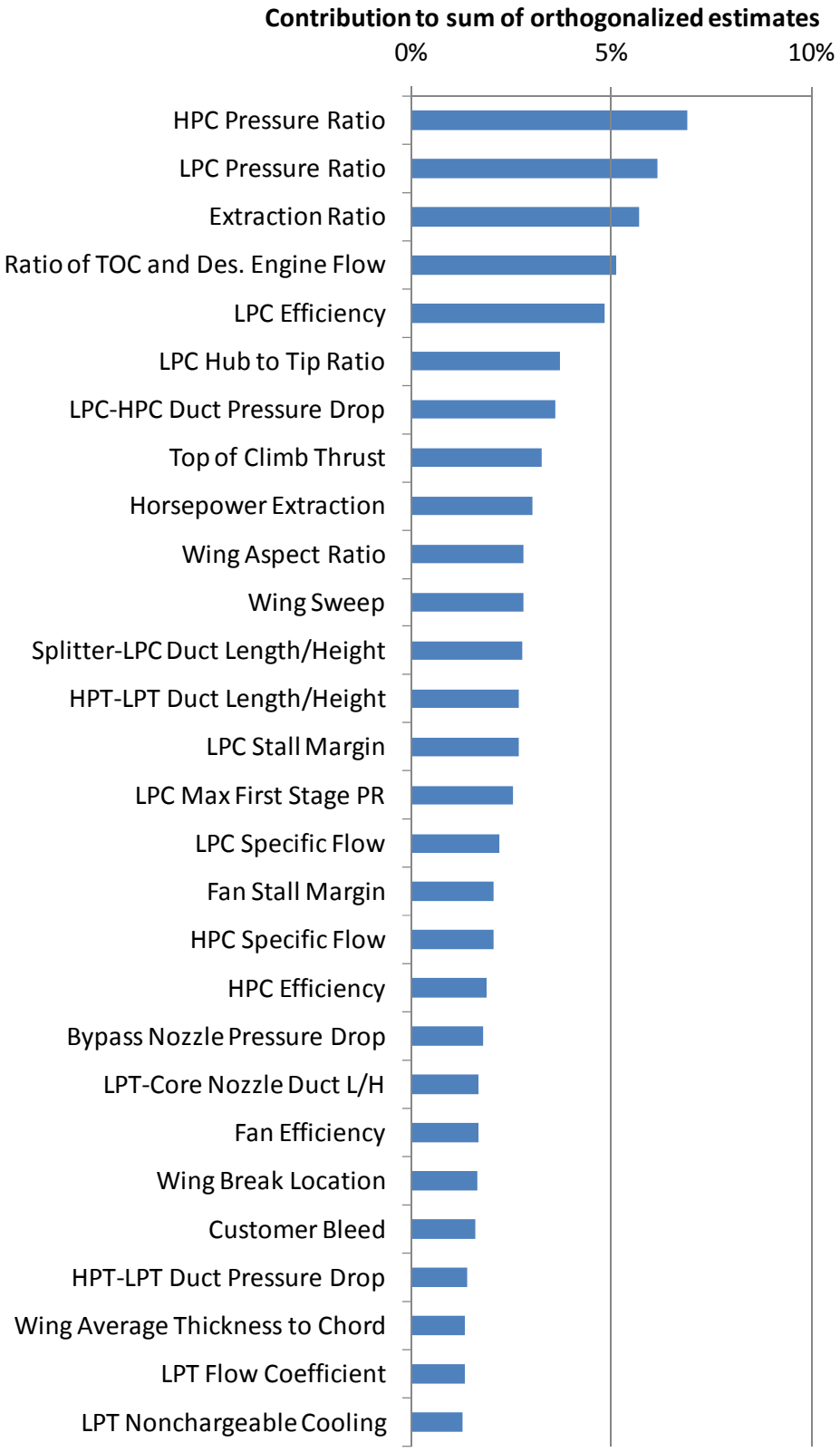

Figure 81. Pareto chart for total mission NO_x for single-aisle reference vehicle.

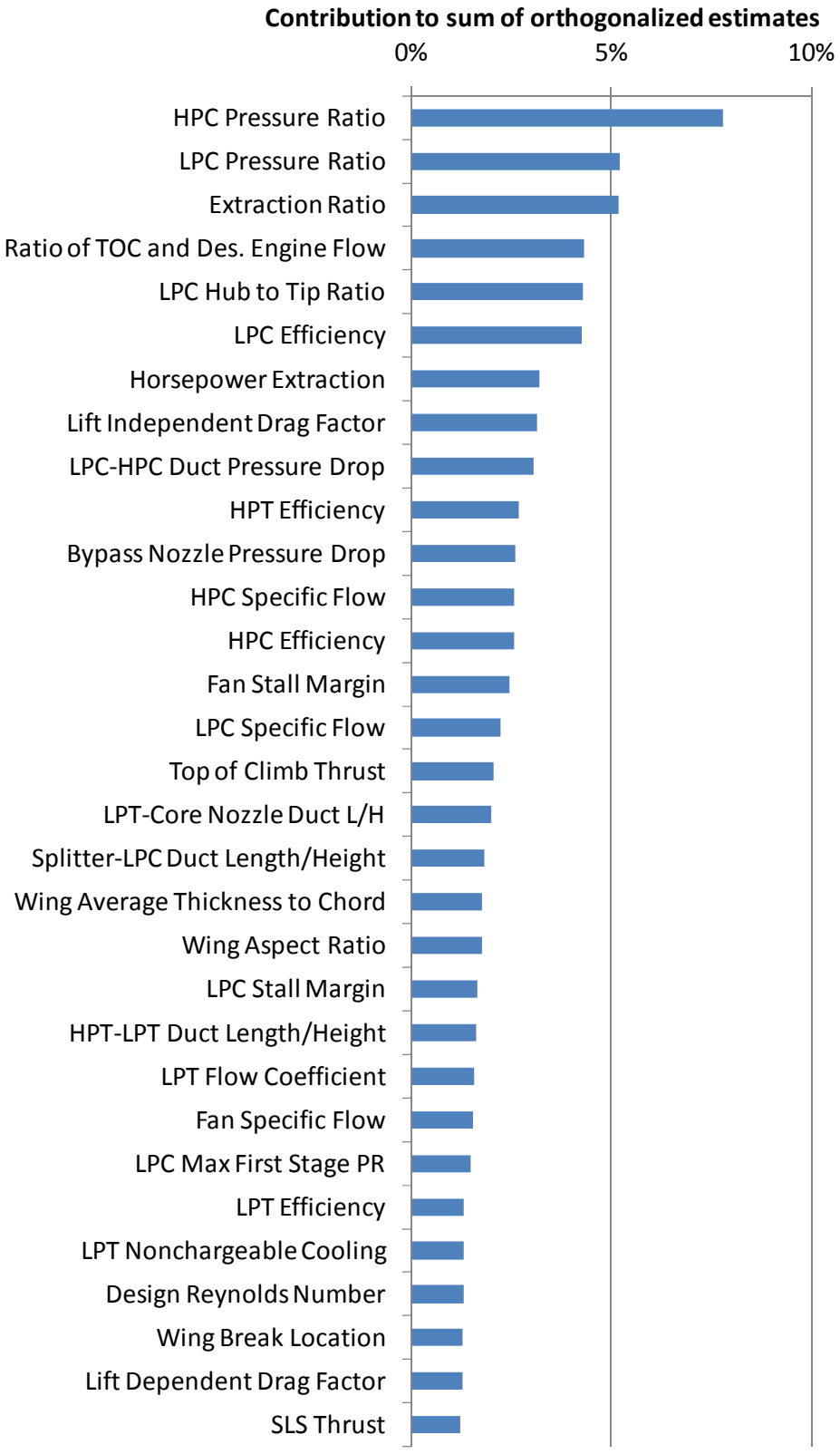

Figure 82. Pareto chart for terminal area NO_x for single-aisle reference vehicle.

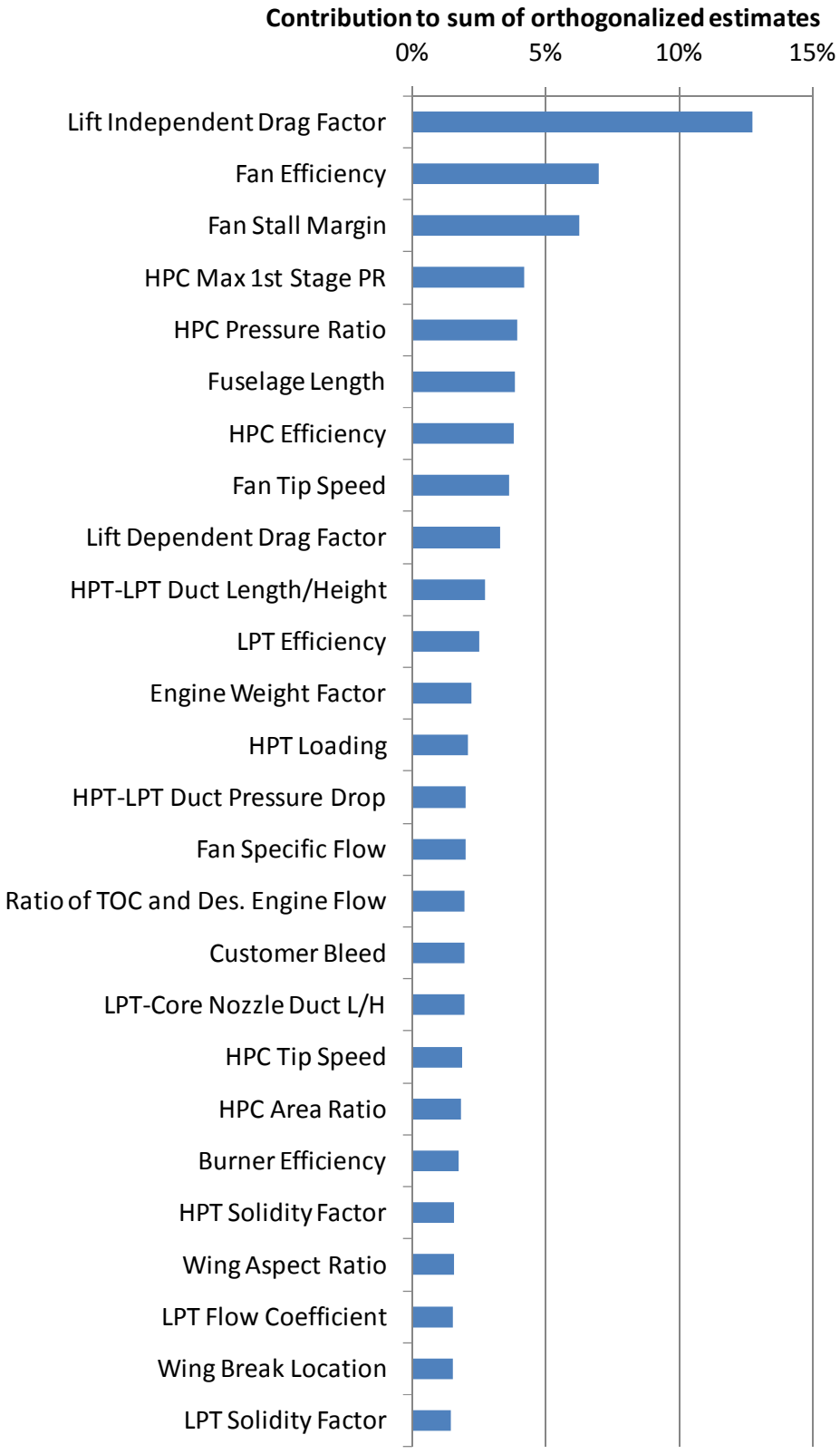

Figure 83. Pareto chart for total mission fuel burn for small twin-aisle reference vehicle.

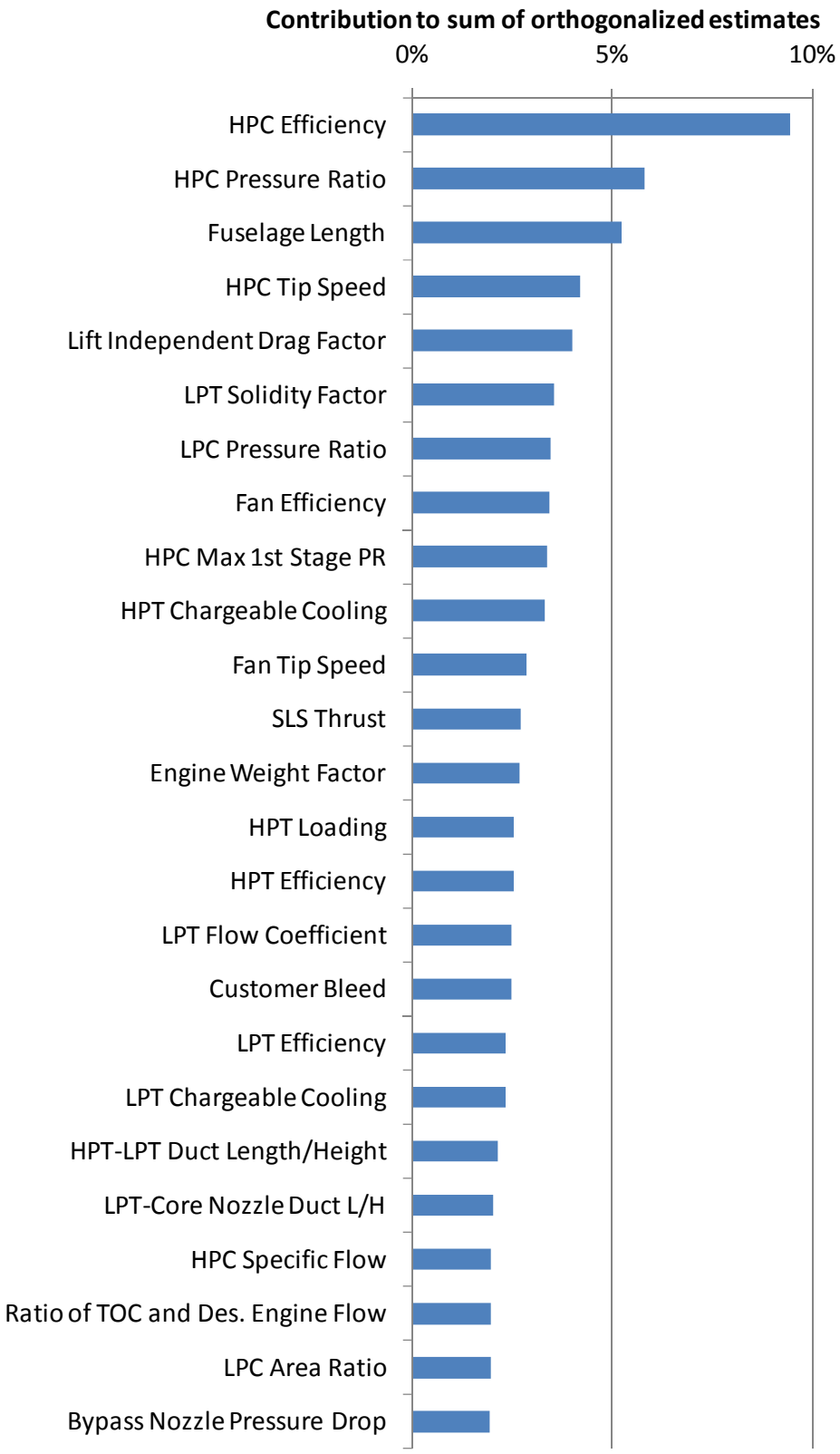

Figure 84. Pareto chart for terminal area fuel burn for small twin-aisle reference vehicle.

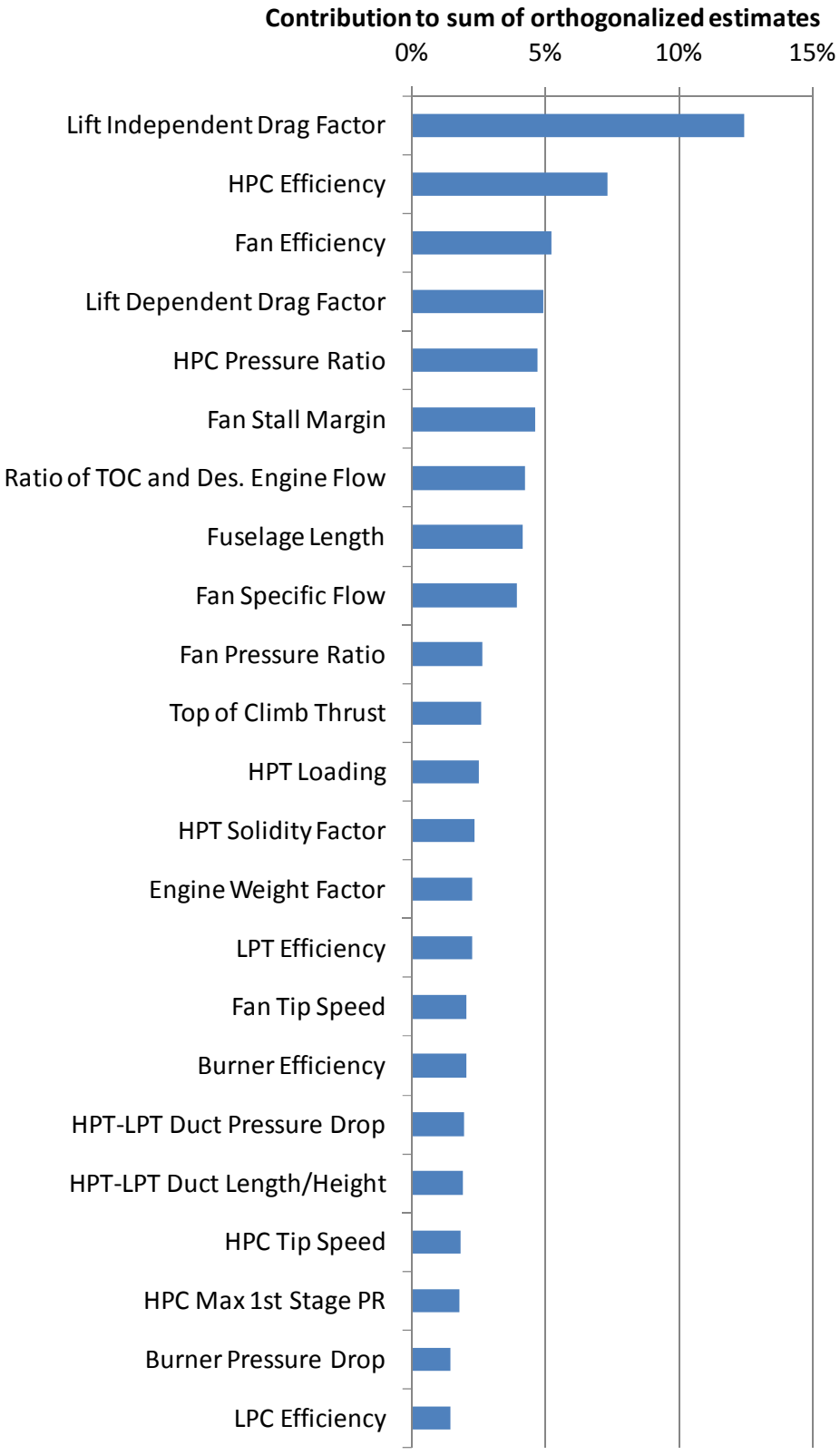

Figure 85. Pareto chart for total mission NO_x for small twin-aisle reference vehicle.

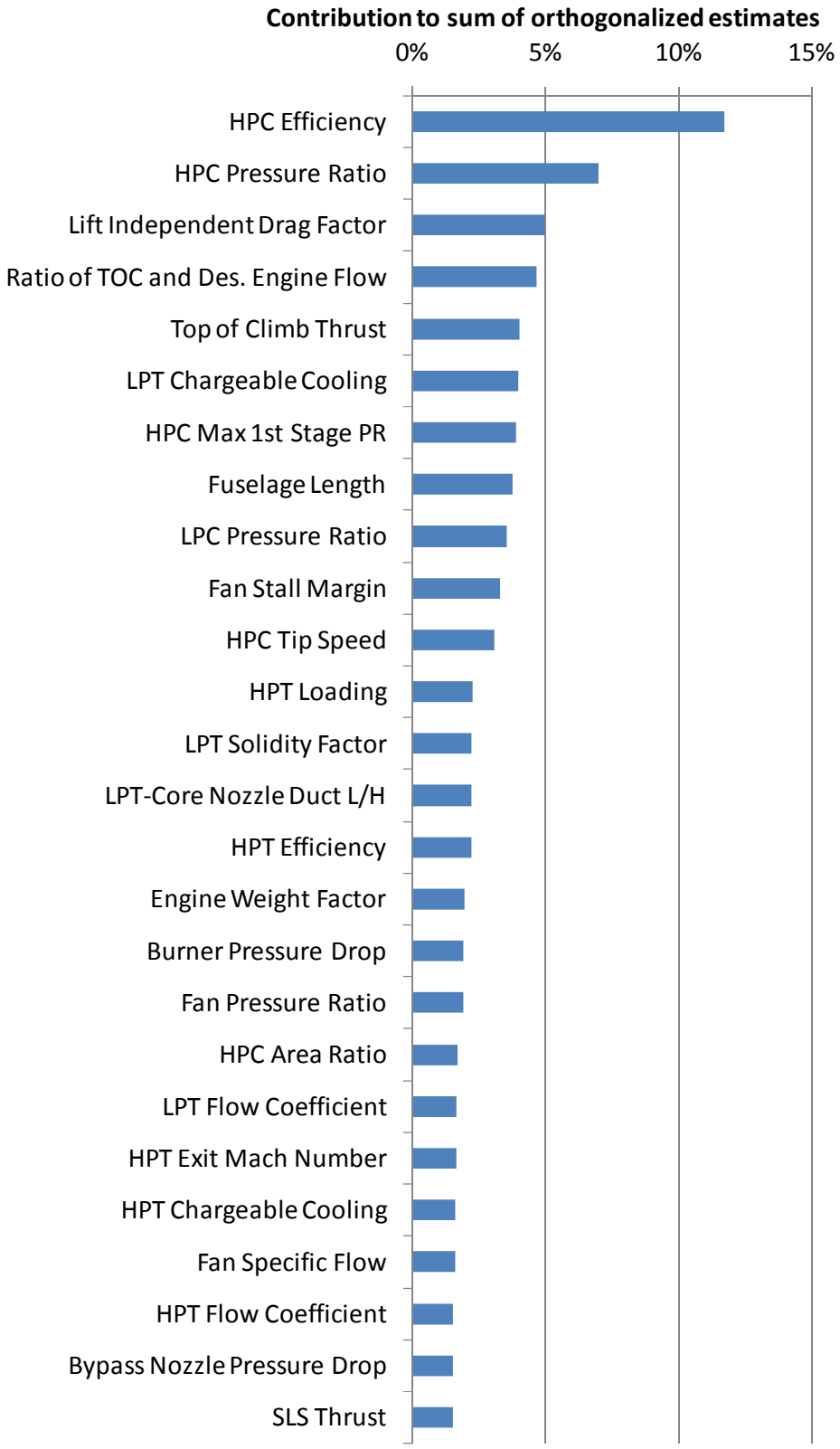

Figure 86. Pareto chart for terminal area NO_x for small twin-aisle reference vehicle.

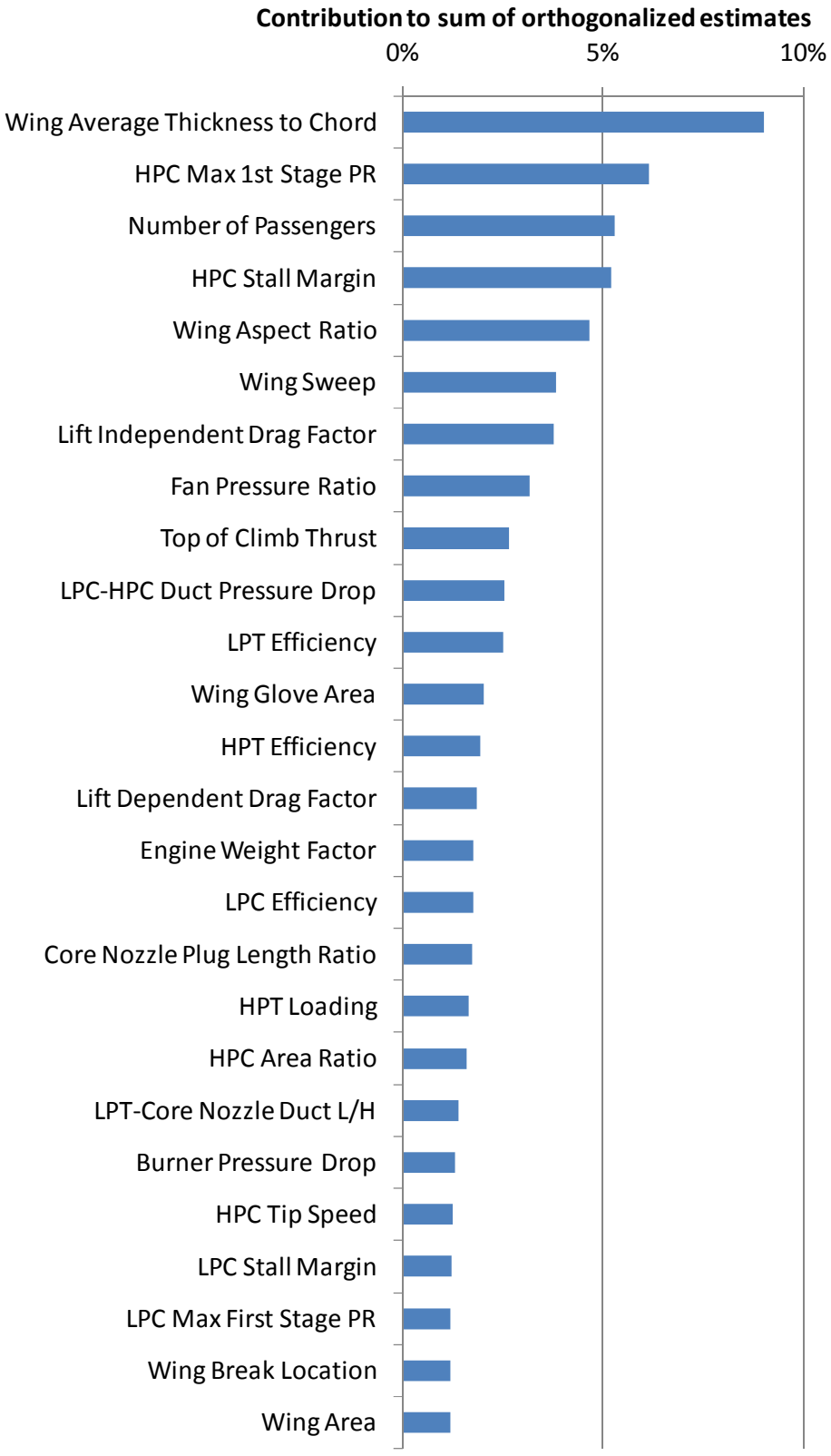

Figure 87. Pareto chart for total mission fuel burn for large twin-aisle reference vehicle.

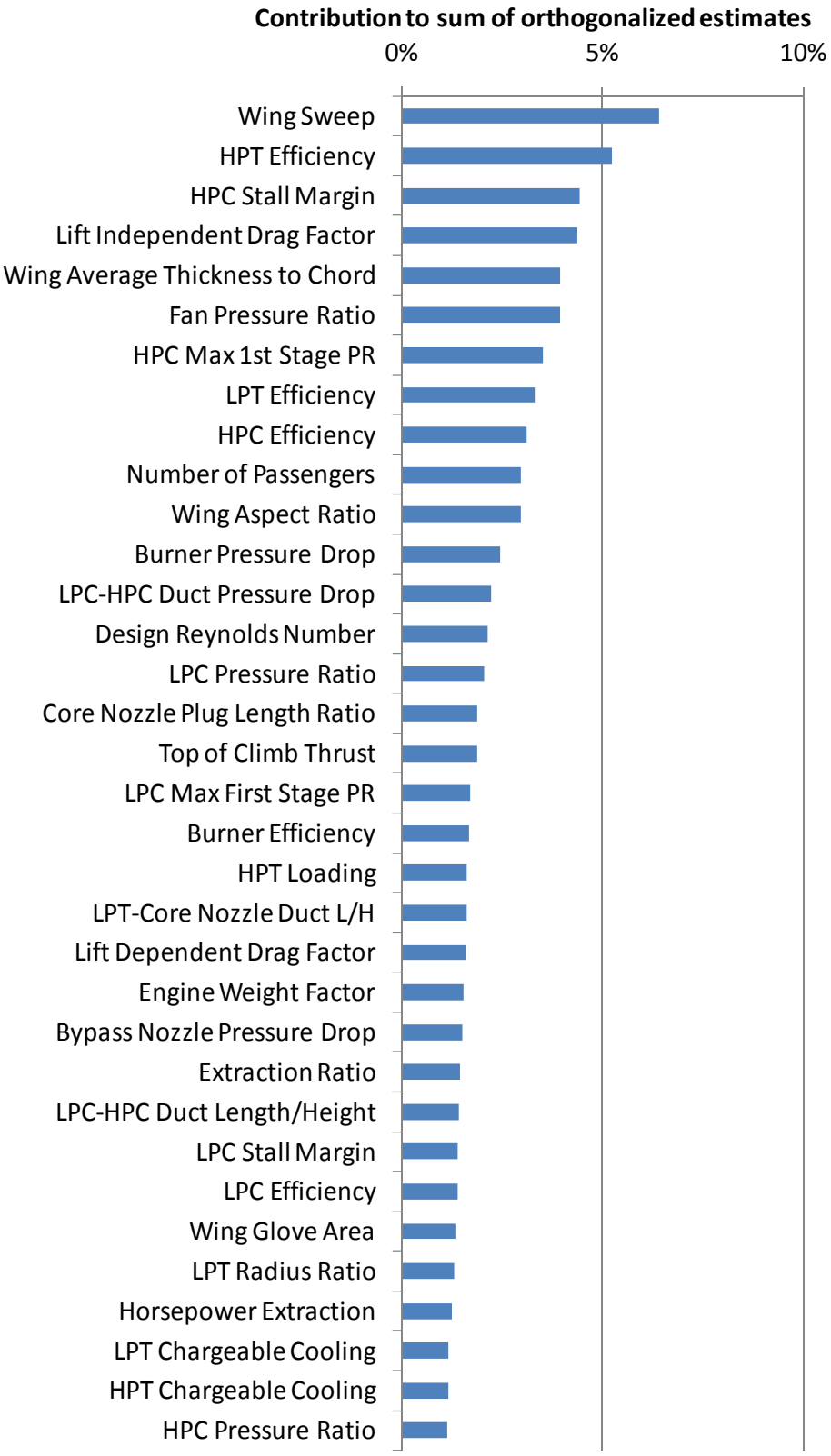

Figure 88. Pareto chart for terminal area fuel burn for large twin-aisle reference vehicle.

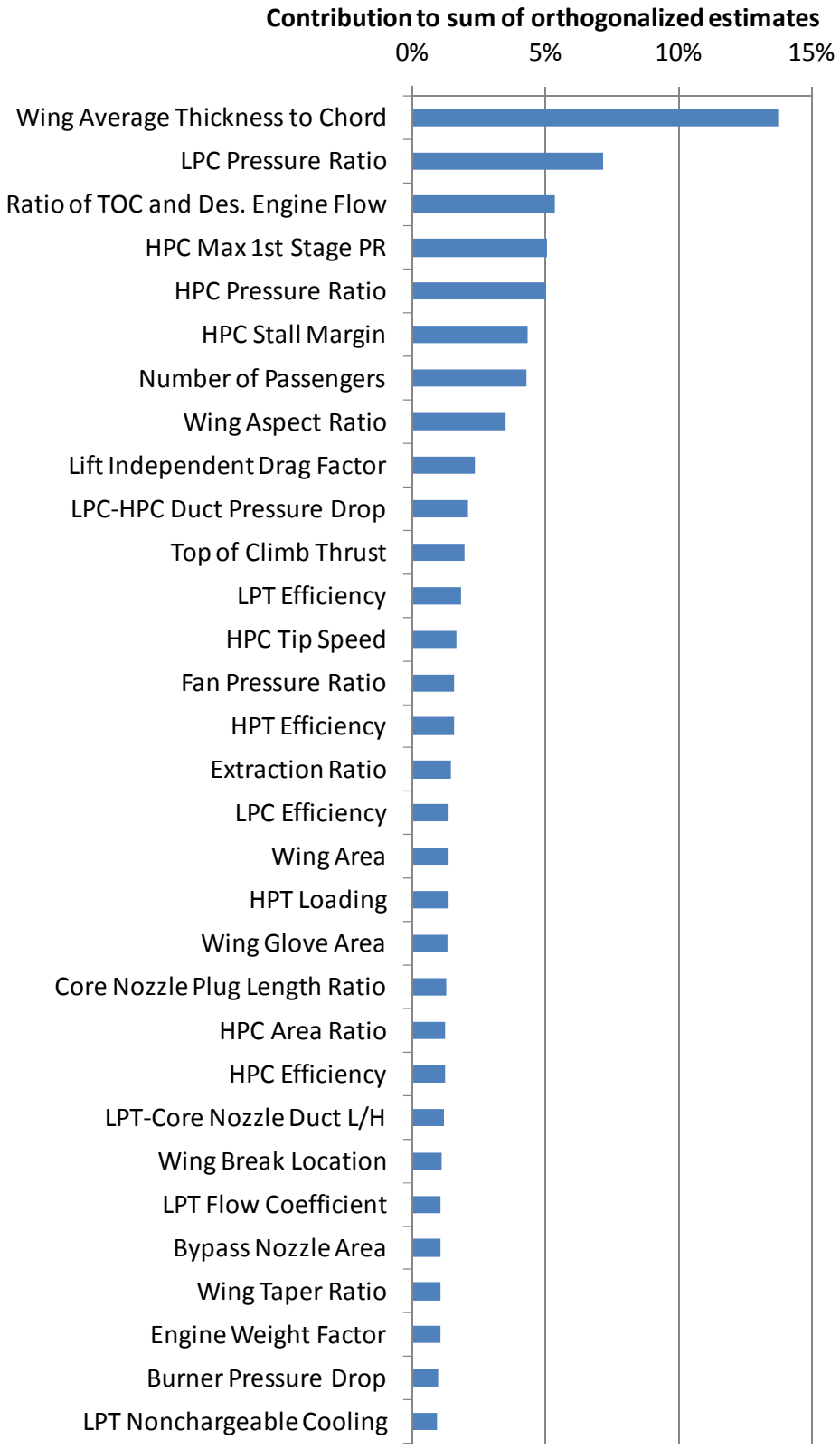

Figure 89. Pareto chart for total mission NO_x for large twin-aisle reference vehicle.

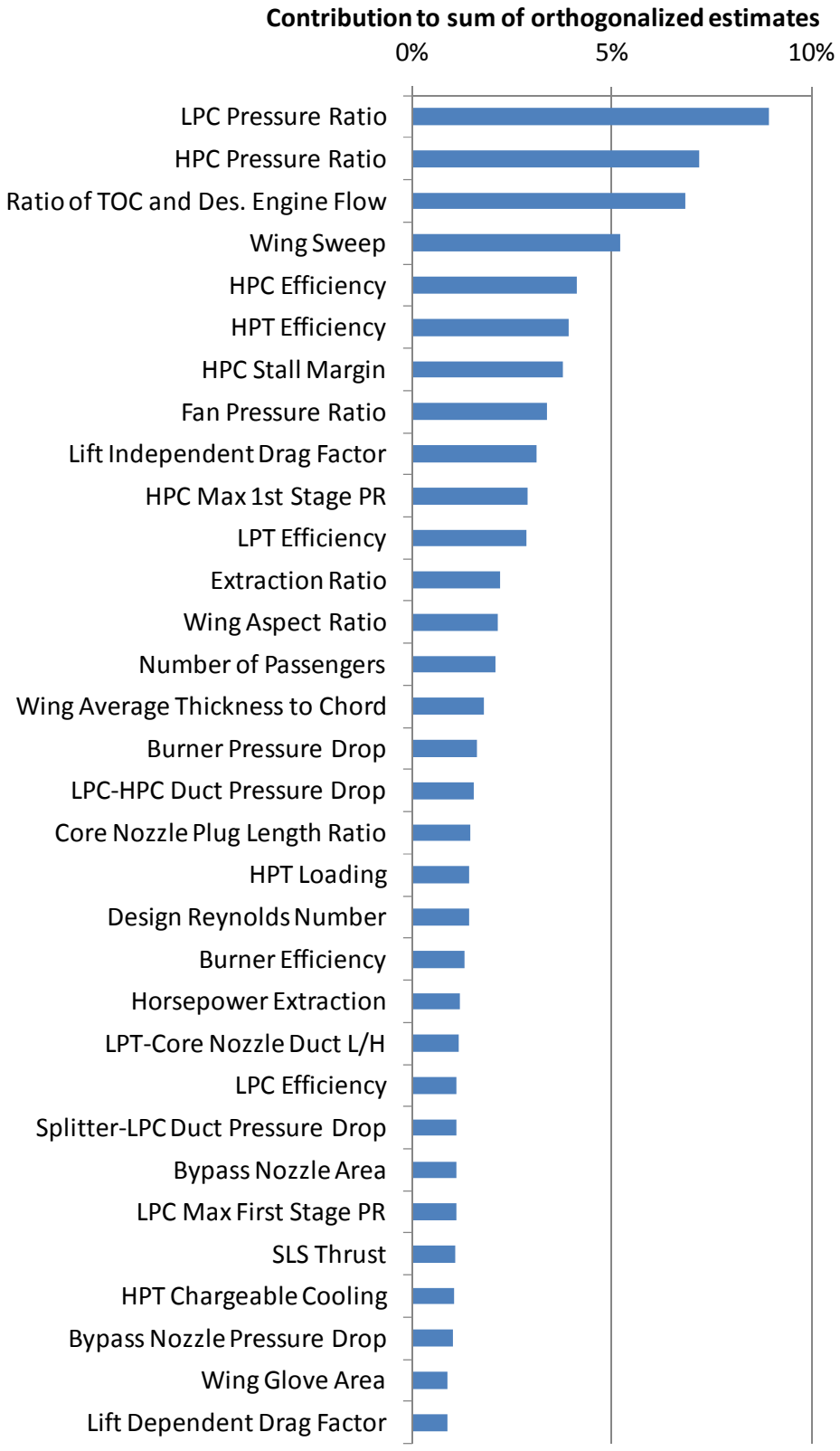

Figure 90. Pareto chart for terminal area NO_x for large twin-aisle reference vehicle.

APPENDIX F

RANGES OF AVERAGE REPLACEMENT DESIGNS OF EXPERIMENTS

This appendix first presents the lists of significant variables for each capability group that encompasses the significant variables for all four metrics. Included are tables containing the minimum and maximum input values for the DOEs used to explore the design space for each capability group in an attempt to develop an averaged replacement vehicle are given. Also included are the final settings of the averaged vehicle in each group.

Table 45. Ranges for regional jet design space exploration (1 of 2).

	Min	Max	Average Replacement
Burner Efficiency	0.985	0.99	0.9881
Burner Pressure Drop (%)	5	5.5	5.2705
Burner Time (s)	0.007	0.009	0.0074
Bypass Nozzle Area Ratio	0.8	0.9	0.8933
Customer Bleed (lb/s)	0	1	0.3806
Design HPC Reynolds Number	325000	375000	306001
Design Reynolds Number	300000	350000	349542
Extraction Ratio	0.55	0.8	0.7327
Fan Efficiency	-0.01	0.01	0.0042
Fan Pressure Ratio	1.58	1.66	1.591
Fan Specific Flow ($lb/s/ft^2$)	42.1	43.5	42.691
Fan Stall Margin	20	30	25.635
Fan Tip Speed Adder (ft/s)	340	430	400.9
HPC Area Ratio	0.196365	0.217035	0.198
HPC Efficiency	-0.001	0.001	-0.00072
HPC Max 1st Stage PR	1.4	1.56	1.454
HPC Pressure Ratio	15.18	20.38	18.046
HPC Specific Flow ($lb/s/ft^2$)	37	41	37.375

Table 46. Ranges for regional jet design space exploration (2 of 2).

	Min	Max	Average Replacement
HPC Stall Margin	20	28	20.436
HPT Solidity Factor	0.92	1.08	0.957
HPT-LPT Duct Length/Height	1.8	2.6	2.144
Lift Dependent Drag Factor	0.8	1.1	1.084
Lift Independent Drag Factor	0.8	1.1	1.084
LPT Chargeable Cooling Factor	0.01	1.05	0.027
LPT Efficiency	0.87	0.9	0.889
LPT Flow Coefficient	5.4	6.4	6.134
LPT Loading	1.05	1.4	1.153
LPT Nonchargeable Cooling Factor	1	1.4	1.207
LPT Radius Ratio	0.9	1.1	1.071
LPT-Core Nozz.Duct Pressure Drop (%)	0.85	1.2	1.18521
LPT-Core Nozzle Duct L/H	0.15	0.5	0.158
Number of Passengers	50	90	75
SLS Thrust (lbf)	11000	15000	14359
LPC-HPC Duct Pressure Drop (%)	0.6	0.8	0.67426
LPC-HPC Duct Length/Height	2.5	3.5	3.021
Vertical Tail Thickness to Chord	0.09	0.12	0.097
Wing Average Thickness to Chord	0.1	0.14	0.132

Table 47. Ranges for single-aisle design space exploration (1 of 2).

	Min	Max	Average Replacement
Burner Pressure Drop (%)	4.4	6.4	4.4113
Burner Time (s)	0.007	0.013	0.0093
Bypass Nozzle Pressure Drop (%)	1.3	1.8	1.5348
Customer Bleed (lb/s)	2	3.5	2.2536
Design HPC Reynolds Number	450000	550000	477518
Design Reynolds Number	350000	450000	426023
Engine Weight Factor	1.55	1.7	1.6292
Extraction Ratio	0.92	1.15	1.0699
Fan Efficiency	-0.02	-0.005	-0.0189
Fan Pressure Ratio	1.65	1.69	1.6725
Fan Specific Flow ($lb/s/ft^2$)	43	44	43.83
Fan Stall Margin	25	35	28.35
Horsepower Extraction (hp)	200	400	224.1
HPC Efficiency	-0.03	-0.01	-0.0197
HPC Max 1st Stage PR	1.38	1.46	1.43
HPC Pressure Ratio	7.80	10.88	8.28
HPC Specific Flow ($lb/s/ft^2$)	29	33	31.1820
HPC Stall Margin	14	20	19.425
HPC Tip Speed Adder (ft/s)	220	320	313.9
HPT Chargeable Cooling Factor	1.7	2.3	1.7143
HPT Efficiency	0.86	0.895	0.8932
HPT Exit Mach Number	0.34	0.39	0.3774
HPT Flow Coefficient	0.94	1	0.9930
HPT Loading	0.9	0.97	0.9700
HPT-LPT Duct Length/Height	0.5	1	0.5596
HPT-LPT Duct Pressure Drop (%)	0.3	1	0.5447
Lift Dependent Drag Factor	0.97	1.1	1.0937
Lift Independent Drag Factor	0.99	1.17	1.1097
LPC Area Ratio	0.5	0.65	0.525

Table 48. Ranges for single-aisle design space exploration (2 of 2).

	Min	Max	Average Replacement
LPC Efficiency	0.02	0.05	0.0224
LPC Hub to Tip Ratio	0.7	0.85	0.8400
LPC Max First Stage PR	1.15	1.3	1.2370
LPC Pressure Ratio	1.8	2.1	2.0794
LPC Solidity Factor	0.9	1.1	1.0940
LPC Specific Flow ($lb/s/ft^2$)	24	28	27.9914
LPC Stall Margin	12	20	15.4087
LPC-HPC Duct Pressure Drop (%)	0.9	1.3	1.0459
LPT Chargeable Cooling Factor	0.7	0.85	0.7891
LPT Efficiency	0.87	0.9	0.8940
LPT Flow Coefficient	6.5	7.5	7.3766
LPT Nonchargeable Cooling Factor	1.7	1.9	1.7855
LPT Radius Ratio	1.25	1.4	1.3307
LPT-Core Nozzle Duct L/H	0.25	0.75	0.2758
Ratio of TOC and Des. Engine Flow	1.01	1.03	1.0143
SLS Thrust (lbf)	26000	27500	26183
Splitter-LPC Duct Length/Height	0.05	0.1	0.0671
Top of Climb Thrust (lbf)	5600	6000	5863.8464
Wing Area (ft^2)	1300	1400	1375.6926
Wing Aspect Ratio	9	9.8	9.0906
Wing Average Thickness to Chord	0.1	0.14	0.1321
Wing Break Location	0.25	0.35	0.2835
Wing Sweep (deg)	20	26	23.77
Wing Taper Ratio	0.2	0.3	0.238

Table 49. Ranges for small twin-aisle design space exploration (1 of 2).

	Min	Max	Average Replacement
Burner Efficiency	0.99	0.997	0.9908
Burner Pressure Drop (%)	2	2.5	2.2155
Bypass Nozzle Pressure Drop (%)	1.9	2.05	2.0016
Customer Bleed (lb/s)	2	3.93	2.7890
Engine Weight Factor	1	1.3	1.0956
Fan Efficiency	-0.005	0.01	0.0080
Fan Pressure Ratio	1.62	1.66	1.6210
Fan Specific Flow ($lb/s/ft^2$)	43.4	43.95	43.8479
Fan Stall Margin	20	30	28.9904
Fan Tip Speed Adder (ft/s)	-100	50	-93.5119
Passenger Cabin Length (ft)	138	207	146.2758
HPC Area Ratio	0.1965	0.2127	0.2045
HPC Efficiency	0	0.02	0.0077
HPC Max 1st Stage PR	1.2	1.35	1.3354
HPC Pressure Ratio	10.6858	15.0421	13.9884
HPC Specific Flow ($lb/s/ft^2$)	37	38	37.9245
HPC Tip Speed Adder (ft/s)	300	400	367.4817
HPT Chargeable Cooling Factor	0.2	0.75	0.336
HPT Efficiency	0.87	0.905	0.9012
HPT Exit Mach Number	0.37	0.38	0.376

Table 50. Ranges for small twin-aisle design space exploration (2 of 2).

	Min	Max	Average Replacement
HPT Flow Coefficient	0.9	1.1	0.9968
HPT Loading	0.4	0.8	0.4443
HPT Solidity Factor	0.95	1.08	1.0388
HPT-LPT Duct Length/Height	0.5	0.8	0.6022
HPT-LPT Duct Pressure Drop (%)	1.3	1.4	1.3500
Lift Dependent Drag Factor	0.9	1.1	1.0332
Lift Independent Drag Factor	0.9	1.1	1.0886
LPC Area Ratio	0.45	0.65	0.5015
LPC Efficiency	0.02	0.03	0.0241
LPC Pressure Ratio	1.4	1.55	1.5020
LPT Chargeable Cooling Factor	1.5	2.5	1.8310
LPT Efficiency	0.895	0.915	0.9005
LPT Flow Coefficient	3.5	3.8	3.7866
LPT Solidity Factor	0.95	1.05	1.0122
LPT-Core Nozzle Duct L/H	0.08	0.12	0.0826
Ratio of TOC and Des. Engine Flow	1.01	1.03	1.0117
SLS Thrust (lbf)	58000	64000	59034.2034
Top of Climb Thrust (lbf)	10900	12500	11924.3424
Wing Aspect Ratio	8	8.8	8.0138
Wing Break Location	0.25	0.35	0.3207

Table 51. Ranges for large twin-aisle design space exploration (1 of 2).

	Min	Max	Average Replacement
Burner Efficiency	0.985	0.997	0.9966
Burner Pressure Drop (%)	3	5	3.0721
Bypass Nozzle Area Ratio	1.05	1.3	1.1977
Bypass Nozzle Pressure Drop (%)	1.6	2	1.8382
Core Nozzle Plug Length Ratio	3.8	4.2	4.1370
Design Reynolds Number	350000	410000	386589
Engine Weight Factor	1.3	1.5	1.4438
Extraction Ratio	1.05	1.3	1.1228
Fan Pressure Ratio	1.5	1.65	1.6493
Horsepower Extraction (hp)	200	400	269
HPC Area Ratio	0.1029	0.1137	0.1030
HPC Efficiency	0	0.02	0.0170
HPC Max 1st Stage PR	1.55	1.59	1.5575
HPC Pressure Ratio	35	42	15.42
HPC Stall Margin	14	20	15.17
HPC Tip Speed Adder (ft/s)	-130	-30	-77.7
HPT Chargeable Cooling Factor	0.35	0.45	0.3749
HPT Efficiency	0.89	0.93	0.921
HPT Loading	0.87	0.99	0.9484
Lift Dependent Drag Factor	1.12	1.2	1.1367
Lift Independent Drag Factor	0.85	0.75	0.8002
LPC Efficiency	0.0171	0.0181	0.0173
LPC Max First Stage PR	1.1	1.2	1.175

Table 52. Ranges for large twin-aisle design space exploration (2 of 2).

	Min	Max	Average Replacement
LPC Pressure Ratio	1.2	1.8	1.4600
LPC Stall Margin	25	34	29.55
LPC-HPC Duct Length/Height	2.5	3.2	3.0087
LPC-HPC Duct Pressure Drop (%)	0.3	1	0.9863
LPT Chargeable Cooling Factor	0.8	0.95	0.8358
LPT Efficiency	0.9	0.9376	0.9234
LPT Flow Coefficient	5.1	5.75	5.7041
LPT Nonchargeable Cooling Factor	1.35	1.47	1.4626
LPT Radius Ratio	0.75	1.25	1.0639
LPT-Core Nozzle Duct L/H	0.15	0.25	0.2056
LPT-CoreNozz. Duct Pressure Drop (%)	0.5	1	0.6488
Number of Passengers	260	280	266
Ratio of TOC and Des. Engine Flow	1.01	1.04	1.0329
SLS Thrust (lbf)	96000	99000	97602
Splitter-LPC Duct Pressure Drop (%)	0.8	1.5	1.4092
Top of Climb Thrust (lbf)	19200	20000	19242
Wing Area (ft^2)	4800	5100	5058
Wing Aspect Ratio	8.5	9.5	8.6201
Wing Average Thickness to Chord	0.1	0.14	0.1166
Wing Break Location	0.3	0.36	0.3344
Wing Glove Area (ft^2)	0.07	0.09	0.0781
Wing Sweep (deg)	32	27	29.04
Wing Taper Ratio	0.14	0.18	0.1748

APPENDIX G

DISTIBUTIONS OF OPERATIONAL VARIATION RESULTS

This appendix provides the results for operational variations presented in the form of the raw distributions that led to the minimum and maximum differences presented in Chapter 4 for Experiment 2. They are presented for each metric of interest by surrogate fleet approach and capability group.

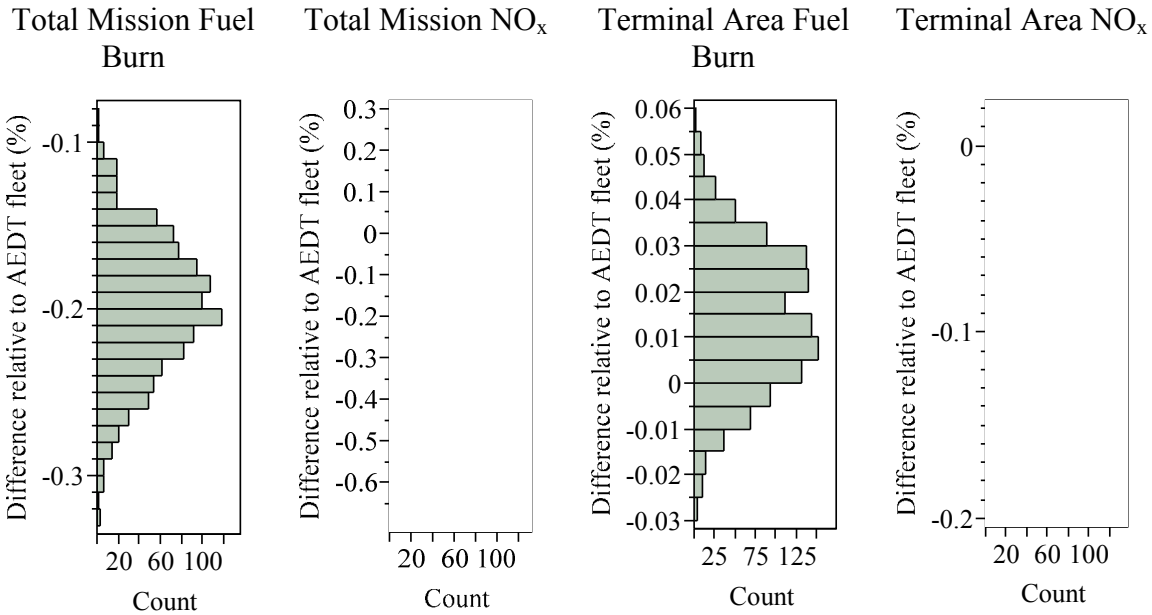

Figure 91. Distributions of results for operational variations for the parametric correction approach with the large twin-aisle group.

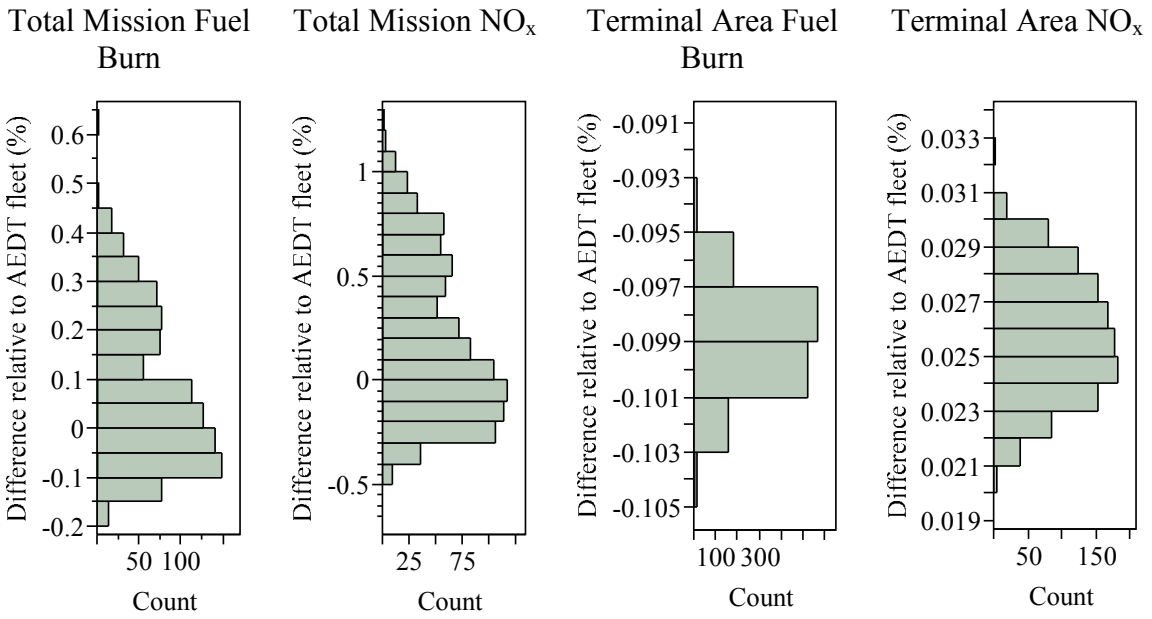

Figure 92. Distributions of results for operational variations for the parametric correction approach with the single-aisle group.

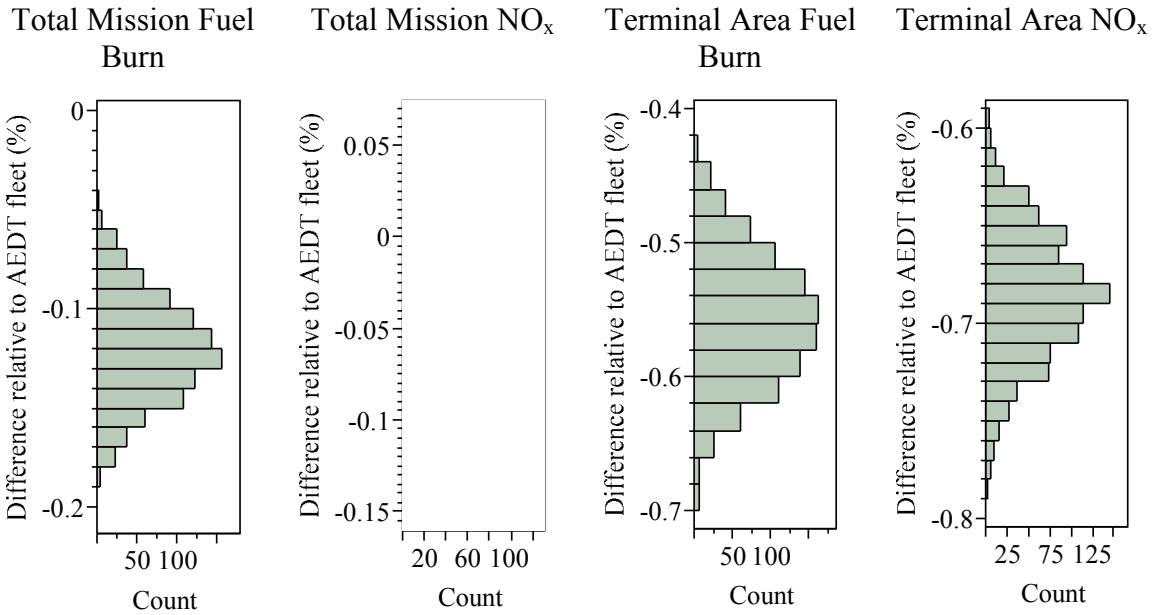

Figure 93. Distributions of results for operational variations for the parametric correction approach with the regional jet group.

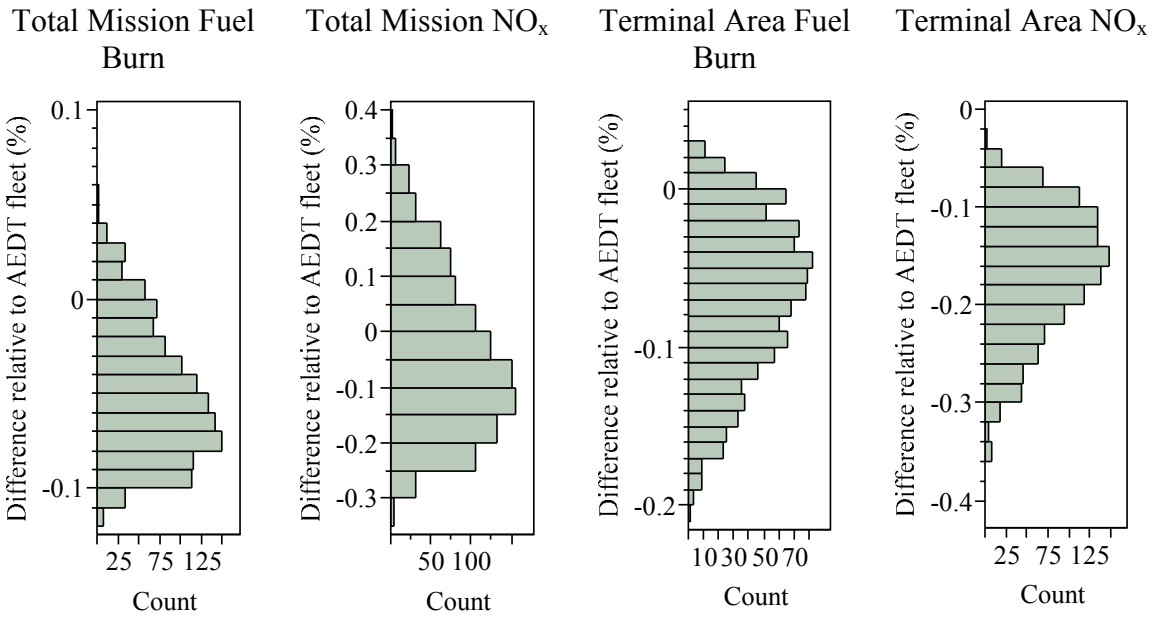

Figure 94. Distributions of results for operational variations for the parametric correction approach with the small twin-aisle group.

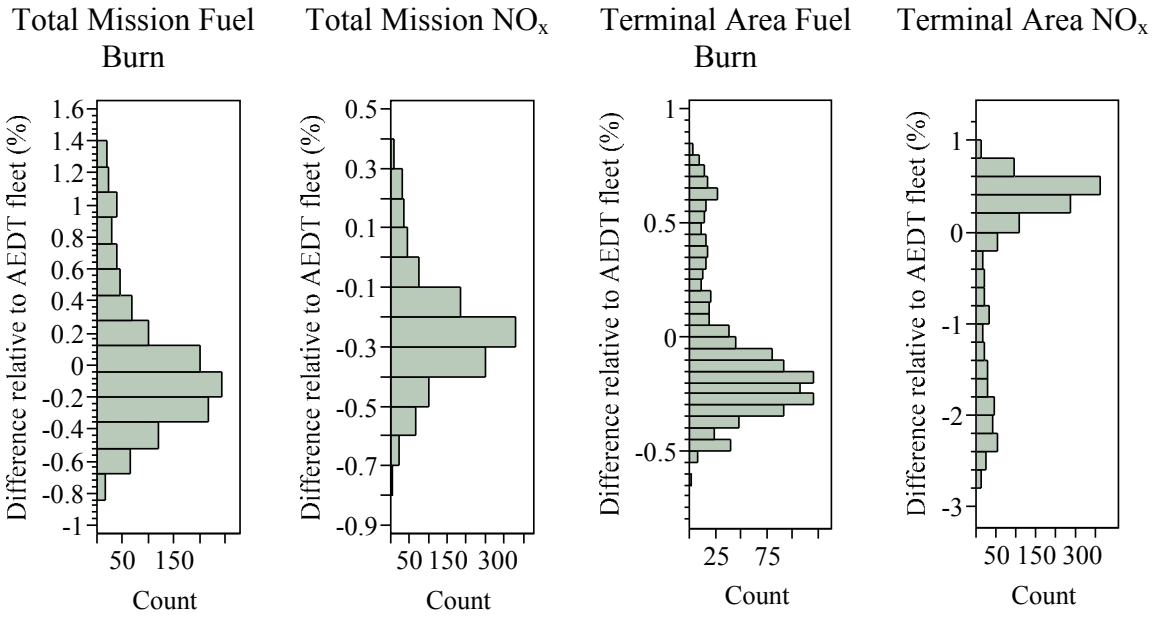

Figure 95. Distributions of results for operational variations for the average replacement approach with the large twin-aisle group.

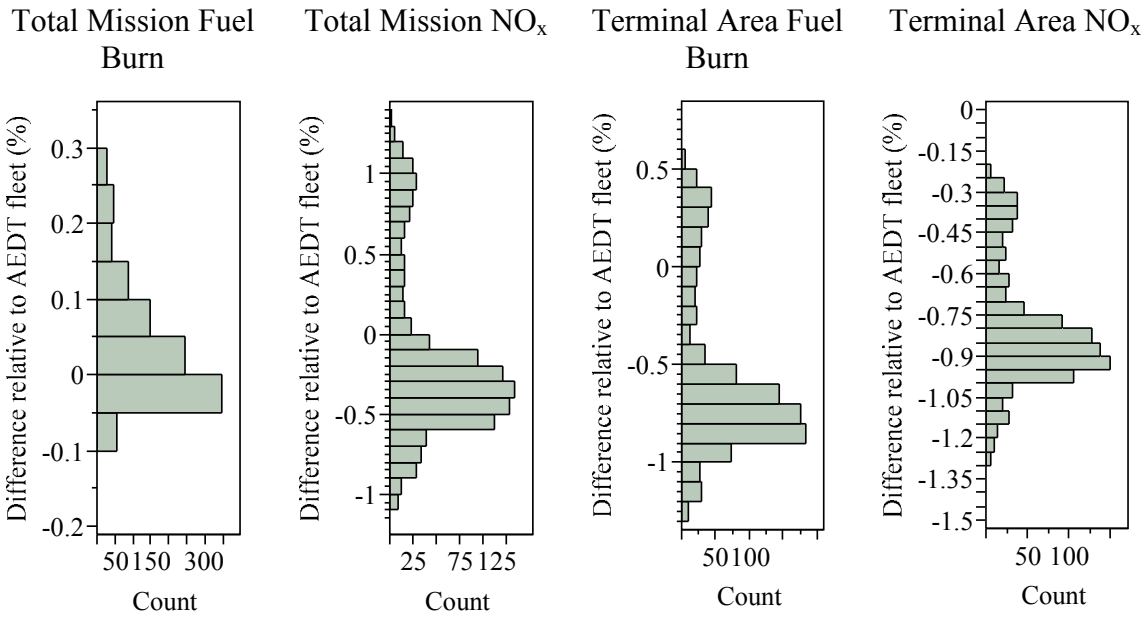

Figure 96. Distributions of results for operational variations for the average replacement approach with the single-aisle group.

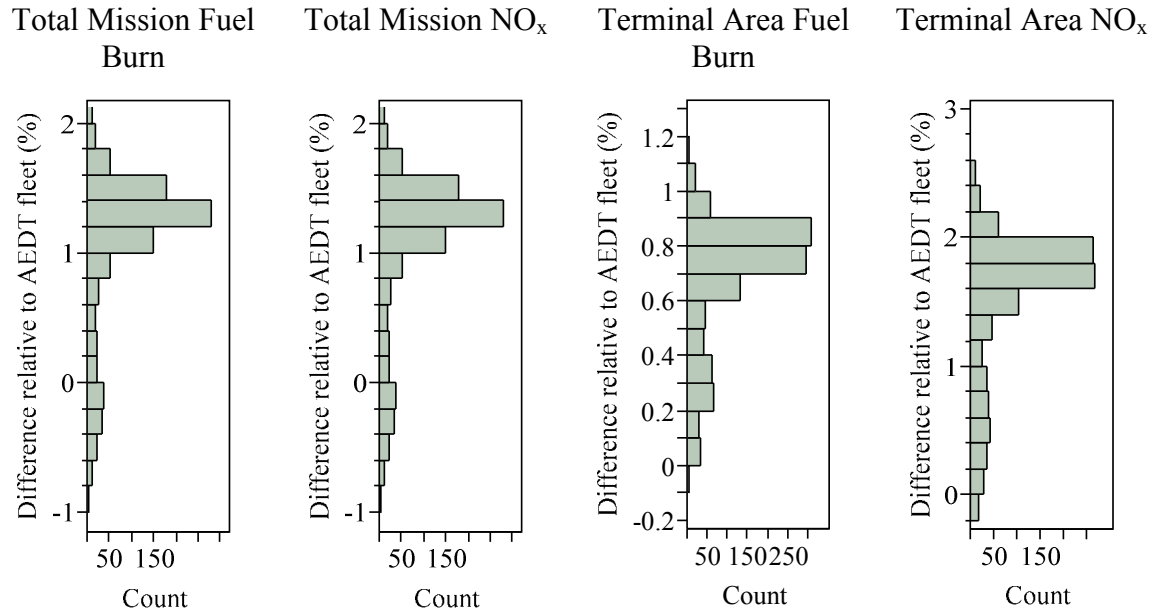

Figure 97. Distributions of results for operational variations for the average replacement approach with the regional jet group.

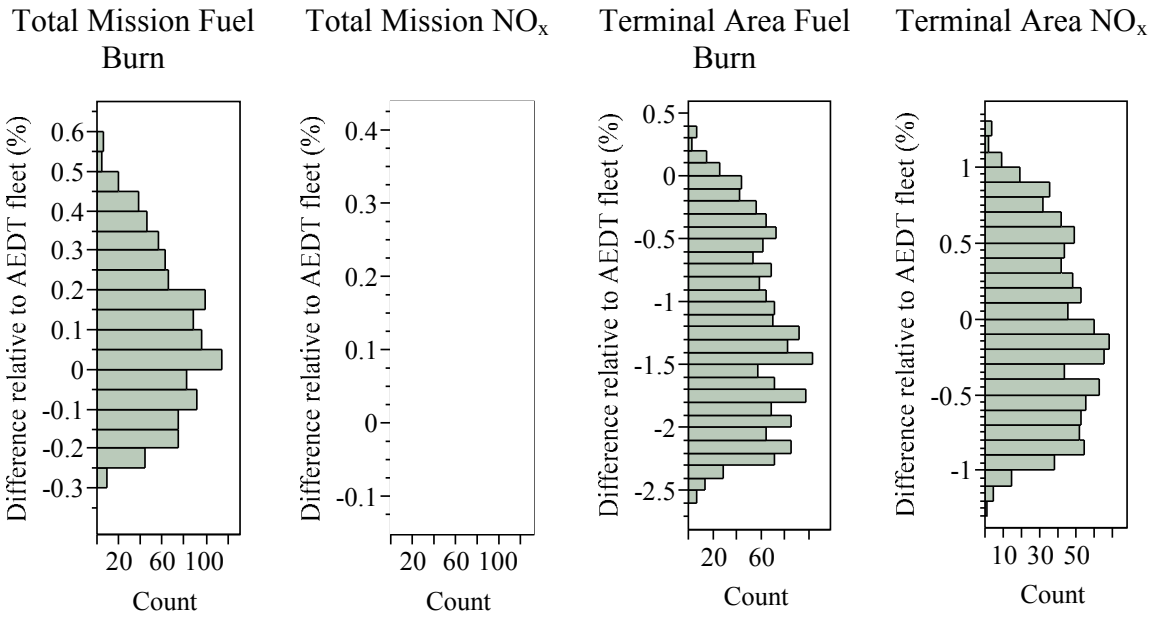

Figure 98. Distributions of results for operational variations for the average replacement approach with the small twin-aisle group.

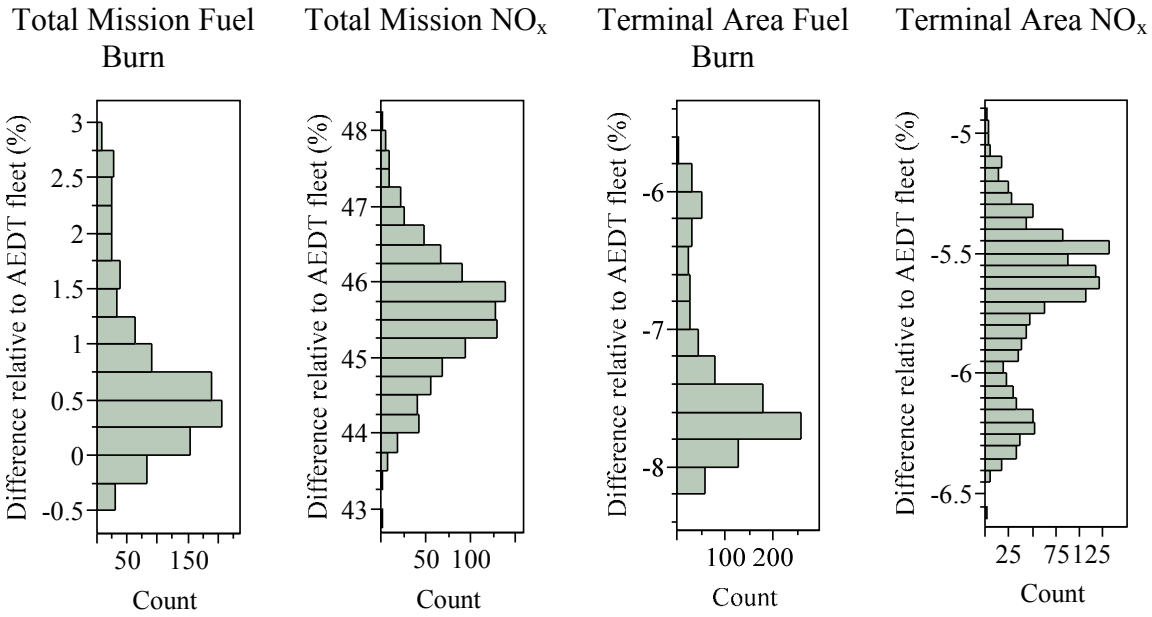

Figure 99. Distributions of results for operational variations for the best-in-class replacement approach with the large twin-aisle group.

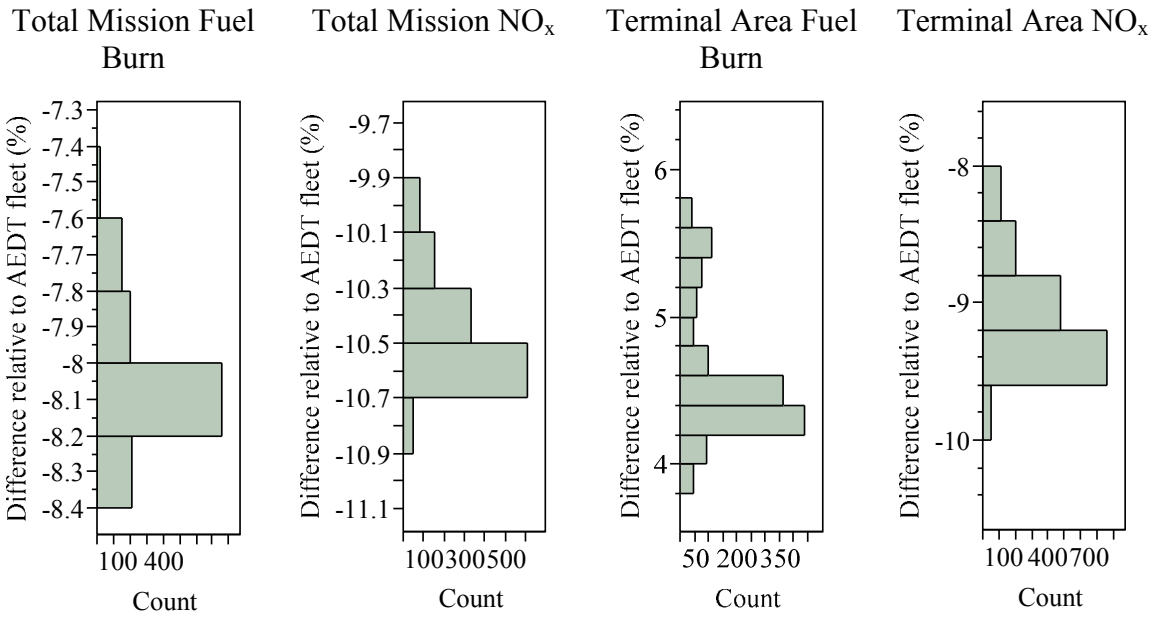

Figure 100. Distributions of results for operational variations for the best-in-class replacement approach with the single-aisle group.

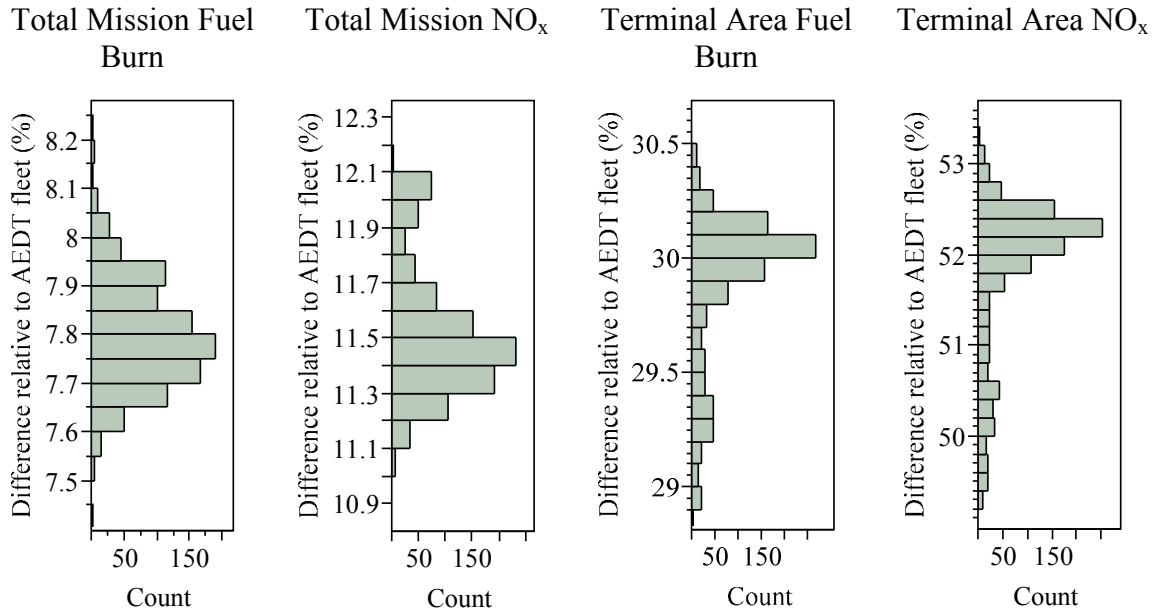

Figure 101. Distributions of results for operational variations for the best-in-class replacement approach with the regional jet group.

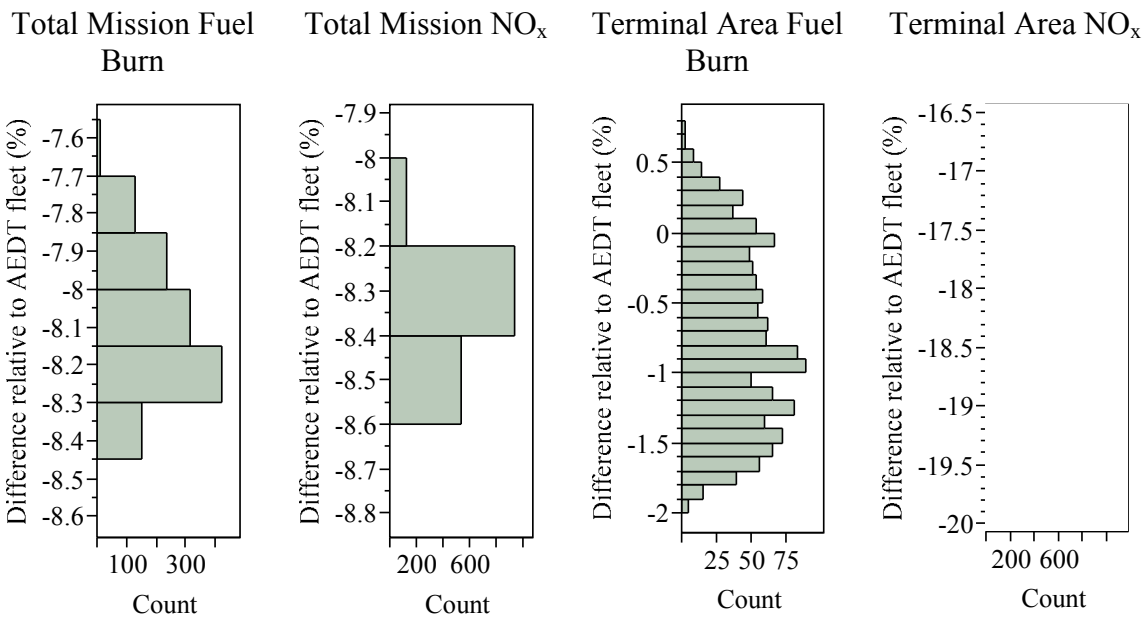

Figure 102. Distributions of results for operational variations for the best-in-class replacement approach with the small twin-aisle group.

APPENDIX H

DOE SETTINGS FOR VIRTUAL FLEET AIRCRAFT

Appendix F contains the DOE settings for the engine cycle and airframe parameters by capability group for the virtual fleet aircraft in the large twin-aisle and single-aisle groups. It is interesting to note that development of the single-aisle virtual fleet required varying the engine thrust and design range of the aircraft. The reason for this is that the relative magnitude of difference in performance between aircraft in the single-aisle fleet is greater than in the large twin-aisle fleet.

Table 53. Engine cycle and airframe parameters for the large twin-aisle virtual fleet.

	Virtual A330 family	**Virtual A340 family**	**Virtual B777 family**
Fan Pressure Ratio	1.5809	1.6483	1.6535
HPC Pressure Ratio	19.8486	15.6604	13.8049
LPC Pressure Ratio	1.6044	1.3207	1.4721
Number of Passengers	255	280	254
Passenger Cabin Length (ft)	151	166	150
Lift Dependent Drag Factor	1.1371	1.1430	1.1733
Lift Independent Drag Factor	0.8532	0.8130	1.0043

Table 54. Engine cycle and airframe parameters for the single-aisle virtual fleet.

	Virtual B737-600 family	**Virtual B737-700 family**	**Virtual B737-800 family**	**Virtual A318 family**	**Virtual A319 family**	**Virtual A320 family**	**Virtual A321 family**
SLS Thrust (lbf)	19356	19356	25406	21281	17811	26192	29967
Design Range (nm)	2700	2750	2950	2500	2750	2950	3350
Extraction Ratio	1.1193	1.1399	1.1070	1.0699	1.1399	1.0990	1.0859
Fan Pressure Ratio	1.6568	1.6722	1.6495	1.6555	1.6722	1.6538	1.6670
LPC Pressure Ratio	1.8324	1.7393	1.8183	1.7318	1.7393	1.8118	1.7858
HPC Pressure Ratio	10.7478	11.2603	11.2134	11.8761	11.2603	11.4514	10.3217
Number of Passengers	110	122	160	95	115	165	185
Passenger Cabin Length (ft)	65.00	76.51	100.34	59.58	75.00	103.48	115.00
Lift Dependent Drag Factor	0.9800	1.0600	1.0424	0.9500	1.0300	1.0424	1.0924
Lift Independent Drag Factor	0.9800	1.0600	1.0418	0.9500	1.0300	1.0418	1.0918

APPENDIX I

TECHNOLOGY IMPACT MATRICES

The following two pages contain the technology impact matrices for the large twin-aisle group and single-aisle group. The values given in each table are in absolute form, meaning that the value in the table would replace the baseline value in the appropriate DOE. These values were taken from [129].

		Active Clearance Control	Aspirated Blades (stage count)	Aspirated Blades (efficiency)	Ceramic Matrix Composites	Advanced TBC	Over the Rotor Foam	Soft Vane	Chevrons	TAPS	TALON X
Input Parameter	**Reference Vehicle Baseline**	**T1**	**T2**	**T3**	**T4**	**T5**	**T6**	**T7**	**T8**	**T9**	**T10**
Active Clearance Control	0	1									
HPC Max FSPR	1.42		2								
HPC Aspect Ratio	1		1.25	1.25							
HPC Aspiration	Off		On	On							
HPC Tip Speed Adder (ft/s)	270		0								
HPC Efficiency Adder	-0.01623		-0.00023	0.00817							
HPT Vane Metal Temperature (deg R)	0				450						
HPT Blade Metal Temperature (deg R)	0					300					
LPT Vane Metal Temperature (deg R)	0				450						
LPT Blat Metal Temperature (deg R)	0					300					
HPT Blade Density (lb/ft3)	0.312				0.0626	0.31512					
HPT Vane Density (lb/ft3)	0.312				0.312	0.31512					
LPT Blade Density (lb/ft3)	0.313				0.0626	0.31613					
LPT Vane Density (lb/ft3)	0.313				0.313	0.31613					
Fan Noise Suppression	1						0.507	0.707			
Jet Noise Suppression	1								0.6		
Nozzle Thrust Coefficient	1								0.995		
NOx Reduction (%)	1									0.48	0.5
Burner Pressure Drop (%)	5.04										
Fan Efficiency Adder	-0.0102						-0.0302				
AC Weight Scalar	1										
Laminar Flow on Upper Wing	Not Specified										
Laminar Flow on Lower Wing	Not Specified										
HLFC Engine Power Extraction	Off										

Figure 103. Technology impact matrix for large twin-aisle group.

		Active Clearance Control	Aspirated Blades (stage count)	Aspirated Blades (efficiency)	Ceramic Matrix Composites	Advanced TBC	Over the Rotor Foam	Soft Vane	Chevrons	TAPS	TALON X
Input Parameter	**Reference Vehicle Baseline**	**T1**	**T2**	**T3**	**T4**	**T5**	**T6**	**T7**	**T8**	**T9**	**T10**
Active Clearance Control	0	1									
HPC Max FSPR	1.582		1.8	1.582							
HPC Aspect Ratio	1		1.25	1.25							
HPC Aspiration	Off		On	On							
HPC Tip Speed Adder (ft/s)	-64.32		-251								
HPC Efficiency Adder	0.016631		0.037631	0.051631							
HPT Vane Metal Temperature (deg R)	0				450						
HPT Blade Metal Temperature (deg R)	0					300					
LPT Vane Metal Temperature (deg R)	0				450						
LPT Blat Metal Temperature (deg R)	0					300					
HPT Blade Density (lb/ft3)	0.312				0.0626	0.31512					
HPT Vane Density (lb/ft3)	0.312				0.312	0.31512					
LPT Blade Density (lb/ft3)	0.313				0.0626	0.31613					
LPT Vane Density (lb/ft3)	0.313				0.313	0.31613					
Fan Noise Suppression	1						0.507	0.707			
Jet Noise Suppression	1								0.6		
Nozzle Thrust Coefficient	1								0.995		
NOx Reduction (%)	1									0.48	0.5
Burner Pressure Drop (%)	3.99										
Fan Efficiency Adder	-0.0132						-0.012				
AC Weight Scalar	1						-0.0252				
Laminar Flow on Upper Wing	Not Specified										
Laminar Flow on Lower Wing	Not Specified										
HLFC Engine Power Extraction	Off										

Figure 104. Technology impact matrix for single-aisle group.

APPENDIX J

SURROGATE MODELS FOR METHODOLOGY DEMONSTRATION TOOL

This appendix contains the stepwise regression equations for the large twin-aisle and single-aisle average replacement vehicles for each technology combination: min fuel burn, min noise, min NO_x, and equally weighted. Each equation takes the form given in Eq. (15)

$$Y = a_1(FD) + a_0 \tag{15}$$

where Y represents a fleet-level metric, a1 and a0 represent the solved for coefficients. Also included are the goodness of fit statistics, which include R^2, mean model fit error, and the standard deviation of model fit error.

Table 55. Regression equations for fixed technology, large twin-aisle average replacement.

Flight Distance		Total Mission Fuel Burn	Total Mission NOx	Terminal Area Fuel Burn	Terminal Area NOx
0-500 nm	a_1	11.07	197.83	-0.01691	-0.27426
	a_0	3004.69	70563	1844.75	32322.03
501-1000 nm	a_1	11.55	159.82	-0.00096	0.14455
	a_0	3009.20	93489	1868.56	32947.02
1001-1500 nm	a_1	11.60	163.21	-0.00026	0.16579
	a_0	3386.41	103592	1898.68	33738.78
1501-2500 nm	a_1	11.38	165.87	-0.00867	-0.05613
	a_0	4646.25	139250	1974.99	35768.33
2501-3500 nm	a_1	12.08	190.12	-0.00633	0.01197
	a_0	4715.05	140388	2053.88	37881.84
3501-4500 nm	a_1	12.29	201.31	-0.00513	0.05025
	a_0	6011.68	177440	2145.96	40363.35
4501-5500 nm	a_1	12.94	225.71	-0.00422	0.08799
	a_0	7306.40	218867	2250.78	43193.15
5501-6500 nm	a_1	12.59	210.99	-0.00059	0.18856
	a_0	11702.45	372204	2366.77	46404.86
> 6501 nm	a_1	12.36	204.87	-0.00942	-0.05873
	a_0	17204.10	542450	2574.80	52213.02

Table 56. Fit statistics for fixed technology, large twin-aisle average replacement.

R2				
Flight Distance	**Total Mission Fuel Burn**	**Total Mission NOx**	**Terminal Area Fuel Burn**	**Terminal Area NOx**
0-500 nm	0.99812	0.98943	0.99174	0.99003
501-1000 nm	0.99910	0.99624	0.99934	0.99940
1001-1500 nm	0.99483	0.97868	0.99940	0.99946
1501-2500 nm	0.99905	0.99583	0.99986	0.99986
2501-3500 nm	0.99997	0.99992	0.99987	0.99987
3501-4500 nm	0.99997	0.99990	0.99989	0.99990
4501-5500 nm	0.99997	0.99991	0.99983	0.99982
5501-6500 nm	0.99999	0.99996	0.99992	0.99992
> 6500 nm	0.99996	0.99988	0.99967	0.99962
Mean Model Fit Error				
Flight Distance	**Total Mission Fuel Burn**	**Total Mission NOx**	**Terminal Area Fuel Burn**	**Terminal Area NOx**
0-500 nm	0.01779	0.11522	0.00000	0.00000
501-1000 nm	-0.10624	-0.17935	-0.06763	-0.10043
1001-1500 nm	-0.09734	-0.17605	-0.06988	-0.10316
1501-2500 nm	-0.11016	-0.23856	-0.06738	-0.09856
2501-3500 nm	-0.09904	-0.19430	-0.08535	-0.12346
3501-4500 nm	-0.09288	-0.18614	-0.08932	-0.12815
4501-5500 nm	-0.13161	-0.24884	-0.10065	-0.14169
5501-6500 nm	-0.07570	-0.11979	-0.13744	-0.18924
> 6500 nm	-0.05488	-0.09229	-0.08042	-0.10864
Standard Deviation of Model Fit Error				
Flight Distance	**Total Mission Fuel Burn**	**Total Mission NOx**	**Terminal Area Fuel Burn**	**Terminal Area NOx**
0-500 nm	1.41977	2.37958	0.01136	0.01157
501-1000 nm	0.49131	0.75419	0.12467	0.18507
1001-1500 nm	0.62484	1.05865	0.12882	0.19011
1501-2500 nm	0.43791	0.79221	0.12066	0.17640
2501-3500 nm	0.15186	0.28892	0.17077	0.23837
3501-4500 nm	0.17964	0.35054	0.16603	0.23627
4501-5500 nm	0.22210	0.42244	0.18019	0.25350
5501-6500 nm	0.11724	0.18661	0.22344	0.30747
> 6500 nm	0.09461	0.15927	0.14264	0.19246

Table 57. Regression equations for min fuel burn, large twin-aisle average replacement.

Flight Distance		Total Mission Fuel Burn	Total Mission NOx	Terminal Area Fuel Burn	Terminal Area NOx
0-500 nm	a_1	10.87	97.27	-0.01681	-0.13540
	a_0	2815.87	32989	1735.52	15228.99
501-1000 nm	a_1	11.35	79.50	-0.00177	0.06040
	a_0	2800.15	43679	1758.20	15523.87
1001-1500 nm	a_1	11.24	78.90	-0.00099	0.07229
	a_0	3352.69	51142	1786.91	15898.36
1501-2500 nm	a_1	11.25	83.11	-0.00967	-0.03857
	a_0	4302.25	64713	1860.37	16861.81
2501-3500 nm	a_1	11.92	94.93	-0.00747	-0.00676
	a_0	4385.23	65434	1935.42	17856.77
3501-4500 nm	a_1	12.13	100.38	-0.00646	0.00973
	a_0	5654.77	83496	2022.59	19019.28
4501-5500 nm	a_1	12.84	113.36	-0.00594	0.02525
	a_0	6751.23	101290	2122.43	20349.10
5501-6500 nm	a_1	12.34	103.45	-0.00255	0.06847
	a_0	11418.43	182077	2229.83	21827.70
> 6501 nm	a_1	12.16	101.32	-0.01085	-0.04403
	a_0	16312.42	255960	2423.68	24497.12

Table 58. Fit statistics for min fuel burn, large twin-aisle average replacement.

R2				
Flight Distance	**Total Mission Fuel Burn**	**Total Mission NOx**	**Terminal Area Fuel Burn**	**Terminal Area NOx**
0-500 nm	0.99795	0.99021	0.99636	0.99636
501-1000 nm	0.99913	0.99642	0.99998	0.99997
1001-1500 nm	0.99401	0.97526	0.99997	0.99996
1501-2500 nm	0.99903	0.99583	0.99991	0.99991
2501-3500 nm	0.99998	0.99993	0.99991	0.99991
3501-4500 nm	0.99996	0.99988	0.99992	0.99992
4501-5500 nm	0.99998	0.99995	0.99994	0.99994
5501-6500 nm	0.99998	0.99995	0.99993	0.99994
> 6500 nm	0.99996	0.99989	0.99984	0.99980
Mean Model Fit Error				
Flight Distance	**Total Mission Fuel Burn**	**Total Mission NOx**	**Terminal Area Fuel Burn**	**Terminal Area NOx**
0-500 nm	0.01898	0.11290	0.00000	0.00000
501-1000 nm	-0.10263	-0.17603	-0.06846	-0.10051
1001-1500 nm	-0.10183	-0.18118	-0.07118	-0.10412
1501-2500 nm	-0.11138	-0.23771	-0.06802	-0.09843
2501-3500 nm	-0.09917	-0.19340	-0.08642	-0.12357
3501-4500 nm	-0.09273	-0.18474	-0.09007	-0.12780
4501-5500 nm	-0.13561	-0.25295	-0.10077	-0.14096
5501-6500 nm	-0.06166	-0.09167	-0.13600	-0.18456
> 6500 nm	-0.05194	-0.08685	-0.07985	-0.10731
Standard Deviation of Model Fit Error				
Flight Distance	**Total Mission Fuel Burn**	**Total Mission NOx**	**Terminal Area Fuel Burn**	**Terminal Area NOx**
0-500 nm	1.52382	2.29314	0.00795	0.00730
501-1000 nm	0.49741	0.76596	0.12618	0.18522
1001-1500 nm	0.67710	1.13721	0.13120	0.19188
1501-2500 nm	0.45451	0.81852	0.12184	0.17621
2501-3500 nm	0.15109	0.28592	0.17054	0.23575
3501-4500 nm	0.18242	0.35203	0.16698	0.23543
4501-5500 nm	0.22863	0.42896	0.18045	0.25226
5501-6500 nm	0.09591	0.14342	0.22118	0.29995
> 6500 nm	0.09005	0.15038	0.14165	0.19015

Table 59. Regression equations for min NO_x, large twin-aisle average replacement.

Flight Distance		Total Mission Fuel Burn	Total Mission NOx	Terminal Area Fuel Burn	Terminal Area NOx
0-500 nm	a_1	10.98	58.61	-0.01683	-0.08106
	a_0	2878.90	20149	1777.90	9306.70
501-1000 nm	a_1	11.46	47.77	-0.00113	0.04062
	a_0	2868.36	26648	1800.98	9487.04
1001-1500 nm	a_1	11.35	47.42	-0.00045	0.04672
	a_0	3424.06	31146	1830.20	9715.50
1501-2500 nm	a_1	11.34	49.87	-0.00906	-0.01948
	a_0	4397.48	39421	1904.75	10302.42
2501-3500 nm	a_1	12.01	56.94	-0.00678	0.00020
	a_0	4503.78	40054	1981.38	10911.50
3501-4500 nm	a_1	12.22	60.25	-0.00571	0.01054
	a_0	5802.45	51030	2070.57	11624.49
4501-5500 nm	a_1	12.94	68.08	-0.00503	0.02079
	a_0	6941.02	62024	2172.71	12440.53
5501-6500 nm	a_1	12.43	62.04	-0.00150	0.04835
	a_0	11681.13	111219	2283.75	13355.37
> 6501 nm	a_1	12.26	60.81	-0.00999	-0.02124
	a_0	16682.87	156371	2484.27	15011.79

Table 60. Fit statistics for min NO_x, large twin-aisle average replacement.

R2				
Flight Distance	**Total Mission Fuel Burn**	**Total Mission NOx**	**Terminal Area Fuel Burn**	**Terminal Area NOx**
0-500 nm	0.99795	0.99003	0.99523	0.99495
501-1000 nm	0.99915	0.99645	0.99923	0.99936
1001-1500 nm	0.99389	0.97494	0.99928	0.99941
1501-2500 nm	0.99905	0.99587	0.99987	0.99990
2501-3500 nm	0.99998	0.99993	0.99987	0.99990
3501-4500 nm	0.99997	0.99989	0.99988	0.99990
4501-5500 nm	0.99998	0.99994	0.99988	0.99990
5501-6500 nm	0.99998	0.99996	0.99992	0.99994
> 6500 nm	0.99996	0.99988	0.99976	0.99972
Mean Model Fit Error				
Flight Distance	**Total Mission Fuel Burn**	**Total Mission NOx**	**Terminal Area Fuel Burn**	**Terminal Area NOx**
0-500 nm	0.01871	0.11318	0.00000	0.00000
501-1000 nm	-0.10252	-0.17585	-0.06869	-0.10117
1001-1500 nm	-0.10180	-0.18158	-0.07087	-0.10381
1501-2500 nm	-0.11083	-0.23730	-0.06790	-0.09860
2501-3500 nm	-0.09942	-0.19413	-0.08613	-0.12373
3501-4500 nm	-0.09328	-0.18590	-0.08987	-0.12807
4501-5500 nm	-0.13640	-0.25455	-0.10103	-0.14170
5501-6500 nm	-0.06234	-0.09250	-0.13707	-0.18684
> 6500 nm	-0.05310	-0.08893	-0.08061	-0.10849
Standard Deviation of Model Fit Error				
Flight Distance	**Total Mission Fuel Burn**	**Total Mission NOx**	**Terminal Area Fuel Burn**	**Terminal Area NOx**
0-500 nm	1.51365	2.29952	0.00891	0.00843
501-1000 nm	0.49130	0.75939	0.12667	0.18646
1001-1500 nm	0.68169	1.13940	0.13067	0.19132
1501-2500 nm	0.45033	0.81197	0.12161	0.17651
2501-3500 nm	0.15210	0.28798	0.17119	0.23742
3501-4500 nm	0.18338	0.35422	0.16692	0.23620
4501-5500 nm	0.22999	0.43177	0.18091	0.25355
5501-6500 nm	0.09683	0.14459	0.22287	0.30362
> 6500 nm	0.09183	0.15379	0.14300	0.19222

Table 61. Regression equations for equally weighted, large twin-aisle average replacement.

Flight Distance		Total Mission Fuel Burn	Total Mission NOx	Terminal Area Fuel Burn	Terminal Area NOx
0-500 nm	a_1	11.10	59.60	-0.01785	-0.08621
	a_0	2928.30	20671	1805.31	9509.97
501-1000 nm	a_1	11.59	48.40	-0.00187	0.03905
	a_0	2917.95	27388	1829.33	9698.34
1001-1500 nm	a_1	11.47	48.05	-0.00114	0.04554
	a_0	3485.11	32011	1859.59	9936.25
1501-2500 nm	a_1	11.47	50.61	-0.00980	-0.02220
	a_0	4473.79	40512	1936.40	10546.10
2501-3500 nm	a_1	12.15	57.84	-0.00748	-0.00190
	a_0	4599.43	41315	2015.56	11179.98
3501-4500 nm	a_1	12.38	61.36	-0.00638	0.00894
	a_0	5896.82	52462	2107.79	11922.89
4501-5500 nm	a_1	13.12	69.57	-0.00564	0.01994
	a_0	7032.39	63645	2213.23	12773.12
5501-6500 nm	a_1	12.56	62.90	-0.00188	0.04945
	a_0	12019.88	115886	2328.10	13728.58
> 6501 nm	a_1	12.40	61.81	-0.01060	-0.02273
	a_0	17130.94	162292	2537.10	15471.84

Table 62. Fit statistics for equally weighted, large twin-aisle average replacement.

R2				
Flight Distance	**Total Mission Fuel Burn**	**Total Mission NOx**	**Terminal Area Fuel Burn**	**Terminal Area NOx**
0-500 nm	0.99791	0.98970	0.99667	0.99678
501-1000 nm	0.99915	0.99639	0.99969	0.99974
1001-1500 nm	0.99396	0.97474	0.99969	0.99975
1501-2500 nm	0.99905	0.99585	0.99994	0.99994
2501-3500 nm	0.99997	0.99993	0.99994	0.99994
3501-4500 nm	0.99996	0.99989	0.99995	0.99995
4501-5500 nm	0.99998	0.99993	0.99990	0.99989
5501-6500 nm	0.99998	0.99996	0.99996	0.99996
> 6500 nm	0.99996	0.99988	0.99976	0.99971
Mean Model Fit Error				
Flight Distance	**Total Mission Fuel Burn**	**Total Mission NOx**	**Terminal Area Fuel Burn**	**Terminal Area NOx**
0-500 nm	0.01941	0.11469	0.00000	0.00000
501-1000 nm	-0.10359	-0.17776	-0.06971	-0.10277
1001-1500 nm	-0.10274	-0.18395	-0.07192	-0.10544
1501-2500 nm	-0.11132	-0.23977	-0.06899	-0.10027
2501-3500 nm	-0.10021	-0.19665	-0.08736	-0.12558
3501-4500 nm	-0.09423	-0.18871	-0.09120	-0.13006
4501-5500 nm	-0.13832	-0.25921	-0.10259	-0.14400
5501-6500 nm	-0.06081	-0.08906	-0.13971	-0.19045
> 6500 nm	-0.05456	-0.09173	-0.08278	-0.11136
Standard Deviation of Model Fit Error				
Flight Distance	**Total Mission Fuel Burn**	**Total Mission NOx**	**Terminal Area Fuel Burn**	**Terminal Area NOx**
0-500 nm	1.51867	2.33113	0.00777	0.00699
501-1000 nm	0.49225	0.76121	0.12852	0.18941
1001-1500 nm	0.67759	1.13921	0.13259	0.19432
1501-2500 nm	0.44857	0.81295	0.12356	0.17951
2501-3500 nm	0.15393	0.29270	0.17437	0.24186
3501-4500 nm	0.18569	0.36021	0.16945	0.23995
4501-5500 nm	0.23328	0.43980	0.18370	0.25770
5501-6500 nm	0.09450	0.13936	0.22718	0.30950
> 6500 nm	0.09450	0.15867	0.14685	0.19732

Table 63. Regression equations for fixed technology, single-aisle average replacement.

Flight Distance		Total Mission Fuel Burn	Total Mission NOx	Terminal Area Fuel Burn	Terminal Area NOx
0-500 nm	a_1	5.09	72.55	-0.01006	-0.18637
	a_0	1158.99	17271.32	685.40	8504.35
501-1000 nm	a_1	5.53	73.67	-0.00222	-0.03372
	a_0	1085.29	19147.93	697.36	8737.61
1001-1500 nm	a_1	5.38	71.65	-0.00188	-0.02631
	a_0	1428.18	25178.08	712.56	9034.50
1501-2500 nm	a_1	5.34	71.52	-0.00599	-0.10745
	a_0	1933.18	34716.41	751.93	9808.32
2501-3500 nm	a_1	5.37	72.05	-0.00553	-0.09780
	a_0	2631.89	47323.36	784.21	10442.85

Table 64. Regression equations for min fuel burn, single-aisle average replacement.

Flight Distance		Total Mission Fuel Burn	Total Mission NOx	Terminal Area Fuel Burn	Terminal Area NOx
0-500 nm	a_1	4.44	60.34	-0.00878	-0.15202
	a_0	958.26	13675.51	580.64	6940.03
501-1000 nm	a_1	4.64	58.02	-0.00265	-0.03988
	a_0	993.23	16683.14	590.04	7112.32
1001-1500 nm	a_1	4.81	60.83	-0.00227	-0.03260
	a_0	954.12	16050.09	601.89	7329.55
1501-2500 nm	a_1	4.47	55.98	-0.00650	-0.10931
	a_0	1515.43	25522.71	634.89	7932.96
2501-3500 nm	a_1	4.63	59.07	-0.00594	-0.09891
	a_0	1927.42	32252.01	658.55	8369.04

Table 65. Regression equations for min NO_x, single-aisle average replacement.

Flight Distance		Total Mission Fuel Burn	Total Mission NOx	Terminal Area Fuel Burn	Terminal Area NOx
0-500 nm	a_1	4.88	20.10	-0.00955	-0.04979
	a_0	1000.06	4296.03	596.13	2134.35
501-1000 nm	a_1	5.24	20.46	-0.00271	-0.01258
	a_0	949.52	4719.02	606.72	2192.03
1001-1500 nm	a_1	5.27	20.75	-0.00247	-0.01112
	a_0	1105.10	5470.73	620.09	2264.96
1501-2500 nm	a_1	5.16	20.22	-0.00606	-0.03093
	a_0	1611.68	8176.37	654.08	2451.30
2501-3500 nm	a_1	5.14	20.18	-0.00584	-0.02930
	a_0	2342.62	11897.71	682.11	2604.19

Table 66. Regression equations for equally weighted, single-aisle average replacement.

Flight Distance		Total Mission Fuel Burn	Total Mission NOx	Terminal Area Fuel Burn	Terminal Area NOx
0-500 nm	a_1	4.53	18.62	-0.00900	-0.04703
	a_0	1015.35	4419.61	600.84	2164.15
501-1000 nm	a_1	4.77	18.25	-0.00266	-0.01194
	a_0	1032.28	5244.97	610.66	2218.59
1001-1500 nm	a_1	4.97	19.41	-0.00240	-0.01033
	a_0	988.75	4984.65	623.09	2287.53
1501-2500 nm	a_1	4.78	18.47	-0.00647	-0.03277
	a_0	1538.10	7915.21	656.24	2471.65
2501-3500 nm	a_1	4.77	18.40	-0.00558	-0.02790
	a_0	2203.58	11309.79	680.31	2606.27

Table 67. Fit statistics for fixed technology, single-aisle average replacement.

R^2				
Flight Distance	**Total Mission Fuel Burn**	**Total Mission NOx**	**Terminal Area Fuel Burn**	**Terminal Area NOx**
0-500 nm	0.99836	0.99808	0.99824	0.99810
501-1000 nm	0.99999	0.99998	0.99995	0.99991
1001-1500 nm	0.99910	0.99833	0.99995	0.99991
1501-2500 nm	0.99988	0.99978	0.99982	0.99968
2501-3500 nm	0.99996	0.99994	0.99880	0.99874
Mean Model Fit Error				
Flight Distance	**Total Mission Fuel Burn**	**Total Mission NOx**	**Terminal Area Fuel Burn**	**Terminal Area NOx**
0-500 nm	0.06447	0.08755	0.00000	0.00000
501-1000 nm	-0.15699	-0.22064	-0.09058	-0.14072
1001-1500 nm	-0.12555	-0.17676	-0.09411	-0.14496
1501-2500 nm	-0.08686	-0.12816	-0.09260	-0.13972
2501-3500 nm	-0.09661	-0.12350	-0.08982	-0.13333
Standard Deviation of Model Fit Error				
Flight Distance	**Total Mission Fuel Burn**	**Total Mission NOx**	**Terminal Area Fuel Burn**	**Terminal Area NOx**
0-500 nm	1.60033	1.52022	0.00839	0.01304
501-1000 nm	0.24661	0.34985	0.16710	0.25993
1001-1500 nm	0.38912	0.51161	0.17360	0.26774
1501-2500 nm	0.21379	0.29616	0.16613	0.25122
2501-3500 nm	0.16021	0.20547	0.16147	0.24002

Table 68. Fit statistics for min fuel burn, single-aisle average replacement.

R2				
Flight Distance	**Total Mission Fuel Burn**	**Total Mission NOx**	**Terminal Area Fuel Burn**	**Terminal Area NOx**
0-500 nm	0.99866	0.99837	0.99862	0.99858
501-1000 nm	0.99828	0.99686	0.99996	0.99993
1001-1500 nm	0.99999	0.99998	0.99996	0.99993
1501-2500 nm	0.99996	0.99994	0.98918	0.98952
2501-3500 nm	0.99996	0.99993	0.98847	0.98870
Mean Model Fit Error				
Flight Distance	**Total Mission Fuel Burn**	**Total Mission NOx**	**Terminal Area Fuel Burn**	**Terminal Area NOx**
0-500 nm	0.05122	0.07880	0.00000	0.00000
501-1000 nm	-0.13402	-0.16868	-0.08426	-0.12781
1001-1500 nm	-0.10531	-0.13348	-0.08776	-0.13211
1501-2500 nm	-0.01806	-0.04306	-0.08824	-0.12986
2501-3500 nm	-0.11766	-0.16094	-0.07979	-0.11646
Standard Deviation of Model Fit Error				
Flight Distance	**Total Mission Fuel Burn**	**Total Mission NOx**	**Terminal Area Fuel Burn**	**Terminal Area NOx**
0-500 nm	1.34357	1.31032	0.00765	0.01124
501-1000 nm	0.61317	0.77026	0.15545	0.23609
1001-1500 nm	0.17376	0.22111	0.16191	0.24399
1501-2500 nm	0.07651	0.10413	0.16536	0.24237
2501-3500 nm	0.19375	0.26515	0.14959	0.21727

Table 69. Fit statistics for min NO_x, single-aisle average replacement.

R2				
Flight Distance	**Total Mission Fuel Burn**	**Total Mission NOx**	**Terminal Area Fuel Burn**	**Terminal Area NOx**
0-500 nm	0.99852	0.99818	0.99858	0.99852
501-1000 nm	0.99917	0.99857	0.99996	0.99992
1001-1500 nm	0.99923	0.99865	0.99996	0.99993
1501-2500 nm	0.99994	0.99988	0.99983	0.99969
2501-3500 nm	0.99996	0.99993	0.99982	0.99968
Mean Model Fit Error				
Flight Distance	**Total Mission Fuel Burn**	**Total Mission NOx**	**Terminal Area Fuel Burn**	**Terminal Area NOx**
0-500 nm	0.06695	0.09787	0.00000	0.00000
501-1000 nm	-0.14077	-0.18819	-0.09191	-0.13842
1001-1500 nm	-0.15828	-0.21420	-0.09492	-0.14174
1501-2500 nm	-0.07078	-0.09771	-0.09195	-0.13473
2501-3500 nm	-0.09428	-0.11863	-0.08868	-0.12806
Standard Deviation of Model Fit Error				
Flight Distance	**Total Mission Fuel Burn**	**Total Mission NOx**	**Terminal Area Fuel Burn**	**Terminal Area NOx**
0-500 nm	1.63908	1.70256	0.00824	0.01227
501-1000 nm	0.41509	0.53080	0.16960	0.25574
1001-1500 nm	0.42112	0.54723	0.17514	0.26187
1501-2500 nm	0.15496	0.21070	0.16505	0.24240
2501-3500 nm	0.15739	0.19824	0.15913	0.23027

Table 70. Fit statistics for equally weighted, single-aisle average replacement.

R2				
Flight Distance	**Total Mission Fuel Burn**	**Total Mission NOx**	**Terminal Area Fuel Burn**	**Terminal Area NOx**
0-500 nm	0.99822	0.99745	0.99867	0.99863
501-1000 nm	0.99825	0.99688	0.99996	0.99992
1001-1500 nm	0.99999	0.99998	0.99996	0.99992
1501-2500 nm	0.99996	0.99994	0.99012	0.99023
2501-3500 nm	0.99995	0.99993	0.99983	0.99970
Mean Model Fit Error				
Flight Distance	**Total Mission Fuel Burn**	**Total Mission NOx**	**Terminal Area Fuel Burn**	**Terminal Area NOx**
0-500 nm	0.07464	0.11089	0.00000	0.00000
501-1000 nm	-0.14403	-0.19146	-0.08475	-0.12910
1001-1500 nm	-0.13107	-0.18041	-0.08801	-0.13304
1501-2500 nm	-0.06146	-0.08801	-0.08667	-0.12842
2501-3500 nm	-0.09155	-0.11571	-0.08110	-0.11878
Standard Deviation of Model Fit Error				
Flight Distance	**Total Mission Fuel Burn**	**Total Mission NOx**	**Terminal Area Fuel Burn**	**Terminal Area NOx**
0-500 nm	1.71723	1.87312	0.00744	0.01099
501-1000 nm	0.59499	0.74720	0.15636	0.23847
1001-1500 nm	0.21600	0.29873	0.16236	0.24573
1501-2500 nm	0.11349	0.15481	0.16150	0.23853
2501-3500 nm	0.15341	0.19417	0.14549	0.21349

REFERENCES

[1] Smith, Margaret Chase. Importance of Aviation & Space in Our World Today. *Above and Beyond: Encyclopedia of Aviation and Space Sciences*, 1967.

[2] FAA Office of Environment and Energy. *Aviation & Emissions: A Primer*. January 2005.

[3] Schaefer, A., et al. *Transportation in a Climate Constrained World.* The MIT Press: Cambridge MA, 2009.

[4] Penner, J.E. et al. *Aviation and the Global Atmosphere: Summary for Policymakers*. Intergovernmental Panel on Climate Change, 1999.

[5] Mygatt, E. "Fueled By Developing Asia, Global Economy Continues to Expand." *Eco-Economy Indicators*, October 12, 2006.

[6] Airbus. *Airbus Global Market Forecast, 2010-2029*, 2010.

[7] Boeing. *Boeing Current Market Outlook, 2010-2029*, 2010.

[8] Federal Aviation Administration. *Terminal Area Forecast Summary, Fiscal Years 2011-2031*. January 2011.

[9] Waitz, I., et al. *Report to the United States Congress: Aviation and the Environment, A National Vision, Framework for Goals and Recommended Actions*. Partnership for AiR Transportation Noise and Emissions Reduction, December 2004.

[10] Lee, J. J., et al. Historical and Future Trends in Aircraft Performance, Cost, and Emissions. *Annual Review of Energy and the Environment*, Volume 26, 2001.

[11] Committee on Aviation Environmental Protection. *Report of the Independent Experts to the Long Term Technology Task Group on the 2006 LTTG NOx Review and the Establishment of Medium and Long Term Technology Goals for NOx. CAEP/7 Working Paper 11*, 2007. Available at http://www.faa.gov/about/office_org/headquarters_offices/aep/research/science_integrated_modeling/media/Independent%20Experts%20Report.pdf.

[12] International Civil Aviation Organization. *Noise Certification Workshop Session 1: ICAO Workshop on Aircraft Noise*. October 2004. Available at http://www.icao.int/icao/en/env/NoiseCertification_04/BIPs/bip1_01.pdf.

[13] International Civil Aviation Organization, "International Civil Aviation Organization: Environmental Unit, CAEP," Available at http://www.icao.int/icao/en/env/caep.htm [28 December 2008].

[14] deLuis, J. *A Process for the Quantification of Aircraft Noise and Emissions Interdependencies*. PhD Dissertation, Georgia Institute of Technology, 2008.

[15] Committee on Aviation Environmental Protection. *Aviation Environmental Design Tool (AEDT) Progress. CAEP/7 Information Paper 24*, January 24, 2007. Available at http://web.mit.edu/aeroastro/partner/reports/caep7/casep7-ip024-aedt.pdf.

[16] Environmental Protection Agency. *Aircraft Contrails Factsheet*. EPA 430-F-00-005, September 2000.

[17] International Civil Aviation Organization. Summary of *Annex 16 to the Convention on International Civil Aviation*. July 1993. Available at http://www.icao.int/eshop/pub/anx_info/an16_info_en.pdf.

[18] *VISION 100—CENTURY OF AVIATION REAUTHORIZATION ACT*. Public Law 108–176. Dec. 12, 2003.

[19] Federal Aviation Administration. *System for assessing Aviation's Global Emissions (SAGE), Version 1.5, validation assessment, model assumptions, and uncertainties*. FAA, Office of Environment and Energy, FAA-AEE-2005-03, September 2005.

[20] Baughcum, S., et al. "Aircraft Emissions: Current Inventories and Future Scenarios." In Penner, J.E. et al., *Aviation and the Global Atmosphere: Summary for Policymakers*. (pp. 293-329) Intergovernmental Panel on Climate Change, 1999.

[21] Fleming, Gregg G. et al. "Using FAA's SAGE Model to Conduct Global Inventories and to Assess Route-Specific Variability in Aviation Fuel Burn, Emissions, and Costs." *25th International Council of the Aeronautical Sciences, Sep. 3.-8. 2006, Hamburg, Germany*, 2006.

[22] Kim, Bryan Y. et al. *System for assessing Aviation's Global Emissions (SAGE), Part 1: Model description and inventory results.* Transportation Research Part D: Transport and Environment, Vol. 12, Issue 5, pp. 325-346, July 2007.

[23] Kim, B. et al. *System for assessing Aviation's Global Emissions (SAGE), Version 1.5, Global Aviation Emissions Inventories for 2000 through 2004.* Federal Aviation Administration Report FAA-EE-2005-02, September 2005.

[24] Fleming, Gregg G. FAA/AEE's Aviation Environmental Design Tool (AEDT) "System for assessing Aviation's Global Emissions (SAGE)." *Technical workshop on emission from aviation and maritime transport*, 4-5 October 2007.

[25] Kim, B. et al. *SAGE Version 1.5 Global Aviation Emissions Inventories for 2000 through 2004*. Federal Aviation Administration Office of Environment and Energy, September 2005.

[26] Gawdiak, Y., Carr, G., and Hasan, S. "JPDO Case Study of NextGen High Density Operations." AIAA 2009-6918. *9th AIAA Aviation Technology, Integration, and Operations Conference (ATIO)*. 21 - 23 September 2009, Hilton Head SC.

[27] Borener, S. et al. "Can NGATS Meet the Demands of the Future?" ATCA Journal of Air Traffic Control. Jan-Mar 2006.

[28] Committee on Aviation Environmental Protection. *CAEP/8 NOx Stringency Cost-Benefit Analysis Demonstration Using APMT-Impacts*, *CAEP/8 Information Paper 30*, 2010. Available at http://web.mit.edu/aeroastro/partner/reports/caep8/caep8-nox-using-apmt.pdf.

[29] Malwitz, A., et al. *System for assessing Aviation's Global Emissions (SAGE), Version 1.5, Validation Assessment, Model Assumptions and Uncertainties*. FAA-EE-2005-03, September 2005.

[30] Graham, M., et al. "Evaluating the Environmental Performance of the U.S. Next Generation Air Transportation System." *Eighth USA/Europe Air Traffic Management Research and Development Seminar*, 2009.

[31] Gopalah, R. and K. Talluri. *Mathematical Models in Airline Schedule Planning: A Survey*. Annals of Operations Research. Vol 76, No 0, pp 155-185.

[32] Dobson, G. and P. Lederer. *Airline Scheduling and Routing in a Hub-and-Spoke System*. Transportation Science, Vol. 27, No. 3, pp 281-291, August 1993.

[33] Joint Planning and Development Office. Next Generation Air Transportation System Integrated Work Plan: A Functional Outline. Volume 1.0, September 30, 2008.

[34] Kirby, Michelle R., et al. Enhancing the Environmental Policy Making Process with the FAA's EDS Analysis Tool. *47th AIAA Aerospace Sciences Meeting Including The New Horizons Forum and Aerospace Exposition 5 - 8 January 2009, Orlando, Florida, AIAA-2009-1262*, 2009.

[35] Committee on Aviation Environmental Protection. *Report of Working Group 3, Part 2: Standards and Technology Goals. CAEP/8 Working Paper 14*, November

30, 2009. Available at http://www.obsa.org/Documentos%20compartidos/CAEP-8-WP-14.pdf.

[36] DeLaurentis, Daniel A. "Understanding Transportation as System-of-Systems Design Problem." *43rd AIAA Aerospace Sciences Meeting and Exhibit 10 - 13 January 2005, Reno, Nevada, AIAA Paper 2005-123*, 2005

[37] Airbus. *Airbus Global Market Forecast, 2007-2026*, 2007.

[38] Committee on Aviation Environmental Protection. *CAEP/6 Information Paper 28*, 2003. Available at http://www.icao.int/anb/Council-Technical-Committees/CAEP6/InformationPapers/ip28a.pdf.

[39] Embraer Commercial Jets. "Embraer ERJ-190." Available at http://www.embraercommercialjets.com/img//download/136.pdf.

[40] Airbus. "Specifications, Airbus A321." Available at http://www.airbus.com/aircraftfamilies/a320/a321/specifications.

[41] The Boeing Company. "Technical Characteristics – Boeing 767-300ER." Available at http://www.boeing.com/commercial/767family/pf/pf_300prod.html.

[42] Committee on Aviation Environmental Protection. *CAEP/6 Information Paper 13*, 2003. Available at http://www.icao.int/anb/Council-Technical-Committees/CAEP6/InformationPapers/ip13.pdf.

[43] Committee on Aviation Environmental Protection. *New NOx Stringency for Aircraft Engines. CAEP/7 Working Paper 47*, December 29, 2006. Available at http://www.tc.gc.ca/media/documents/ca-opssvs/caep7__wp47.pdf.

[44] International Civil Aviation Organization, *Group on International Aviation and Climate Change (GIACC). Report of Working Group 3, Agenda Item 3: Planning of actions and policy elements to be developed by the Group*. GIACC/3-WP/4 Available at http://www.icao.int/icao/en/atb/meetings/GIACC/2009/Giacc_3/Docs/Giacc3_wp04_en.pdf.

[45] Bombardier Aircraft. "Fiscal Year 2007/08 Deliveries." Available at http://www2.bombardier.com/en/3_0/pdf/aircraft_deliveries_2007-08_1.pdf.

[46] Kirby, Mary. "Embraer commercial aircraft deliveries drop 25% in 2009." *Air Transport Intelligence news*. December 1, 2010.

[47] The Boeing Company. "Orders and Deliveries." Available at http://active.boeing.com/commercial/orders/index.cfm.

[48] Airbus. "Airbus for Analysts." Available at http://www.airbus.com/tools/airbusfor/analysts.

[49] 2006 Global Fleet Operations courtesy of the Volpe National Transportation Systems Center, June 2009.

[50] Committee on Aviation Environmental Protection. *Review of the Fleet and Operations Module (FOM) Assumptions and Limitations. CAEP/8 Working Paper 10*, 2007. Available at http://www.wyle.com/PDFs/archive/CAEP8.PDF

[51] Kirby, M. et al. "Development of an Interactive Capability to Trade Off New Technologies and Future Aircraft to Reduce Aviation Environmental Impacts."*27th International Congress of the Aeronautical Sciences*. 2010.

[52] Ranson, Lori. "American CEO Arpey cites economic struggles with 757s." *Air Transport Intelligence*, July 16, 2009.

[53] Francis, Leithen. "AirAsia wants to delay delivery of eight A320s in 2010." *Air Transport Intelligence*, July 16, 2009.

[54] Thrasher, T., e; al. *NOx Demonstration Analysis, Round 3*, AEDT Nox Demonstration Third Analysis, Round 3 Final Report, November 6, 2006.

[55] Mattson, C.A. and Messac, A., "Concept Selection in n-Dimension using s-Pareto Frontiers and Visualization." *9th AIAA/ISSMO Symposium on Multidisciplinary Analysis and Optimization September 04–06, 2002 Atlanta, GA, AIAA–2002–5418, 2002*, 2002.

[56] Graham, M., et al. "Evaluating the Environmental Performance of the U.S. Next Generation Air Transportation System." *Eighth USA/Europe Air Traffic Management Research and Development Seminar (ATM2009)*, Napa CA, 2009.

[57] Collier, F. "NASA's Subsonic Fixed Wing Project." NASA Fundamental Aeronautics Program Annual Meeting, October 7, 2008.

[58] Murphy, C. and T. Thompson. "IPSA Environmental Analysis." Presented to the JPDO Environmental Working Group Operations Standing Committee, May 17, 2010.

[59] *User Manual for the Base of Aircraft Data (BADA). Revision 3.6*, European Organisation for the Safety of Air Navigation, September 2004.

[60] Harris, W. L., et al. *FAA Aviation Environmental Design Tool (AEDT) Workshop #1 Letter Report*. Transportation Research Board, Washington DC, March 31 - April 2, 2004.

[61] Barter, G., *Exploration and Assessment of the Environmental Design Space for Commercial Aircraft and Future Technologies*, Master's Thesis. Massachusetts Institute of Technology, 2004

[62] Roberts, J. W. *Further Calculations of the Performance of Turbofan Engines Incorporating a Wave Rotor*. MS Thesis, Naval Postgraduate School, September 1990.

[63] Koch, P. N., A. Barlow, J. Allen, and F. Mistree. "Configuring Turbine Propulsion Systems Using Robust Concept Exploration." *Proceedings of The 1996 ASME Design Engineering Technical Conferences and Computers in Engineering Conference*. August 18-22, 1996, Irvine, California, 1996.

[64] Kirby, M. R. and Mavris, D. N. "The Environmental Design Space." *26th International Congress of the Aeronautical Sciences*. 14-19 September, 2008.

[65] Caves, B.E., L.R. Jenkinson, and D.P. Rhodes. "Adapting Civil Aircraft Conceptual Design Methods to Account for Broader Based Constraints." *AIAA/SAE 1997 World Aviation Congress, AIAA Paper 1997-5595*, 1997.

[66] "Integrated Wing Introduction." http://www.integrated-wing.org.uk, Accessed July 23, 2009.

[67] Ellsmore, P. D. and K. E. Restrick. "Application of RETIVO to Civil Aircraft." *7th AIAA Aviation Technology, Integration and Operations Conference (ATIO) September 2007, Belfast, Northern Ireland, AIAA Paper 2007-7808*, 2007.

[68] Cadot-Burillet, Delphine, et. al. "Technology Evaluator: a Global Way of Assessing Low Noise Technologies." *13th AIAA/CEAS Aeroacoustics Conference (28th AIAA Aeroacoustics Conference), AIAA Paper 2007-3669*, 2007

[69] Koenig, J. and T. Hellstrom. "The Clean Sky 'Smart Fixed Wing Aircraft Integrated Technology Demonstrator': Technology targets and project status." *27th International Council of the Aeronautical Sciences, Sep. 19.-24. 2010, Nice, France*, 2010.

[70] Lissys Ltd. "Piano.Aero: Commercial Aircraft Analysis Software." Available at http://www.lissys.demon.co.uk/index2.html.

[71] Zeinali, M. and D. Rutherford. "Trends in Aircraft Efficiency and Design Parameters." International Council on Clean Transportation, 2010.

[72] Mavris, D. N., L.L. Phan, and E. Garcia. "Formulation and Implementation of an Aircraft System – Subsystem Interrelationship Model for Technology

Evaluation." *25th International Council of the Aeronautical Sciences, Sep. 3.-8. 2006, Hamburg, Germany*, 2006.

[73] Reis, G. "Systems Architectural Development: A New Paradigm for Early-Stage Design." PACE America Inc., February 2010.

[74] Torenbeek, E. *Synthesis of Subsonic Airplane Design.* Delft: Delft University Press, 1982.

[75] Gologan, C. and D Schmitt. "Comparison of Powered-Lift Turbofan Aircraft with Conventional Turboprop Aircraft for ESTOL Application." *27th International Council of the Aeronautical Sciences, Sep. 19.-24. 2010, Nice*, *France*, 2010.

[76] Pace. *Pacelab APD Data Sheet*. Pace Aerospace Engineering and Information Technology GmbH (http://www.pace.de/en/), 2006.

[77] Pace. *Pacelab Mission*. Pace Aerospace Engineering and Information Technology GmbH, 2009. Available at http://www.pace.de/get_document2.php?id=983.

[78] Committee on Aviation Environmental Protection. *Update on U.S. Aviation Environmental Research and Development Efforts*. CAEP/8 Information Paper 33, December 16, 2009. Available at http://web.mit.edu/aeroastro/partner/reports/caep8/caep8-r-and-d.pdf.

[79] Mavris, D. "Environmental Design Space Overview." *TRB AEDT/APMT Workshop #4*, December 6-8, 2006. Available at http://www.faa.gov/about/office_org/headquarters_offices/apl/research/models/history/media/05_DM_Overview-EDS_2006-11-28_FINAL.pdf.

[80] Converse, G.L.; and Giffin, R.G., *Extended Parametric Representation of Compressors Fans and Turbines. Vol. I - CMGEN User's Manual* NASA CR-174645, 1984.

[81] Berton, J. J. and R. M. Plencner. *An Interactive Preprocessor for the NASA Engine Performance Program*. NASA Technical Memorandum 105786, August 1992.

[82] Fishbach, L. H. and M. J. Caddy. *NNEP - THE NAVY NASA ENGINE PROGRAM*. NASA Technical Memorandum X-71857, December 1975.

[83] Sehra, A. K. "The Numerical Propulsion System Simulation….A Vision for Virtual Engine Testing." *The 2006 ASME TURBO EXPO, May 8 – 11, 2006*, 2006.

[84] Follen, G. J. *An Object Oriented Extensible Architecture for Affordable Aerospace Propulsion Systems*. NASA Glenn Research Center, 2002.

[85] Schutte, J. S. *Simultaneous, Multi-design Point Approach to Gas Turbine On-design Cycle Analysis for Aircraft Engines*. PhD Dissertation. Georgia Institute of Technology, 2009.

[86] Kirby, M.R. *A Method for Technology Identification, Evaluation, and Selection in Conceptual and Preliminary Aircraft Design*. PhD Dissertation, Georgia Institute of Technology, 2001.

[87] Kirby, M.R. and D.N. Mavris. *A Technique for Selecting Emerging Technologies for a Fleet of Commercial Aircraft to Maximize R&D Investment.* SAE Paper 2001-01-3018, 2001.

[88] Burgelman, R.A., Maidique, M.A., Wheelwright, S.C., *Strategic Management of Technology and Innovation*, 2nd Edition, Irwin McGraw-Hill, Boston, 1988.

[89] Patel, C. *A Multi-objective Stochastic Approach to Combinatorial Technology Space Exploration*. PhD Dissertation, Georgia Institute of Technology, August 2009.

[90] Mavris, D.N., Baker, A.P., Schrage, D.P., "Implementation of a Technology Impact Forecast Technique on a Civil Tiltrotor", *Proceedings of the 55th National Forum of the American Helicopter Society*, Montreal, Quebec, Canada, May 25-27, 1999.

[91] Aviation Integrated Modelling (AIM) Project, http://www.aimproject.aero/, Accessed July 28, 2009.

[92] Reynolds, T. G., et. al. "Modelling Environmental & Economic Impacts of Aviation: Introducing the Aviation Integrated Modelling Project." *7th AIAA Aviation Technology, Integration and Operations Conference (ATIO) September 2007, Belfast, Northern Ireland, AIAA Paper 2007-7751*, 2007.

[93] Institute for Aviation and the Environment, University of Cambridge. "Modelling Environmental & Economic Impacts of Aviation: Introducing the Aviation Integrated Modelling Project." IIT Bombay Presentation, October 26, 2007.

[94] Evans, A. *Simulating Airline Operational Responses to Environmental Constraints.* Ph.D. Dissertation, University of Cambridge, 29 Mar 2010.

[95] Dray, L. et al. *Mitigation of Aviation Emissions of Carbon Dioxide: Analysis for Europe*. Transportation Research Record: Journal of the Transportation Research Board, Issue 2177, pp. 17-26, 2010.

[96] Evans, A. and A. Schaefer. "Simulating Flight Routing Network Responses to AirportCapacity Constraints in the US." *9th AIAA Aviation Technology, Integration, and Operations Conference (ATIO) 21 - 23 September 2009, Hilton Head, South Carolina, AIAA-2009-6934*, 2009.

[97] Dray, L. et al. "Air Transport Within An Emissions Trading Regime: A Network-based Analysis of the United States and India." *88th Transportation Research Board Annual Meeting, Washington, DC,* January 2009.

[98] Vlek, S. and M. Vogels. *AERO – Aviation Emissions and Evaluation of Reduction Options*. Air & Space Europe, Vol. 2, No. 3, pp. 41-44, 2000.

[99] Aviation Emissions and Evaluation of Reduction Options (AERO) Main Report Part I: Description of the AERO Modelling System, December 2000.

[100] Anger, A. and J. Koehler. *Including aviation emissions in the EU ETS: Much ado about nothing? A review.* Transport Policy, Vol. 17, pp. 38–46, 2010.

[101] Edmondson, D. et al. *Quantifying the Environmental and Economic Impacts of Market Based Instruments to Reduce Aircraft Emissions.* Report written for the Dutch Civil Aviation Department, 2005.

[102] Waitz, Ian, et al. *Requirements Document for the Aviation Environmental Portfolio Management Tool*. PARTNER Report No. PARTNER-COE-2006-001, June 2006.

[103] Committee on Aviation Environmental Protection, CAEP/6 Working Paper 49, 2004. Available at http://www.icao.int/anb/Council-Technical-Committees/CAEP6/WorkingPapers/wp49.pdf

[104] Iovinelli, R. and C. Roof. "Aviation Environmental Design Tool (AEDT) Beta1a Demonstration." Presented to UC Davis Symposium Luncheon, 1 Mar 2010. Available at http://airquality.ucdavis.edu/pages/events/2010/aerovision/IOVINELLI.pdf.

[105] Koopman, J. and A. Hansen. "Aviation Environmental Design Tool Presentation." Presented to Public Tools Colloquium. 2 Dec 2010. Available at http://web.mit.edu/aeroastro/partner/envtoolcollo-12-10/files/aedt-demo.pdf.

[106] Boeker, E. and G. Fleming. "Functional Description of the FAA's Aviation Environmental Design Tool's Aircraft Acoustics Module." Noise-*Con, 28-30 Jul 2008, Dearborn MI*, 2008.

[107] Emissions and Dispersion Modeling System (EDMS) User's Manual. Prepared for the Federal Aviation Administration Office of Environment and Energy byCSSI, Inc., Washington DC, Nov. 2009.

[108] Roof, C., et al. *Aviation Environmental Design Tool (AEDT) System Architecture*. Prepared for: Federal Aviation Administration Office of Environment and Energy, January 29, 2007.

[109] SAE Committee A-21, Aircraft Noise. *Procedure for the Calculation of Noise in the Vicinity of Airports*, Aerospace Information Report No. 1845, Warrendale, PA: Society of Automotive Engineers, Inc., March 1986.

[110] Becker, K., et al. "A Process for Future Aviation Environmental Impacts: A Surrogate Fleet Analysis Approach for NextGen." *9th AIAA Aviation Technology, Integration, and Operations Conference (ATIO) 21 - 23 September 2009, Hilton Head, South Carolina, AIAA-2009-6934*, 2009.

[111] Roy, D.P., B. Devereux, B. Grainger, S. White. *Parametric Geometric Correction of Airborne Thematic Mapper Imagery*. Int. J. Remote Sensing, vol. 18, no. 9, 1865-1887, 1997.

[112] Phillips, P. and B. Hansen. *Statistical Inference in Instrumental Variables Regression with I(1) Processes*. The Review of Economic Studies, Vol. 57, No. 1, pp. 99-125, 1990.

[113] Anderson, J. *Fundamentals of Aerodynamics*. Mcgraw Hill: Boston, 2001.

[114] Hahn, R. W. *An economic analysis of scrappage*. RAND Journal of Economics, Vol. 26, No. 2, Summer 1995. pp. 222-242.

[115] Biltgen, P.T., T. Ender, and D.N. Mavris. "Development of a Collaborative Capability-Based Tradeoff Environment for Complex System Architectures." *44th AIAA Aerospace Sciences Meeting and Exhibit 9 - 12 January 2006, Reno, Nevada, AIAA 2006-728*, 2006.

[116] Barros, P.A., M. R. Kirby, and D. N. Mavris. "A Review of Calibration under Uncertainty within the Environmental Design Space." *47th AIAA Aerospace Sciences Meeting Including The New Horizons Forum and Aerospace Exposition 5 - 8 January 2009, Orlando, Florida AIAA 2009-274*, 2009.

[117] Hornberger, G. M., and B.J. Cosby, *Selection of parameter values in environmental models using sparse data: A case study*, Applied Mathematics and Computation, 17 (1985), 335-55.

[118] Hornberger, G. M., B. J. Cosby, and J. N. Galloway. *Modeling the effects of acid deposition: Uncertainty and spatial variability in estimation of long-term sulfate dynamics in a region*. Water Resources Research, 22(8) (1986), 1293-1302.

[119] Trabalka, J. R., Edmonds J. A., Reilly, J. M., Gardner, R. H. and Reichle, D. E., "Atmospheric CO2 projections with globally averaged carbon cycle models", in Trabalka, J. R. and Reichle, D. E. (eds). *The Changing Carbon Cycle: A Global Analysis*, New York: Springer-Verlag, 1986.

[120] Roth, Bryce, and Dimitri N. Mavris. *Estimation of Turbofan Engine Performance Model Accuracy and Confidence Bounds*. International Society for Air Breathing Engines, ISABE 2003-1208, 2003.

[121] Rose, Kenneth A. et al. *Parameter Sensitivities, Monte Carlo Filtering, and Model Forecasting Under Uncertainty*. Journal of Forecasting, Vol. 10, pp117-133, 1991.

[122] Simpson, Timothy W., Timothy M. Mauery, John J. Korte, and Farrokh Mistree. "Comparison of Response Surface and Kriging Models for Multidisciplinary Design Optimization." *7th AIAA/USAF/NASA/ISSMO Symposium on Multidisciplinary Analysis & Optimization September 2-4, 1998, St. Louis MI, AIAA, Vol. 1, pp. 381-391, AIAA-98-4755*, September 1998.

[123] Brot, A. "Using Probabilistic Simulations in Order to Minimize Fatigue Failures in Metallic Structures." Presented to the Israel Annual Conference on Aerospace Sciences, 2005.

[124] Venables, W. N., Ellis, N., Punt, A. E., Dichmont, C. M., and Deng, R. A. 2009. *A simulation strategy for fleet dynamics in Australia's northern prawn fishery: effort allocation at two scales*. ICES Journal of Marine Science, 66: 631–645.

[125] Noel, G., et al. "Assessment of the Aviation Environmental Design Tool." *Eighth USA/Europe Air Traffic Management Research and Development Seminar (ATM2009)*, 2009.

[126] Malwitz, A., et al. *System for assessing Aviation's Global Emissions (SAGE), Version 1.5, Validation Assessment, Model Assumptions and Uncertainties*. FAA-EE-2005-03, September 2005.

[127] Lee, Joosung J. *Modeling aviation's global emissions, uncertainty analysis, and applications to policy*. PhD Thesis, Massachusetts Institute of Technology (MIT), February 2005.

[128] Skalecky, J. "CLEEN Planned Solicitation." CLEEN Market Research Conference, May 15, 2008.

[129] Mavris, D. and M. Kirby. "EDS Capability Demonstration for Assessing the CLEEN Program Final Report". Submitted to Federal Aviation Administration, Office of Environment & Energy. 2 February 2010.

[130] Boeing: Airport Noise and Emissions Regulations - Airports with Noise and Emissions Restrictions. Available at http://www.boeing.com/commercial/noise/list.html Retrieved September 20, 2010.

[131] Jung, Y. "Fuel Consumption and Emissions from Airport Taxi Operations." *Green Aviation Summit*, NASA Ames Research Center, Sept 8-9, 2010.

[132] Clarke, J.P. et al. *Development, design, and flight test evaluation of a continuous descent approach procedure for nighttime operation at Louisville International Airport.* Partnership for AiR Transportation Noise and Emission Reduction, Report No. PARTNER-COE-2006-002, January 9, 2006.

[133] Fletcher, S.G. and K. Ponnambalam. *Estimation of Reservoir Yield and Storage Distribution Using Moments Analysis*. Journal of Hydrology vol. 182, pp. 259-275, 1996.

[134] Kumaraswamy, P. *A Generalized Probability Density Function for Double-bounded Random Processes*. Journal of Hydrology, 46, pp 79—88, 1980.

[135] Box, G.E.P. and J.S. Hunter. The 2k-p Fractional Factorial Designs Part I. *Technometrics*. 3(3), pp311-351, 1961.

[136] Stowe, R. A. and R.P. Mayer. *Efficient Screening of Process Variables*. Industrial and Engineering Chemistry, 58 (2), pp36-40, 1966.

[137] Carter, C. *Seven Basic Quality Tools.* HRMagazine. Vol. 37, Iss. 1, pp 81-84. Jan 1992.

[138] Craft, R. and Leake, C. *The Pareto Principle in Organizational Decision Making*. Management Decision. Vol. 40, Iss. 8, pp. 729-733. 2002.

[139] Juran, J. *The Non-Pareto Principle; Mea Culpa.* Selected Papers No. 18. Juran Institute, 1975.

[140] Sall, J. and A. Lehmann. *JMP start statistics. A guide to statistics and data analysis using JMP and JMP In software*. Belomont CA: Duxbury Press, 1996.

[141] Yang, W. and Y. Tarng. Design Optimization of Cutting Parameters for Turning Operations Based on the Taguchi Method. Journal of Materials Processing Technology 84 (1998) 122–129.

[142] Barros, P.A., M.R. Kirby, and D.N. Mavris. *Impact of Sampling Technique Selection on the Creation of Response Surface Models*. SAE Transactions. 113(1), 2004.

[143] Helton, J., *Uncertainty and sensitivity analysis techniques for use in performance assessment for radioactive waste disposal*. Reliability Engineering and System Safety, 42 (2-3) pp. 327 -367, 1993.

[144] Smith, P. J., Shafi, M., and Gao, H., *Quick simulation: a review of importance sampling techniques in communications systems*. IEEE Journal on Selected Areas in Communications, 15 (4) pp. 597-613, 1997.

[145] SAS Institute Inc., JMP Release 7, Design of Experiments Guide, Cary, NC, 2007.

[146] Sacks, J., W. Welch, T. Mitchell, and H. Wynn. *Design and Analysis of Computer Experiments*. Statistical Science, 4(4), 1989.

VITA

Keith Frederick Becker was born in Portland, Oregon and lived with his family in New York and Florida before graduating from Flagler Palm Coast High School in 1999 and beginning undergraduate work in Aerospace Engineering at the Georgia Institute of Technology. He completed his Bachelor of Science degree in 2003, having also served as Vice-Chair of the Georgia Tech chapter of AIAA, Vice-President of the Georgia Tech chapter of Sigma Gamma Tau, Aerospace Engineering Representative to the Student Government Association, and an active member in Tau Beta Pi. Keith began graduate studies in May 2003 under the advisement of Professor Jeff Jagoda in the Aerospace Combustion Lab at Georgia Tech, and completed his Master of Science degree in the summer of 2004. Following this, Keith began doctoral studies at the Aerospace Systems Design Lab at Georgia Tech under the advisement of Professor Dimitri Mavris, and he anticipates completing this work in August 2011.